NOTICE

The quality of this microform is heavily dependent upon the quality of the original thesis submitted for microfilming. Every effort has been made to ensure the highest quality of reproduction possible.

If pages are missing, contact the university which granted the degree.

Some pages may have indistinct print especially if the original pages were typed with a poor typewriter ribbon or if the university sent us an inferior photocopy.

Previously copyrighted materials (journal articles, published tests, etc.) are not filmed.

Reproduction in full or in part of this microform is governed by the Canadian Copyright Act, R.S.C. 1970, c. C-30.

AVIS

La qualité de cette microforme dépend grandement de la qualité de la thèse soumise au microfilmage. Nous avons tout fait pour assurer une qualité supérieure de reproduction.

S'il manque des pages, veuillez communiquer avec l'université qui a conféré le grade.

La qualité d'impression de certaines pages peut laisser à désirer, surtout si les pages originales ont été dactylographiées à l'aide d'un ruban usé ou si l'université nous a fait parvenir une photocopie de qualité inférieure.

Les documents qui font déjà l'objet d'un droit d'auteur (articles de revue, tests publiés, etc.) ne sont pas microfilmés.

La reproduction, même partielle, de cette microforme est soumise à la Loi canadienne sur le droit d'auteur, SRC 1970, c. C-30.

Canada

ON DIFFERENTIAL DETECTION OF DIGITALLY MODULATED SIGNALS

A THESIS
SUBMITTED TO THE SCHOOL OF
GRADUATE STUDIES AND RESEARCH
OF THE UNIVERSITY OF OTTAWA
IN PARTIAL FULFILLMENT OF THE REQUIREMENTS
FOR THE DEGREE OF
DOCTOR OF PHILOSOPHY
IN
ELECTRICAL ENGINEERING

By
Mustafa Abbas Yongaçoğlu
1987

ISBN 0-315-40756-5

UNIVERSITÉ D'OTTAWA
UNIVERSITY OF OTTAWA

For my Mother

started with you
continuing with your memory

ABSTRACT

The objective of this thesis is to introduce new transmitter and receiver structures to improve the bandwidth efficiency and/or power efficiency of differentially detected phase-shift keyed (PSK) and continuous phase modulated (CPM) signals.

For frequency division multiple access operations when the channel includes nonlinearities, a differentially detected controlled transition PSK (DCTPSK) modem is introduced. This modem employs a new signal format which can be demodulated using a conventional differential detector.

It is shown that in an adjacent channel interference environment, more carriers can share the same channel by using DCTPSK modems compared to using differentially detected quaternary PSK (DQPSK) or differentially detected minimum shift keying (DMSK) modems. Similarly, for certain bandwidth efficiencies, DCTPSK modems require less transmit power than DQPSK or DMSK modems.

A DCTPSK modem has been designed and implemented, and its performance has been evaluated using a laboratory set-up and also via satellite link. The measurement results indicate that the modem suffers about 2 dB E_b/N_0 degradation due to various hardware imperfections.

In order to improve the bit error rate (BER) performance of the DCTPSK modem, two new receiver processing techniques have been introduced. In addition to the conventional one-bit differential detectors, the new receivers also utilize two-bit differential detectors.

The first new technique uses symbol-by symbol detection which combines the outputs of the one-bit and two-bit differential detectors. Thus an E_b/N_0 improvement of 1.2 dB is achieved (at BER=10^{-4}).

The second receiver processing technique is based on using a four-state sequential decoder. The E_b/N_0 improvement achieved with this technique is about 1.7 dB.

These new receiver processing techniques are directly applicable to DQPSK, and the same concepts can be utilized for other modulation techniques as well.

The work on CPM signals focuses on the differential detection of Gaussian

minimum shift keying (GMSK). When conventional receivers are used, the performance of differentially detected GMSK is about 7 dB inferior to its coherent counterpart. This difference is largely due to a large amount of intersymbol interference in the differentially detected signal. It is shown here that by applying decision feedback to the differential detectors, the destructive effect of intersymbol interference can be partially removed. Various new receivers have been studied where the outputs of more than one detector are combined. The best BER performance obtained here is when the outputs of the modified two-bit and three-bit differential detectors are jointly utilized. For a system with a bandwidth-time product (B_tT) of 0.25, this new receiver provides about 4 dB E_b/N_o advantage over currently known differentially detected GMSK receivers. Furthermore, the improvement is greater for systems with B_tT values smaller than 0.25.

ACKNOWLEDGEMENTS

While working for my Ph.D. degree, I accumulated various intellectual debts for which a mere acknowledgement is small repayment.

I wish to thank my supervisor Dr. K. Feher for the technical guidance, financial support and the excellent facilities he provided me at the University of Ottawa.

Many colleagues and friends facilitated my work. With D. Makrakis I had long (sometimes perplexing) but generally very fruitful discussions. H. Ohnishi's expertise and efforts were crucial in building the DCTPSK modem. D. Prendergast provided valuable help with the hardware implementation and satellite measurements.

Several brave colleagues read earlier versions of this thesis in its entirety and tried to reduce the errors, ambiguous statements and confusing notation. If I have failed in these respects, it is through no fault of B. Mazur, D. Makrakis, J.S. Seo and P. Mathiopoulos. I am immensely grateful to each of these friends, particularly to my ex-manager B. Mazur.

I would like to thank Dr. W. Steenaart and Dr. Y.F. Lum, the members of my Ph.D. advisory committee, for their valuable suggestions. I acknowledge the examiners of the thesis defence: Dr. G.J.P. Lo, Dr. S. Mahmoud and Dr. W. McGee for their comments and contributions to the final version of the thesis.

Finally, I thank my sisters, my friends who are away, and Adrienne Edwards for being my vital source of encouragement and support throughout this long process.

Contents

List of Figures

List of Tables

List of Abbreviations

ACI: Adjacent channel interference.

AWGN: Additive white Gaussian noise.

BER: Bit error rate.

BPF: Bandpass filter.

BPSK: Binary PSK.

BT: 3 dB bandwidth-time product.

CPM: Continuous phase modulation.

CWF: Combining with feedback.

DBPSK: Differentially detected binary PSK.

DCTPSK: Differentially detected controlled transition PSK.

DGMSK: Differentially detected GMSK.

DMSK: Differentially detected MSK.

DOQPSK: Differentially detected offset quaternary PSK.

DQPSK: Differentially detected quaternary PSK.

GLPF: Gaussian lowpass filter.

GMSK: Gaussian minimum shift keying.

FDMA: Frequency division multiple access.

FM: Frequency modulation.

HF: High frequency.

IF: Intermediate frequency.

IJF: Intersymbol and jitter free.

ISI: Intersymbol interference.

LO: Local oscillator.

LPF: Lowpass filter.

MSK: Minimum shift keying.

NEC: Nonredundant error correction.

NRZ: Non-return to zero.

OQPSK: Offset quaternary PSK.

PSK: Phase-shift keying.

PWM: Pulse width modulation.

P/S: Parallel to serial conversion.

QPSK: Quaternary (or quadri) PSK.

SSD: Signal-state diagram.

S/P: Serial to parallel conversion.

TFM: Tamed frequency modulation.

VCO: Voltage controlled oscillator.

Chapter 1

INTRODUCTION AND OVERVIEW

1.1 SYSTEM ENGINEER'S PROBLEM

When a new communications service is to be introduced, one of the major tasks the system engineer must perform is the selection of the appropriate modulation-demodulation (modem) technique. For this purpose several factors must be taken into account. These include:

- bandwidth efficiency,
- detection efficiency,
- channel characteristics,
- acquisition time,
- implementation complexity,
- compatibility with existing services and equipment, and
- cost.

Bandwidth efficiency is defined as the ratio of the data rate to channel bandwidth (in units of b/s/Hz). For instance, the bandwidth may be defined as the bandwidth required to contain a certain percentage (e.g., 99% or 99.99 %) of the transmitted power.

Detection efficiency[1] is measured in terms of the ratio of the energy per bit to noise power density required to achieve a given bit error rate (BER). In a practical context, a more frequently used criterion is the power efficiency which also takes into account various sources of interference and the operating mode of the power amplifiers.

Channel characteristics refer to a large number of physical phenomena related to the transmission medium, and various (potentialy) inflexible channel parameters (e.g., filters and amplifiers). In addition to the ever present thermal noise, the major channel imperfections might be:

- intersymbol interference,
- adjacent channel interference,
- co-channel interference,
- multipath fading and shadowing,
- frequency uncertainties and phase noise, and
- nonlinear amplifiers.

Implementation complexity includes circuit complexity, environmental constraints, size, weight and suitability to large scale integration.

Compatibility with existing services and equipment is often a system requirement, and *cost* is often the most crucial parameter in the final decision.

Generally, the selection is done after weighting each parameter and evaluating the tradeoffs. Some modem techniques are precluded easily when the preliminary analysis indicates that they cannot meet the minimum service requirements. A short list of candidates is thus formed, from which more detailed analysis will lead to the final selection.

[1] This is also refered to as communications efficiency in the engineering literature.

Let us assume that the system engineer started by satisfying the bandwidth efficiency requirement, and determined the candidate modulation techniques which provide bandwidth efficiencies in the range of 0.5 to 1 b/s/Hz. The next step would be selecting the appropriate demodulation technique, which we consider below.

1.2 REVIEW OF DEMODULATION TECHNIQUES

Digitally modulated signals can be demodulated

- coherently, or
- noncoherently.

There are numerous ways of demodulating a received signal coherently or noncoherently, and in this section only the general properties of the various demodulation techniques are briefly reviewed.

1.2.1 Coherent Demodulation

In coherent systems, an estimate of the carrier phase is used as a reference in the demodulation process. Coherent detection is the most power efficient demodulation approach when additive white Gaussian noise (AWGN) is the major channel disturbance. Conversely, in applications where multipath fading, Doppler shifts or phase noise are considerable, it is difficult to obtain and maintain a coherent phase reference in the receiver. The phase error due to these disturbances results in high error floors [1–4], i.e., increasing the transmit power does not reduce the BER below a certain value.

A coherent phase estimate is usually derived directly from the modulated signal[2]. Because of the frequency instabilities and phase jitter inherent in transmitter and receiver systems, carrier recovery loop bandwidths

[2]The modulated signal, in general, does not contain a discrete component at the carrier frequency.

cannot be made arbitrarily small. Consequently, in practice, a noisy phase estimate is obtained and only partially coherent reception can be claimed [5].

Another problem with coherent detection is its sometimes poor acquisition performance. As the spectrum of the transmitted signal becomes narrower, the problem of finding the exact phase of the carrier becomes more difficult [4–8]. A common method of finding the phase is to use a band-pass filter or a phase locked loop with some suitable loop-bandwidth. However, as the loop bandwidth is decreased, the signal acquisition time becomes larger [9]. This becomes a major problem when the transmitted information is sent in bursts (e.g., packet data or voice activated digital speech), as fast acquisition is then needed to maintain a high transmission efficiency [10,11].

One way to relax the carrier recovery requirements and improve the BER performance of a coherent receiver experiencing adverse phase variations is to transmit a tone along with the information bearing signal. Several such schemes have been described in the literature [12–19]. Some of these techniques require additional bandwidth (e.g., [12,17,18]), while all of them require more power than the conventional coherent detection.

1.2.2 Noncoherent Demodulation

In noncoherent demodulation, the phase coherence requirement is either relaxed or completely removed. The noncoherent demodulation techniques which are suitable to narrowband signals (i.e., with bandwidth efficiencies greater than 0.5 b/s/Hz) are:

- limiter discriminator detection, and
- differential detection.

1.2.2.1 Limiter Discriminator Detection

In limiter discriminator detection no phase coherence is necessary. The receiver consists of a predetection bandpass filter, a limiter discriminator,

and a postdetection filter (see Figure 1.1). The predetection filter limits the noise entering the detector, while the actual demodulation is performed by the limiter discriminator circuit. The noisy baseband signal is further filtered by postdetection filter which can be implemented as an integrate sample and dump circuit or a low-pass filter. At the end of each bit interval the output of the filter is sampled to determine the transmitted bit.

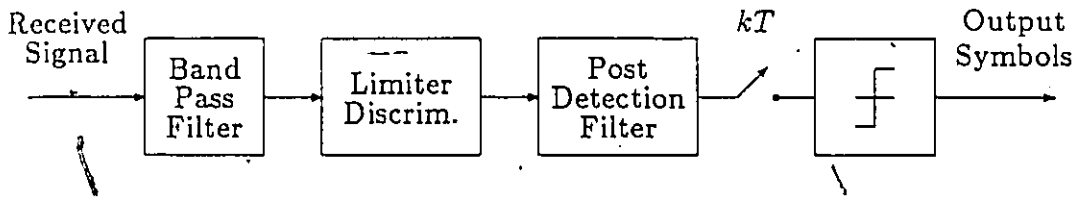

Figure 1.1: Block diagram of a limiter discriminator detector.

1.2.2.2 Differential Detection

Another alternative to coherent detection is differential detection[3] where information is encoded into relative phase differences between successive symbols (rather than absolute phases). Provided that the unknown phase θ contained in the received signal varies slowly (that is, slow enough for it to be considered essentially constant over two bit intervals), then the phase difference between waveforms received in two successive bit intervals will be independent of θ. At the receiver the signal can be demodulated by comparing the phases of the consecutive symbols (see Figure 1.2). Thus

[3]Differential detection is also often refered to as differentially coherent detection or phase comparison detection. Differential detection should not be confused with differentially encoded coherent detection. The latter method is a coherent demodulation technique where carrier recovery is mandatory, and the purpose of the differential encoding is only to avoid a phase ambiguity in the recovered carrier.

a carrier recovery circuit is avoided and faster signal acquisition may be achieved.

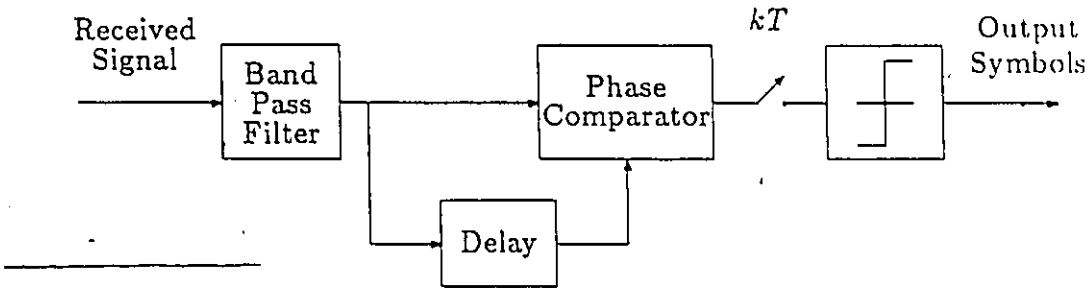

Figure 1.2: Block diagram of a differential (phase comparison) detector.

1.3 DIFFERENTIAL DETECTION VERSUS LIMITER DISCRIMINATOR DETECTION

Let us return to the system engineer's task of selecting the modulation-demodulation technique. Assuming that coherent detection is precluded (e.g., due to a fast signal acquisition requirement or the properties of the transmission medium); then the selection is between differential detection and limiter discriminator detection.

Differential detection can be applied to both phase-shift keyed (PSK) and digital frequency modulated (FM) signals; whereas limiter discriminator detection is mainly suitable to digital FM signals[4]. Various investigations indicate that neither scheme exhibits unequivocal superiority over the other one [1,21]. For example, differential detection is less sensitive

[4]Limiter discriminator detection can be applied to binary PSK signals, but the BER performance is inferior to that of differential detection [20].

to co-channel interference [1,22], and delay distortion [23]; whereas limiter discriminator detection is less sensitive to random FM and frequency offsets [3,24]. The performances of both schemes under multipath fading conditions are comparable [1,2,4,25]. For both schemes error performance improvement techniques have been proposed [26–33] and more powerful receiver processing techniques are emerging. Thus, the final selection of the type of noncoherent detection to be used can be made only when the system requirements of a specific application are defined.

Research on improving the performance of both noncoherent detection techniques is continuing [34–37]. This thesis is devoted to developing new signal formats and receiver processing techniques suitable to differential detection. Yet, some of the concepts introduced here are also (directly or with some modifications) applicable to limiter discriminator detection [38].

1.4 APPLICATION AREAS OF DIFFERENTIAL DETECTION

Differential detection is used or being considered for various applications such as satellite communications, cellular mobile radio, voiceband data transmission, lightwave communications, and spread spectrum communications.

In satellite communications, major application areas are:

- regenerative satellite systems [39–45], and
- mobile satellite communications [46-55].

In regenerative satellite systems, differential detection provides a simpler and more reliable on-board regenerative unit where size and weight reductions are desirable. In mobile communications (satellite or cellular radio [56]) the major advantages of differential detection are an increased tolerance to phase noise and fading, an improved acquisition time, and a reduced the receiver complexity.

In voice band data transmission, differential detection is used in 1200

b/s and 2400 b/s modems [57–59]. In this case the major reason for using differential detection is to eliminate the need for carrier recovery circuits.

In lightwave communications, due to technological difficulties, coherent detection is not currently applicable [60][5]. Hence differential detection and other noncoherent detection techniques are the only available options.

In frequency hopped spread spectrum systems, differential detection is employed because of its fast acquisition properties [62–64].

All of the above applications are for signals with bandwidth efficiencies in the range of 0.5 to 2 b/s/Hz[6].

1.5 RESEARCH CONTRIBUTIONS OF THIS THESIS

Although the system engineer is already faced with the problem of selecting the most suitable modem technique from a large set, the researchers are aware of various shortcomings of the existing modems. Therefore, a significant amount of research is being devoted to improving the power or bandwidth efficiency (or both) of digital modulation-demodulation techniques.

I have chosen to study the subject of differential detection of digitally modulated signals in this context. The research tasks performed and the results obtained in this thesis can be summarized as follows.

1. A new signal format was developed, which can be demodulated by a conventional differential detector, and provides power/bandwidth efficiency advantages under certain operating conditions (in comparison to some well known techniques such as quaternary PSK (QPSK) and minimum shift keying (MSK). The modem technique developed as the result of this work is named differentially detected controlled transition phase shift keying (DCTPSK).

[5] With the recent technological advances, coherent detection may soon be applicable to lightwave communications [61].

[6] Where, for instance, bandwidth is defined in terms of 99% power occupancy.

2. New receiver structures for differentially detected PSK type signals were developed. The motivation here was to improve the BER performance of the DCTPSK modem. The receiver structures proposed for DCTPSK improve the bit error rate performance up to 1.7 dB over conventional structures. Furthermore, the same receivers can also be utilized in the differential detection of QPSK signals and result in similar gains.

3. New receiver structures for the differential detection of Gaussian minimum shift keying (GMSK) were developed. The starting point in this case was the observation that GMSK has very attractive spectral properties, but when it is differentially detected, an E_b/N_0 penalty of 7 dB is incurred in comparison to the coherent detection of GMSK [65]. This implies that the conventional differential detectors are not suitable to the GMSK signal. The ensuing work resulted in new receiver structures which improve the BER performance of differentially detected GMSK signals by about 4 dB.

1.6 THESIS ORGANIZATION

Including this introductory chapter, this thesis consists of five chapters and two appendices, and is organized as follows.

Chapter 2 presents relevant background material on the differential detection of digitally modulated signals. The purpose of this chapter is to review the principle of differential detection and to introduce the basic concepts upon which the research material of Chapter 3 and Chapter 4 is built. In Section 2.1 the properties of the differentially detected phase shift keyed signals are discussed. This section serves as a preamble to Chapter 3 where a new PSK-type modem is introduced. In Section 2.2 the differential detection of continuous phase modulated (CPM) signals is discussed. The core of this section deals with Gaussian minimum shift keying. For comparison with differentially detected GMSK, a brief discussion on other bandwidth efficient CPM signals (such as Tamed Frequency Modulation) is also included. The last section of this chapter summarizes the bandwidth and detection efficiencies of various differentially detected signals.

Chapter 3 introduces the aforementioned new quadrature modulation technique designed for Frequency Division Multiple Access (FDMA) operations when the transmitters utilize nonlinear amplifiers. This technique is called differentially detected controlled transition phase shift keying. The bit error rate performance of DCTPSK is first evaluated using a conventional differential detector. Then in Section 3.6 two new receiver structures are introduced. The new receivers require twice the number of differential detectors and additional baseband processsing to improve the bit error rate performance of DCTPSK. The implementation of the DCTPSK modem and the results of the performance evaluation measurements are presented in Section 3.7. The modem circuit diagrams and the operating instructions are given in Appendix A.

Chapter 4 deals with improving the BER performance of differentially detected GMSK. For this purpose we first analyze how intersymbol interference degrades its performance when conventional differential detectors are employed. An approach to reduce the effects of intersymbol interference is therefore determined. This leads to receiver structures which employ decision feedback. Then the performance of the proposed receivers is evaluated.

Finally, in Chapter 5, the conclusions reached from the work performed for this thesis are summarized, and various suggestions for future research on differential detection are given.

The listings of the computer programs which were used to evaluate the bit error rate performances of the systems employing differential detection are presented in Appendix B.

Chapter 2

DIFFERENTIAL DETECTION (BACKGROUND MATERIAL)

The aim of this chapter is to review the basic principles of differential detection and discuss the performances of various existing modem techniques which use differential detection. Thus, this section will serve as the background for the original research material to be presented in Chapter 3 and Chapter 4.

In Section 2.1, the application of differential detection to PSK systems is reviewed. First, we discuss the most frequently used schemes: differentially detected binary PSK (DBPSK) and differentially detected quaternary PSK (DQPSK). Then, we demonstrate why conventional differential detection is not used for offset-QPSK type signals.

Section 2.2 deals with the differential detection of continuous phase modulated signals. First, the general mathematical description of CPM signals is given. Then, the differential detection of minimum shift keying is discussed. The relevance of the differentially detected MSK (DMSK) to our work is that DMSK is a candidate for similar applications that DCTPSK is intended for (e.g. mobile-satellites). A more bandwidth efficient version

of MSK is Gaussian MSK. Since Chapter 4 is devoted to developing new receivers for GMSK, at this point only the conventional two-bit differential detection of GMSK is briefly dicsussed. For comparison with GMSK, a brief description of two popular CPM techniques, namely, Duobinary MSK and Tamed Frequency Modulation is given.

In Section 2.3 the bandwidth and detection efficiency of the modems discussed in Section 2.1 and 2.2 are compared and various tradeoffs are discussed.

2.1 DIFFERENTIAL DETECTION OF PHASE SHIFT KEYED SIGNALS

Differential detection was first applied to binary PSK (BPSK) signals [66], where information is transmitted in the phase of the modulated carrier. Later, differential detection of m-ary[1] signals was also introduced [67–70]. In this section differentially detected binary PSK, differentially detected quaternary PSK and differentially detected Offset-QPSK (DOQPSK) are discussed.

2.1.1 Differentially Detected Binary PSK

DBPSK is suited to applications where the bandwidth efficiency is not required to exceed 0.8 b/s/Hz and the system does not include nonlinear amplifiers. In early applications, differential detection was considered mainly as an alternative to coherent detection to provide a simpler implementation. Later, it was also shown that differential detection is less sensitive to phase noise and fading than coherent detection [24,71,72].

[1] Where $m = 4, 8, 16$.

2.1.1.1 Transmitter

The block diagram of a DBPSK transmitter is given in Figure 2.1. The input data can be represented by

$$s(t) = \sum_{k=-\infty}^{\infty} a_k p(t - kT_b) \tag{2.1}$$

where T_b is the bit duration[2], $a_k \pm 1$ and

$$p(t) = \begin{cases} 1, & \text{for} \quad -T_b/2 \leq t \leq T_b/2 \\ 0 & \text{elsewhere.} \end{cases} \tag{2.2}$$

The differential encoder maps the input sequence $\{a_k = \pm 1\}$ into another binary sequence $\{b_k = \pm 1\}$ by using the operation

$$b_k = a_k b_{k-1}. \tag{2.3}$$

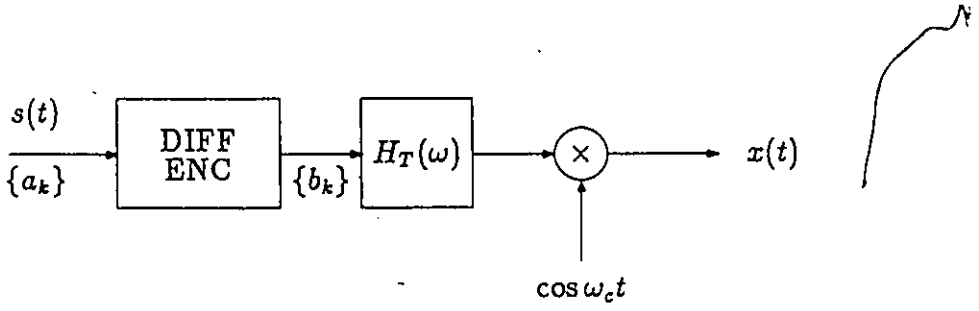

Figure 2.1: Block diagram of a DBPSK transmitter.

The transmitted signal can be represented by

$$x(t) = \sum_{k=-\infty}^{\infty} b_k p(t - kT_b) \cos \omega_c t \tag{2.4}$$

[2]For BPSK, the bit duration T_b is equal to the symbol duration T_s.

where ω_c is the angular frequency of the carrier. As a result of the differential encoding process, the transmitted signal $x(t)$ changes its phase by π radians when $a_k = -1$ and keeps the same phase when $a_k = 1$.

Another way of expressing the transmitted signal is

$$x(t) = \cos(\omega_c t + \theta_k) \quad \text{for} \quad (k-1)T_b \leq t \leq kT_b \tag{2.5}$$

where

$$\theta_k = \frac{b_k \pi}{2}. \tag{2.6}$$

In a bandlimited system, the transmitted signal can be represented as

$$x(t) = \left(\sum_{k=-\infty}^{\infty} b_k p(t - kT_b) * h_T(t) \right) \cos \omega_c t \tag{2.7}$$

where $h_T(t)$ is the impulse response of the transmit filter $H_T(\omega)$, and $*$ denotes the convolution operation.

2.1.1.2 Receiver

There are two receiver configurations for the differential detection of a PSK signal. The first configuration is the classical integrate sample and dump (ISD) receiver shown in Figure 2.2. The received signal is first demodulated by multiplying with two noncoherent carriers in quadrature: $\cos(\omega_c t + \varphi)$ and $\sin(\omega_c t + \varphi)$; where φ is an unknown phase constant. The resultant in-phase and quadrature waveforms are integrated and sampled synchronously at $t = kT_b$. The phase θ_k is computed from the samples. The phase difference is obtained by subtracting θ_{k-1} from θ_k. Then the phase difference is mapped into the output bit. The structure shown in Figure 2.2 is applicable to m-ary PSK signals as well. As m changes, the decision rule has to be changed [73], and T_b is replaced by T_s.

The mathematical analysis of the ISD receiver is given in various references, including [73–78]. This receiver yields the optimum sample by sample detection when the signal is not bandlimited [78]. Note that the configuration of Figure 2.2 requires the recovery of the carrier frequency (but not the phase).

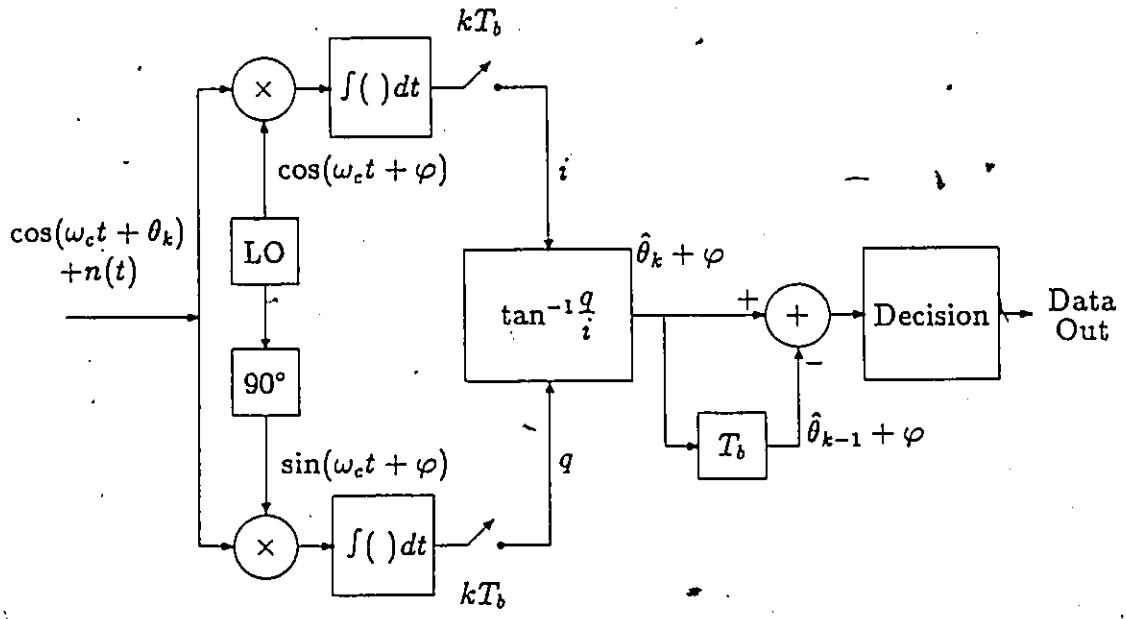

Figure 2.2: Block diagram of an integrate sample and dump type receiver for DBPSK. LO is the local oscillator.(Reproduced from [73]).

The second differential detector configuration is suitable to bandlimited signals and is more representative of real systems; because in satellite communications and mobile radio the allocated bandwidth is generally only slightly larger than the symbol rate. The required bandlimiting is performed by either premodulation lowpass filtering or post modulation bandpass filtering. The block diagram of the receiver for the bandlimited DBPSK signals is shown in Figure 2.3. The received signal is passed

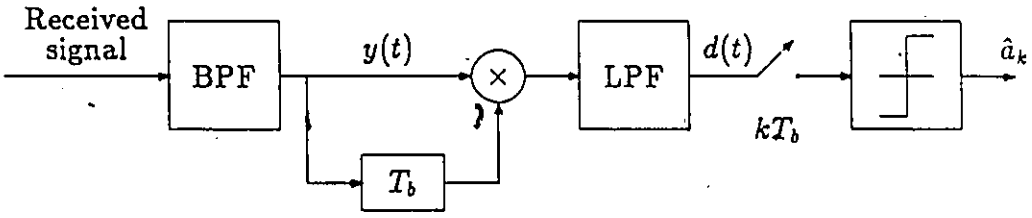

Figure 2.3: Block diagram of DBPSK receiver for bandlimited signals.

through a predetection bandpass filter (BPF) to limit the noise entering the differential detector. The signal at the output of the BPF can be represented as

$$y(t) = [\sum_{k=-\infty}^{\infty} b_k p(t - kT_b)\cos(\omega_c t + \psi)] * h_s(t) + n(t) \qquad (2.8)$$

where $h_s(t)$ is the equivalent IF filter response which characterizes the overall filtering (i.e., transmit filtering plus predetection bandpass filtering), ψ is an arbitrary phase angle, and $n(t)$ is the narrow-band Gaussian noise which can be represented as

$$n(t) = n_c(t)\cos\omega_c t + n_s(t)\sin\omega_c t. \qquad (2.9)$$

Assuming that $h_s(t)$ has a Fourier transform which is symmetrical around ω_c, it can be related to its lowpass equivalent $h(t)$ by

$$h_s(t) = 2h(t)\cos\omega_c t. \qquad (2.10)$$

By using (2.9), (2.10) and noting that $h(t)$ has a bandwidth much smaller than ω_c, we can rewrite (2.8) as

$$y(t) = \sum_{k=-\infty}^{\infty} b_k g_k(t) \cos(\omega_c t + \psi) + n_c(t) \cos \omega_c t + n_s(t) \sin \omega_c t \qquad (2.11)$$

where

$$g_k(t) = \int_{-\infty}^{\infty} p(\tau - kT_b) h(t - \tau) d\tau. \qquad (2.12)$$

The differential detection is performed by multiplying $y(t)$ with a T_b second delayed version of itself and then low-pass filtering the product (see Figure 2.3). At the input of the LPF we have

$$d'(t) = y(t) y(t - T_b). \qquad (2.13)$$

The lowpass filter has a flat frequency response up to $2/T_b$ [57], and removes the second harmonic terms of $d'(t)$. Assuming that $\omega_c T_b = 2n\pi$, the signal at the output of the LPF is given by

$$d(t) = \frac{1}{2}\Big(\sum_{k=-\infty}^{\infty} b_k g_k(t)\Big)\Big(\sum_{j=-\infty}^{\infty} b_j g_j(t - T_b)\Big) + w(t) \qquad (2.14)$$

where $w(t)$ lumps all the signal times noise and noise times noise terms together (i.e., the noise is signal dependent). At the sampling instant $t = nT_b$, let

$$\begin{aligned} d_n &= d(nT_b), \\ g_{k,n} &= g_k(nT_b), \\ w_n &= w(nT_b). \end{aligned} \qquad (2.15)$$

Then (2.14) can be rewritten as

$$d_n = \frac{1}{2}\Big(\sum_k b_k g_{k,n}\Big)\Big(\sum_j b_j g_{j,n-1}\Big) + w_n \qquad (2.16)$$

or

$$d_n = \frac{1}{2} b_n b_{n-1} g_{n,n}^2 + \frac{1}{2} \sum_{k \neq n} \sum_{j \neq n-1} b_k b_j g_{k,n} g_{j,n-1} + w_n. \qquad (2.17)$$

In (2.17), the first term is the signal, the second term represents intersymbol interference (ISI), and the last term is the noise.

Observe from (2.12) that if $h(t)$ satisfies the first Nyquist criterion [79], then

$$g_{k,j} = \begin{cases} 1 & \text{for } j = k \\ 0 & \text{for } j \neq k. \end{cases} \tag{2.18}$$

Thus the decision variable d_n is given by

$$d_n = \frac{1}{2} b_n b_{n-1} + w_n. \tag{2.19}$$

Substituting $a_n = b_n b_{n-1}$ (see Eqn. (2.3)), we obtain

$$d_n = \frac{1}{2} a_n + w_n. \tag{2.20}$$

Hence the polarity of d_n produces an estimate of the transmitted bit a_n. Following the mathematical description given above, the associated waveforms at various points of the DBPSK modem are shown in Figure 2.4.

The eye-diagram of the differentially detected BPSK signal at the input of the threshold comparator is displayed in Figure 2.5. The combined transmit and receive filter assumed by this figure has a raised-cosine characteristic with a roll-off factor $\alpha = 0.5$; hence at the sampling instants the signal does not suffer from ISI.

2.1.1.3 BER Performance in an AWGN Channel

Approaches to the probability of error analysis of DBPSK systems may be classified into two categories : the "indirect analogy" method [67–69,76,77]. and the "characteristic function" method [80,81]. The indirect analogy method means that the computation of the error probability is based on the knowledge of other communication systems such as binary orthogonal systems. This technique does not require the probability density function (pdf) of the decision variable because the probability of bit error (P_b) expression can always be brought to a form that is equivalent to that of a binary orthogonal system.

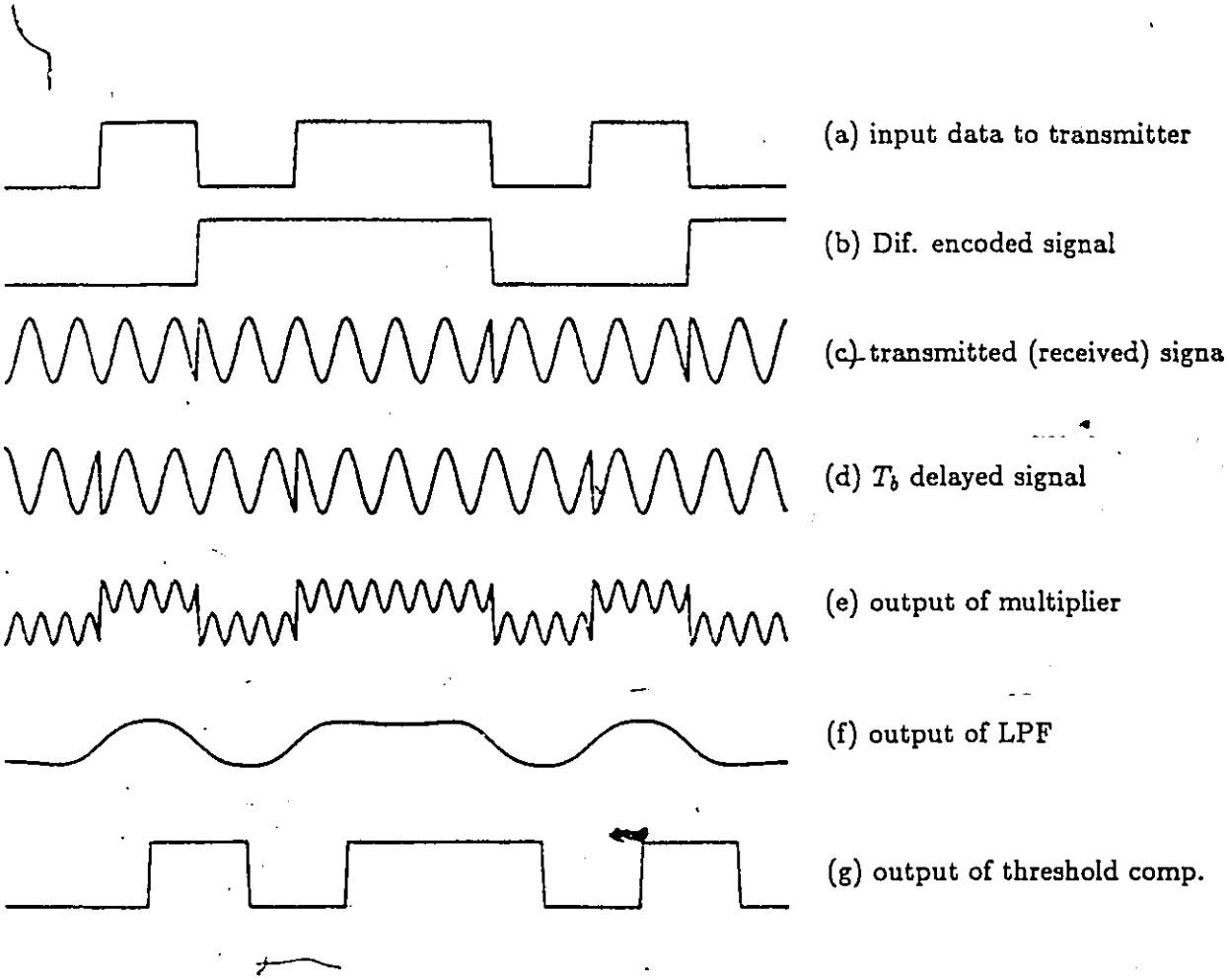

Figure 2.4: Waveforms at various points of a DBPSK modem.

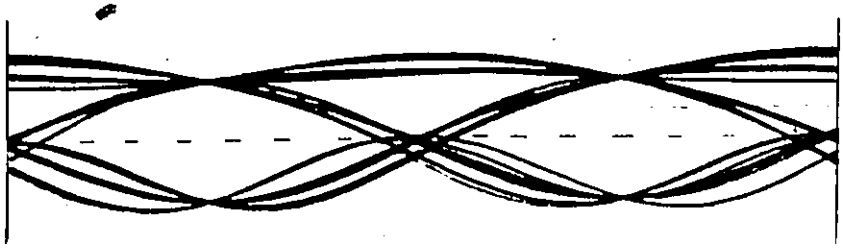

Figure 2.5: Eye-diagram of a DBPSK signal at the input of the threshold detector. The channel filters have an overall raised cosine characteristic with $\alpha = 0.5$.

The characteristic function method utilizes the pdf of the decision variable (i.e., phase) and computes the error rate taking into account both the noise correlation and ISI [80].

By using either method, when input bits are equiprobable and additive Gaussian noise is the only source of degradation, the probability of error expression for DBPSK is given by

$$P_b = \exp(-E_b/N_o)/2 \tag{2.21}$$

where E_b is the energy per bit and N_0 is the one-sided noise spectral density.

Conversely, the probability of error expression for coherently detected BPSK is [82]:

$$P_b = \frac{1}{2}\mathrm{erfc}\sqrt{\frac{E_b}{N_o}}. \tag{2.22}$$

A comparison of (2.21) and (2.22) indicates that for a BER of 10^{-4}, DBPSK requires only one dB more E_b/N_0 than coherent BPSK[3].

[3]BER performance curves corresponding to (2.21) and (2.22) are plotted in Figure 2.10 of Section 2.1.2.4.

2.1.1.4 Improving the BER Performance

When the signal is differentially encoded so that

$$\cos(\theta_k - \theta_{k-1}) = \cos(\frac{\pi b_k}{2} - \frac{\pi b_{k-1}}{2}) = b_k b_{k-1} = a_k, \tag{2.23}$$

then, not only the phases two sampling instants apart, but the entire signal phase, is correlated. To see this, observe that

$$\begin{aligned} \cos(\theta_k - \theta_{k-2}) &= a_k a_{k-1} && (2.24)\\ \cos(\theta_k - \theta_{k-3}) &= a_k a_{k-1} a_{k-2} && (2.25)\\ &\vdots \qquad\qquad \vdots \\ \cos(\theta_k - \theta_{k-n}) &= a_k a_{k-1} \cdots a_{k-n+1}. && (2.26) \end{aligned}$$

The conventional differential detector is based on the relationship given by (2.23), i.e., the phase comparison is between two consecutive samples. If the conventional one-bit delay detector is refered to as a first order detector, then the phase comparisons described by (2.24) – (2.26) require second, third,..., n^{th} order detectors.

Various receiver structures have been developed which make better use of the correlation in the signal phase and improve the BER performance by employing more than one detectors [26–28,30]. For DBPSK the improvement achieved by using both a first and second order detector is about 0.3 dB. However, for other modulation schemes, by utilizing more than one detectors, bit error rate improvements may correspond to, say, 1.5 dB reduction in the required E_b/N_0. Two such higher-order receiver structures developed to improve the BER performance of the DCTPSK modem are presented in Section 3.6.

2.1.1.5 Spectrum

A BPSK modulator performs the frequency translation of a baseband signal to a carrier frequency ω_c (see (2.4)). Hence the shape of the spectrum is completely determined by the baseband signal[4]. For the infinite band (IB)

[4]This assumes that there is no post modulation filtering or nonlinear amplification.

signal defined by (2.1) and (2.2), the power spectrum is given by [82]:

$$S_{IB}(\omega) = T_b[\frac{\sin((\omega-\omega_c)T_b/2}{(\omega-\omega_c)T_b/2}]^2. \tag{2.27}$$

To utilize the available bandwidth more efficiently, the transmitted BPSK signal is generally filtered. The spectrum of the filtered signal $S_F(\omega)$ is given by:

$$S_F(\omega) = S_{IB}(\omega)|H_T(\omega)|^2 \tag{2.28}$$

where $H_T(\omega)$ is the Fourier transform of the transmit BPF (or the bandpass equivalent of the transmit LPF). Note that the spectrum of the modulated signal does not depend upon the way the signal is detected, i.e., coherent or differentially detected BPSK signals have the same spectrum.

The theoretical bandwidth efficiency of BPSK modulation is 1 b/s/Hz [82]. Using practical filters[5] a bandwidth efficiency of 0.8 b/s/Hz can be achieved. However, when the system includes nonlinear amplifiers, the filtered sidelobes of the BPSK signal are restored. In such cases, to minimize the adjacent channel interference (ACI), BPSK systems are operated with much lower bandwidth efficiencies.

2.1.2 Differentially Detected Quaternary PSK

DBPSK, as presented in Section 2.1.1, is the simplest differential detection system, and achieves a good bit error rate performance of only about 1 dB away from coherent BPSK. However, the bandwidth efficiency of BPSK is low. By using two quadrature channels, the bandwidth efficiency of binary PSK can be doubled. This quadrature modulation technique is refered to as Quaternary-Phase Shift Keying[6]. Differentially detected QPSK is extensively used in voice-band modems [59,83], and HF communications [84]; and is being considered for regenerative satellite systems [39–45] and also for aeronautical satellite communications [46,47].

[5]For instance, a raised cosine filter with a roll-off factor $\alpha = 0.25$.

[6]Or quadri-phase shift keying.

2.1.2.1 Transmitter

The block diagram of a DQPSK transmitter is shown in Figure 2.6. The input binary sequence $\{c_k = \pm 1\}$ has a rate of T_b^{-1}. First, $\{c_k\}$ is serial to

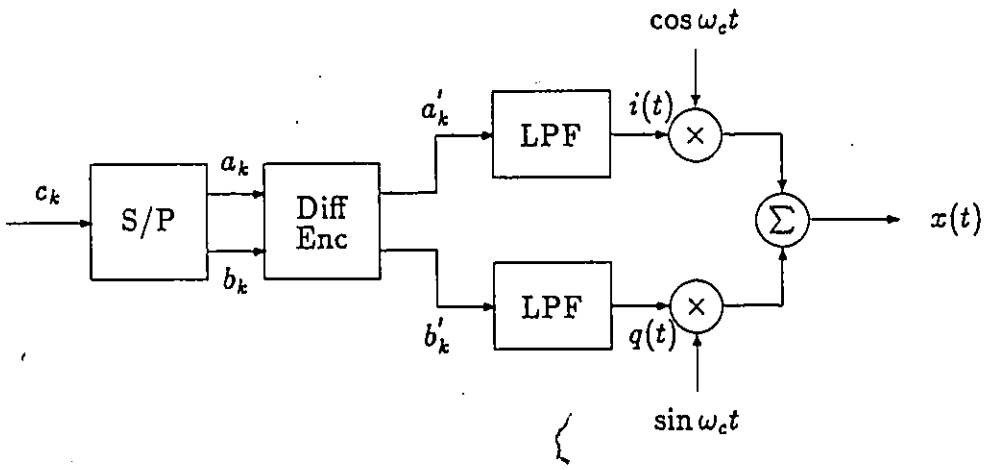

Figure 2.6: Block diagram of a DQPSK transmitter.

parallel converted (S/P) into two binary sequences $\{a_k\}$ and $\{b_k\}$ such that

$$\{a_k\} = \{c_{2k}\} \quad \text{for all } k \tag{2.29}$$

$$\{b_k\} = \{c_{2k+1}\} \quad \text{for all } k. \tag{2.30}$$

Then, $\{a_k\}$ and $\{b_k\}$ are differentially encoded to produce the sequences $\{a'_k\}$ and $\{b'_k\}$.

The input signals to the quadrature modulators, refered to as the I and Q-channel signals respectively, can be represented by

$$i(t) = \sum_{k=-\infty}^{\infty} a'_k p(t - kT_s) \tag{2.31}$$

$$q(t) = \sum_{k=-\infty}^{\infty} b'_k p(t - kT_s). \tag{2.32}$$

In an infinite bandwidth system,

$$p(t) = \begin{cases} 1 & \text{for } -T_s/2 \leq t \leq T_s/2; \\ 0 & \text{elsewhere.} \end{cases} \tag{2.33}$$

In the case where the transmitted signal is bandlimited, $p(t)$ in (2.31) and (2.32) is replaced by the impulse response of the lowpass filter. Note that the input to the transmitter has a rate of T_b^{-1}, whereas each quadrature channel has a rate of T_s^{-1} (where $T_s = 2T_b$).

The baseband signals $i(t)$ and $q(t)$ modulate the quadrature carriers $\cos\omega_c t$ and $\sin\omega_c t$ respectively. The transmitted signal can thus be represented by

$$x(t) = i(t)\cos\omega_c t + q(t)\sin\omega_c t. \tag{2.34}$$

The transmitted signal of (2.34) can also be represented in terms of its envelope and phase as

$$x(t) = s(t)\cos(\omega_c t + \theta(t)) \tag{2.35}$$

where

$$s(t) = \sqrt{i^2(t) + q^2(t)} \tag{2.36}$$

and

$$\theta(t) = \tan^{-1}\frac{q(t)}{i(t)}. \tag{2.37}$$

Observe from (2.31), (2.32) and (2.36) that when the signal is filtered, $i(t)$ and $q(t)$ may assume zero amplitude simultaneously. This means that the signal envelope $s(t)$ experiences 100% fluctuations.

A signal-state diagram (SSD) conveniently displays the amplitude and phase variations of a signal. To draw the SSD of the signal described by (2.34), assume that the x and y-axes represent the carriers $\cos\omega_c t$ and $\sin\omega_c t$ respectively. Then drawing $i(t)$ versus $q(t)$ produces the signal-state diagram.

The SSD of the unfiltered QPSK signal is shown in Figure 2.7. The instantaneous carrier phase changes resulting from the modulation of the carrier by the data are 0, $\pm\pi/2$ and π radians.

The SSD of QPSK signal when the signal is filtered and the Nyquist 1 criterion is satisfied is as shown in Figure 2.8. Again every T_s second the signal is at one of the corner states. However, this time the phase changes of 0, $\pm\pi/2$ and π radians are not instantaneous.

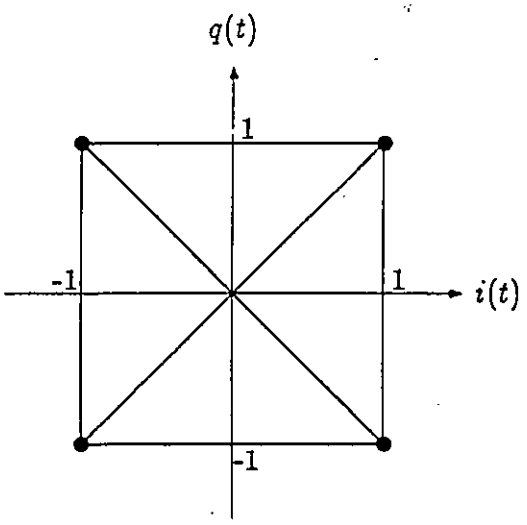

Figure 2.7: Signal-state diagram of an unfiltered QPSK signal.

2.1.2.2 Receiver

The differential detection of a QPSK signal is similar to that of a BPSK signal; however, for QPSK two differential detectors are needed. The receiver block diagram is shown in Figure 2.9. The signal at the output of the BPF can be represented as

$$y(t) = s'(t)\cos(\omega_c t + \theta'(t)) + n_c(t)\cos\omega_c t + n_s(t)\sin\omega_c t. \qquad (2.38)$$

If the transmit and predetection filters satisfy the first Nyquist criterion, then $s'(kT_s)$ is a constant and $\theta'(kT_s) = \theta(kT_s) = n\pi/2$.

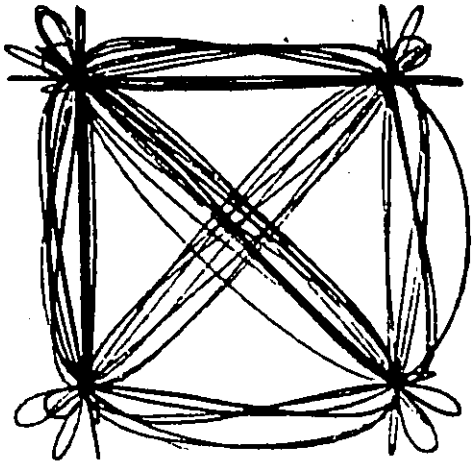

Figure 2.8: Signal-state diagram of a filtered QPSK signal. The filter has a raised-cosine characteristic with $\alpha = 0.5$ (including a $x/\sin x$ equalizer).

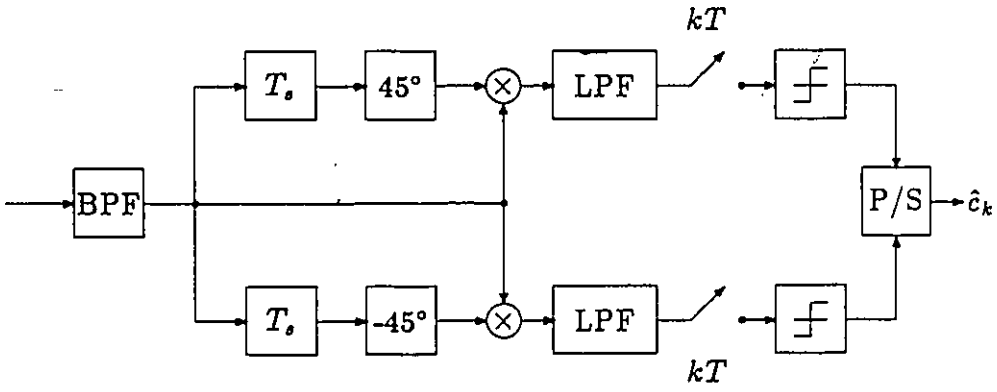

Figure 2.9: Block diagram of DQPSK receiver for bandlimited signals.

The differential encoding at the transmitter ensures that

$$\Delta\theta_k = \theta(kT_s) - \theta((k-1)T_s) = \theta_k - \theta_{k-1} = m_k\frac{\pi}{2} \tag{2.39}$$

where

$$\begin{array}{llllll} m_k = 0 & \text{for} & a_k = & 1 & \text{and} & b_k = 1 \\ m_k = 1 & \text{for} & a_k = & 1 & \text{and} & b_k = -1 \\ m_k = 2 & \text{for} & a_k = & -1 & \text{and} & b_k = -1 \\ m_k = 3 & \text{for} & a_k = & -1 & \text{and} & b_k = 1. \end{array} \tag{2.40}$$

In the I-channel detector, the received signal is multiplied by a T_s second delayed and 45° shifted version of itself, i.e.,

$$d_I'(t) = y(t)y(t-T_s)_{45°} \ . \tag{2.41}$$

The lowpass filter which follows the multiplier has a flat characteristic up to $2/T_s$, and the signal at the output of the LPF can be represented as

$$d_I(t) = s(t)s(t-T_s)\cos(\theta(t) - \theta(t-T_s) + \pi/4) + w_I(t) \tag{2.42}$$

where $w_I(t)$ represents the combined noise terms.

At the sampling instant $t = kT_s$, the input to the I-channel threshold comparator can be written as

$$d_{k,I} = s_k s_{k-1}\cos(\theta_k - \theta_{k-1} + \pi/4) + w_{k,I}. \tag{2.43}$$

Note that s_k and s_{k-1} are positive quantities, and in the absence of noise by using the relations given in (2.39) and (2.40) we find

$$\text{sgn}[d_{k,I}] = a_k, \tag{2.44}$$

where

$$\text{sgn}[x] = \begin{cases} 1 & \text{for} \quad x \geq 0; \\ -1 & \text{for} \quad x < 0. \end{cases} \tag{2.45}$$

In the Q-channel detector, the received signal is multiplied by a T_s second delayed and $-45°$ shifted version of itself. At the sampling instant $t = kT_s$, the output of the Q-channel detector is:

$$d_{k,Q} = s_k s_{k-1}\sin(\theta_k - \theta_{k-1} + \pi/4) + w_{k,Q}. \tag{2.46}$$

Again in the absence of ISI and noise,

$$\text{sgn}[d_{k,Q}] = b_k. \tag{2.47}$$

The output data sequence $\hat{c}_k$ is obtained by parallel to serial conversion (P/S) of the I and Q-channel detector outputs.

2.1.2.3 BER Performance in an AWGN Channel

The calculation of the probability of bit error for DQPSK is similar but significantly more complex than that for DBPSK. The probability of error is evaluated via the probability density function of the phase [74,85,86]. Assuming that there is no ISI, the probability of bit error is given by [74]:

$$P_b = Q(a,b) - \frac{1}{2} I_o(ab) \exp[-\frac{1}{2}(a^2 + b^2)] \tag{2.48}$$

where $Q(a,b)$, $I_\alpha(x)$, a and b are defined as:

$$Q(a,b) = \exp[-\frac{1}{2}(a^2 + b^2)] \sum_0^\infty (\frac{a}{b})^k I_k(ab), \tag{2.49}$$

$$I_\alpha(x) = \sum_{k=0}^{\infty} \frac{(x/2)^{\alpha+2k}}{k!\,(\alpha+k)!)} \quad \text{for} \quad x \geq 0, \tag{2.50}$$

$$a = \sqrt{\frac{E_b}{2N_o}}(\sqrt{2+\sqrt{2}} - \sqrt{2-\sqrt{2}}), \tag{2.51}$$

$$b = \sqrt{\frac{E_b}{2N_o}}(\sqrt{2+\sqrt{2}} + \sqrt{2-\sqrt{2}}). \tag{2.52}$$

The probability of bit error performances of DBPSK, DQPSK and coherent BPSK[7] obtained by evaluating equations (2.21), (2.22), and (2.48) are plotted in Figure 2.10. Observe that at high E_b/N_0 values, DQPSK is approximately 2.3 to 2.5 dB poorer in performance than coherent PSK. Hence coherent BPSK can be easily replaced by DBPSK. However, the tradeoff between coherent QPSK and DQPSK is a more complex one.

For m-ary PSK systems (where $m > 4$), the difference between coherent and differential PSK asymptotically becomes 3 dB [79,p.253].Note that the BER performance of DQPSK is rather close to this asymptotic value.

[7]BER performances of coherent BPSK and coherent QPSK are identical.

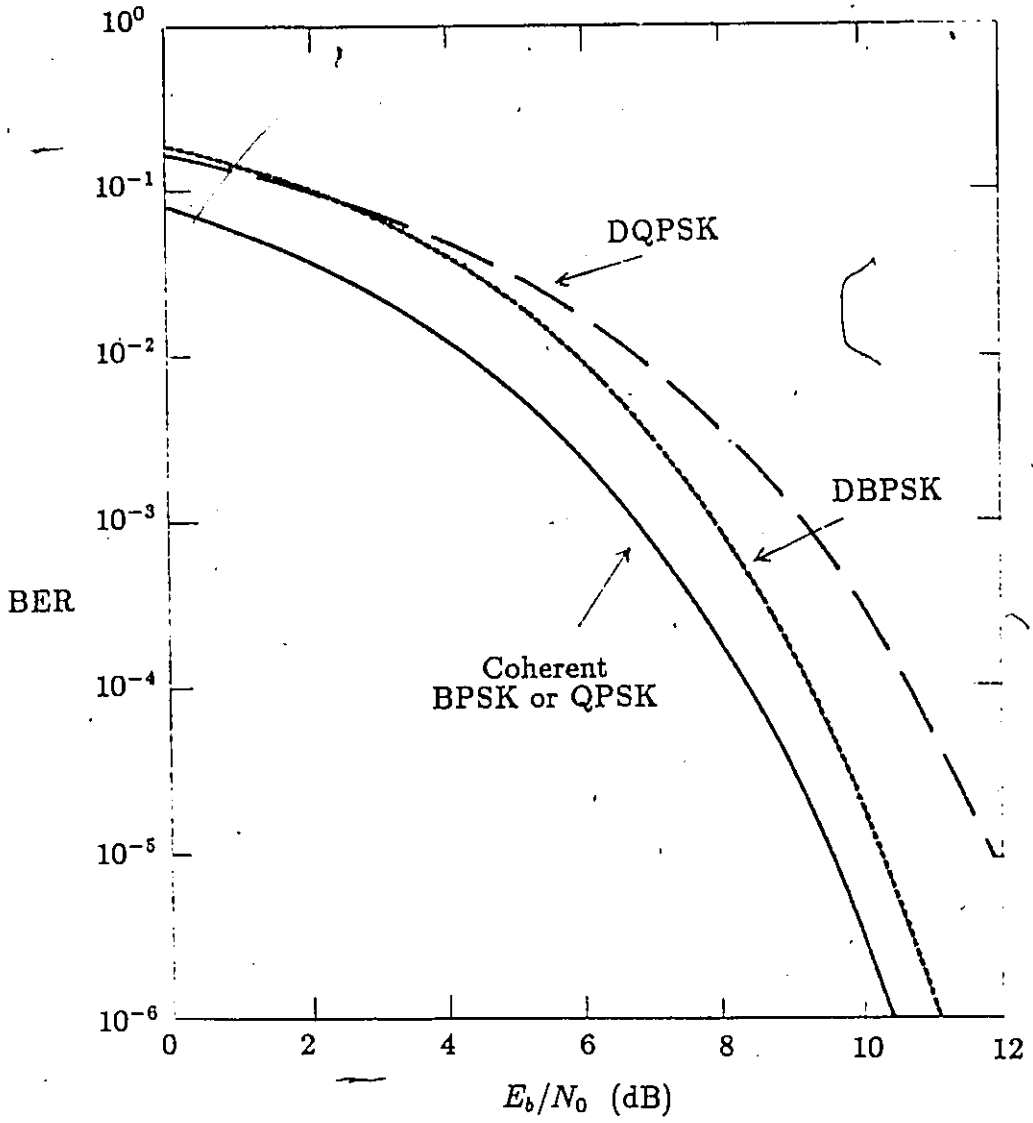

Figure 2.10: BER curves for DBPSK, DQPSK and coherent BPSK (or QPSK).

2.1.2.4 Spectrum

The power spectrum of the DQPSK signal is similar to the spectrum of the DBPSK signal. For the infinite bandwidth DQPSK signal, by replacing $T_b = T_s/2$ in (2.27), we obtain

$$S_{IB}(\omega) = T_s \left[\frac{\sin((\omega - \omega_c)T_s/4}{(\omega - \omega_c)T_s/4} \right]^2. \tag{2.53}$$

Note that for an input data rate of, say, 100 kb/s, the first spectral null of the DBPSK signal is 100 kHz away from the center frequency; whereas the first spectral null of the DQPSK signal is at 50 kHz.

The theoretical bandwidth efficiency of QPSK signal is 2 b/s/Hz [82]. Using practical filters, a bandwidth efficiency in the range of 1.6 b/s/Hz can be achieved.

When the system includes nonlinear amplifiers, the filtered sidelobes of the QPSK signal are restored. This is demonstrated in Figure 2.11; where (i) unfiltered, (ii) filtered, and (iii) filtered and then hardlimited spectra of QPSK are plotted. The filter used is a square-root raised cosine with $\alpha = 0.5$ and includes a $x/\sin x$ equalizer[8]. A hardlimiter represents a pessimistic model of the amplitude response of a nonlinear amplifier. A typical class-C power amplifier may have the characteristics shown in Figure 2.12 (reproduced from [87]).

The spectral regrowth of a nonlinearly amplified DQPSK is a major disadvantage for using it in an adjacent channel interference environment. For this reason, in Chapter 3 we shall introduce a new modem which reduces the spectral regrowth while retaining the basic structure of a DQPSK modem.

[8] In short-hand notation: $(x/\sin x + \sqrt{\alpha = 0.5})$.

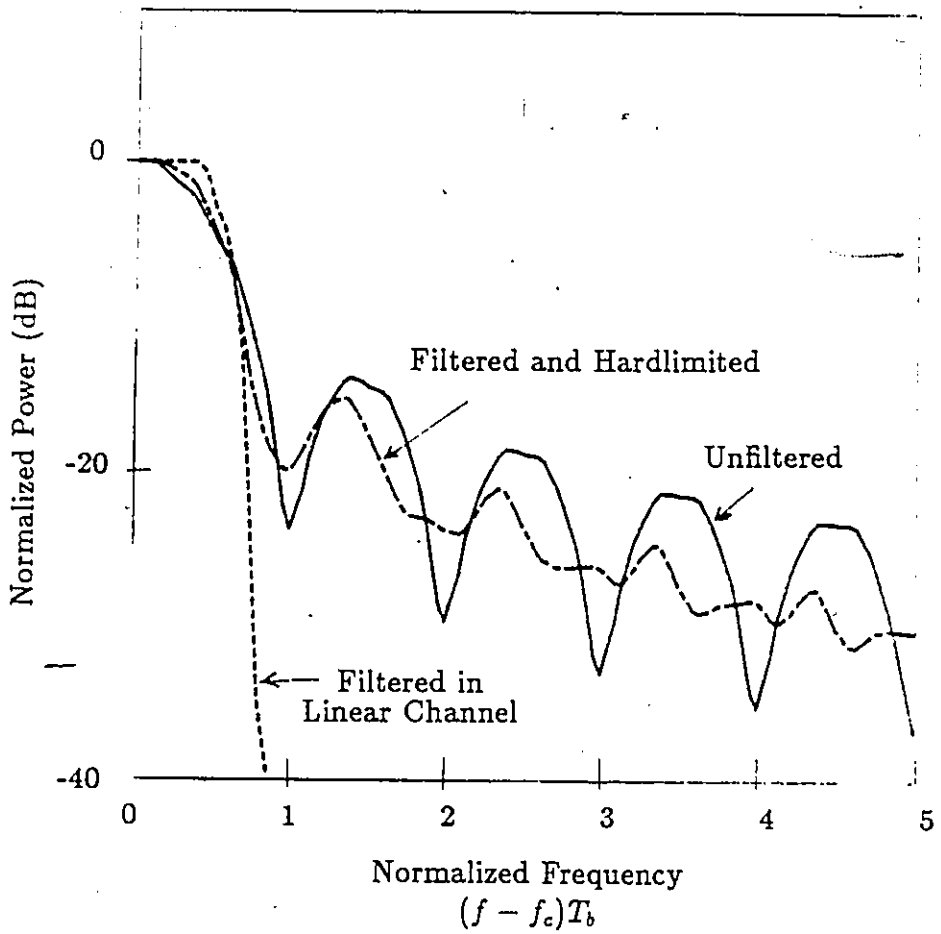

Figure 2.11: Spectra of DQPSK signals: (i) unfiltered, ii) filtered $(x/\sin x + \sqrt{\alpha = 0.5})$, and (iii) filtered and then hardlimited.

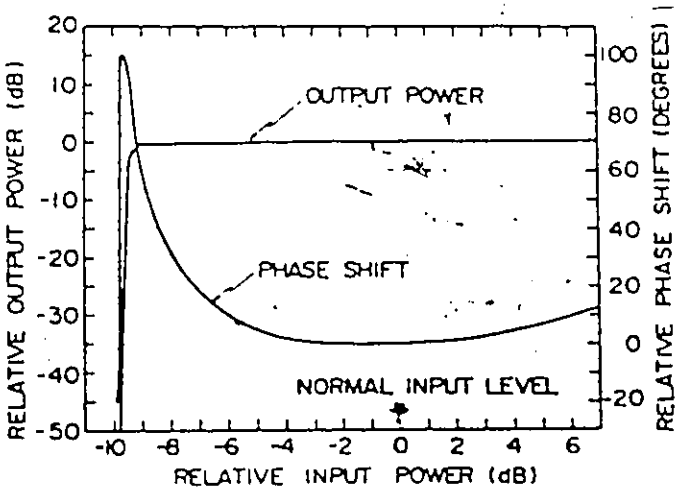

図 2　典型的なC級電力増幅器の AM/AM特性と AM/PM特性

Fig. 2　AM/AM and AM/PM characteristics of a typical class-C power amplifier.

Figure 2.12: AM/AM and AM/PM characteristics of a typical class-C power amplifier. Reproduced from [87].

2.1.3 Differential Detection of Offset-QPSK Type Signals

In the previous section we have seen that a filtered QPSK signal may have 100% envelope fluctuation and if it is passed through a nonlinearity the filtered sidelobes are mostly restored. A variant of QPSK is Offset-QPSK [82]. In comparison to a QPSK signal, the spectral regrowth of a filtered OQPSK signal after a nonlinearity is much less. This can be observed from Figure 2.13 where the spectra of filtered QPSK and OQPSK after a hardlimiter are plotted. The transmitter filter used is: $x/\sin x + \sqrt{\alpha} = 0.5$. Note that the spectra of QPSK and OQPSK before the hardlimiter are identical (see Figure 2.13).

When coherent detection is employed, the ideal theoretical BER performances of QPSK and OQPSK are identical [82]. A natural question at this point is: *Are the BER performances of differentially detected QPSK and OQPSK identical ?* The answer is *NO,* and the mechanism which causes the performance difference is explained below.

2.1.3.1 Transmitter

The block diagram of an OQPSK transmitter (including a differential encoder) is shown in Figure 2.14. The input binary sequence $\{c_k = \pm 1\}$ has a rate of T_b^{-1}. First, $\{c_k\}$ is serial to parallel converted into two binary sequences $\{a_k\}$ and $\{b_k\}$ such that

$$\{a_k\} = \{c_{2k}\} \quad \text{for all } k \tag{2.54}$$

and

$$\{b_k\} = \{c_{2k+1}\} \quad \text{for all } k. \tag{2.55}$$

Then, $\{a_k\}$ and $\{b_k\}$ are differentially encoded to produce the sequences $\{a'_k\}$ and $\{b'_k\}$. The differential encoding required here is the same as that of DBPSK, i.e.,

$$a'_k = a_k a'_{k-1}, \tag{2.56}$$

and

$$b'_k = b_k b'_{k-1}. \tag{2.57}$$

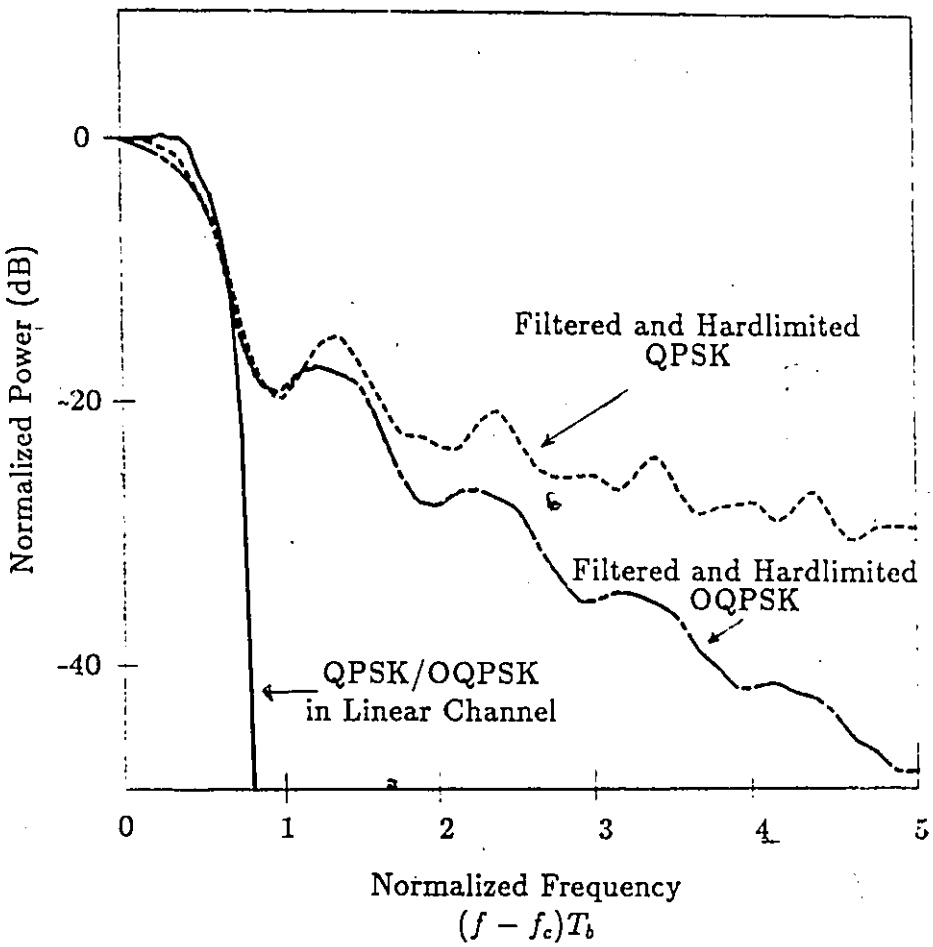

Figure 2.13: Spectra of filtered QPSK and OQPSK signals before and after a hardlimiter. The filter is $x/\sin x + \sqrt{\alpha = 0.5}$

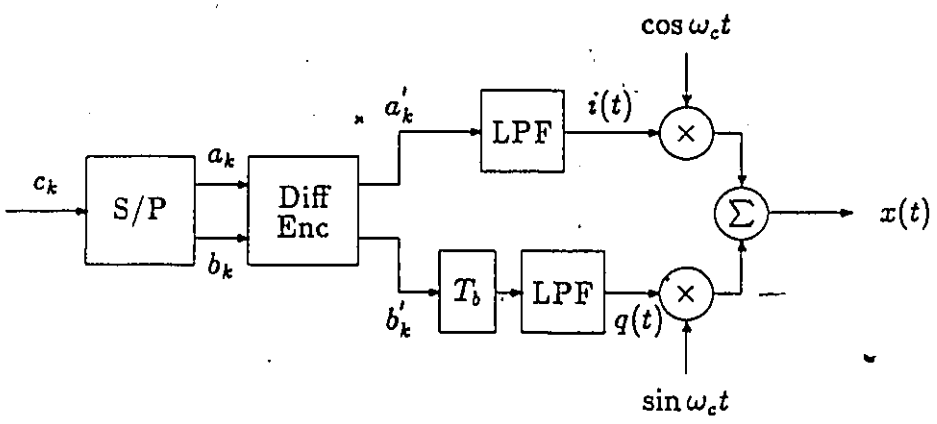

Figure 2.14: Block diagram of an OQPSK transmitter (including a differential encoder).

In OQPSK, one of the quadrature channel signals is delayed by $T_b = T_s/2$ seconds. Thus the instantaneous phase change of 180° is eliminated and the possible phase changes (every T_b seconds) are 0°, +90° and −90°. The differential encoding ensures that when $c_k = 1$, the phase of the signal changes by ±90°; and when $c_k = -1$ the phase remains the same.

The transmitted OQPSK signal can be represented as

$$x(t) = \sum_{k=-\infty}^{\infty} a'_k p(t - kT_s)\cos\omega_c t + \sum_{k=-\infty}^{\infty} b'_k p(t - kT_s - \frac{T_s}{2})\sin\omega_c t \quad (2.58)$$

where T_s is the symbol interval ($T_s = 2T_b$), and $p(t)$ is the baseband pulse shaping. By changing the baseband pulse shaping, various Offset-QPSK type signals have been obtained [88–91].

Equation (2.58) can also be written as

$$x(t) = i(t)\cos\omega_c t + q(t)\sin\omega_c t \quad (2.59)$$

where $i(t)$ and $q(t)$ are the I and Q-channel modulating signals. The waveforms associated with the OQPSK transmitter of Figure 2.14 are shown in

Figure 2.15.

The SSD of the unfiltered OQPSK signal is shown in Figure 2.16. This SSD is obtained by drawing trace (d) versus trace (e) of Figure 2.15. Note that the signal occupies one of the four corner states for a full bit interval, and the transitions from one state to another are instantaneous.

In Figure 2.17 the SSD of a filtered OQPSK signal is shown. The filter used in this case is a $x/\sin x+\alpha = 1$. The signals $i(t)$ and $q(t)$ corresponding to this SSD are trace (f) and (g) of Figure 2.15. Note that when the signal is filtered, the transitions from one state to another take a finite duration.

2.1.3.2 Receiver

The receiver block diagram of a differentially detected OQPSK (DOQPSK) is shown in Figure 2.18. Since the signal phase may change every bit interval, the required delay is T_b seconds.

For illustrative purposes, let us first consider the differential detection of an unfiltered (i.e., infinite bandwidth) OQPSK signal. At the sampling instant $t = kT_b$, the signal is at one of the corner states (see Figure 2.19). Let us denote the signal phase as θ_k, and the differential phase angle as $\Delta\theta_k$; where

$$\Delta\theta_k = \theta_k - \theta_{k-1}. \tag{2.60}$$

Recall from the differential encoding rule that for the unfiltered signal, $\Delta\theta_k$ can take three values: 0°, +90° and −90°. The decoding rule is given by:

$$\hat{c}_k = \begin{cases} 1 & \text{if} \quad |\Delta\hat{\theta}_k| \geq 45°, \\ -1 & \text{otherwise;} \end{cases} \tag{2.61}$$

where $\hat{c}_k$ is the estimate of the transmitted bit c_k.

The differential detection of an unfiltered OQPSK signal is not of any practical value, because an unfiltered OQPSK signal does not provide any advantages over a QPSK signal.

Let us now focus on the filtered OQPSK signal, and assume that the composite transmit and receive filter has a raised-cosine characteristic with an $\alpha = 1$. In this case the transitions take place in a finite duration. At

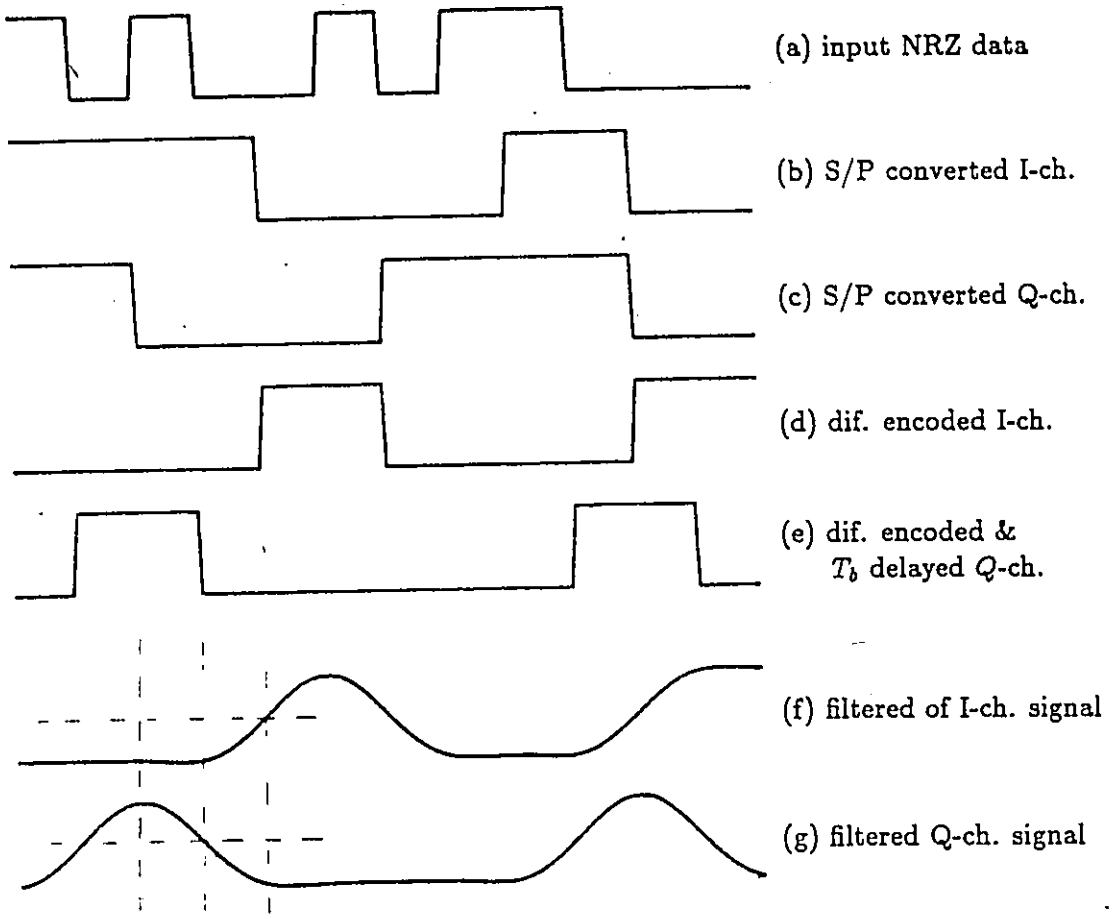

Figure 2.15: Waveforms associated with an OQPSK transmitter.

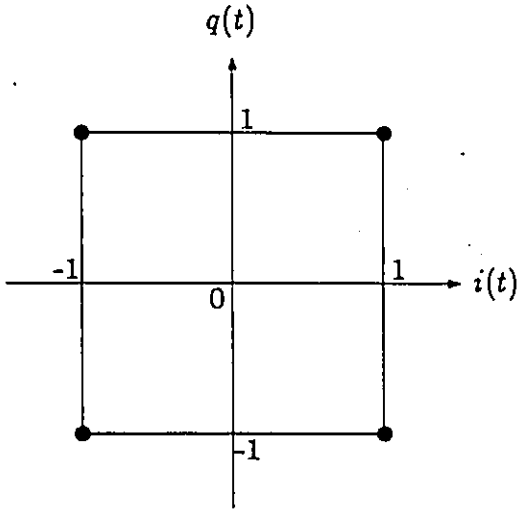

Figure 2.16: Signal-state diagram of an unfiltered OQPSK signal.

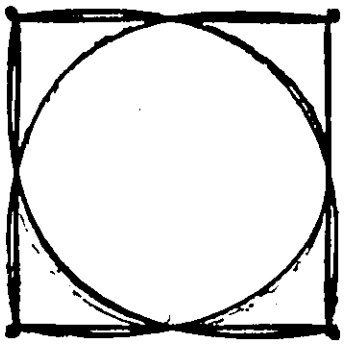

Figure 2.17: Signal-state diagram of a filtered OQPSK signal. The filter is a $x/\sin x + \alpha = 1$.

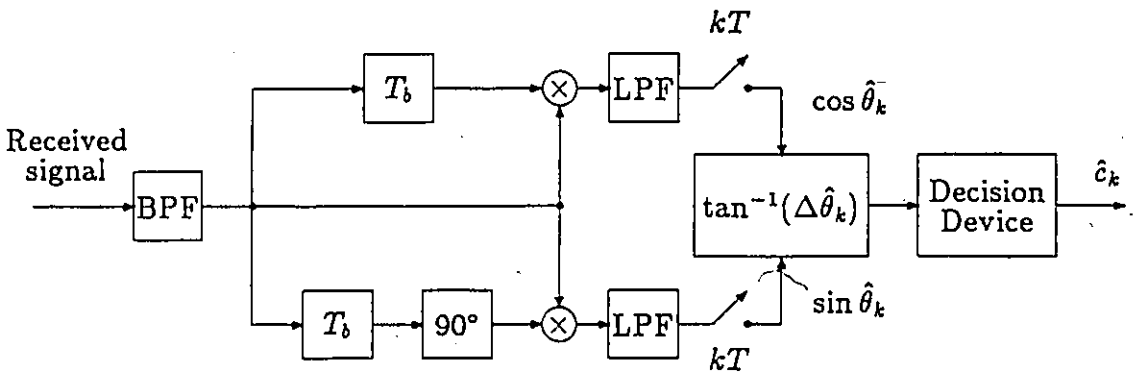

Figure 2.18: Block diagram of DOQPSK receiver.

the sampling instant $t = kT_b$, the signal is at one of the 8 states shown in Figure 2.20.a. Observe that in this case the minimum differential phase angle between two states (i.e., the "phase margin") can be as small as 45°. The phase margin can be increased by sampling at $t = kT_b + T_b/2$; then the possible signal phases are as shown in Figure 2.20.b. Note that there are four clusters, and in each cluster there are four points[9]. From one sampling instant to the next, if the signal stays within the same cluster, then the output of the decision device is a "+1". If the signal moves from one cluster to the other, then the output of the decision device is a "–1".

2.1.3.3 BER Performance in an AWGN Channel

The bit error rate performance of DOQPSK has been estimated by using computer simulations[10], and the result is plotted in Figure 2.21. The assumed composite transmit and receive filter has a raised-cosine characteristic with $\alpha = 1$, and the sampling time is $kT_b + T_b/2$. In Figure 2.21, the

[9]Only the corner points are free from ISI.
[10]Program listings are given in Appendix B.

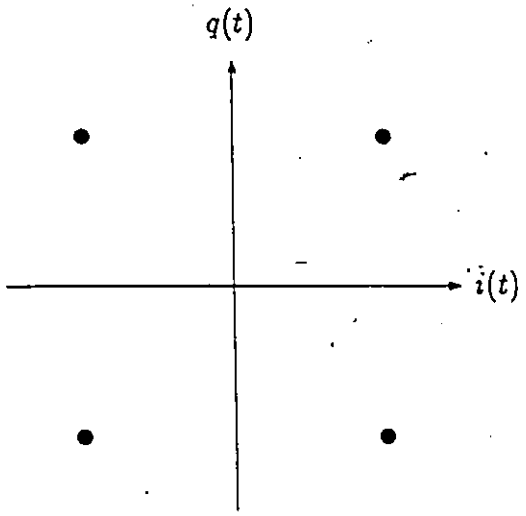

Figure 2.19: Signal states of unfiltered OQPSK at sampling instants ($t = kT_b$).

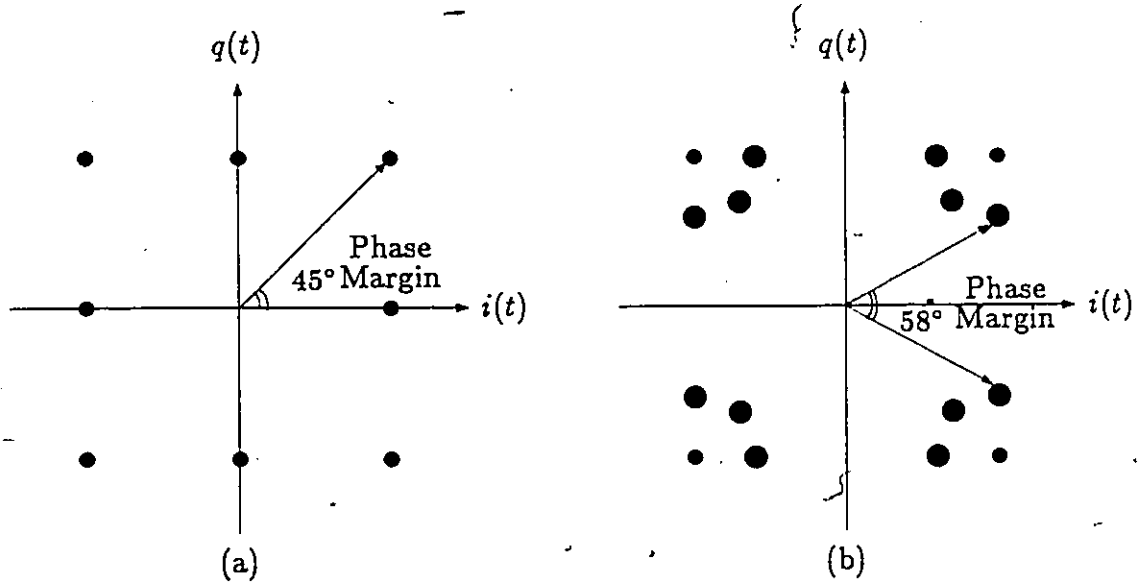

Figure 2.20: Signal states of filtered OQPSK at sampling instants (a) $t = kT_b$; (b) $t = kT_b + T_b/2$. The filter is a $x/\sin x + \alpha = 1$.

ideal theoretical BER performance of DQPSK is also plotted. A comparison of the two curves indicates that to achieve a BER of 10^{-4}, DOQPSK requires about 3 dB more E_b/N_0 than DQPSK. The difference in performance is attributed to the difference in the phase margin. In DQPSK the phase margin is 90°, whereas in DOQPSK the phase margin is about 58°. A factor in determining the phase margin is the filter roll-off factor α. Figure 2.21 indicates that as α is reduced from 1 to 0.5, the performance degrades significantly.

There are several Offset-QPSK type signals (e.g., [88-90]; however, we have not seen any references on the application of differential detection to any of them. This can be explained by the fact that when Offset-QPSK type signals are differentially detected (by using conventional symbol-by-symbol detectors), the phase margin is reduced. Consequently, the BER performance is significantly inferior to that of DQPSK. This argument also applies to other signal constellations where the phase margin is small. For example in Tamed Frequency Modulation the phase margin is 45°, and the resulting performance is significantly inferior to DQPSK [92].

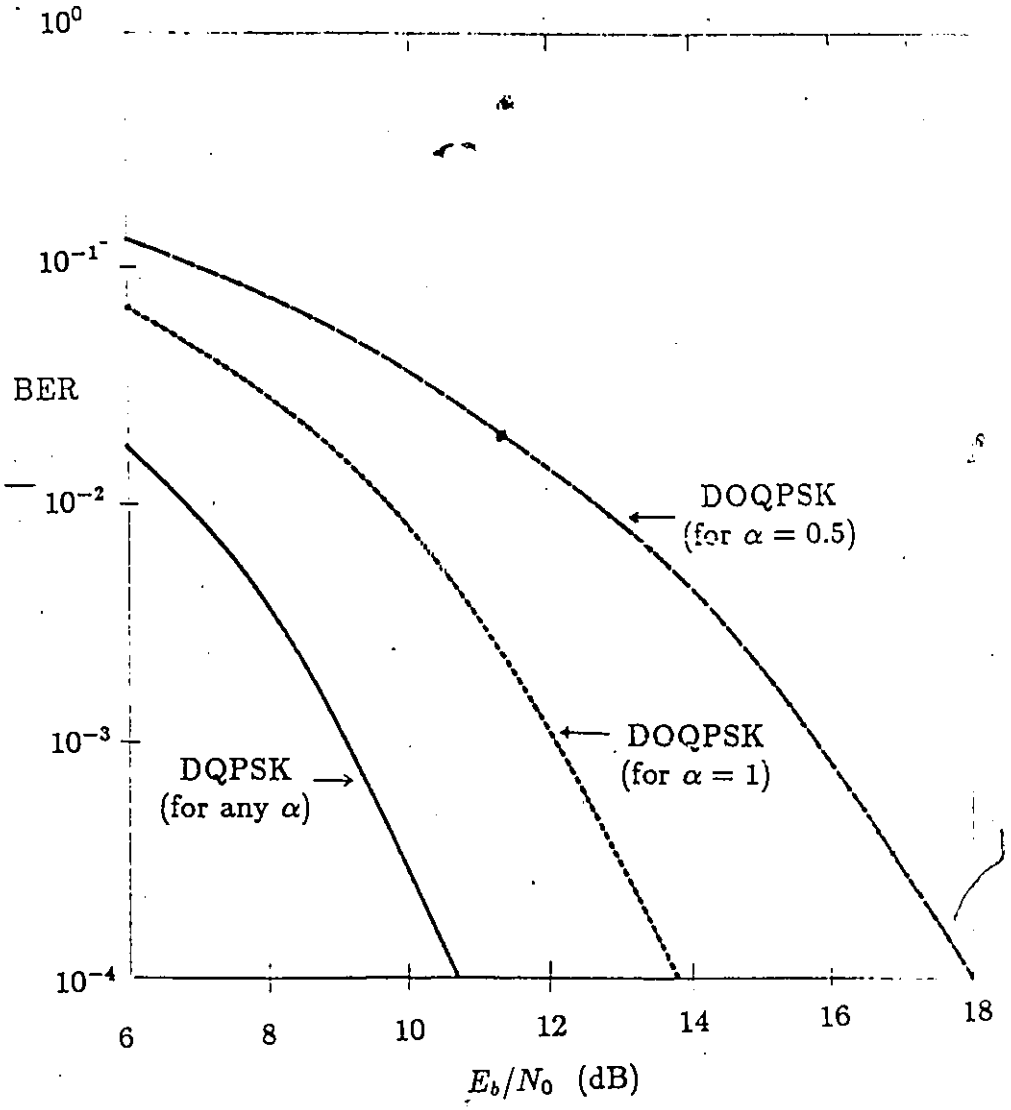

Figure 2.21: BER performance of DQPSK and DOQPSK. The filter has a raised-cosine characteristic (including a $x/\sin x$ equalizer). DQPSK is sampled at $t = kT_s$ and DOQPSK is sampled ~~at $t = kT_b + T_b/2$~~.

2.2 DIFFERENTIAL DETECTION OF CONTINUOUS PHASE MODULATED SIGNALS

In digital transmission, low adjacent channel interference necessitates low spectral sidelobes, which, in an environment where efficient (i.e., near saturated) operation of power amplifiers is also required, implies that constant envelope signals must be used. In PSK systems, the discontinuities in the phase were seen in the last section to result in high spectral sidelobes. The filtering applied to reduce the sidelobes resulted in nonconstant envelope signals which made the modulations more sensitive to nonlinearities. A class of digital modulation schemes which satisfy both the constant envelope and the low spectral sidelobe properties are called Continuous Phase Modulation (CPM) schemes [93][11].

In CPM systems, the transmitted signal can be represented as

$$x(t) = \cos(\omega_c t + \phi(t)) \tag{2.62}$$

where ω_c is the carrier frequency and $\phi(t)$ is the information carrying phase which can be expressed as

$$\phi(t) = 2\pi h \sum_k a_k g(t - kT). \tag{2.63}$$

In (2.63), h is the modulation index, $\{a_k\}$ are the m-ary data symbols which take the values $\pm 1, \pm 3 \cdots \pm (m-1)$, and $g(t)$ is the phase response defined by

$$g(t) = \int_{-\infty}^{t} p(\tau) d\tau \tag{2.64}$$

where $p(t)$ is the pulse shaping.

The shape of $p(t)$ determines the smoothness of the information carrying phase. The rate of change of phase (i.e., the instantaneous frequency) is proportional to the modulation index h. If the pulse shape $p(t)$ is normalized so that

$$\int_{-\infty}^{\infty} p(t) dt = 1/2 \tag{2.65}$$

[11] In [93] Sundberg provides an extensive bibliography on CPM systems.

then the maximum phase change over any symbol interval is $(m-1)h\pi$.

By choosing different pulse shapes $p(t)$, and by varying the parameters h and m, a great variety of CPM schemes can be obtained. In this thesis we shall keep $h = 0.5$ and $m = 2$, and the bandwidth/power tradeoff will be achieved by varying the pulse shaping. This approach has the advantages of being simpler (because the receiver structure remains essentially the same) and also provides compatibility with coherent systems, where $h = 0.5$ is frequently chosen so that a simple quadrature receiver can be used [94,95].

2.2.1 Differentially Detected Minimum Shift Keying

Minimum Shift Keying is the simplest and the most widely used form of CPM, which can be more precisely refered to as continuous phase binary frequency shift keying. Coherent MSK was introduced in 1961 [96]. The differential detection of MSK was first reported by Hubbard in 1967 [97][12]. Later, various aspects of DMSK were studied [65,98–102]. In this section we shall review the principle of DMSK and briefly discuss its major properties.

2.2.1.1 Transmitter

In MSK, the modulation index h is equal to 0.5, the input symbols a_k take the values ± 1 and the pulse shape is given by

$$p(t) = \begin{cases} \frac{1}{2T} & \text{for } 0 \le t \le T \\ 0 & \text{otherwise} \end{cases} \tag{2.66}$$

where T is the bit interval (i.e., $T = T_b$)[13]. Since the pulse is confined to a one-bit interval, the phase change over any bit interval is exactly $\pm\pi/2$.

In a particular interval, the phase $\phi(t)$ can be expressed as

$$\phi(t) = (\frac{a_k \pi}{2T})t + \psi_k \quad \text{for} \quad kT - T \le t \le kT \tag{2.67}$$

[12]Hubbard refers to DMSK as FM-Differentially Coherent BPSK.

[13]In the rest of this section T refers to T_b.

where

a_k = input data (± 1) transmitted at rate T^{-1},
ψ_k = constant phase valid for $kT - T \leq t \leq kT$.

To satisfy the phase continuity condition, the necessary requirement is

$$\psi_k - \psi_{k-1} = (a_{k-1} - a_k)(k-1)\frac{\pi}{2}. \tag{2.68}$$

The MSK transmitter is generally implemented in the form of an OQPSK transmitter with sinusoidal pulse shaping. The equivalance of the transmitted signal using an FM type or an OQPSK type modem is shown in various references, including [103,104].

2.2.1.2 Receiver

The block diagram of a DMSK receiver is shown in Figure 2.22. This

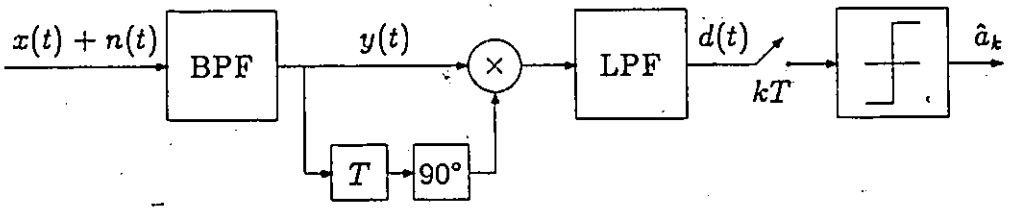

Figure 2.22: Block diagram of a DMSK receiver.

receiver is basically the same as the one used for the differential detection of BPSK. The received signal is

$$z(t) = \cos(\omega_c t + \phi(t)) + n(t) \tag{2.69}$$

where $n(t)$ is the white Gaussian noise. At the output of the BPF the signal can be represented as

$$y(t) = r'(t)\cos(\omega_c t + \phi'(t)) + n_c(t)\cos\omega_c t + n_s(t)\sin\omega_c t \tag{2.70}$$

where $r'(t)$ is the envelope of the filtered signal, $\phi'(t)$ is the distorted signal phase, and $n_c(t)$ and $n_s(t)$ are the components of the narrowband Gaussian noise. The BPF introduces ISI, and its effect is taken into account in the simulations. To simplify the following discussion, we shall assume that the effect of the predetection BPF on the phase and the envelope of the signal is negligible, i.e., $r'(t) = 1$ and $\phi'(t) = \phi(t)$.

The differential detection is performed by multiplying $y(t)$ with a T second delayed and 90° phase shifted version of itself and then low-pass filtering the product. The output of the multiplier is given by

$$\begin{aligned} d'(t) &= y(t)y(t-T)_{90°} \\ &= -\frac{1}{2}\sin(2\omega_c t - \omega_c T + \phi(t) + \phi(t-T)) \\ &\quad + \frac{1}{2}\sin(\omega_c T + \phi(t) - \phi(t-T)) + n'_T(t) \end{aligned} \tag{2.71}$$

where $n'_T(t)$ lumps together all the terms containing the noise components. The LPF and removes the second harmonic terms. Assuming that $\omega_c T = 2\pi n$, then the signal at the input of the decision device is

$$d(t) = \frac{1}{2}\sin(\phi(t) - \phi(t-T)) + n_T(t). \tag{2.72}$$

At the sampling instant $t = kT$, by substituting the expression of $\phi(t)$ (see (2.67)) into (2.72), the decision variable can be written as

$$d(kT) = \frac{1}{2}a_k + n_T(kT) \tag{2.73}$$

Then,

$$\hat{a}_k = \text{sgn}\,[d(kT)] \tag{2.74}$$

Note that the receiver for DMSK (i.e., Figure 2.22) is considerably simpler than the one required for DQPSK.

2.2.1.3 BER Performance in an AWGN Channel

The BER performance of DMSK has been analytically calculated by Ogose et al [105] and also by Simon and Wang [65]. The analytical calculations use the probability distribution function for the phase difference between the two vectors after they have been perturbed by narrowband Gaussian noise [85]. The BER performance of DMSK has also been estimated via simulation techniques [98,101,106]. The results obtained by analytical calculations and by simulations are in good agreement. The simulation approach is more suitable if the receiver includes complex processing circuitry, and is also more flexible in terms of specifying different filter types and parameters.

The analytically calculated BER performance of DMSK is reproduced in Figure 2.23. In the same figure, we have also included the BER performance results of our simulations [106]. In both approaches, the predetection BPF used has a Gaussian characteristic with a BT=1.25 (i.e., the optimum value for the predetection Gaussian filter). Observe that the analytical and simulation results match quite closely. To provide a reference point, the ideal theoretical BER performance of of DBPSK is also plotted. By comparing the performances of the two modems, it can be observed that for the same bit error rate (e.g., 10^{-4}), DBPSK requires about 3 dB less E_b/N_0 than DMSK. This is due to the fact that DMSK suffers from ISI; whereas for DBPSK the conditions of no ISI can be satisfied (see Section 2.1.1.2).

2.2.1.4 Spectrum

The easiest way to calculate the power spectrum of MSK is to treat it as an OQPSK signal with a symbol shaping function $v(t)$ defined by

$$v(t) = \begin{cases} \cos\frac{\pi t}{2T} & |t| \leq T \\ 0 & \text{elsewhere.} \end{cases} \tag{2.75}$$

Then the spectral density $S(\omega)$ is given by [104]

$$S(\omega) = |\mathcal{F}[v(t)]|^2 = 16\pi^2 T\left(\frac{\cos(\omega-\omega_c)T}{\pi^2 - 4(\omega-\omega_c)^2T^2}\right)^2 \tag{2.76}$$

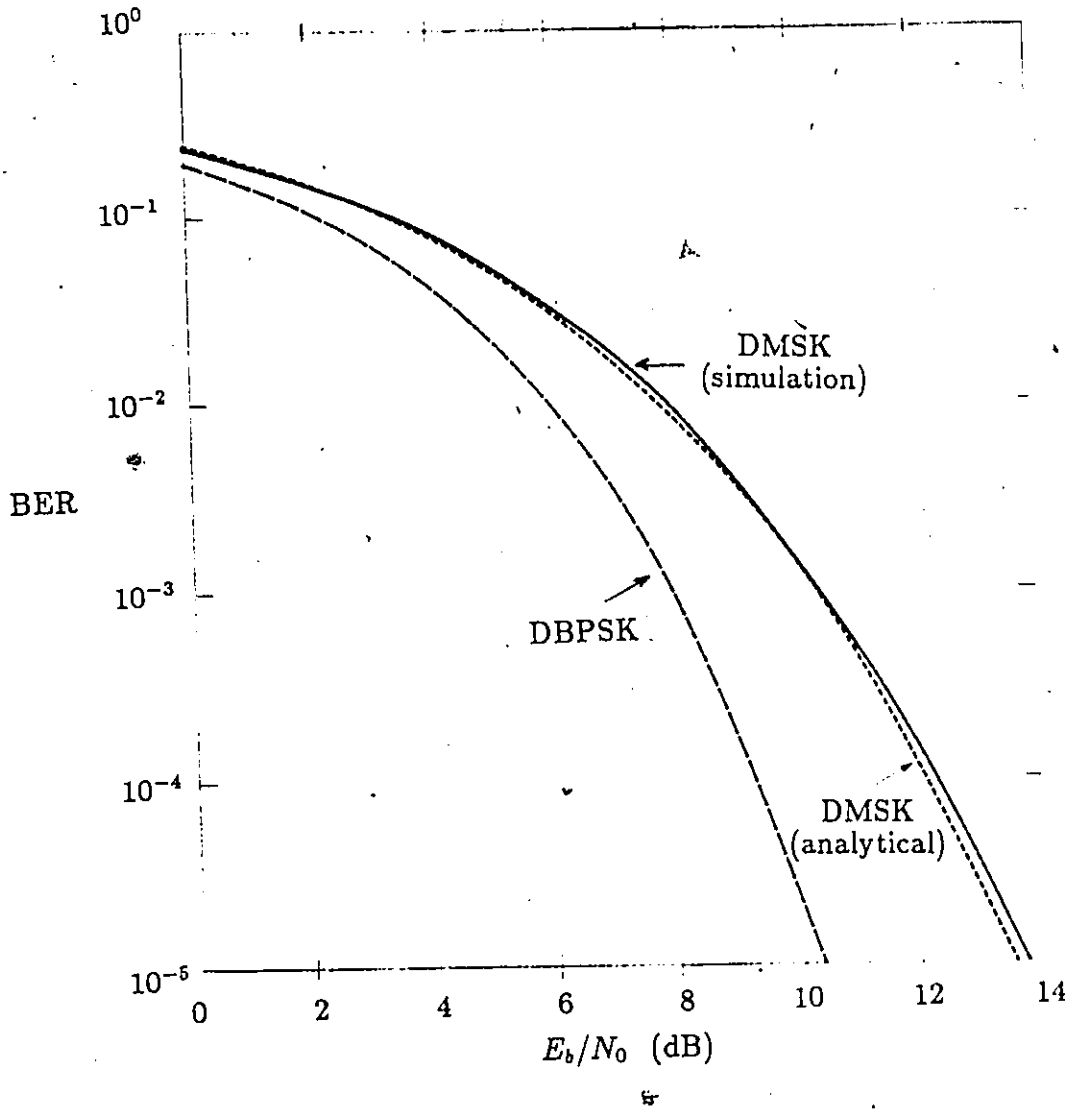

Figure 2.23: BER performance of DMSK.

where $\mathcal{F}$ represents the Fourier transform. A comparison of (2.76) and (2.53) indicates that MSK has a 50% larger mainlobe than QPSK but its sidelobes decay faster (at the rate of ω^4 rather than ω^2).

2.2.2 Gaussian Minimum Shift Keying

Gaussian Minimum Shift Keying provides constant envelope signals with a compact spectrum. It was introduced initially for digital transmission in mobile radio communications systems [94].

2.2.2.1 Modem Requirements for Land Mobile Communications

In land mobile radio communications the major properties required from a modem technique can be enumerated as follows:

- A bandwidth efficiency of 0.65 b/s/Hz or better;
- Out-of-band power attenuation of more than 60 dB;
- Constant envelope transmitted signal;
- Fast signal acquisition.

Let us briefly examine why these requirements are imposed. The first requirement is needed to achieve the same bandwidth efficiency as analog voice transmission by using digital voice transmission. The existing mobile radio systems use analog FM for the transmission of voice in a 25 kHz channel spacing. Comparable quality digital voice transmission requires a bit rate of 16 kb/s [11,94,107]. Hence the bandwidth efficiency should be 0.65 b/s/Hz or better.

Since the analog and digital voice may be transmitted in adjacent channels, to keep the degradation of the analog voice at a tolerable level, the power spilling into the adjacent channel should be 60 dB less than the power in the main channel.

The constant envelope signals are required to efficiently utilize the transmit power amplifiers and to reduce the effect of fading on the receiver performance.

The rapid signal acquisition property is required because the signal is subject to frequent fading. For this reason, in mobile communications noncoherent detection schemes are preferred.

MSK or PSK schemes cannot satisfy the 0.65 b/s/Hz bandwidth efficiency, the 60 dB out-of-band power attenuation and constant envelope properties simultaneously. However, in recent years, a number of modulation techniques have been invented to satisfy the above listed requirements [92,94,108,109]. The best known of these schemes are Tamed Frequency Modulation (TFM) and Gaussian Minimum Shift Keying. The major properties of differentially detected GMSK are described below.

2.2.2.2 Transmitter

The block diagram of a GMSK transmitter consisting of a differential encoder, a Gaussian low-pass filter (GLPF) and an FM modulator is shown in Figure 2.24 The differences between a GMSK transmitter and a MSK

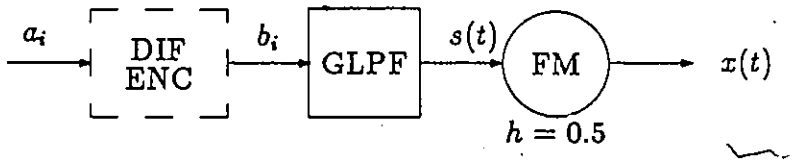

Figure 2.24: Block diagram of a GMSK transmitter. The differential encoder is not needed for one-bit differential detection.

transmitter are the additional differential encoder and the GLPF. The differential encoder is required for the two-bit (and higher order) differential detection. For two-bit differential detection, it performs the operation described by

$$b_i = -a_i b_{i-1}. \tag{2.77}$$

The input to the GLPF is a non-return to zero (NRZ) sequence. The output of the GLPF can be expressed as

$$s(t) = \sum_{i=-\infty}^{\infty} b_i p(t - iT) \tag{2.78}$$

where $\{b_i = \pm 1\}$ and $p(t)$ is the *pulse*[14] response of the transmit GLPF given by [110] :

$$p(t) = \frac{1}{2T}(Q(k_1 B_t T(-\frac{t}{T})) - Q(k_1 B_t T(1 - \frac{t}{T})) \tag{2.79}$$

In (2.79), B_t is the 3 dB bandwidth of the GLPF[15], $k_1 = 7.546$

$$Q(x) = \frac{1}{\sqrt{2\pi}} \int_x^{\infty} \exp(-y^2/2) dy. \tag{2.80}$$

The output of the FM modulator can be expressed as:

$$x(t) = \cos(\omega_c t + \phi(t) + \psi) \tag{2.81}$$

where ω_c is the carrier frequency , ψ is the initial phase (which can be assumed as zero) and $\phi(t)$ is the excess-phase defined by

$$\phi(t) = k_m \int_{-\infty}^{t} s(\tau) d\tau = k_m \sum_{j=-\infty}^{\infty} b_j \int_{-\infty}^{t} p(\tau - jT) d\tau \tag{2.82}$$

where k_m is a constant equal to $\pi/2T$ (so that the modulation index h=0.5).

The transmitter block diagram of Figure 2.24 is a conceptual one. Implementing the GMSK transmitter using an FM modulator leads to certain practical difficulties (e.g., VCO drift). For this reason, implementing the transmitter in the form of a quadrature modulator which uses a look-up table is prefered [109].

The spectrum of the GMSK signal for various values of $B_t T$ is calculated via computer simulations and is plotted in Figure 2.25.

[14]Contrary to the more familiar impulse response.

[15]thus $B_t T$ is the bandwidth-time product.

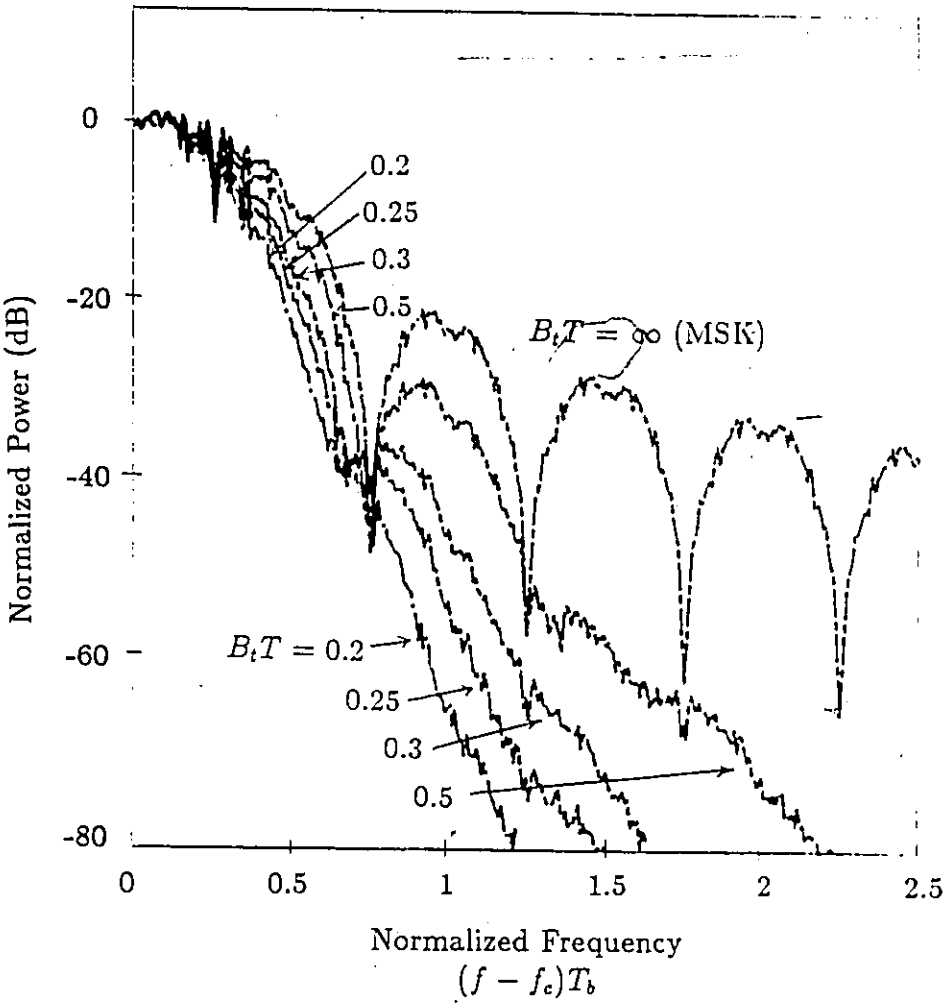

Figure 2.25: Spectrum of GMSK for various B_tT values.

2.2.2.3 Conventional Two-Bit Differential Detection

The GMSK signal can be detected by using an n-bit differential detector (where $n = 1, 2, ...$). However, it has been shown that a two-bit differential detector yields better performance than a one-bit differential detector [110,111]. In this section we shall review only the two-bit differential detector.

Figure 2.26 illustrates the block diagram of the conventional two-bit differential detector. The output of the two-bit detector $d_2(t)$ is obtained

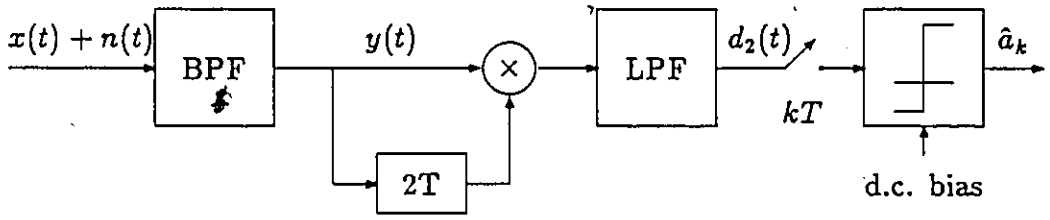

Figure 2.26: Block diagram of the conventional two-bit differential detector.

by multiplying $y(t)$ with a $2T$ seconds delayed version of itself and then lowpass filtering the product, i.e.,

$$d_2(t) = r(t)r(t-2T)\cos(k_m \sum_{j=-\infty}^{\infty} b_j \int_{t-2T}^{t} p(\tau - jT)d\tau) + n_2(t) \qquad (2.83)$$

where $n_2(t)$ represents all the noise terms.

At the time instant kT, $d_2(t)$ is given by

$$d_2(kT) = r(kT)r(kT-2T)\cos(\sum_{j=-\infty}^{\infty} b_j V_{k-j}) + n_2(kT) \qquad (2.84)$$

where

$$V_{k-j} = k_m \int_{kT-2T}^{kT} p(\tau - jT)d\tau \tag{2.85}$$

In this section, for illustrative purposes, only the case where $B_tT = 0.25$ is considered. This value of B_tT optimizes the spectrum utilization in cellular mobile radio communications [112,113]. The effect of varying the B_tT on the BER performance is discussed in Chapter 4.

The values of V_i for $B_tT = 0.25$ are as follows:

$$V_0 = V_1 = 70.6°.$$

$$V_{-1} = V_2 = 18.2°$$

$$V_i \approx 0 \quad \text{for} \quad i \geq 3 \quad \text{and} \quad i \leq 2.$$

Thus, we can rewrite (2.84) as:

$$d_2(kT) = r(kT)r(kT - 2T)\cos(\Delta V_k) + n_2(kT) \tag{2.86}$$

where

$$\Delta V_k = b_{k+1}V_{-1} + b_kV_0 + b_{k-1}V_1 + b_{k-2}V_2. \tag{2.87}$$

The differential phase angles ΔV_k corresponding to the 16 possible combinations of $\{b_{k-2}b_{k-1}b_kb_{k+1}\}$ have been tabulated in Table 2.1. Using Table 2.1, the phase-states at the decision instants for the two-bit differential detector are shown in Figure 2.27.

To determine the polarity of the output bit, as a first approximation, let us assume that the decision threshold is the y-axis. When the phase difference (ΔV_k) is to the left of the y-axis, $-b_kb_{k-1}$ is "+1"; otherwise $-b_kb_{k-1}$ is "−1". Recall that $a_k = -b_kb_{k-1}$. Hence, as a first approximation, the decision law is given by

$$\hat{a}_k = \begin{cases} 1 & \text{for} \quad -\pi/2 \leq \Delta V_k \leq \pi/2 \\ -1 & \text{elsewhere.} \end{cases} \tag{2.88}$$

From Figure 2.27 we see that the phase-states at the output of the two-bit differential detector are not symmetrical with respect to the y-axis. As a result of this, the corresponding eye-diagram shown in Figure 2.28 is also

Bit Combinations				State	ΔV_k
b_{k-2}	b_{k-1}	b_k	b_{k+1}		(in degrees)
1	1	-1	1	7	37.6
1	-1	1	1	7	37.6
1	1	-1	-1	8	0.0
1	-1	1	-1	8	0.0
-1	1	-1	1	8	0.0
-1	-1	1	1	8	0.0
-1	1	-1	-1	9	-37.6
-1	-1	1	-1	9	-37.6
1	-1	-1	1	10	-103.6
1	-1	-1	-1	11	-141.2
-1	-1	-1	1	11	-141.2
-1	-1	-1	-1	12	-178.8
1	1	1	1	12	178.8
1	1	1	-1	13	141.2
-1	1	1	1	13	141.2
-1	1	1	-1	14	103.6

Table 2.1: Differential phase angles ΔV_k of the two-bit detector corresponding to various input data combinations ($B_t T = 0.25$). Contributions of b_{k+2} and b_{k-3} are ignored.

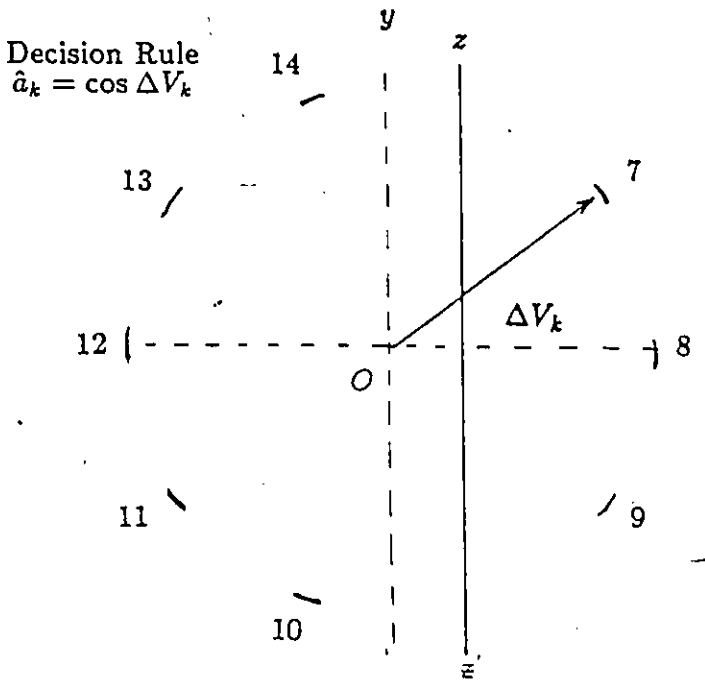

Figure 2.27: Possible differential phase angles ΔV_k in conventional two-bit differential detection ($B_tT = 0.25$).

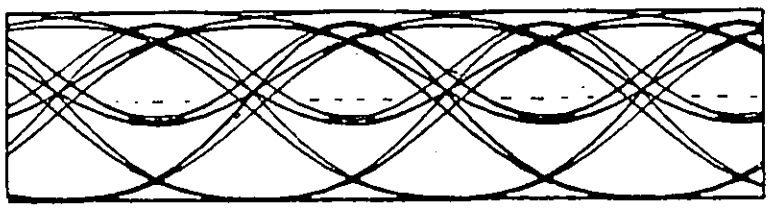

Figure 2.28: Eye-diagram of the conventional two-bit differential detector at the output of the LPF ($B_tT = 0.25$).

asymmetric. To improve the performance, in Figure 2.27 the thresholds should be placed midway between the states 7 and 14, and the states 9 and 10. This is equivalent to inserting a bandpass limiter after the BPF and applying a dc bias to the threshold comparator [65] (i.e., the new threshold is the zz' line in Figure 2.27.).

2.2.2.4 BER Performance of Conventional Two-Bit Differential Detection

The analytical calculation of BER performance of DGMSK is similar to that of DMSK. The additional factors to be considered are:

- In DMSK the ISI is only due to the predetection BPF, and it extends over 3 bit intervals. Thus in determining the phase angle between two vectors, the averaging should be done over all possible three bit combinations. In DGMSK the ISI is due to transmit GLPF and the predetection BPF, and extends over a longer time interval. For example, when $B_tT = 0.25$, then the averaging should use 5 bit combinations [110].
- In the two-bit differential detection of MSK, the asymmetry in the received signal levels is negligible. In the two-bit differential detection of GMSK, the asymmetry is significant and an adjustable threshold is necessary (the threshold level is dependent on E_b/N_0).

Taking these factors into account, Simon and Wang have calculated the BER performance of two-bit differential detection [110]. For the system where $B_tT = 0.25$, the analytically obtained BER curves (when the predetection BPF bandwidth and the threshold levels are optimized) are shown in Figure 2.29.

For evaluating the BER performance of the two-bit differential detection scheme, we have used simulations based on the Monte Carlo error counting technique. Using the optimum parameters given by Simon and Wang [110], the curves obtained via simulations are also plotted in Figure 2.29, and the close agreement between the simulation and analytical results is observed.

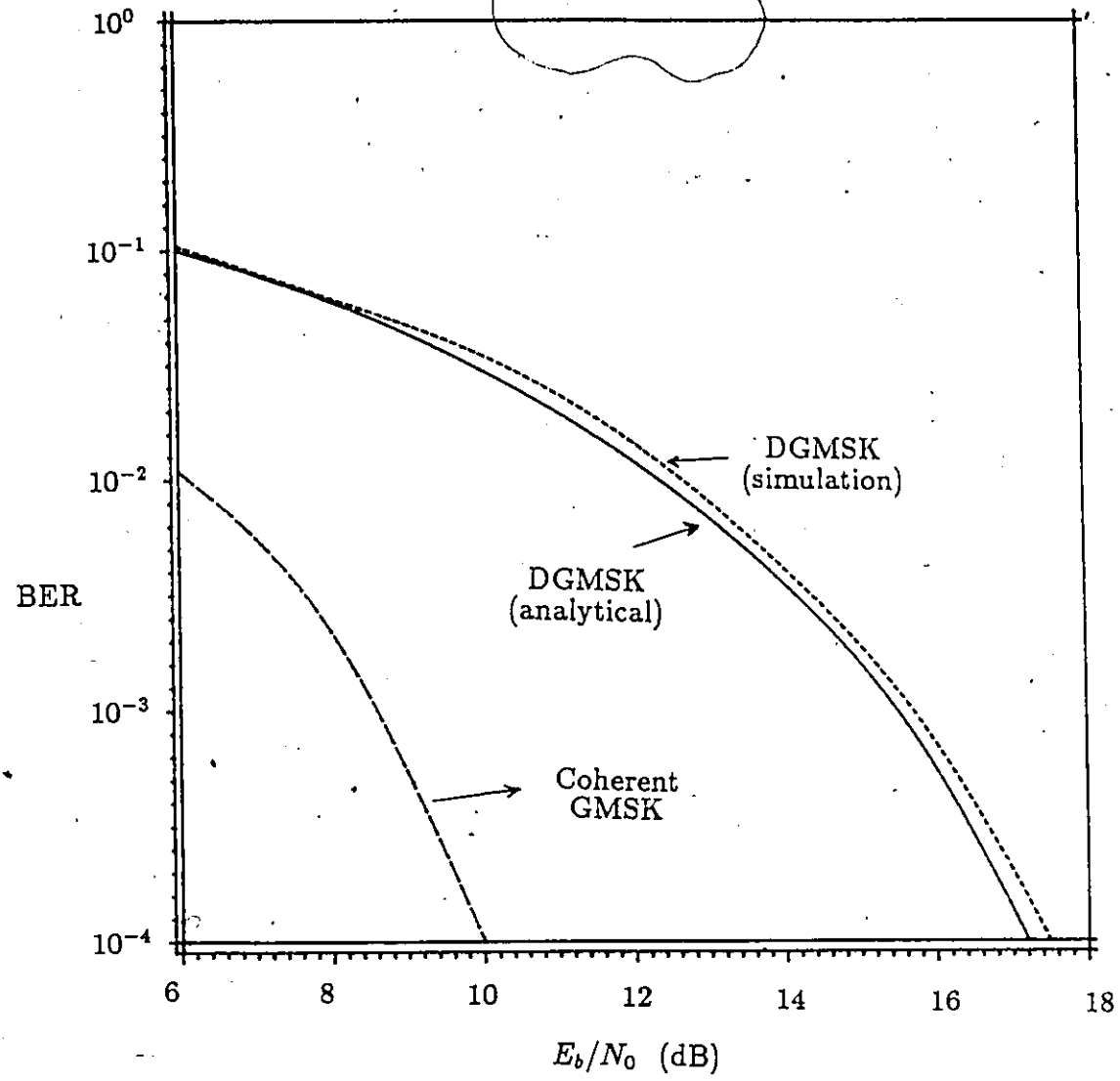

Figure 2.29: BER performance of GMSK using conventional two-bit differential detection. Transmit LPF has $BT = 0.25$, predetection BPF has $BT = 1.25$ (both filters are Gaussian).

2.2.3 Tamed Frequency Modulation

Tamed Frequency Modulation was introduced specifically for digital mobile radio communications [108]. The block diagram of a TFM transmitter is shown in Figure 2.31. The difference between TFM and GMSK is the pulse response of the premodulation filter. The spectrum of TFM is almost identical to the spectrum of GMSK with $B_tT = 0.22$ (see Figure 2.30).

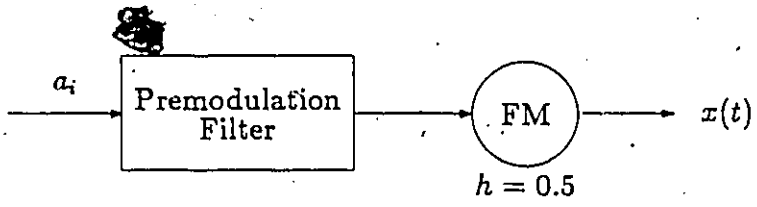

Figure 2.30: Block diagram of a TFM transmitter.

Using the notation introduced at the beginning of this section, the pulse shaping function $p(t)$ for TFM can be represented by [93]:

$$p(t) = \frac{1}{8}[p_0(t-T) + 2p_0(t) + p_0(t+T)], \tag{2.89}$$

where

$$p_0(t) \approx \sin(\frac{\pi t}{T})[\frac{1}{\pi t} - \frac{2 - \frac{2\pi t}{T}\cot(\frac{\pi t}{T}) - \frac{\pi^2 t^2}{T^2}}{\frac{24\pi t^3}{T^2}}]. \tag{2.90}$$

TFM can be differentially detected by using a conventional two-bit symbol-by-symbol differential detector. However, the resulting BER performance is rather poor [92][16]. Our simulation results indicate that for a BER of 10^{-4}, an E_b/N_0 of 20.5 db is required. This can be explained by the fact that in TFM the signal phase changes by $\pm 90°$ or $\pm 45°$ over a bit interval. Hence the phase margin is only 45°.

[16]This conclusion is reached in [92]; but a quantitative result for BER $< 10^{-2}$ is not presented.

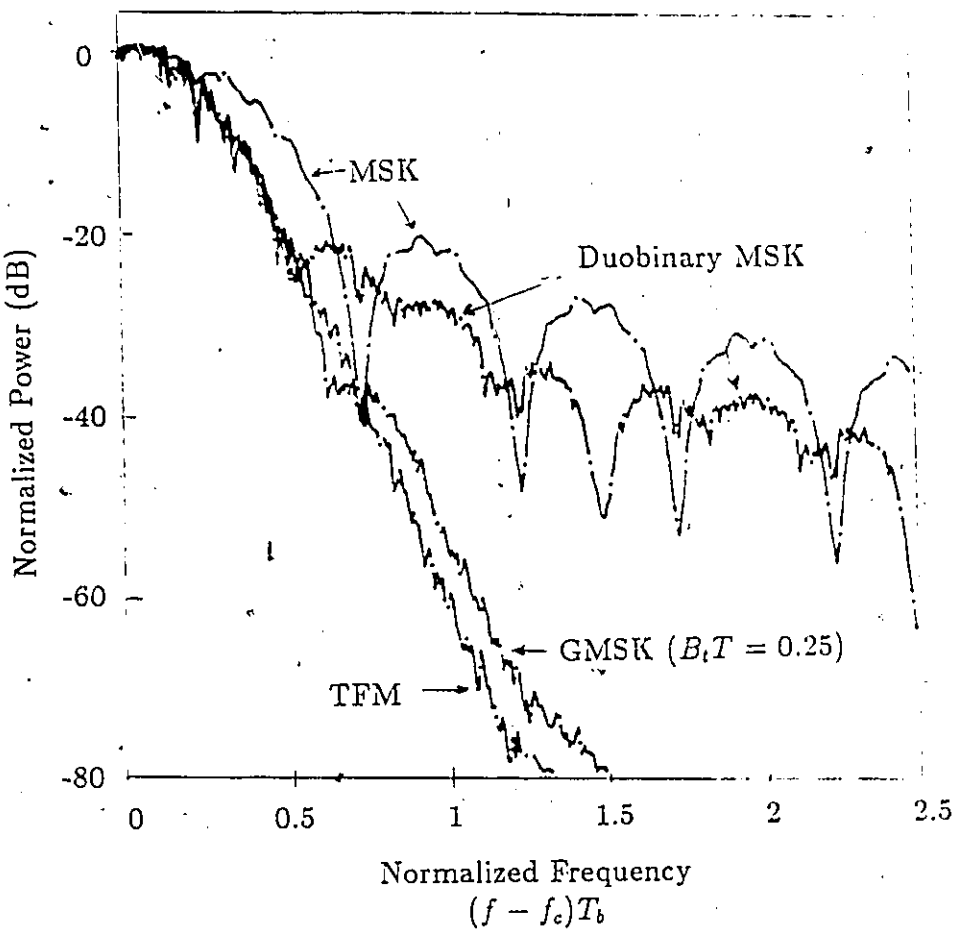

Figure 2.31: Spectra of MSK, Duobinary MSK, GMSK and TFM signals.

2.2.4 Duobinary MSK

Duobinary MSK is obtained by inserting a duobinary encoder at the input of an MSK transmitter. The block diagram of a Duobinary MSK transmitter is shown in Figure 2.32. The operation performed by the encoder is described by

$$b_k = \frac{1}{2}(a_k + a_{k-1}), \tag{2.91}$$

where a_k takes the values ± 1 and b_k takes the values ± 1 and 0. Hence the input to the FM modulator can be described by

$$s(t) = \sum_k b_k p(t), \tag{2.92}$$

where

$$p(t) = \begin{cases} \frac{1}{2T} & \text{for } 0 \le t \le T \\ 0 & \text{otherwise.} \end{cases} \tag{2.93}$$

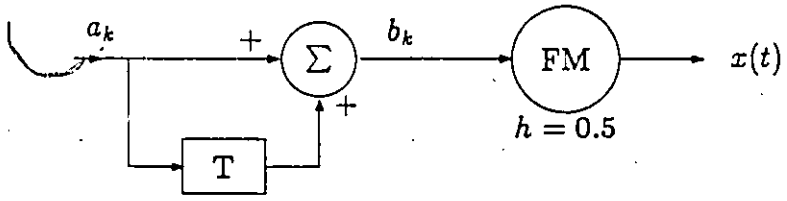

Figure 2.32: Block diagram of a Duobinary MSK transmitter.

The spectrum of Duobinary MSK is plotted in Figure 2.31. It can be observed that Duobinary MSK is not as bandwidth efficient as GMSK or TFM; but it provides a bandwidth efficiency advantage over MSK.

The differential detection of Duobinary MSK is similar to that of DMSK [114]. In comparison to DMSK, to achieve a BER of 10^{-4}, differentially detected Duobinary MSK requires about 4 dB more E_b/N_0 [114]. Hence the above noted bandwidth efficiency advantage over DMSK is traded off for detection efficiency.

2.3 CONCLUSIONS

We have reviewed the differential detection of PSK and CPM signals. It is often desirable to compare the bandwidth and power efficiencies of these modulation schemes. Yet, defining comparison criteria which applies equally well to both PSK and CPM signals is difficult.

PSK signals are generally filtered and thus have nonconstant envelopes. The major application of PSK is in linear or mildly nonlinear channels. On the other hand, CPM signals are particularly suitable to nonlinear channels because of their constant envelope property. Any post modulation filtering annihilates this constant envelope property. Therefore CPM signals are usually not filtered[17].

Given a certain channel characteristic and adjacent channel interference conditions, a performance comparison of PSK versus CPM schemes is meaningful. But for a general discussion, we shall treat them separately.

PSK

The theoretical bandwidth efficiency of m-ary PSK signals is $\log_2(m)$ b/s/Hz[18]. However, using practical filters, the bandwidth efficiency achieved is less than the theoretical limit.

Assuming that the transmit filter used has a square-root raised-cosine characteristic with $\alpha = 1$ (plus an x/sinx equalizer), then the 99% and 99.99% bandwidth efficiencies of DBPSK, DQPSK and DOQPSK signals are as shown in Table 2.2. When the bandwidth is defined as the percent power containment bandwidth in this manner[19], then it is a function of the roll-off factor α. Reducing the α increases the bandwidth efficiency as shown in Table 2.2.

The E_b/N_0 required to achieve a BER of 10^{-4} is also given in Table 2.2. Note that BER performance with only conventional differential detectors is considered (i.e., additional receiver processing is not taken into account). In comparison to coherent detection, DBPSK provides the best detection

[17]Rarely, a mild transmit filtering is applied.

[18]This assumes that a brickwall filter with a cutoff frequency of $1/2T_s$ is employed.

[19]Various other definitions of bandwidth (e.g., null to null bandwidth, 3 dB bandwidth etc.) are given in [115].

efficiency. However the bandwidth efficiency of DBPSK is half of that of DQPSK or DOQPSK.

In DBPSK and DQPSK, as long as the raised cosine shaping is equally split between the transmitter and the receiver, then the BER performance is independent of the roll-off factor α. In DOQPSK this is not the case, and the performance degrades significantly as α is reduced from 1 to 0.5.

The bandwidth efficiency and detection efficiency values given in Table 2.2 are valid only for linear channels. In nonlinear channels the filtered sidelobes will be partially restored, and hence the bandwidth efficiency drops. Furthermore, equal splitting of the raised-cosine characteristic between the transmit and receive filters while satisfying the first Nyquist criterion is no longer possible. Consequently, the detection efficiency is reduced as well.

CPM

The bandwidth and detection efficiency of DMSK, differentially detected Duobinary MSK, DGMSK, and differentially detected TFM signals are given in Table 2.3. The percent power containment bandwidth assumes that no postmodulation filtering is applied. The detection efficiency is based on conventional differential detectors, i.e., no additional receiver processing is applied.

Among the four CPM schemes considered, TFM has the best bandwidth efficiency, and DMSK has the best detection efficiency. Table 2.3 demonstrates the tradeoff involved between the bandwidth efficiency and detection efficiency.

In important criterion which is not included in Tables 2.2 and 2.3 is the modem complexity. As the systems become more bandwidth efficient, the modem complexity is increased. Further increase in the modem complexity may be introduced if the detection efficiency traded off for bandwidth efficiency is to be partially recovered by sophisticated (i.e., non-conventional) receiver structures. For example, in the case of DGMSK with $B_tT = 0.25$, a new receiver described in Chapter 4 improves the detection efficiency by about 4 dB.

Modulation Type	99% Bandwidth Efficiency (b/s/Hz)	99.99% Bandwidth Efficiency (b/s/Hz)	E_b/N_0 for BER=10^{-4} (dB)	Degradation with respect to Coherent PSK (dB)
DBPSK	0.55†	0.5†	9.3	0.9
	0.72*	0.67*		
DQPSK	1.1†	1.0†	10.7	2.3
	1.44*	1.34*		
DOQPSK	1.1†	1.0†	13.6†	5.2†
	1.44*	1.34*	18.0*	9.6*

Table 2.2: Bandwidth and detection efficiency of conventional DBPSK, DQPSK and DOQPSK. † Raised-cosine is equally split between the transmitter and receiver and the roll-off factor $\alpha = 1$. * Raised-cosine is equally split with $\alpha = 0.5$.

Modulation Type	99% Bandwidth Efficiency (b/s/Hz)	99.99% Bandwidth Efficiency (b/s/Hz)	E_b/N_0 for BER=10^{-4} (dB)	Degradation with respect to Coherent MSK (dB)
DMSK	0.85	0.17	12.3	3.9
Duobinary MSK	1.15	0.25	16.1	7.7
DGMSK ($B_tT = 0.25$)	1.22	0.77	17.2	8.8
TFM	1.25	0.8	20.5	12.1

Table 2.3: Bandwidth and detection efficiency of differentially detected MSK, Duobinary MSK, GMSK and TFM.

Chapter 3

DIFFERENTIALLY DETECTED CONTROLLED TRANSITION PSK (DCTPSK)

3.1 INTRODUCTION

In Chapter 2, we have seen that DBPSK has good detection efficiency but it is not bandwidth efficient. DQPSK is twice more bandwidth efficient than DBPSK, but this is at the expense of reduced detection efficiency. DQPSK is suited to single carrier operation or to applications where the amplifiers are operated in the linear region. When DQPSK is used in configurations including nonlinear amplifiers, the filtered sidelobes are restored. Consequently, in a multicarrier adjacent channel interference environment, DQPSK cannot efficiently utilize the available bandwidth. Conversely, nonlinearly amplified, differentially detected OQPSK has less spectral regrowth than DQPSK, but its BER performance is rather poor. In conclusion, the existing differentially detected PSK signals do not provide a good bandwidth/power efficiency tradeoff in nonlinear channels.

CPM signals, due to their constant envelope property, suffer very little from nonlinear amplification [116,117]. Among the differentially detected

CPM signals, MSK has the best detection efficiency. However, MSK has a wide main-lobe (50% wider than QPSK) which limits the efficient utilization of the available bandwidth by multiple MSK carriers. As differential detection is applied to more bandwidth efficient CPM signals (e.g., TFM or GMSK), the detection efficiency drops drastically[1].

Based on these conclusions, one of the objectives of my research was to design a modem which would outperform DQPSK and DMSK modems when nonlinear amplifiers are used in closely spaced multicarrier operation.

This chapter introduces a new modem technique to fulfill the objectives mentioned above. In this modem tehnique, the modulator modifies the well-known DQPSK signal so as to control the path of the phase transitions, and the demodulator employs differential detection. Hence, the technique used in the new modem is called Differentially detected Controlled Transition Phase Shift Keying (DCTPSK).

In the description of DCTPSK which follows, first the transmit baseband pulse shaping is introduced; then the operating principle of the modem is demonstrated with the aid of waveforms at various points in the system. After presenting the spectral properties of the DCTPSK signal, the BER performance of the modem is evaluated in a multicarrier adjacent channel interference environment. In Section 3.6, two novel receiver structures which improve the BER performance of the DCTPSK modem are then presented. A description of a laboratory model hardware DCTPSK modem is given in Section 3.7. Finally, the experimental results of the modem back to back and satellite link measurements are presented, and various sources of performance impairments are discussed.

3.2 PULSE SHAPING

The starting point of designing the new modem was a consideration of the signal-space diagram of various quadrature modulated signals. To reduce spectral regrowth after a nonlinearity, the signal phase transitions should be

[1] At this point, our discussion is confined to using conventional differential detection. As it will be shown in Chapter 4, by introducing more complex receiver structures, the loss in detection efficiency can be partially recovered.

controlled such that the signal envelope never falls below a certain minimum level [86]. Let us illustrate this with an example. The SSD of QPSK is redrawn in Figure 3.1. Assuming that the signal is at state A, then AB,

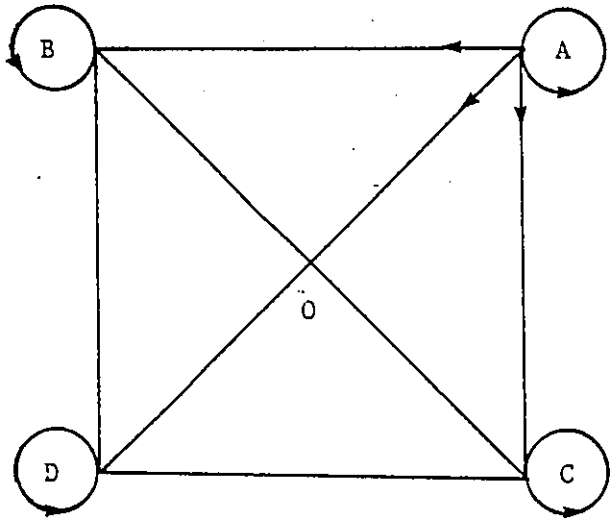

Figure 3.1: Signal-space diagram of QPSK

AC, AD and AA transitions correspond to carrier phase changes of $+90°$, $-90°$, $180°$ and $0°$ respectively. During the AB and AC transtions, the envelope fluctuates at most 3 dB. However, during the AD transition, the envelope momentarily becomes zero which represents a 100% fluctuation.

Figure 3.2 depicts another SSD, where again AA, AB, AC and AD are all legitimate transitions. However, in this case, when the AD transition takes place, the trajectory is AEFD rather than AOD. By changing the trajectory, the envelope fluctuation is limited to 4 dB. Consequently, the spectral regrowth after a nonlinearity may likewise be kept at a low level.

It should be noted that SSD only indicates the transition paths. Another important aspect, the speed of transition from one state to another state, is not conveyed by the SSD. Hence, signals such as QPSK and IJF-QPSK [89] may have the same SSD, yet the corresponding spectra are different. In unfiltered QPSK the transitions are instantaneous, whereas in IJF-QPSK the transitions are smooth and take one symbol duration. The smoother phase transitions of IJF-QPSK result in a more compact spectrum than

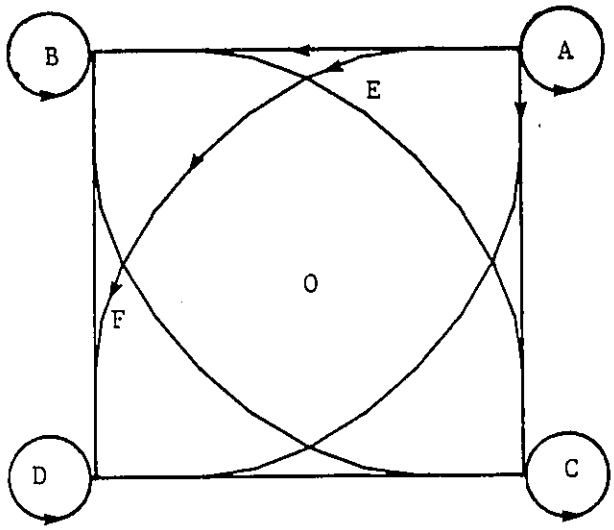

Figure 3.2: Signal-space diagram of DCTPSK

QPSK; this design approach is also exploited in DCTPSK.

Choosing transitions with smooth functions and also limiting the amplitude fluctuation are only one dimension of the signal design. The other dimension is the suitability to differential detection, and this requires that the differential phase angles be large at the sampling instants.

The phase characteristics of a number of candidate waveform elements which satisfy the compact spectrum requirement (i.e., smooth transitions) and have the SSD of Figure 3.2 were studied. Through an iterative process, the waveform elements which follow were found to satisfy these objectives.

The encoding rules of the selected waveform elements can be formulated in the following manner. Let $\{a'_k\}$ and $\{b'_k\}$ be the differentially encoded input symbols which take the values ± 1, then

1. If $a'_k = a'_{k-1}$ and $b'_k = b'_{k-1}$, then in both channels transmit constant amplitude signals, i.e.,

$$i(t) = a'_k \quad \text{for} \quad 0 \leq t \leq T_s \tag{3.1}$$

and similarly

$$q(t) = b'_k \quad \text{for} \quad 0 \leq t \leq T_s \tag{3.2}$$

where T_s is the symbol duration (i.e., $T_s = 2T_b$).

2. If $a'_k = a'_{k-1}$ and $b'_k = -b'_{k-1}$, then in the I-channel transmit a constant amplitude signal, and in the Q-channel transmit a segment of a sinusoid. In other words,

$$i(t) = a'_k \qquad \text{for} \quad 0 \le t \le T_s \tag{3.3}$$

and

$$q(t) = b'_k \cos(\frac{\pi t}{T_s}) \qquad \text{for} \quad 0 \le t \le T_s \tag{3.4}$$

3. Similarly, if $a'_k = -a'_{k-1}$ and $b'_k = b'_{k-1}$, then

$$i(t) = a'_k \cos(\frac{\pi t}{T_s}) \qquad \text{for} \quad 0 \le t \le T_s \tag{3.5}$$

and

$$q(t) = b'_k \qquad \text{for} \quad 0 \le t \le T_s \tag{3.6}$$

4. If $a'_k = -a'_{k-1}$ and $b'_k = -b'_{k-1}$, then $i(t)$ and $q(t)$ signals must change signs at different times. For this case we transmit

$$i(t) = \begin{cases} -a'_k & \text{for} \quad 0 \le t \le T_s/4 \\ -a'_k \cos(4\pi(t/T_s - 1/4)/3) & \text{for} \quad T_s/4 \le t \le T_s \end{cases} \tag{3.7}$$

and

$$q(t) = \begin{cases} -b'_k \cos(4\pi t/3T_s) & \text{for} \quad 0 \le t \le 3T_s/4 \\ -b'_k & \text{for} \quad 3T_s/4 \le t \le T_s \end{cases} \tag{3.8}$$

3.3 MODULATOR-DEMODULATOR DESCRIPTION AND ASSOCIATED WAVEFORMS

The DCTPSK system is formed by applying the signal processing described in Section 3.2 to a quadrature modulator and using differential detection at the receiver. A block diagram of the resulting system is given in Figure 3.3.

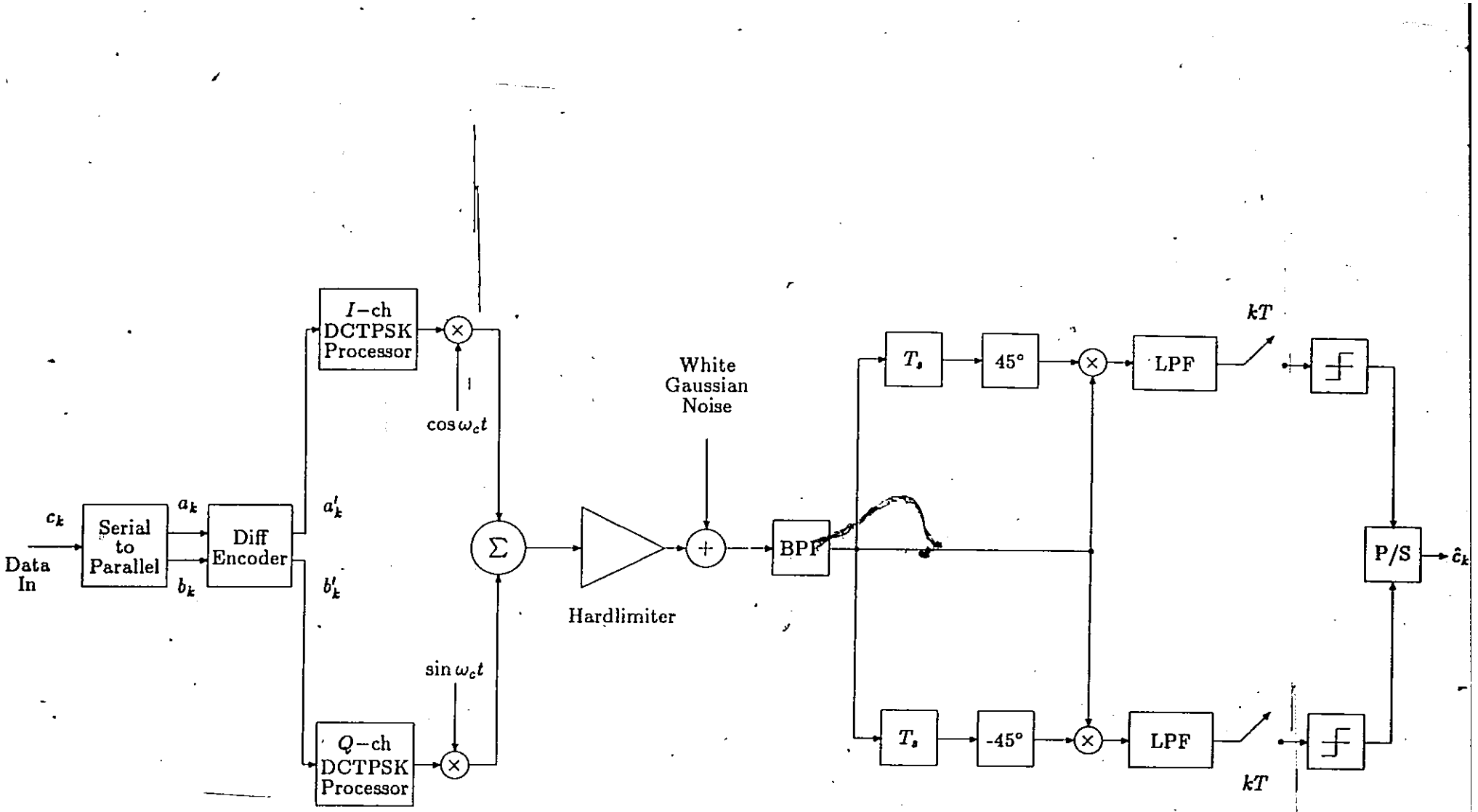

Figure 3.3: Block Diagram of a DCTPSK system model.

The operation of the modem of Figure 3.3 can best be explained with the aid of the waveforms at various points in the system. The input non-return to zero (NRZ) data (Figure 3.4, trace (a)) of $1/T_b$ bits/second is first serial to parallel converted into two binary streams (traces (b) and (c)), each with a bit rate of $1/T_s$ bits/second ($T_s=2T_b$). These two binary streams are then fed into a differential encoder. The rules applied by the differential encoder are:

$$a'_k = \overline{(a_k \oplus b_k)}(a_k \oplus a'_{k-1}) + (a_k \oplus b_k)(b_k \oplus b'_{k-1}) \tag{3.9}$$

$$b'_k = \overline{(a_k \oplus b_k)}(b_k \oplus b'_{k-1}) + (a_k \oplus b_k)(a_k \oplus a'_{k-1}) \tag{3.10}$$

where $\{a_k\}$, $\{b_k\}$ are the uncoded and $\{a'_k\}$, $\{b'_k\}$ are the coded sequences, and $\oplus$ and $+$ represent the logical operations of exclusive-OR and OR respectively. The differentially encoded sequences (trace (d) and (e)) are fed into the DCTPSK processors The processor for the I-channel operates slightly differently from the Q-channel processor, as described in Section 3.2.

The DCTPSK processors consist of two stages: the first stage uses the present and the immediately past I and Q-channel input bits to determine the corresponding transition. The second stage generates the selected pulse shape which may be implemented, for example, in the form of a look-up table. The outputs of the I and Q-channel processors are depicted by traces (f) and (g) of Figure 3.4 respectively. These baseband signals modulate the quadrature carriers $\cos \omega_c t$ and $\sin \omega_c t$ (traces (h) and (i)). The transmitted signal, trace (j), is the sum of (h) and (i).

The waveforms associated with the receiver are given in Figure 3.5. The noisy receive signal (trace (a)) is first passed through a BPF to reject out-of band noise. For the detection of the I-channel signal, the predetection filtered received signal (see trace (b)) is multiplied by a 45° shifted and T_s second delayed version of itself (see trace (c)). The second harmonic terms resulting from the multiplication (see (d)) are removed by the LPF (see trace (e)). Then the baseband signal is passed through a decision device to obtain an estimate of the I-channel signal (see trace (f)). A similar process takes place in the Q-channel detector. Finally, the decoded I and Q-channel streams are parallel to serial converted to produce the output data stream at the rate of $1/T_b$ bits per second.

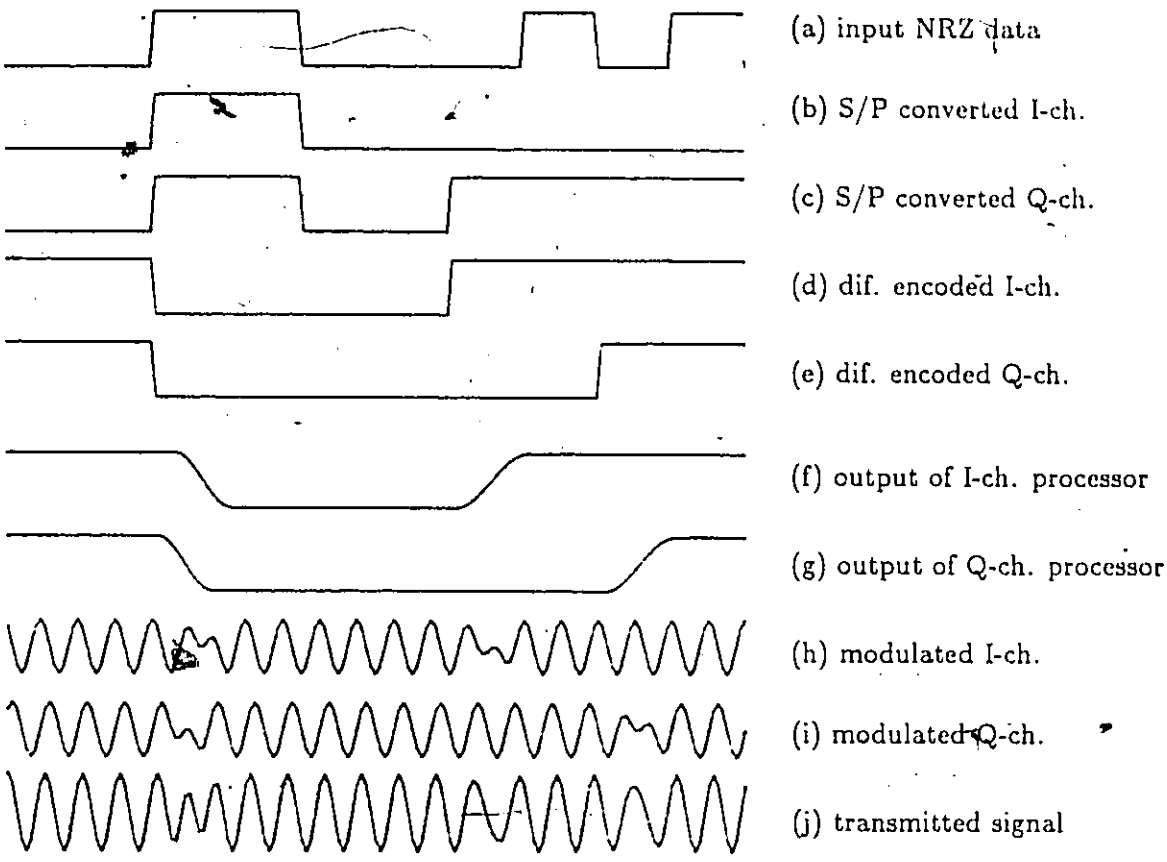

Figure 3.4: DCTPSK Modulator Waveforms

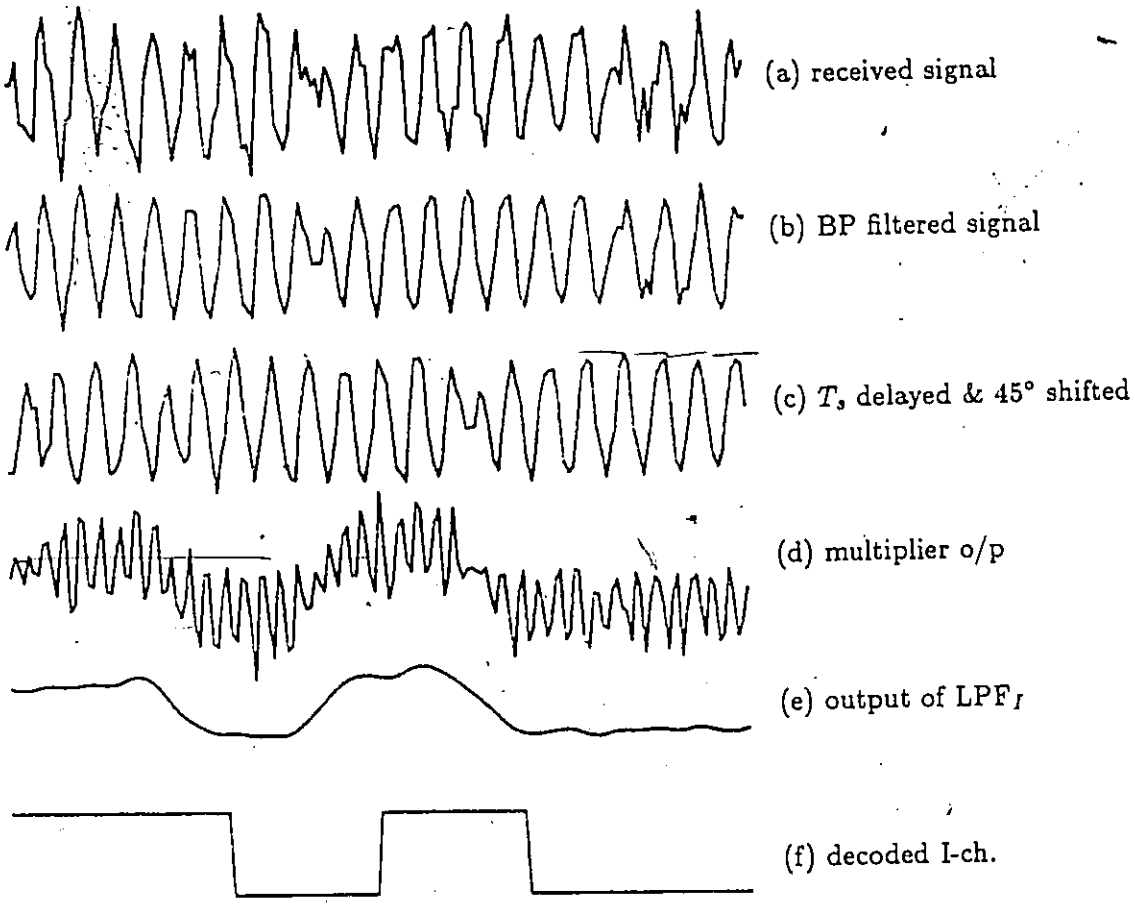

Figure 3.5: DCTPSK Demodulator Waveforms.

3.4 SPECTRUM

The power spectra of DQPSK and DCTPSK obtained by using a laboratory set-up are shown in Figure 3.6. The spectrum of DCTPSK displays much lower sidelobes than DQPSK, and this suggests that DCTPSK can be employed without any additional filtering at the transmitter.

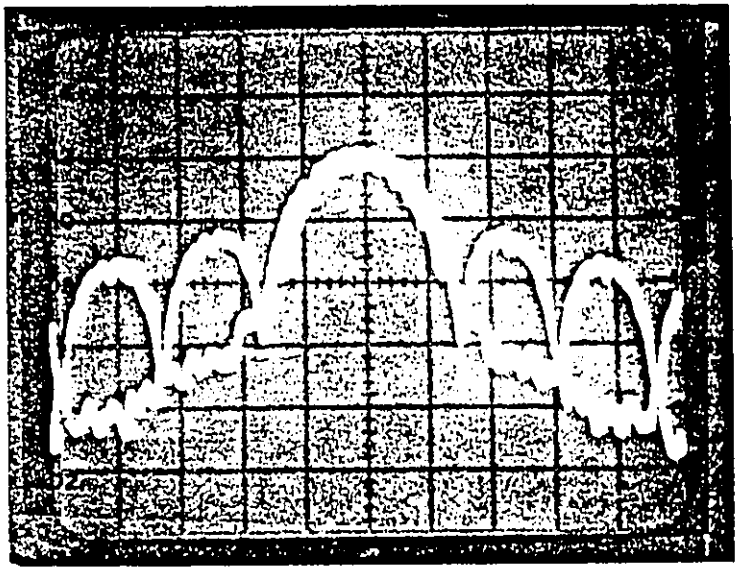

Figure 3.6: Measured spectra of DQPSK (upper trace) and DCTPSK (lower trace). Vert: 10 dB/div; Horiz: 20 kHz/div; resolution bandwidth: 10 kHz; bit rate=64 kb/s; carrier frequency 70 MHz.

The power spectra of DCTPSK, DQPSK and DMSK have also been estimated by computer simulations and plotted in Figure 3.7. The fractional out-of-band power as a function of normalized frequency (i.e., bandwidth in units of bit rate) of unfiltered DQPSK, DMSK and hardlimited DCTPSK are plotted in Figure 3.8[2]. The percent energy containment bandwidths of

[2]Note that unfiltered DQPSK and DMSK have constant envelopes and hardlimiting for spectrum estimatation is unnecessary.

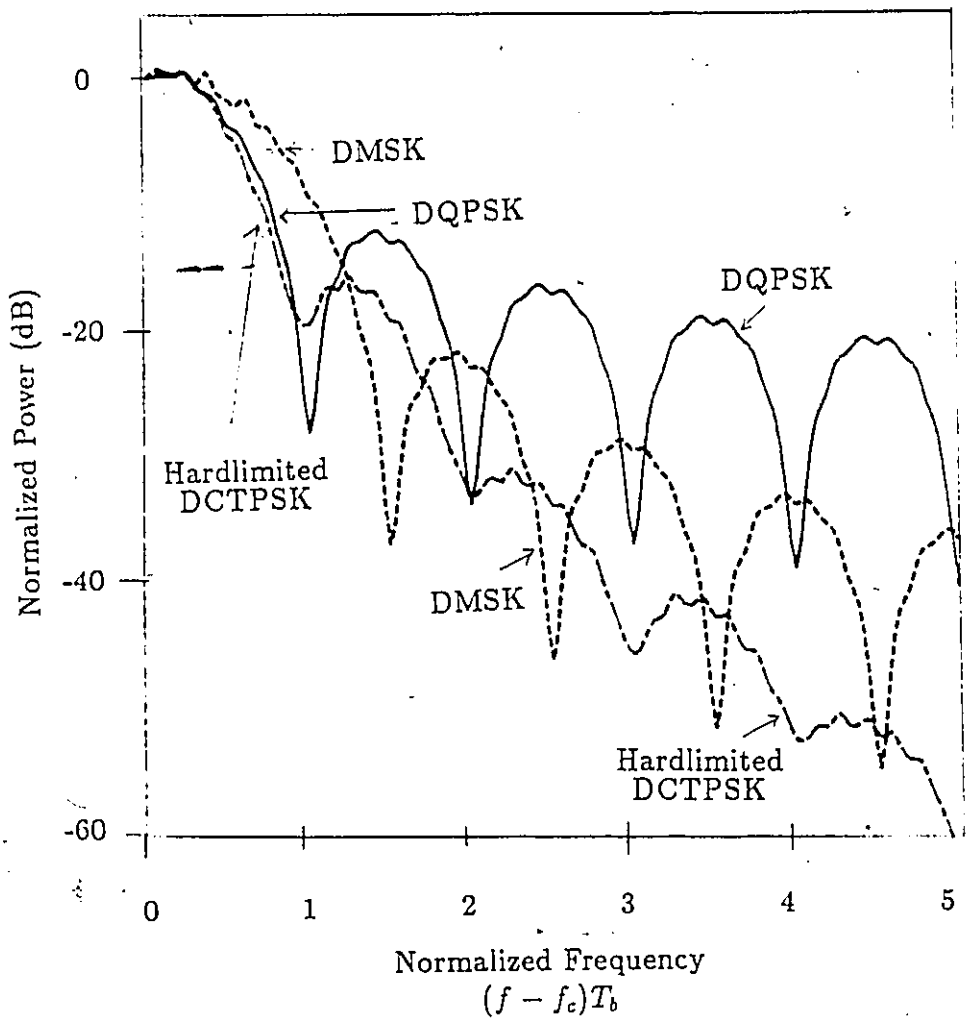

Figure 3.7: Power spectra of unfiltered DQPSK, DMSK and DCTPSK in a hardlimited channel.

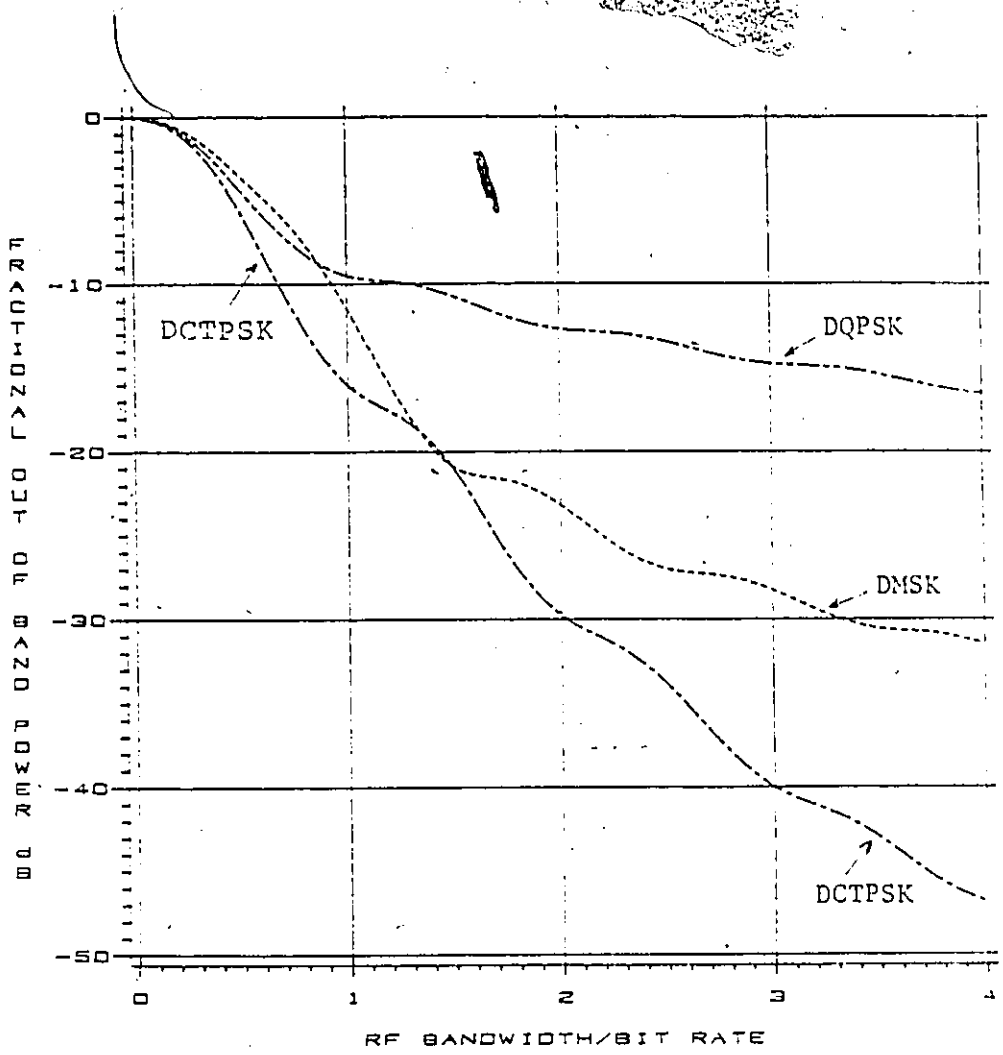

Figure 3.8: Fractional out-of-band power of unfiltered DQPSK, DMSK and DCTPSK in a hardlimited channel.

these signals similarly are given in Table 3.1. From Figures 3.6 and 3.8,

Modulation Type	Required RF bandwidth/bit rate	
	99% (20 dB)	99.99% (40 dB)
QPSK	10.3	620
MSK	1.2	5.7
DCTPSK (Hardlimited)	1.4	3.0

Table 3.1: Percent energy containment bandwidth of DQPSK, DMSK and DCTPSK signals.

and Table 3.1, it can be observed that DCTPSK has a compact main-lobe and low spectral components at high frequencies. The advantage of such a spectrum will be apparent when we next consider system operation in an adjacent channel interference environment.

3.5 BER PERFORMANCE IN MULTICARRIER CHANNELS

The specific case we wish to consider is that of *single carrier per transmitter* DCTPSK in a multicarrier channel when the transmitter includes a nonlinear amplifier. Multicarrier operation is here meant to refer to the situation where several users share the same channel by frequency division multiple access (e.g., as in some designs for mobile satellite communications). In many such cases, it is important that the transmit amplifier be used as efficiently as possible; and this in turn dictates operation close to the amplifier's saturation point, in the nonlinear region of amplifier operation. To provide us with a reference for comparisons, the performance of DQPSK and DMSK modem techniques are also evaluated under the same operating conditions.

The impairments considered in the modem evaluations described below are:

- thermal noise,

- bandlimiting,
- AM/AM conversion due to hardlimiting,
- adjacent channel interference from neighbouring carriers.

To estimate the BER performance of the cited modem techniques with the above listed impairments, we have used computer simulation methods based on Monte Carlo error counting techniques. The block diagram of the simulation model is given in Figure 3.9. The reason for choosing the Monte

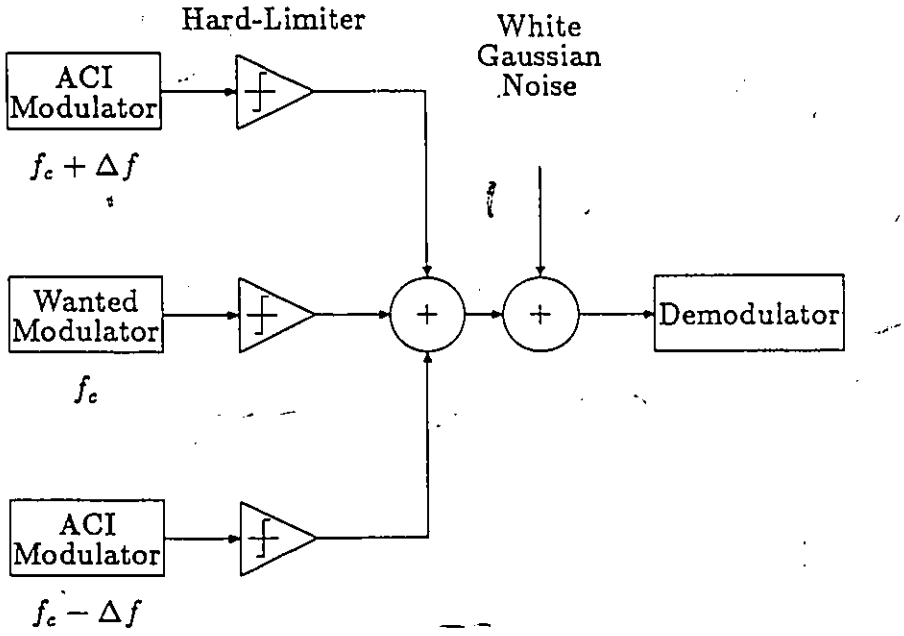

Figure 3.9: Simulation model of a hardlimited multicarrier system.

Carlo technique and the program listings are given in Appendix B.

3.5.1 Selection of Transmit and Receive Filters

To utilize the available bandwidth efficiently, the out-of-band energy and the corresponding adjacent channel interference must be reduced. This can be achieved by bandlimiting the transmitted and received signal. The bandlimiting causes envelope fluctuations and time dispersion which then result in ISI and degraded performance. Thus, a tradeoff exists for the selection of the transmit and receive filters.

In selecting the transmit and receive filter characteristics, the desired properties are:

- minimizing the thermal noise at the receiver;
- minimizing the ISI;
- minimizing the AM/AM conversion due to hardlimiting;
- limiting the transmitter output spectrum to minimize the interference into adjacent channels.

All four properties stated above cannot in general be met simultaneously. Hence, in practice, the transmit and receive filters are selected such that the performance with the various impairments is near optimum. For each modem technique, the transmit filtering (and/or pulse shaping) and receive filtering which yield marginally suboptimum BER performance are as follows.

DCTPSK achieves its low out-of-band energy properties by using pulse shaping. Hence there is no need for any additional transmit filtering. As a predetection BPF, various raised-cosine family filters, Butterworth and Chebycheff filters have been evaluated. The best results have been obtained when a fourth-order phase equalized Butterworth filter is used with a bandwidth-time product, i.e., BT_b, of 0.75.

For DQPSK, in a linear channel, the sidelobes can be filtered out completely (i.e., no ACI), and the optimum performance is obtained by splitting the Nyquist-1 [79] shaping equally between the transmitter[3] and the predetection BPF. However, in a nonlinear satellite channel, equal splitting

[3]The transmitter also includes a x/sinx amplitude equalizer.

of the Nyquist-1 shaping no longer results in the optimum performance [118]. Taking the ACI into consideration, our simulation results indicate that for the hardlimited DQPSK signal, the near optimum performance is obtained when the transmit filter and predetection BPF are both a fourth order Butterworth type with $BT_b = 0.65$. The same filtering strategy is also proposed in [118].

DMSK has a wider main-lobe than DQPSK and DCTPSK, and therefore it requires a wider predetection BPF. If the ACI is not present, the best performance is obtained when the transmitted DMSK signal is not filtered and the predetection filter is a fourth-order equalized Butterworth with $BT_b = 1.1$. The same result has also been reported in [98]. When ACI is taken into account, a transmit filter is necessary; and a predetection BPF with a smaller BT_b performs better. We have found the best transmit and predetection filter combination as fourth-order Butterworth filters with $BT_b = 1.2$ and $BT_b = 0.9$ respectively.

The transmit and predetection filters used in DCTPSK, DQPSK and DMSK modems are summarized in Table 3.2.

Modem	Transmit Filter	Predetection Filter
DQPSK	4th order Butterworth with $BT_b = 0.65$	4th order Butterworth with $BT_b = 0.65$
DMSK	4th order Butterworth with $BT_b = 1.2$	4th order Butterworth with $BT_b = 0.9$
DCTPSK	not necessary	4th order Butterworth with $BT_b = 0.75$

Table 3.2: Filtering strategies for DQPSK, DMSK and DCTPSK modems.

3.5.2 BER Curves

To evaluate BER performance in a multicarrier environment, it is assumed here that the signal in the wanted channel is heavily attenuated (e.g., due to fading) whereas the signals in the adjacent channels may not be subject to attenuation concurrently. This is depicted in Figure 3.10.

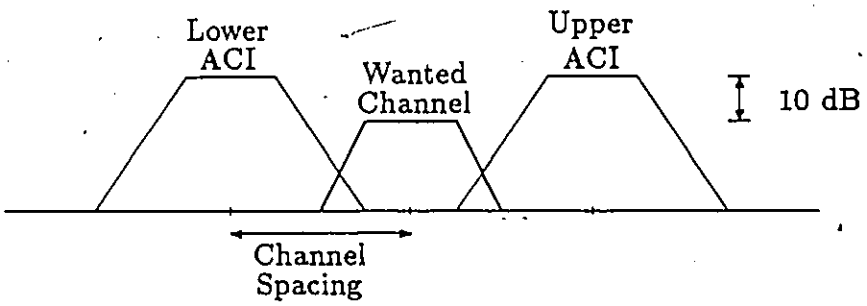

Figure 3.10: Adjacent channel interference model.

The degradation of each modem is evaluated and plotted in Figure 3.11 where it is assumed that the relative power of each interfering channel is 10 dB higher[4] than the wanted channel (with the same type of modulation and data rate). The reference point is the ideal theoretical performance of a DQPSK modem in a linear AWGN channel (i.e., no ACI). For example, for a BER $= 10^{-3}$, the ideal DQPSK modem requires an E_b/N_0 of 9.4 dB [74]. From Figure 3.11 we can conclude that as the bandwidth efficiency is increased (or equivalently as the channel spacing is reduced), DCTPSK performs better than DMSK and DQPSK. More specifically, if the total margin allocated to the combined degradations due to ISI, amplifier nonlinearities and ACI is 4 dB, then using DCTPSK, 20% or 40% more carriers may share the same channel as compared to DMSK and DQPSK respectively.

Another way of displaying the performances of the three modems is to keep the channel spacing and the relative signal (wanted and interfering)

[4]For example the MSAT system design given in [50] assumes a 13 dB fade margin.

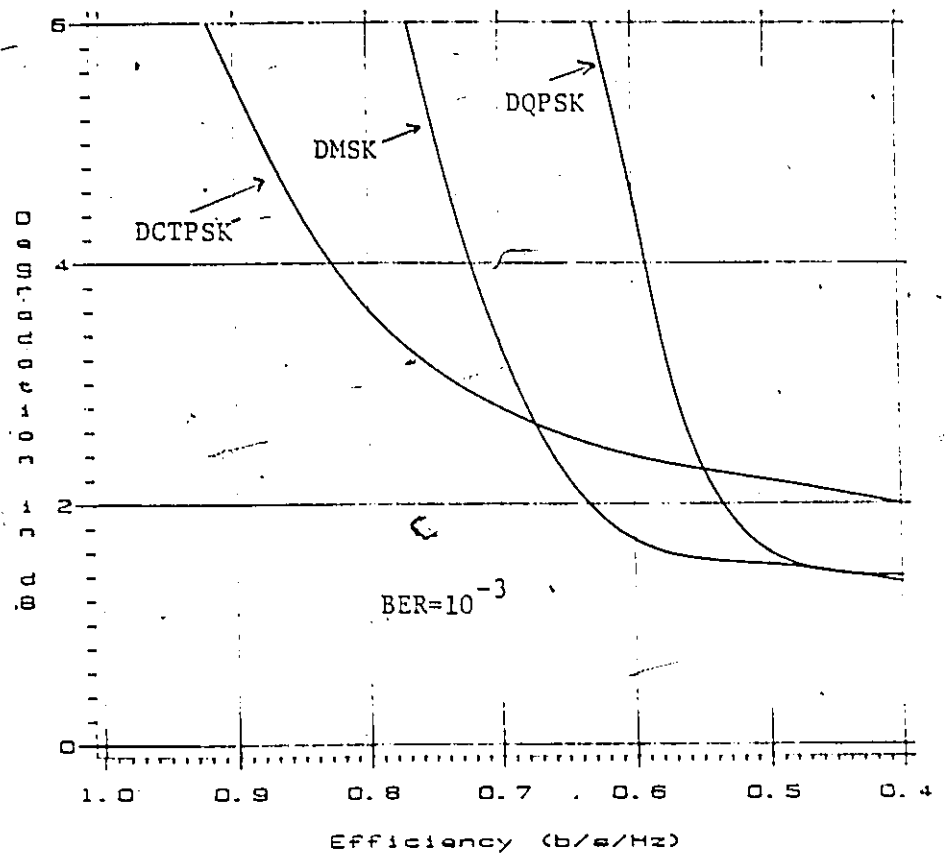

Figure 3.11: Performance comparison of DQPSK, DMSK and DCTPSK modems in a hardlimited multichannel system. Relative powers of the adjacent channel interferers are 10 dB higher than wanted channel. Degredation is with respect to theoretical ideal performance of DQPSK.

powers fixed and evaluate BER performance of the wanted channel. Assuming that the wanted channel experiences a 10 dB fade, BER versus C/N curves for the channel spacing of 0.75 b/s/Hz are given in Figure 3.12. The noise bandwidth used for the C/N measurement is $1/T_b$. From Figure 3.12 the following observations can be made:

- For DQPSK, the curves exhibit a tailing off at rather high BER values (i.e., 5×10^{-2}). This results from keeping the relative transmit powers of the wanted and interfering channel signals the same. Increasing the C/N ratio only reduces the contribution of the thermal noise; yet the ACI remains the same. Therefore operating a DQPSK modem with a nonlinear amplifier at such bandwidth efficiencies is prohibitive.

- Filtered DMSK has lower spectral components than DQPSK, hence the tailing off occurs at much lower bit error rates.

- For DCTPSK, at low C/N values, the effect of ISI is more dominant than ACI. Consequently at a BER of about 10^{-2} the performances of DMSK and DCTPSK are comparable. However, for lower bit error rates (e.g., 10^{-4}), DCTPSK offers a power efficiency advantage of more than 3 dB. Also note that DCTPSK is less sensitive to nonlinearities than DQPSK. Hence the operating point of the nonlinear amplifier (i.e., back-off) is not critical.

3.6 IMPROVING THE BER PERFORMANCE OF DCTPSK

In Section 2.1.1.4 it was mentioned that the BER performance of differentially detected systems can be improved by introducing additional processing at the receiver. The well-known nonredundant error correction (NEC) technique [26,30,28] can be directly applied to DCTPSK. Yet, two new techniques introduced in this section are more powerful than the NEC technique.

The first new technique to be introduced uses a symbol-by-symbol detector which combines the signal samples of the one-symbol and two-symbol

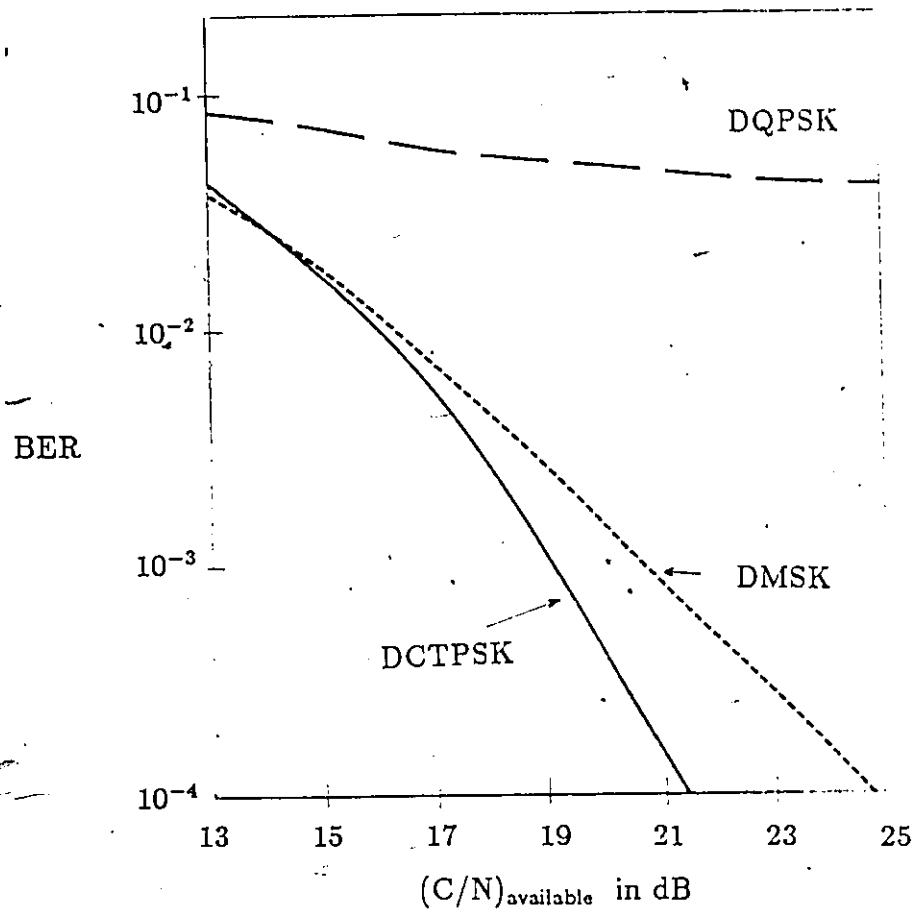

Figure 3.12: BER performance of DCTPSK, DMSK and DCTPSK modems in an ACI environment. Relative powers of the adjacent channel interferers are 10 dB higher than the wanted channel, and the bandwidth efficiency is 0.75 b/s/Hz. The filters used are given in Table 3.2.

detectors. The receiver structure is obtained by applying the maximum likelihood ratio test. The second structure introduced is a sequential detector. It uses the one-symbol and two-symbol detector outputs for maximum likelihood sequence estimation. Before presenting these new receivers, we shall first develop the underlying concepts and introduce the associated notation.

3.6.1 System Model

The DCTPSK receiver presented in Section 3.3 consisted of two differential detectors (one for each quadrature channel). Since the signal in the delay arm was delayed by one T_s period, these detectors are refered to as one-symbol detectors. The additional detectors introduced in this section delay the received signal by $2T_s$ and are called two-symbol detectors. The block diagram of a DCTPSK receiver which uses a one-symbol and a two-symbol detector for each quadrature channel is shown in Figure 3.13.

Following the notation used in Section 2.1.2.2, at the sampling instant $t = kT_s$ the output of each detector can be represented as

$$d_{1I}(k) = \cos(\theta_k - \theta_{k-1} - \frac{\pi}{4}) + n_{1I}(k) \tag{3.11}$$

$$d_{1Q}(k) = \cos(\theta_k - \theta_{k-1} + \frac{\pi}{4}) + n_{1Q}(k) \tag{3.12}$$

$$d_{2I}(k) = \cos(\theta_k - \theta_{k-2} - \frac{\pi}{4}) + n_{2I}(k) \tag{3.13}$$

$$d_{2Q}(k) = \cos(\theta_k - \theta_{k-2} + \frac{\pi}{4}) + n_{2Q}(k). \tag{3.14}$$

Recall from Section 2.1.2.2 that the transmitted phases are related such that

$$\theta_k - \theta_{k-1} = m_k \frac{\pi}{2} \tag{3.15}$$

where

$$\begin{array}{llllll} m_k = 0 & \text{for} & a_k = & 1 & \text{and} & b_k = 1 \\ m_k = 1 & \text{for} & a_k = & 1 & \text{and} & b_k = -1 \\ m_k = 2 & \text{for} & a_k = & -1 & \text{and} & b_k = -1 \\ m_k = 3 & \text{for} & a_k = & -1 & \text{and} & b_k = 1. \end{array} \tag{3.16}$$

Equations (3.11) to (3.16) will be used in describing the new receiver structures.

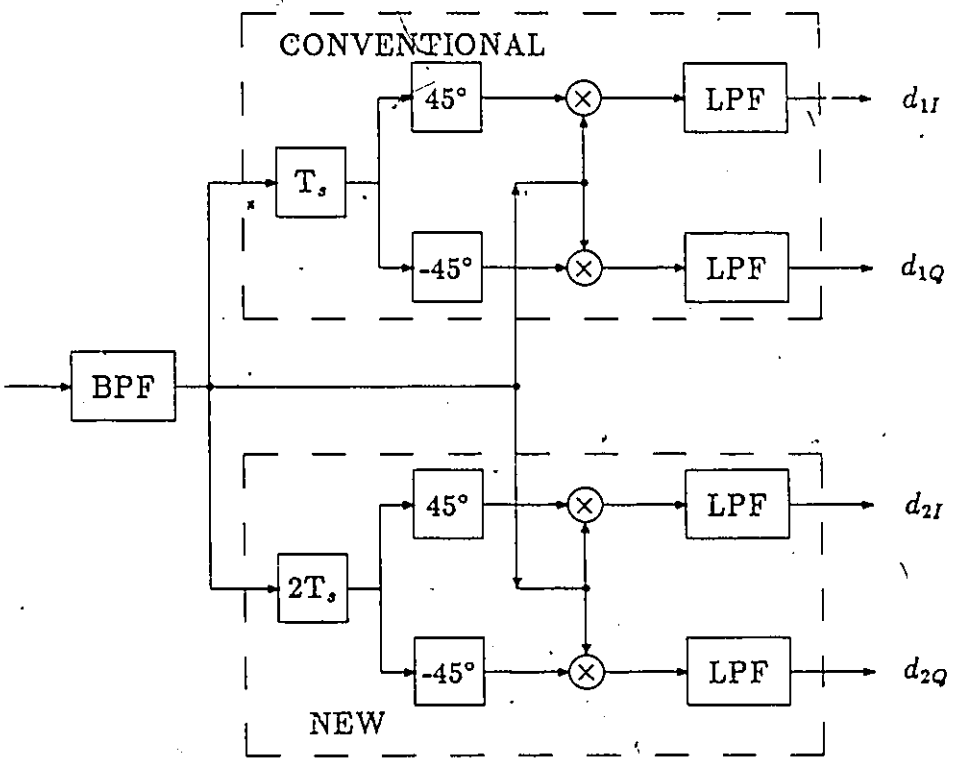

Figure 3.13: Block diagram of a DCTPSK receiver which uses one-symbol and two-symbol differential detectors.

3.6.2 A Symbol-by-Symbol Detector Using Combining With Feedback (CWF)

We want to use the outputs of the one-bit and two-bit detectors to estimate the input symbols a_k and b_k (or equivalently m_k). To establish the required relationships, we form the maximum likelihood ratio test (MLRT) given by

$$\frac{f(d_{1I}(k), d_{1Q}(k), d_{2I}(k), d_{2Q}(k)|m_k = \eta_1, \hat{m}_{k-1})}{f(d_{1I}(k), d_{1Q}(k), d_{2I}(k), d_{2Q}(k)|m_k = \eta_2, \hat{m}_{k-1})} \begin{array}{c} \hat{m}_k = \eta_1 \\ > \\ < \\ \hat{m}_k = \eta_2 \end{array} 1. \quad (3.17)$$

In (3.17), η_1 and η_2 are the hypotheses which take the values $\{0, 1, 2, 3\}$ while $\eta_1 \neq \eta_2$. To determine $\hat{m}_k$, the MLRT is applied three times. Suppose that initially $\eta_1 = 0$ and $\eta_2 = 1$. If the first MLRT yields $\hat{m}_k = \eta_1$, then in the second test we take $\eta_1 = 0$ and $\eta_2 = 2$. Suppose that this time we find $\hat{m}_k = \eta_2$. In the last test, we compare $\eta_1 = 3$ and $\eta_2 = 2$, and the result is the estimate of the transmitted phase difference, i.e., $\hat{m}_k$.

We assume that $f(d_{1I}(k), d_{1Q}(k), d_{2I}(k), d_{2Q}(k))$ is the probability density function of jointly normal random variables. The mean and variance of the noise components are calculated as

$$E[n_{1I}(k)] = E[n_{1Q}(k)] = E[n_{2I}(k)] = E[n_{2Q}(k)] = 0 \quad (3.18)$$

$$E[n_{1I}^2(k)] = E[n_{1Q}^2(k)] = E[n_{2I}^2(k)] = E[n_{2Q}^2(k)] = 2\sigma^2 \quad (3.19)$$

$$E[n_{1I}(k)n_{2I}(k)] = E[n_{1Q}(k)n_{2Q}(k)] = \sigma^2 \cos(m_{k-1}\frac{\pi}{2}) \quad (3.20)$$

$$E[n_{1I}(k)n_{2Q}(k)] = -E[n_{1Q}(k)n_{2I}(k)] = \sigma^2 \sin(m_{k-1}\frac{\pi}{2}) \quad (3.21)$$

$$E[n_{1I}(k)n_{1Q}(k)] = E[n_{2I}(k)n_{2Q}(k)] = 0. \quad (3.22)$$

Then we can write (see [120]),

$$\begin{aligned} &f(d_{1I}(k), d_{1Q}(k), d_{2I}(k), d_{2Q}(k)|m_k, \hat{m}_{k-1}) = \\ &\frac{1}{12\pi^2\sigma^4} \exp(-\frac{1}{9\sigma^4}[A^2(k) + B^2(k) + C^2(k) + D^2(k) \\ &-A(k)C(k)\cos(\hat{m}_{k-1}\frac{\pi}{2}) + A(k)D(k)\sin(\hat{m}_{k-1}\frac{\pi}{2}) \\ &-B(k)C(k)\sin(\hat{m}_{k-1}\frac{\pi}{2}) - B(k)D(k)\cos(\hat{m}_{k-1}\frac{\pi}{2})]) \end{aligned} \quad (3.23)$$

where

$$A(k) = d_{1I}(k) - \cos(m_k\frac{\pi}{2} - \frac{\pi}{4}) \quad (3.24)$$

$$B(k) = d_{1Q}(k) - \cos((m_k + \hat{m}_{k-1})\frac{\pi}{2} + \frac{\pi}{4}) \quad (3.25)$$

$$C(k) = d_{2I}(k) - \cos(m_k\frac{\pi}{2} - \frac{\pi}{4}) \quad (3.26)$$

$$D(k) = d_{1Q}(k) - \cos((m_k + \hat{m}_{k-1})\frac{\pi}{2} + \frac{\pi}{4}). \quad (3.27)$$

Substituting (3.23) into (3.17) and then simplifying the MLTR expressions, we find that when $\hat{m}_{k-1}$ is given, then $\hat{a}_k$ and $\hat{b}_k$ can be estimated in one iteration by the following relationships:

(i) If $\hat{m}_{k-1} = 0$, (i.e., $a_{k-1} = 1$ and $b_{k-1} = 1$) then

$$\hat{a}_k = \text{sgn}(d_{1I}(k) + d_{2I}(k)) \quad (3.28)$$

$$\hat{b}_k = \text{sgn}(d_{1Q}(k) + d_{2Q}(k)); \quad (3.29)$$

(ii) if $\hat{m}_{k-1} = 1$, (i.e., $a_{k-1} = 1$ and $b_{k-1} = -1$) then

$$\hat{a}_k = \text{sgn}(d_{1I}(k) - d_{2Q}(k)) \quad (3.30)$$

$$\hat{b}_k = \text{sgn}(d_{1Q}(k) + d_{2I}(k)); \quad (3.31)$$

(iii) if $\hat{m}_{k-1} = 2$, (i.e., $a_{k-1} = -1$ and $b_{k-1} = -1$) then

$$\hat{a}_k = \text{sgn}(d_{1I}(k) - d_{2I}(k)) \quad (3.32)$$

$$\hat{b}_k = \text{sgn}(d_{1Q}(k) - d_{2Q}(k)); \quad (3.33)$$

(iv) if $\hat{m}_{k-1} = 3$, (i.e., $a_{k-1} = -1$ and $b_{k-1} = 1$) then

$$\hat{a}_k = \text{sgn}(d_{1I}(k) + d_{2Q}(k)) \quad (3.34)$$

$$\hat{b}_k = \text{sgn}(d_{1Q}(k) - d_{2I}(k)). \quad (3.35)$$

The block diagram of the detector based on these decision laws is illustrated in Figure 3.14. The performance of the DCTPSK system using the receiver structure described above is evaluated in Section 3.6.4.

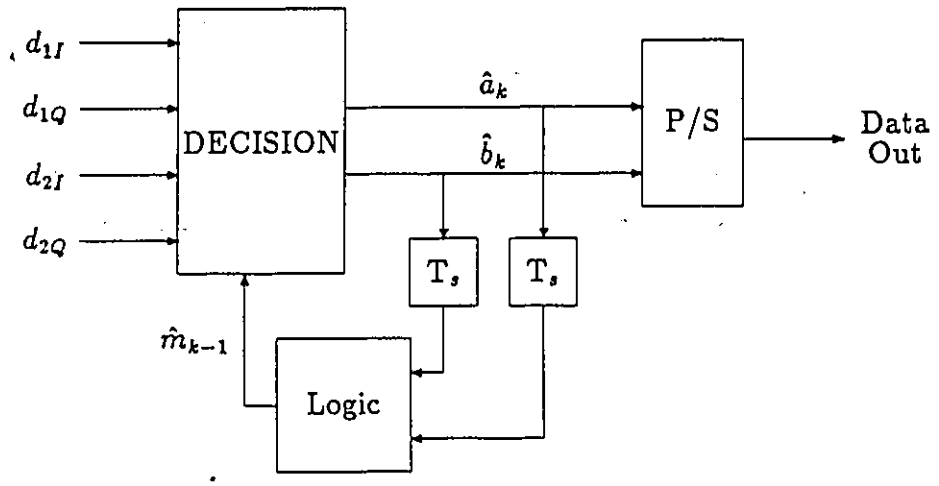

Figure 3.14: Block diagram of a detector which uses combining with feedback. (For the applicable decision laws see equations (3.29)–(3.35)).

3.6.3 A Simple Sequential Decoder

Having introduced a new receiver based on symbol-by-symbol detection, the next step is processing the outputs of the one and two bit detectors sequentially. In this case the decisions will depend not only on $d_{1I}(k)$, $d_{1Q}(k)$, $d_{2I}(k)$ and $d_{2Q}(k)$, but also on the history of the received signal.

For this purpose, we use a maximum likelihood sequence estimation method which finds, in terms of a predefined measure, the symbol sequence which is closest to the received signal [119]. This corresponds to selecting the data sequence which minimizes the mean square error $P(l)$, i.e.,

$$\begin{aligned} P(l) \;=\; & \underset{\text{over all } m_k}{\text{minimum}} \Big[\sum_{k=0}^{l} A^2(k) + B^2(k) + C^2(k) + D^2(k) \\ & -A(k)C(k)\cos(\hat{m}_{k-1}\frac{\pi}{2}) + A(k)D(k)\sin(\hat{m}_{k-1}\frac{\pi}{2}) \\ & -B(k)C(k)\sin(\hat{m}_{k-1}\frac{\pi}{2}) - B(k)D(k)\cos(\hat{m}_{k-1}\frac{\pi}{2})\Big] \end{aligned} \tag{3.36}$$

where $A(k), B(k), C(k)$ and $D(k)$ were defined in (3.24) – (3.27).

Since m_k can take the values $\{0,1,2,3\}$, a four-state Viterbi decoder [119] can solve this minimization problem recursively. Discarding the terms common to all metrics, (3.36) can be restated as a maximization problem in the form of

$$R(k) = \max(u_k(0), u_k(1), u_k(2), u_k(3)) \tag{3.37}$$

where $u_k(j)$ are the metrics for the surviving paths ending in state j at the time instant kT. The trellis diagram of the decoder is shown in Figure 3.15.

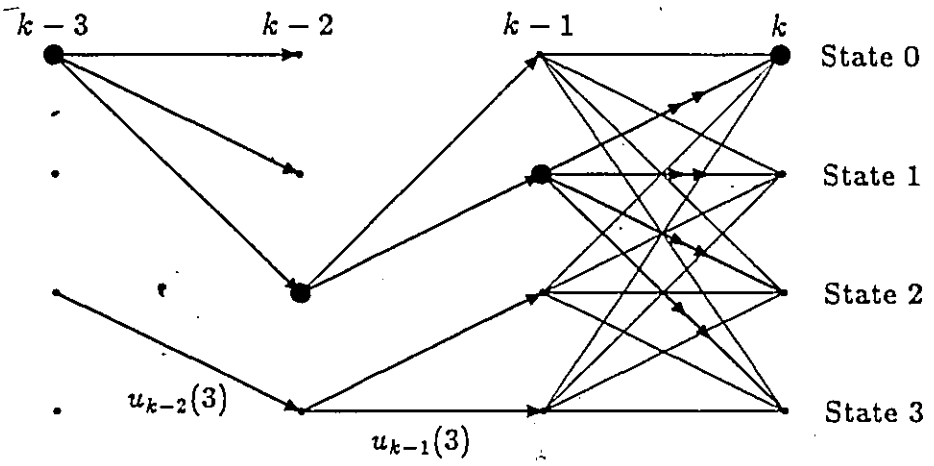

Figure 3.15: Trellis diagram of a four-state sequential decoder for DCTPSK.

The metric $u_k(j)$ can be expressed as

$$\begin{aligned} u_k(j) \;=\; & \underset{q=0,1,2,3}{\text{maximum}} \; [G_k(q,j) + u_{k-1}(q) + 2d_{1I}(k)\cos(j\frac{\pi}{2} - \frac{\pi}{4}) \\ & -2d_{1Q}(k)\sin(j\frac{\pi}{2} - \frac{\pi}{4})] \end{aligned} \tag{3.38}$$

where

$$\begin{aligned} G_k(q,j) \;=\; & 2d_{2I}(k)\cos((j+q)\frac{\pi}{2} - \frac{\pi}{4}) - 2d_{2Q}(k)\sin((j+q)\frac{\pi}{2} - \frac{\pi}{4}) \\ & -\cos(q\frac{\pi}{2})(d_{1I}(k)d_{2I}(k) + d_{1Q}(k)d_{2Q}(k)) \\ & +\sin(q\frac{\pi}{2})(d_{1I}(k)d_{2Q}(k) - d_{1Q}(k)d_{2I}(k)). \end{aligned} \tag{3.39}$$

In our simulations, we have observed that when the last two terms in (3.39) are ignored, the loss in BER performance is only 0.1 dB. Therefore, to provide substantial simplification in the computations, these terms can be omitted. Then,

$$G_k(q,j) \approx 2d_{2I}(k)\cos((j+q)\frac{\pi}{2}-\frac{\pi}{4}) - 2d_{2Q}(k)\sin((j+q)\frac{\pi}{2}-\frac{\pi}{4}). \quad (3.40)$$

The steps of the resulting sequential decoding algorithm are briefly as follows:

Step 1: determine the surviving paths at instant k.
This means computing $u_k(0)$, $u_k(1)$, $u_k(2)$ and $u_k(3)$. For each $u_k(j)$ we compute four quantities and select the largest one as the metric of the surviving path. Four computations for each metric and four computations for each state require a total of 16 computations.

Step 2: select the maximum among $u_k(0)$, $u_k(1)$, $u_k(2)$ and $u_k(3)$.

Step 3: trace the selected path L steps back and decode m_{k-L}.
As we shall see in the next section, L is generally 1 or 2.

Let us demonstrate the operation of the decoder with the aid of the trellis diagram given in Figure 3.15. All 16 possible paths between instants $k-1$ and k are indicated. At the k^{th} instant only four of these transitions (one for each state) are kept and the others are discarded[5]. Then the state with the largest metric is selected (indicated by a solid circle). In this example, $R(k) = u_k(0)$ is selected. When the decoding depth is one symbol, the surviving path terminating at $R(k)$ is traced back one step and the symbols for the $(k-1)^{th}$ instant are decoded. In Figure 3.15 this is m_{k-1}, and therefore $\hat{a}_{k-1} = 1$ and $b_{k-1} = -1$. For a decoding depth of two symbols, at the k^{th} instant the symbols for the $(k-2)^{th}$ instant are decoded. In Figure 3.15 this corresponds to state m_{k-2}, or equivalently $a_{k-2} = -1$ and $b_{k-2} = -1$.

[5]The surviving paths are indicated by double arrows.

3.6.4 BER Performance of New Receivers

We have evaluated the BER performance of DCTPSK for four different receiver structures via computer simulation[6]. These receivers employ:

- conventional differential detection,
- nonredundant error correction [26,28,30],
- a symbol-by-symbol detector using combining with feedback,
- a four-state sequential decoder with decoding depths 1 and 2.

The system configuration is shown in Figure 3.16. The predetection BPF is a fourth-order phase equalized Butterworth with BT_s=0.65. The BER performances of the four detectors in an additive white Gaussian noise channel are plotted in Figure 3.17. The four-state sequential decoder, even with a decoding depth of one symbol, outperforms the other decoders and provides about 1.7 dB improvement over the conventional differential detection (all comparisons here are made at a BER of 10^{-4}). Increasing the decoding depth to 2 brings an additional improvement 0.3 dB. Our simulation results indicate that the improvement gains for decoding depths greater than 2 are marginal; and the associated complexity is not warranted.

The combining with feedback decoder achieves the second best performance and offers about 1.2 dB improvement over the conventional detector.

The nonredundant error correction decoder is about 0.3 dB inferior to CWF decoder and provides about 0.9 dB improvement over the conventional detector.

The performance curves of Figure 3.17 indicate that as the receiver processing complexity is increased, the penalty for using differential detection (rather than coherent detection) is reduced. Note that all three performance improvement techniques require the same amount of IF processing. With the recent advances in digital signal processing, the additional baseband processing involved in the CWF detector or the four-state sequential decoder may not be a heavy burden for future receivers.

[6]The program listings are in given in Appendix B.

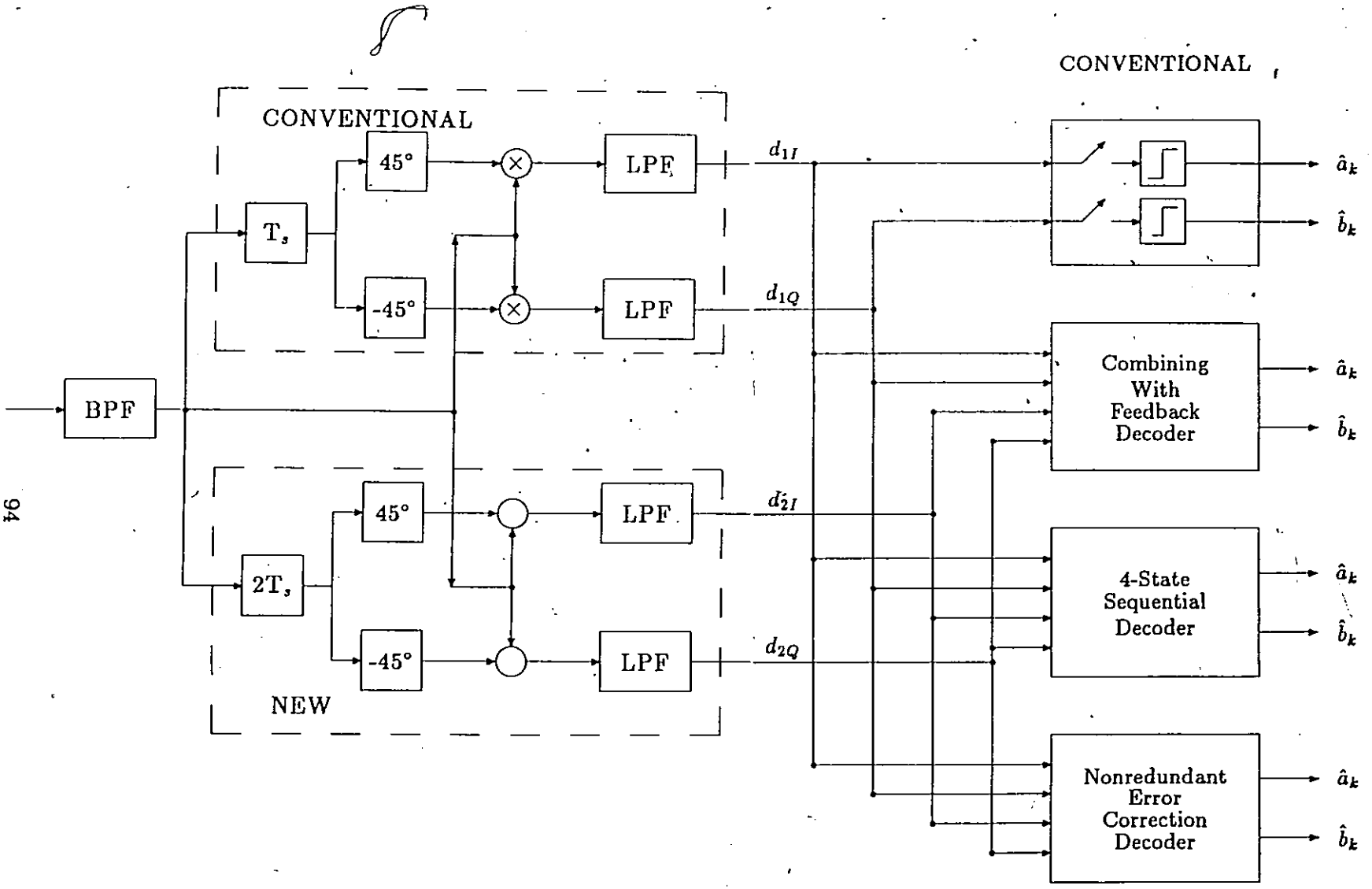

Figure 3.16: Block diagram of a DCTPSK system with various detectors.

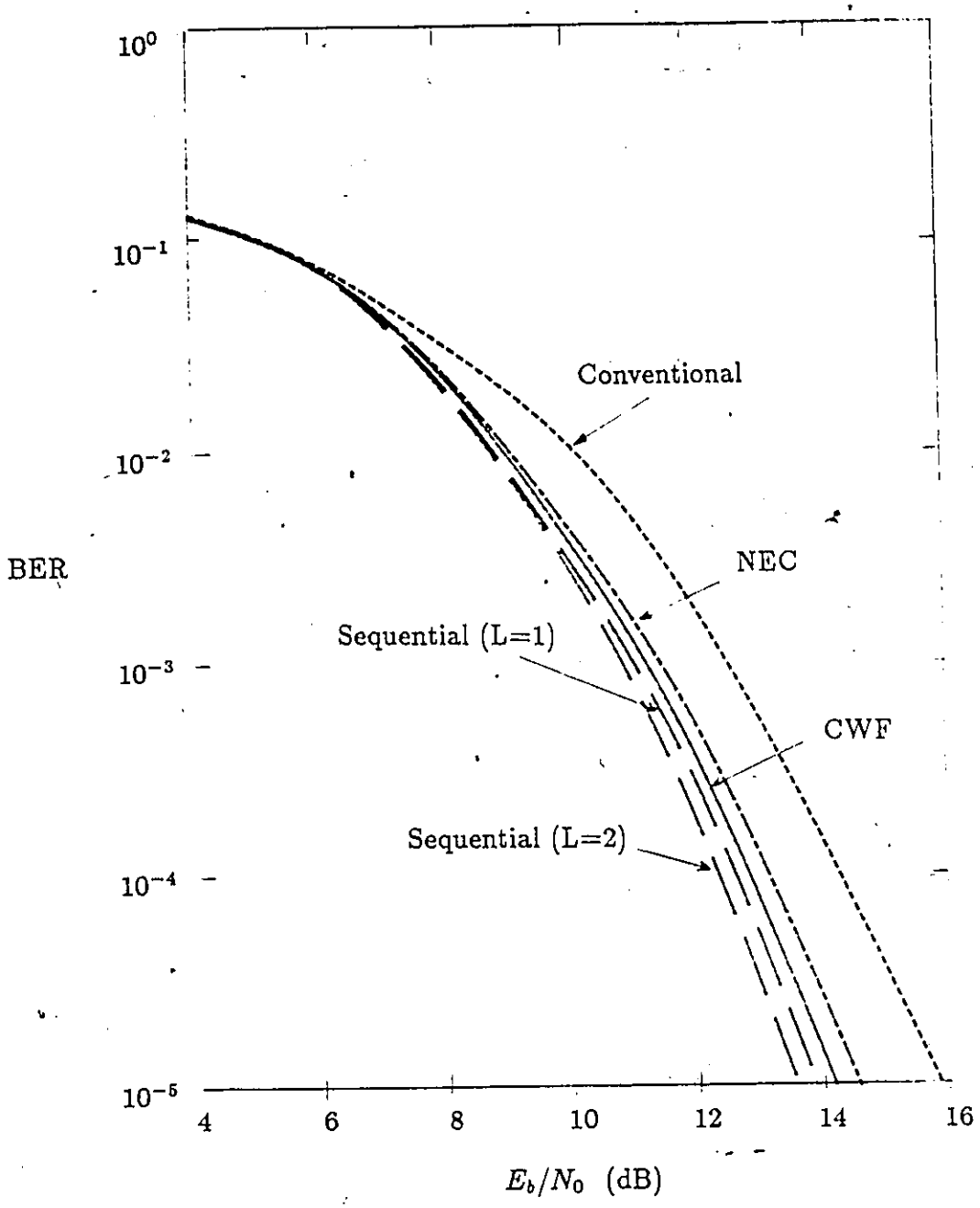

Figure 3.17: BER performances of various DCTPSK detectors. Transmitted signal is hardlimited and there is no ACI.

3.7 HARDWARE IMPLEMENTATION AND EXPERIMENTAL RESULTS

As a proof of concept, and to gain additional insight into some of the problems involved, we implemented a DCTPSK modem. In this section we first discuss the design of the modem and describe the experimental set-up. Then the experimental results are presented and various sources of impairments are identified. The modem circuit diagrams and operating instructions are given in Appendix A.

3.7.1 Design of the Modem

In the design of the modem the major system parameters to be selected were:

- bit rate,
- intermediate frequencies (IF),
- predetection BPF characteristic, and
- type of delay element to be used.

We shall briefly discuss how each of these parameters were selected.

Bit Rate

The lowest limit on the bit rate is imposed by the system frequency uncertainties; whereas the highest bit rate is determined by the power and bandwidth allocations.

Since we have frequently refered to the MSAT system, a natural choice for the bit rate of our modem would be 2.4 kb/s. However, the local oscillator drift of our satellite earth station is specified as 2 kHz/day [121]. Therefore, to reduce the frequency uncertainty errors, we were forced to choose a data rate much higher than 2.4 kb/s.

The bandwidth allocated to us by the Department of Communications was 100 kHz. Thus the maximum data rate we could transmit was about

150 kb/s.[7] Considering that most of the modems in our laboratory operate at 64 kb/s, we chose the bit rate as 64 kb/s.

Intermediate Frequencies

In the uplink, single IF stage is sufficient and the frequency dictated by the earth station is 70 MHz. Similarly, in the downlink, the output of the downconverter is 70 MHz. To determine whether a second IF stage is needed or not, let us briefly consider the implications of the frequency stability requirements.

Assuming that the allowable phase error $\Delta\vartheta$ is 5° (this corresponds to a E_b/N_o penalty of about 1.2 dB [24]), then the maximum delay variation is given by:

$$\Delta T_s = \Delta\vartheta/\omega_{IF}. \tag{3.41}$$

The required delay stability is

$$\frac{\Delta T_s}{T_s} = \frac{\Delta\vartheta}{T_s\omega_{IF}}. \tag{3.42}$$

Substituting $T_s = 15.6\mu s$ and $\omega_{IF} = 14\pi \times 10^7$, we obtain $\Delta T_s/T_s$ as 1.27×10^{-5}. An inexpensive delay element cannot maintain such a stability. To relax the stability requirements, a second IF stage was used. The center frequency of the second IF stage was selected as 256 kHz. In this case a 5° phase error requires a stability of 3.4×10^{-3}, which can be easily provided.

Predetection BPF

The necessary characteristic of the predetection bandpass filter was determined by computer simulations. For this purpose, the performance of the modem was evaluated for Butterworth, Chebycheff and raised-cosine type filters. The best performane was obtained with a fourth-order Butterworth filter with $BT = 0.65$. The implemented filter has a center frequency of 256 kHz. The amplitude characteristic of the filter matches the specifications closely, but to keep the implementation simple, its phase was not equalized.

[7] This is based on a 99% power containment bandwidth.

Delay Element

In the implementation of the differential detector, a crucial component is the delay element. In high bit rate (e.g., 120 Mb/s) systems, the delay elements are implemented as microwave filters or transmission lines. For a regenerative TDMA system, COMSAT implemented them as microwave integrated circuit filters [44], whereas AEG used waveguide filters [40]. For the bit rate and the operating frequency we chose, such delay lines are impractical.

For long delays (e.g., 0.4 ms for 2.4 kb/s) bucket brigade devices or charge coupled devices could be used. But 15.6 μs is rather short for these analog devices. Hence we had to implement a digital delay element using shift registers.

To avoid the analog to digital converters and digital multipliers, we used a simpler technique. The block diagram of the differential detector we used is shown in Figure 3.18 and the associated waveforms are given in Figure 3.19. The received signal (at 256 kHz) is passed through a threshold detector, and the output binary sequence is applied to a multi-stage shift register. Then the phase comparison is equivalent to a binary exclusive-OR operation. Note that for the intermediate frequency and the bit rate we chose, a phase shift of $\pi/4$ corresponds to a delay of $T_s/16$. The output of the exclusive-OR circuit is a pulse width modulated (PWM) sequence. This PWM signal is passed through a lowpass filter, which acts as an integrator. Then the binary decisions are based on whether the pulse is wider or narrower than $T_{IF}/2$ (where T_{IF} is the duration of a one IF cycle).

In the modulator, the baseband processing (i.e. S/P conversion, differential encoding and the signal processing) is performed by semiconductor circuits. The demodulator is also implemented by using semiconductors, except for the BPF. Thus, in the future, most of the modem can be integrated as a monolithic integrated circuit.

3.7.2 Experimental Set-Up

The experimental set-up used to evaluate the performance of the modem is illustrated in Figure 3.20. The important parameters for the experiments were as follows :

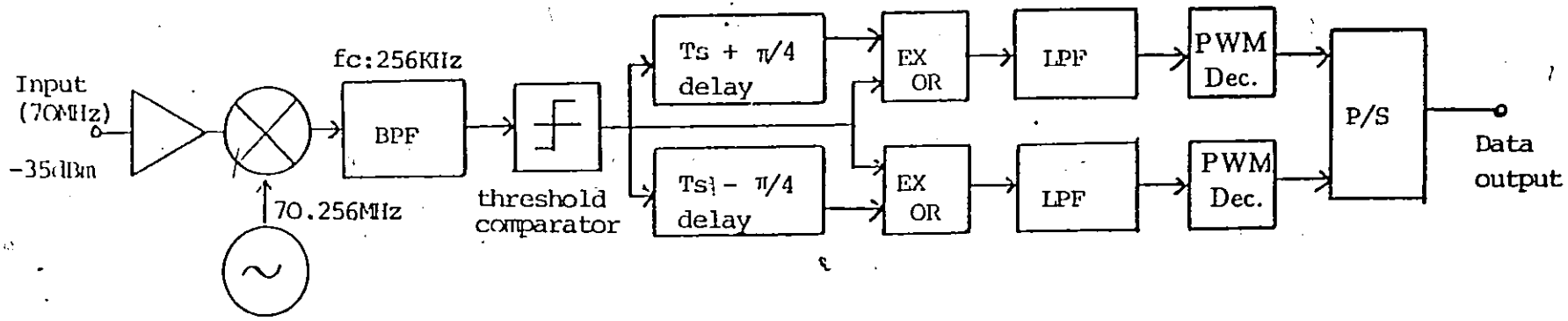

Figure 3.18: Block diagram of hardware differential detector.

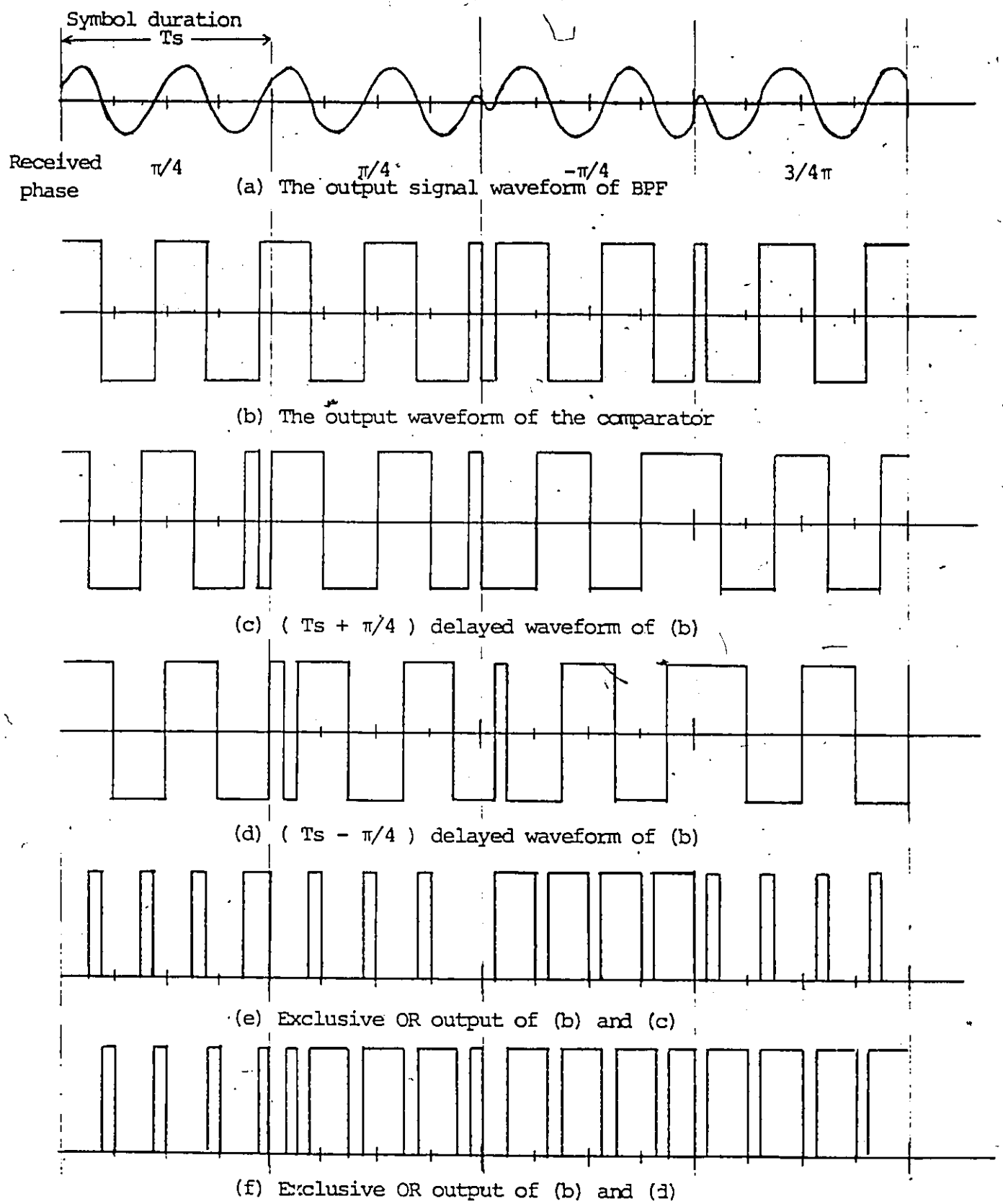

Figure 3.19: Waveforms associated with the implemented differential detector.

Carrier frequency: 70 MHz,

Test data: Pseudo random binary sequence of length $2^{20} - 1$,

Noise source: (i) DCD 3002 IF noise generator, or
(ii) 14/12 GHz Satellite Link;

BPF for C/N Measurements: Third-order Butterworth with a noise bandwidth of 1.3 MHz;

Predetection BPF: fourth-order Butterworth at 256 KHz with a noise bandwidth of 40 KHz;

BER improvement technique: None.

The modulator generates the data clock and this is fed to the data error analyzer which generates a pseudo random binary sequence. The input data is processed and the modulated DCTPSK signal is transmitted at 70 MHz.

If only a modem back-to-back evaluation is performed, the transmitted signal is corrupted by using a Gaussian noise generator. In the case of a real satellite link (as indicated by the dashed lines in Figure 3.20) sufficient noise for a performance evaluation is inherent in the system.

The noisy signal centered at 70 MHz is passed through a BPF of known noise bandwidth for measuring the carrier and noise power.

At the demodulator, the signal is down converted to 256 kHz, passed through a predetection BPF and then applied to the differential detectors. The output of the demodulator is connected to the Data Error Analyzer for counting the errors.

Digital signal processing techniques permit us to generate the signals which are quite close to the analytical expressions given in Section 3.1. The eye-diagrams of the I and Q channel baseband DCTPSK signals are shown in Figure 3.21. By applying these signals to channels 1 and 2 of an oscilloscope and using the XY mode, we obtain the SSD shown in Figure 3.22.

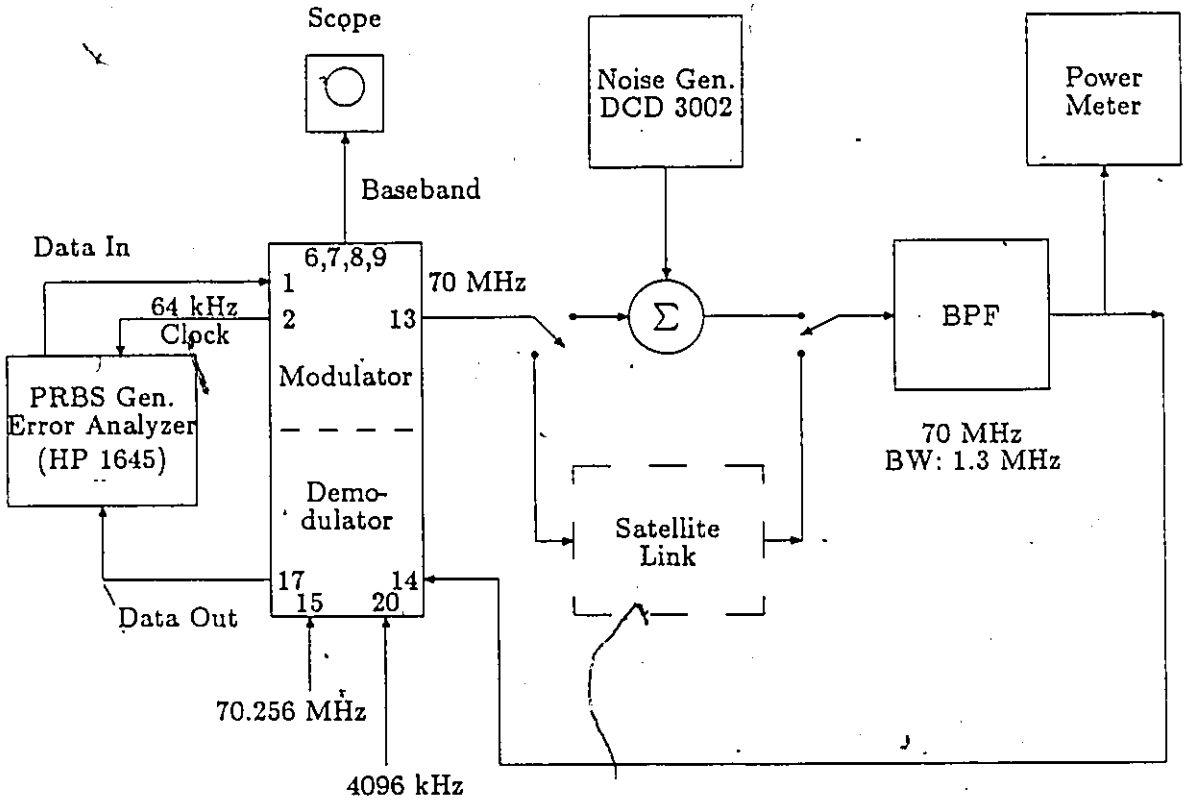

Figure 3.20: Experimental set-up.

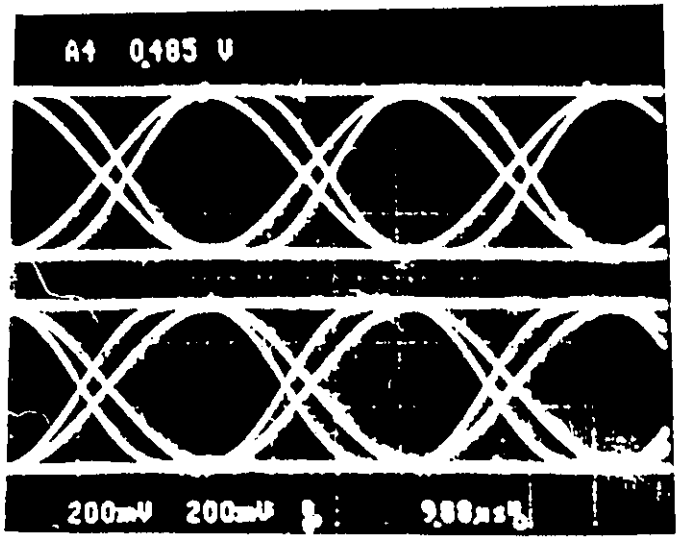

Figure 3.21: Experimental I and Q-channel eye-diagrams at transmitter.

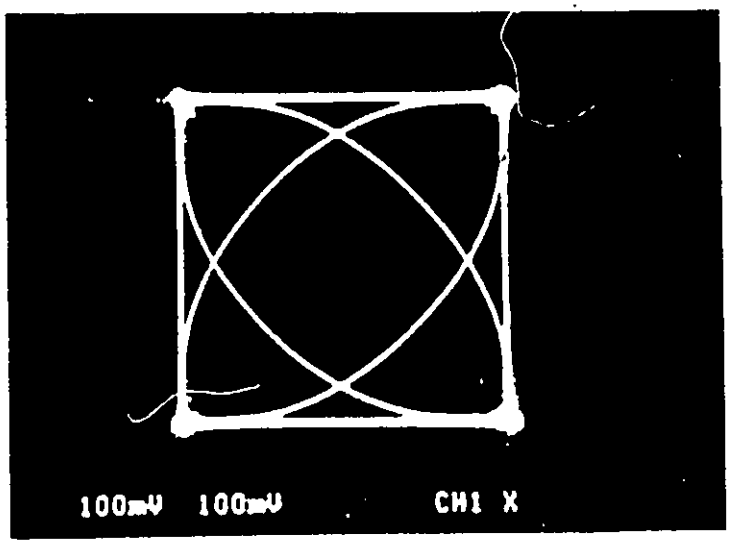

Figure 3.22: Experimental signal-space diagram of DCTPSK.

3.7.3 Measurement Results

The performance of the DCTPSK modem was evaluated in a back-to-back configuration as well as using the 14/12 GHz satellite earth station of the University of Ottawa. The steps followed in each case are described below.

3.7.4 Back-to-Back Evaluation

For the back-to-back evaluation, the set-up of Figure 3.20 is used. The transmitted signal plus generated noise were passed through a filter centered at 70 MHz with a noise bandwidth of 1.3 MHz. The carrier power was measured with the noise suitably attenuated. Then the noise power was measured by attenuating the carrier.

The measured C/N values can be translated into E_b/N_o values by using the relationship

$$\frac{E_b}{N_o} = \frac{C}{N}\frac{BW}{f_b} \tag{3.43}$$

where BW is the noise bandwidth of the IF filter (i.e. 1.3 MHz) and f_b is the bit rate (i.e., 64 kb/s). In dB form (3.43) can be rewritten as

$$(\frac{E_b}{N_o})_{dB} = (\frac{C}{N})_{dB} + 10\log(\frac{BW}{f_b}). \tag{3.44}$$

Substituting the values used for BW and f_b, we find

$$\frac{E_b}{N_o} = \frac{C}{N} + 13 \quad \text{in dB.} \tag{3.45}$$

Repeating the carrier power and noise power mesurements several times and reading the corresponding BER, we obtained the curve shown in Figure 3.23.

3.7.5 Satellite Channel Evaluation

We also evaluated the performance of the DCTPSK modem using the 14/12 GHz Anik–B satellite. The block diagram of the satellite link is shown in Figure 3.24.

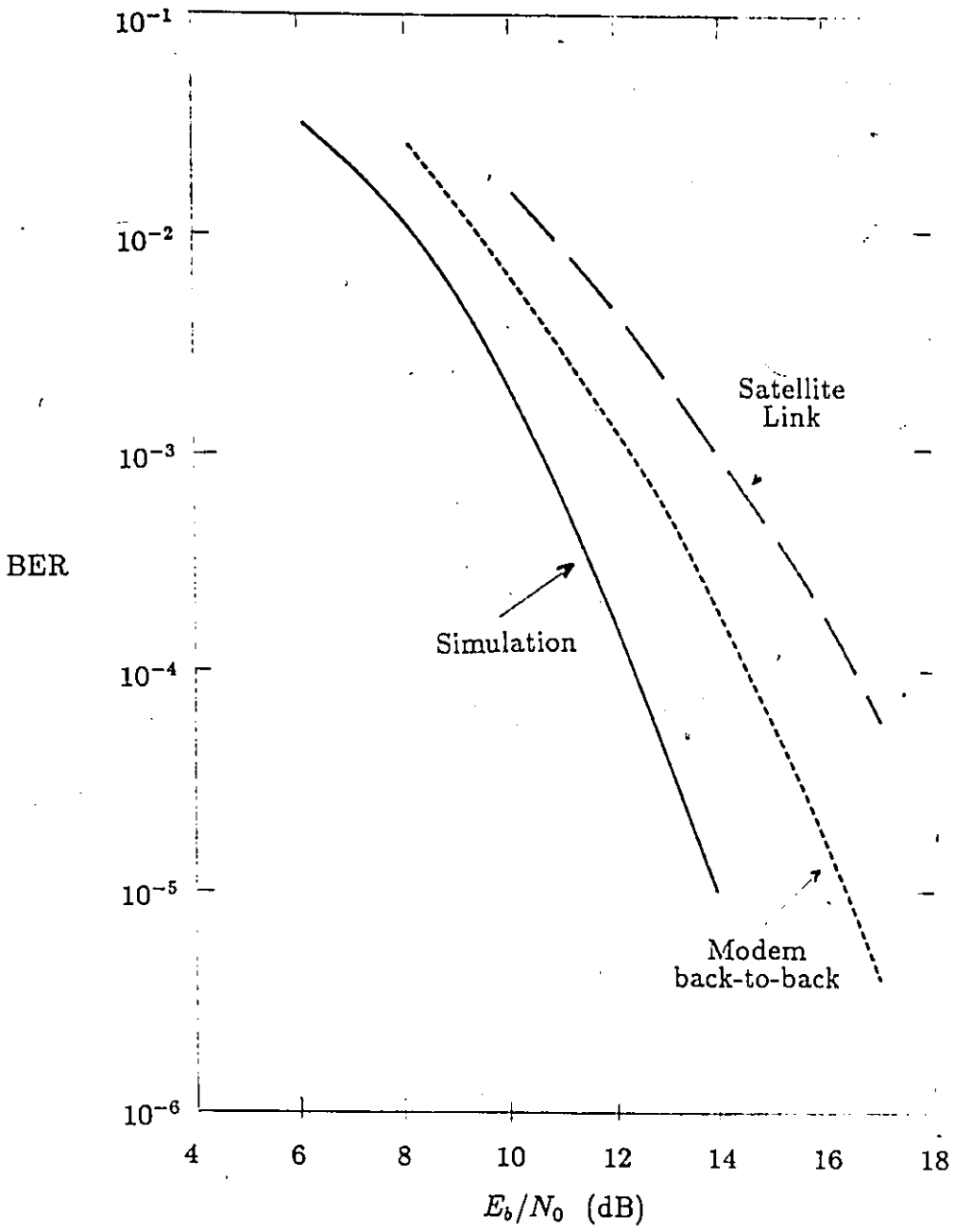

Figure 3.23: Results of DCTPSK modem bit error rate measurements. No BER improvement technique is used.

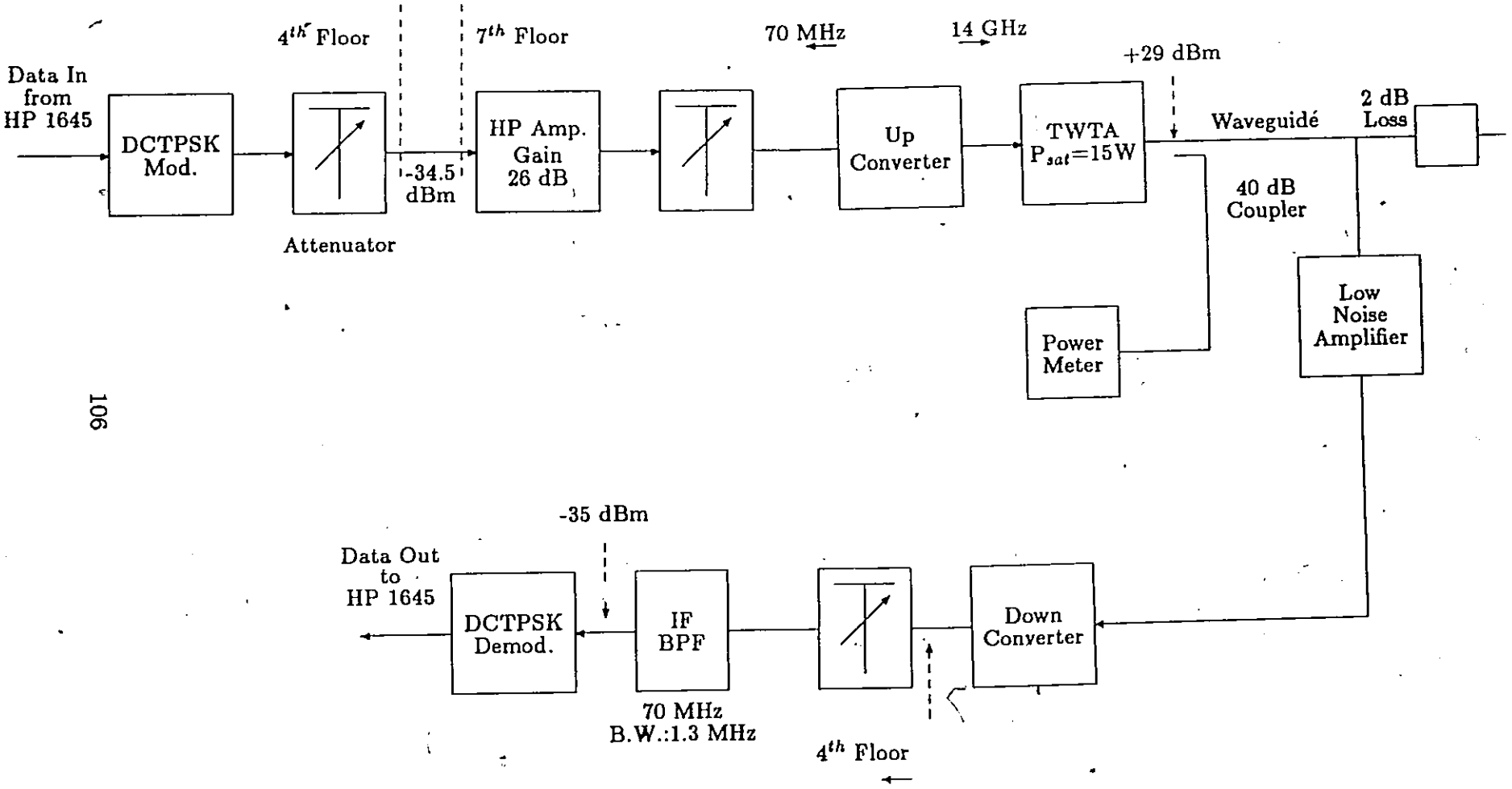

Figure 3.24: Satellite link block diagram.

The major differences between the back-to-back and satellite link measurements can be summmarized as follows:

- The maximum power we were allowed to transmit was 0.8 W (i.e., 29 dBm). Thus the power levels at various points in the link required careful adjustments (as indicated in Fig. 3.19).
- Since the modem did not have a clock recovery circuit, the sampling time was manually adjusted.
- Since the noise was continuously present, the C/N values were obtained by measuring (C+N) and N separately and then calculating C.

The BER measurements obtained by using the satellite link are plotted also in Figure 3.23.

3.7.6 Discussion of Experimental Results

In Figure 3.23 we have plotted the BER curves obtained by:

- computer simulation,
- modem back-to-back measurements, and
- satellite link measurements.

It can be observed from Figure 3.23 that there is a 2 dB difference between the computer simulation results and the modem back-to-back measurements. An additional 2 dB degradation is incurred when the modem was evaluated via the satellite link. The major sources causing this discrepancy can be classified into three categories:

- modulator imperfections,
- satellite link impairments, and
- demodulator imperfections.

Let us briefly discuss the sources of imperfections in each category which were not included in the computer simulations.

Modulator

In our modulator we identified two imperfections; these are:

- The phase difference between the quadrature carriers (i.e. $\cos\omega_c t$ and $\sin\omega_c t$) is not 90° but about 88°. This causes some crosstalk.
- The baseband waveshapes are generated by a table look-up technique. Due to a inevitable quantization error there is a small deviation from the ideal waveshapes.

Satellite Link

In our simulations the satellite link was treated as a bent pipe; and the only impairment accounted for was the thermal noise. In fact, the satellite link is the contributor of various other impairments such as

- frequency uncertainties,
- amplitude and phase variations introduced by satellite filters,
- intermodulation distortion due to multiple carriers sharing the same transponder,
- modulation transfer due to carriers operating in burst mode,
- adjacent channel interference from neighbouring carriers,
- cochannel interference from other systems.

We did not quantify the individual contributions of these impairments, but their overall effect can be deduced by comparing the satellite link measurements with the modem back-to-back measurements.

Demodulator

The phase of the predetection filter is not equalized and consequently the received signal experiences some phase distortion which is not accounted for in the simulations.

Our demodulator uses a sampling rate of 4096 kHz, an IF frequency of 256 kHz and a shift register of length 129. The resulting phase resolution is 22.5°. We could enhance the phase resolution to 11.25° by doubling the sampling rate and the shift register length. Then an improvement of a few tenths of a dB is expected [117]. However the circuit complexity would increase significantly, therefore we did not implement it.

Based on the foregoing discussion it be could concluded that the imperfections which exist in the modem can be reduced considerably. Yet the results obtained with the laboratory model DCTPSK modem accomplished our objective of proving the concept.

3.8 CONCLUSIONS

A new modem technique, namely, differentially detected controlled PSK, has been introduced. Its encoding rules, waveforms, signal space diagram, eye-diagram and spectrum has been presented.

The BER performance of DCTPSK in a hardlimited multicarrier channel is obtained. It has been shown that more carriers may share the same channel using DCTPSK in an adjacent channel interference environment than by using DMSK or DQPSK.

For improving the BER performance of DCTPSK, two novel receiver structures have been proposed. The first new technique uses a symbol-by-symbol detector which combines the signal samples of the one-bit and two-bit detectors. The second structure introduced was a four-state sequential decoder. The improvements achieved with these receivers are about 1.2 to 1.7 dB respectively.

As a proof of concept, we also implemented a laboratory model DCTPSK modem. The experimental results of the modem back-to-back and via satellite link measurements have been presented and various sources of impairments have been discussed.

In conclusion, the DCTPSK modem is a potential candidate for applications where a channel is to be efficiently shared by multiple users. Furthermore, the new receivers developed for DCTPSK could also be used for other quadrature modulated signals.

Chapter 4

DIFFERENTIAL DETECTION OF GMSK USING DECISION FEEDBACK

4.1 INTRODUCTION

In Section 2.2.2.1, we reviewed the requirements of mobile radio communications and mentioned that the differential detection of GMSK is a major candidate for mobile applications.

Another potential application area for DGMSK is a multicarrier satellite communications system. As the bandwidth efficiency is increased, the BER performance degradation of DMSK, DQPSK and DCTPSK increase drastically. Particularly for bandwidth efficiencies better than 0.8 b/s/Hz, operating these systems with nonlinear amplifiers is impractical. However, due to the compact spectrum of GMSK, adjacent channel interference becomes considerable only for bandwidth efficiencies in excess of 1 b/s/Hz. Hence there is a range of bandwidth utilization values and ACI conditions for which DGMSK is attractive for satellite communications applications as well.

The use of the conventional one-bit differential detector with GMSK results in poor communications efficiency, therefore earlier literature focuses on two-bit differential detection [105,110]. In terms of communications efficiency, the conventional two-bit differential detector [110] is about 7 dB inferior to the coherent detection of GMSK[1]. Hence, there is ample room for improvements by introducing additional processing at the receiver.

Considering both the mobile radio and multicarrier satellite communications applications, in this chapter new receiver structures are introduced to improve the BER performance of DGMSK.

The chapter outline is as follows. First the principle of the differential detection of GMSK using a conventional one-bit, two-bit and three-bit differential detector is analyzed. Then, we determine how to apply decision feedback to these detectors. After demonstrating that the decision feedback significantly reduces the destructive effect of intersymbol interference in the individual detectors, we propose receiver structures where two detectors can be jointly utilized. Finally, the results of a BER performance evaluation of various DGMSK receivers are presented.

4.2 TRANSMITTER

The block diagram of a GMSK transmitter is shown in Figure 4.1. The transmitter consists of a differential encoder, a Gaussian low-pass filter (GLPF) and an FM modulator. The differential encoder is required for two-bit and three-bit differential detection. The input symbols to the differential encoder are denoted as a_k, and the output symbols as b_k. For the one-bit differential detection a differential encoder is not needed; i.e., $a_k = b_k$. For two-bit differential detection, the differential encoding rule is given by

$$b_k = -a_k b_{k-1}. \tag{4.1}$$

Similarly, for three-bit differential detection, the differential encoding rule is:

$$b_k = -a_k b_{k-1} b_{k-2}. \tag{4.2}$$

The input to the GLPF is a non-return to zero (NRZ) sequence. The output

[1] This is when the premodulation filter $B_t T = 0.25$, and for a BER=10^{-4}.

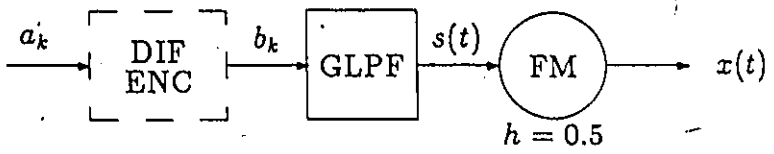

Figure 4.1: Block diagram of a GMSK transmitter. The differential encoder is not needed for one-bit differential detection.

of the GLPF can be expressed as

$$s(t) = \sum_{i=-\infty}^{\infty} b_i p(t - iT) \tag{4.3}$$

where $\{a_i = \pm 1\}$ and $p(t)$ is the *pulse* response of the transmit GLPF given by [110]:

$$p(t) = \frac{1}{2T}[Q(k_1 B_t T(-\frac{t}{T})) - Q(k_1 B_t T(1 - \frac{t}{T}))]. \tag{4.4}$$

In (4.4), B_t is the 3 dB bandwidth of the GLPF, T is the bit duration[2] (thus, $B_t T$ is the bandwidth-time product of the transmit GLPF), $k_1 = 7.546$ and

$$Q(x) = \frac{1}{\sqrt{2\pi}} \int_x^{\infty} \exp(-y^2/2) dy. \tag{4.5}$$

The pulse response of the transmit GLPF for various $B_t T$ values is shown in Figure 4.2.

The output of the FM modulator can be expressed as:

$$x(t) = A_0 \cos(\omega_c t + \phi(t) + \psi) \tag{4.6}$$

In (4.6), A_0 is the constant envelope of the signal, ω_c is the carrier frequency, ψ is the initial phase (which can be assumed as zero) and $\phi(t)$ is the excess-phase defined by

$$\phi(t) = k_m \int_{-\infty}^{t} s(\tau) d\tau = k_m \sum_{j=-\infty}^{\infty} b_j \int_{-\infty}^{t} p(\tau - jT) d\tau \tag{4.7}$$

[2]Throughout this chapter $T = T_b$.

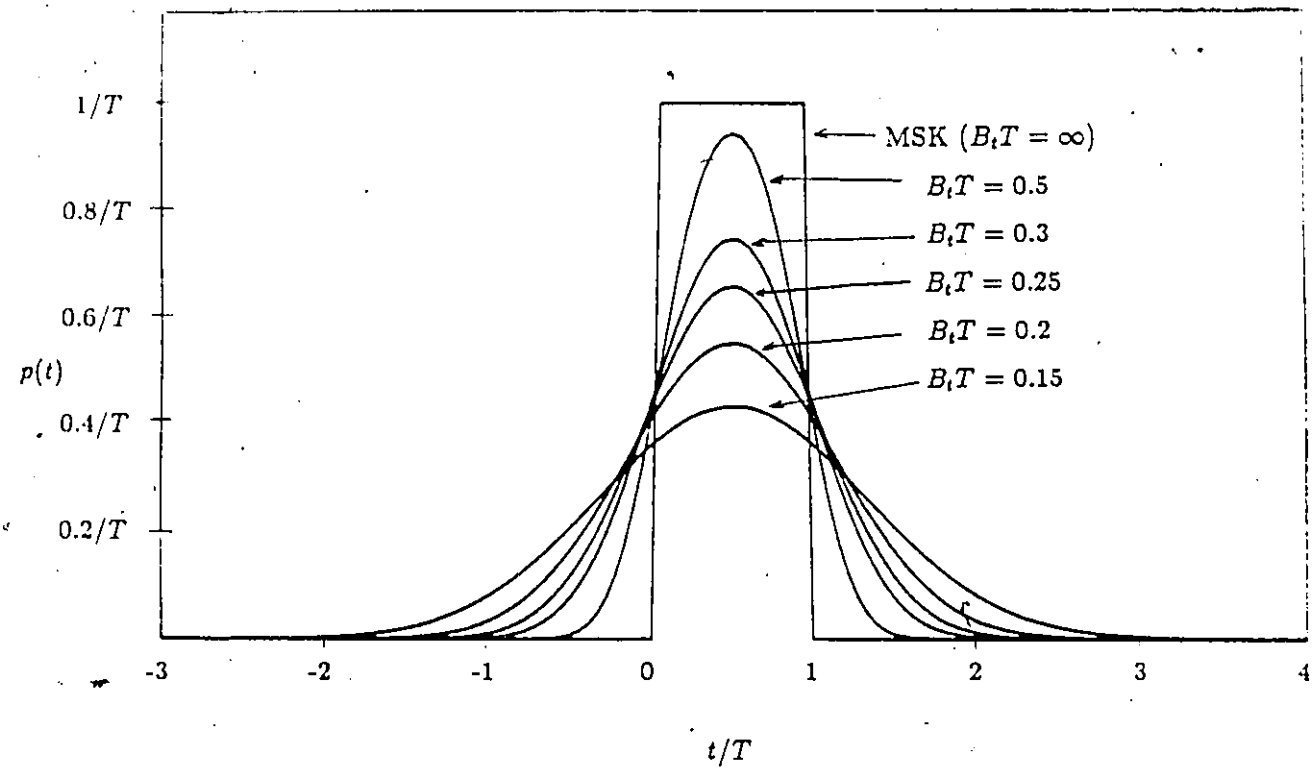

Figure 4.2: Pulse response of GLPF as a function of BT product.

where k_m is a constant equal to $\pi/2T$ (so that the modulation index $h = 0.5$).

4.3 CONVENTIONAL RECEIVERS

In PSK systems, if there is no ISI, a one-bit differential detector has as good a performance as a two-bit or a three-bit detector. Therefore for implemenational simplicity, a one-bit detector is preferred. For GMSK signals this is not the case. In this section we investigate how "n" affects the differential detection process.

4.3.1 Conventional One-Bit Differential Detection

The block diagram of the conventional one-bit differential detector is illustrated in Figure 4.3. The signal at the input of the predetection band-pass

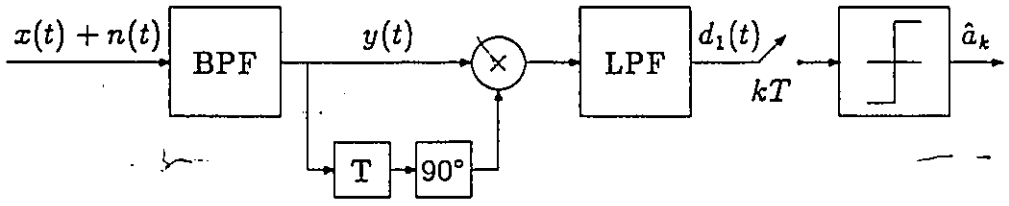

Figure 4.3: Block diagram of a one-bit differential detector.

filter is corrupted by additive white Gaussian noise with a one-sided spectral density N_0. The signal at the output of the BPF, $y(t)$, can be represented as

$$y(t) = r(t)\cos(\omega_c t + \phi'(t)) + n_c(t)\cos\omega_c t - n_s(t)\sin\omega_c t \qquad (4.8)$$

where $r(t)$ is the time varying envelope of the signal, $\phi'(t)$ is the distorted signal phase, and $n_c(t)$ and $n_s(t)$ are respectively the in-phase and quadrature components of the narrowband noise. In the mathematical analysis which follows, we shall assume that $\phi'(t) = \phi(t)$. However, in evaluating the system performance by simulation, the distortion due to the filtering is included.

The output of the one-bit detector $d_1(t)$ is obtained by lowpass filtering the product of $y(t)$ and a T seconds delayed and 90° phase shifted version of itself (see Figure 4.3), i.e.,

$$d_1(t) = r(t)r(t-T)\sin(k_m \sum_{j=-\infty}^{\infty} b_j \int_{t-T}^{t} p(\tau - jT)d\tau) + n_1(t) \qquad (4.9)$$

where $n_1(t)$ lumps all the noise terms together.

At the time instant kT, $d_1(t)$ has the following form

$$d_1(kT) = r(kT)r(kT-T)\sin(\sum_{j=-\infty}^{\infty} b_j\theta_{k-j}) + n_1(kT) \qquad (4.10)$$

where

$$\theta_{k-j} = k_m \int_{kT-T}^{kT} p(\tau - jT)d\tau. \qquad (4.11)$$

The values of θ_i for different B_tT have been tabulated in Table 4.1. Here, θ_0 represents the signal and $\theta_{-2}, \theta_{-2}, \theta_{-1}, \theta_1$, θ_2 and θ_3 are the ISI terms. For $|i| \geq 3$, θ_i is negligible. This observation enables us to rewrite (4.10) as:

$$d_1(kT) = r(kT)r(kT-T)\sin(\Delta\theta_k) + n_1(kT) \qquad (4.12)$$

where

$$\Delta\theta_k = b_{k+2}\theta_{-2} + b_{k+1}\theta_{-1} + b_k\theta_0 + b_{k-1}\theta_1 + b_{k-2}\theta_2. \qquad (4.13)$$

For B_tT=0.25, the differential phase angles $\Delta\theta_k$ corresponding to all possible input data combinations have been tabulated in Table 4.2. The diagrams in which all possible differential phase angles at the sampling instants (i.e., $\Delta\theta_k$) are shown will be referred to as *phase-state diagrams.* Using Table 4.2, the phase-state diagram of the one-bit detector is shown in Figure 4.4. From Figure 4.4 the following observations can be made:

B_tT	θ_{-3}	θ_{-2}	θ_{-1}	θ_0	θ_1	θ_2	θ_3	$\Delta\theta_{min}$	$\Delta\theta_{min}^{DF}$
0.15	0.3	4.55	21.85	36.6	21.85	4.55	0.3	—	19.6
0.2	—	1.7	20.6	45.4	20.6	1.7	—	1.6	-46.2
0.25	—	0.6	18.2	52.4	18.2	0.6	—	29.6	67.2
0.3	—	0.2	15.9	57.8	15.9	0.2	—	51.2	83.4
0.4	—	—	12.5	65.0	12.5	—	—	80.0	105.0
0.5	—	—	10.3	69.4	10.3	—	—	97.6	118.2
1.0	—	—	5.9	78.2	5.9	—	—	132.8	144.6
∞ (MSK)	—	—	—	90.0	—	—	—	180.0	180.0

Table 4.1: Phase shifts (in degrees) corresponding to signal, θ_o, and ISI terms (θ_i, for $i \neq 0$) as a function of transmit Gaussian filter B_tT for the one-bit differential detector. $\Delta\theta_{min}$ and $\Delta\theta_{min}^{DF}$ are the minimum differential phase angles before and after applying decision feedback.

Bit Combinations			State	$\Delta\theta_k$
b_{k-1}	b_k	b_{k+1}		(in degrees)
1	1	1	1	88.8
1	1	-1	2	52.4
-1	1	1	2	52.4
-1	1	-1	3	16.0
1	-1	1	4	-16.0
1	-1	-1	5	-52.4
-1	-1	1	5	-52.4
-1	-1	-1	6	-88.8

Table 4.2: Differential phase angles $\Delta\theta_k$ of the one-bit detector corresponding to various input data combinations ($B_tT = 0.25$). The contributions of b_{k-2} and b_{k+2} are ignored.

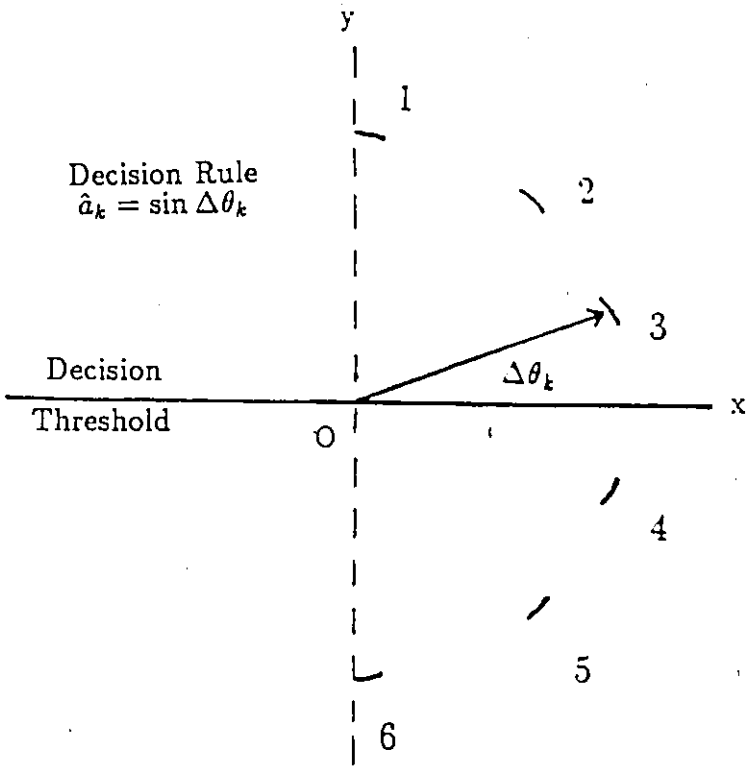

Figure 4.4: Phase-state diagram of a one-bit differential detector.

- The phase-states are symmetric with respect to the x-axis; consequently the corresponding eye-diagram shown in Figure 4.5 is also symmetric.

- The decision threshold is the x-axis. When the phase difference ($\Delta\theta_k$) is above the x-axis, b_k is decoded as "+1"; otherwise b_k is decoded as "-1", i.e.,

$$\hat{b}_k = \text{sgn}[d_1(kT)] \tag{4.14}$$

where $\text{sgn}[x] = 1$ for $x \geq 0$ and $\text{sgn}[x] = -1$ for $x < 0$. Recall that for one-bit differential detection, $a_k = b_k$.

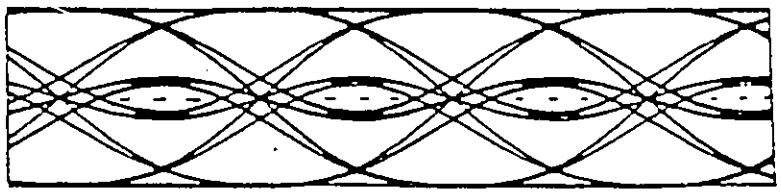

Figure 4.5: Eye-diagram of a conventional one-bit differential detector.

To investigate the effect of B_tT upon one-bit differential detection performance, we have also included in Table 4.1 the phase separation between the closest states with the opposite polarity (i.e., states 3 and 4). This quantity is refered to as the minimum differential phase angle $\Delta\theta_{min}$ and is defined as

$$\Delta\theta_{min} = 2(\theta_0 - \sum_{i \neq 0} \theta_i). \tag{4.15}$$

From Table 4.1, we can observe that the conventional one-bit differential detector has positive $\Delta\theta_{min}$ values for B_tT values greater than 0.2. If the ISI caused by the predetection BPF is also taken into account, the smallest B_tT for which the one-bit differential detection can operate (with a very poor performance) is about 0.22.

4.3.2 Conventional Two-Bit Differential Detection

The block diagram of the conventional two-bit differential detector is illustrated in Figure 4.6. The output of the two-bit detector $d_2(t)$ is obtained

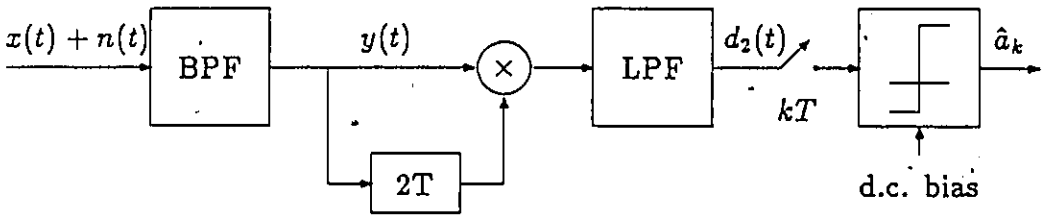

Figure 4.6: Block diagram of the conventional two-bit differential detector.

by multiplying $y(t)$ with a $2T$ seconds delayed version of itself and then lowpass filtering the product, i.e.,

$$d_2(t) = r(t)r(t-2T)\cos(k_m \sum_{j=-\infty}^{\infty} b_j \int_{t-2T}^{t} p(\tau - jT)d\tau) + n_2(t) \qquad (4.16)$$

where $n_2(t)$ represents all the noise terms.

At the time instant kT, $d_2(t)$ is given by

$$d_2(kT) = r(kT)r(kT-2T)\cos(\sum_{j=-\infty}^{\infty} b_j V_{k-j}) + n_2(kT) \qquad (4.17)$$

where

$$V_{k-j} = k_m \int_{kT-2T}^{kT} p(\tau - jT)d\tau. \qquad (4.18)$$

The values of V_i for different B_tT have been tabulated in Table 4.3, where V_0 and V_1 represent the signal and V_{-2}, V_{-1}, V_2, V_3 are the ISI terms. V_i is almost zero for $i \geq 4$ and $i \leq -3$. Therefore we can rewrite (4.17) as

B_tT	V_{-3}	V_{-2}	V_{-1}	V_0	V_1	V_2	V_3	V_4	ΔV_{min}	ΔV_{min}^{DF}
0.15	0.3	4.85	26.4	58.45	58.45	26.4	4.85	0.3	—	52.4
0.18	—	2.7	23.9	63.4	63.4	23.9	2.7	—	20.4	73.6
0.2	—	1.7	22.3	66.0	66.0	22.3	1.7	—	36.0	84.0
0.25	—	0.6	18.8	70.6	70.6	18.8	0.6	—	63.6	102.4
0.3	—	0.2	16.2	73.6	73.6	16.2	0.2	—	81.6	114.4
0.4	—	—	12.5	77.5	77.5	12.5	—	—	105.0	130.0
0.5	—	—	10.3	79.7	79.7	10.3	—	—	118.2	138.8
1.0	—	—	5.9	84.1	84.1	5.9	—	—	144.6	156.4
∞	—	—	—	90.0	90.0	—	—	—	180.0	180.0

Table 4.3: Phase-shifts (in degrees) corresponding to signal terms (V_o and V_1) and ISI terms as a function of transmit Gaussian filter B_tT for the two-bit differential detector. ΔV_{min} and ΔV_{min}^{DF} are the minimum differential phase angles before and after applying decision feedback.

$$d_2(kT) = r(kT)r(kT-2T)\cos(\Delta V_k) + n_2(kT) \tag{4.19}$$

where

$$\Delta V_k = b_{k+2}V_{-2} + b_{k+1}V_{-1} + b_kV_0 + b_{k-1}V_1 + b_{k-2}V_2 + b_{k-3}V_3. \tag{4.20}$$

For B_tT=0.25, the differential phase angles ΔV_k corresponding to all possible input data combinations have been tabulated in Table 4.4. Using Table 4.4, the phase-states at the decision instants for the two-bit differential detector are shown in Figure 4.7.

To determine the polarity of the output bit, as a first approximation, let us assume that the decision threshold is the y-axis. When the phase difference (ΔV_k) is to the right of the y-axis, (b_kb_{k-1}) is "–1"; otherwise (b_kb_{k-1}) is "+1". Suppose for a moment that the differential encoder in Figure 4.1 was omitted (i.e., $a_k = b_k$). Then, the $\hat{b}_k$ can be determined by using the knowledge of the already decoded $\hat{b}_{k-1}$. However, with this approach an error in $\hat{b}_{k-1}$ will affect the succeeding decisions. The differential encoder

Bit Combinations				State	ΔV_k
b_{k-2}	b_{k-1}	b_k	b_{k+1}		(in degrees)
1	1	-1	1	7	37.6
1	-1	1	1	7	37.6
1	1	-1	-1	8	0.0
1	-1	1	-1	8	0.0
-1	1	-1	1	8	0.0
-1	-1	1	1	8	0.0
-1	1	-1	-1	9	-37.6
-1	-1	1	-1	9	-37.6
1	-1	-1	1	10	-103.6
1	-1	-1	-1	11	-141.2
-1	-1	-1	1	11	-141.2
-1	-1	-1	-1	12	-178.8
1	1	1	1	12	178.8
1	1	1	-1	13	141.2
-1	1	1	1	13	141.2
-1	1	1	-1	14	103.6

Table 4.4: Differential phase angles ΔV_k of the two-bit detector corresponding to various input data combinations ($B_t T = 0.25$). The contributions of b_{k+2} and b_{k-3} are ignored.

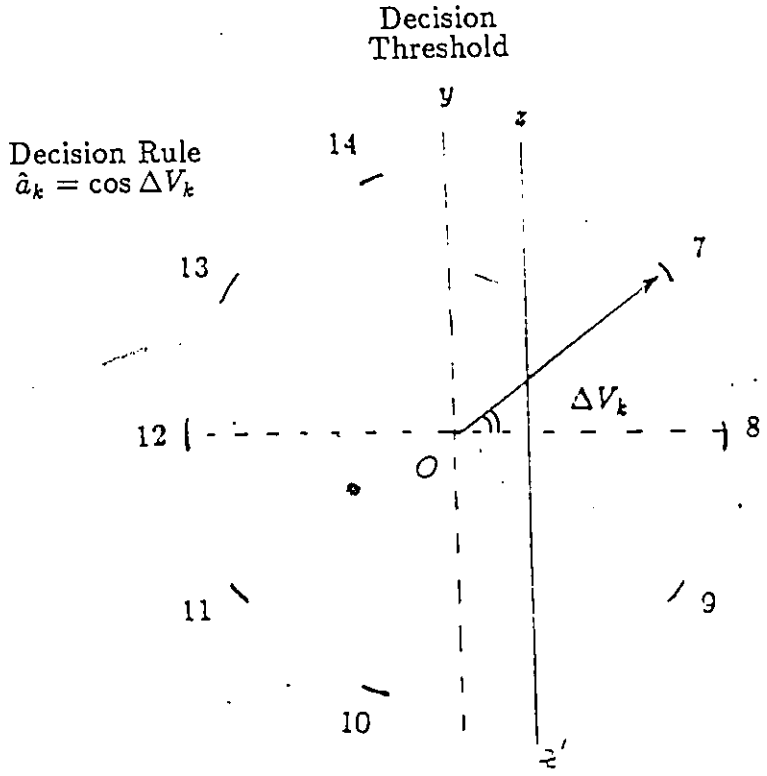

Figure 4.7: Phase-state diagram of conventional two-bit differential detection ($B_tT = 0.25$).

defined by (4.1) circumvents this problem; because

$$a_k = -b_k b_{k-1}. \tag{4.21}$$

Hence,

$$\hat{a}_k = \text{sgn}[d_2(kT)]. \tag{4.22}$$

Observe from Figure 4.7 that the phase-states at the output of the two-bit differential detector are not symmetrical with respect to the y-axis. As a result of this, the corresponding eye-diagram shown in Figure 4.8 is also asymmetric. To improve BER performance in this case, it has been

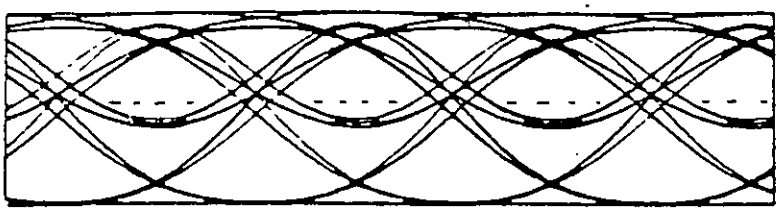

Figure 4.8: Eye-diagram of a conventional two-bit differential detector ($B_tT = 0.25$).

proposed [110] to insert a bandpass limiter after the BPF and to apply a dc bias to the threshold comparator. This is equivalent to shifting the decision region to the zz' line in Figure 4.7.

For the two-bit detector, the minimum differential phase angle is defined as

$$\Delta V_{min} = (V_0 + V_1) - 2 \sum_{i \neq 0,1} V_i. \tag{4.23}$$

The values of ΔV_{min} for various B_tT's have been tabulated in Table 4.3. A comparison of Table 4.1 and Table 4.3 reveals that for all B_tT values, the minimum differential phase angle of the two-bit detector is greater than that

of the one-bit detector (i.e., $\Delta V_{min} > \Delta\theta_{min}$). From Table 4.3 we can also conclude that the conventional two-bit differential detection is applicable to systems with $B_tT \geq 0.18$.

4.3.3 Three-Bit Differential Detection

We have seen that in comparison with a one-bit detector, a two-bit detector increases the minimum differential phase angle and widens the corresponding eye-opening. Then the natural question is whether using an n-bit differential detector ($n \geq 3$) offers any advantages? To determine this, let us examine the operation of the conventional 3-bit differential detector.

The output of the 3-bit differential detector (see Figure 4.9) is given by

$$d_3(kT) = r(kT)r(kT - 3T)\sin(\Delta U_k) + n_3(kT) \tag{4.24}$$

where

$$\Delta U_k = b_{k+2}U_{-2} + b_{k+1}U_{-1} + b_kU_0 + b_{k-1}U_1 + b_{k-2}U_2 + b_{k-3}U_3 + b_{k-4}U_4 \tag{4.25}$$

and

$$U_{k-j} = k_m \int_{kT-3T}^{kT} p(\tau - jT)\,d\tau. \tag{4.26}$$

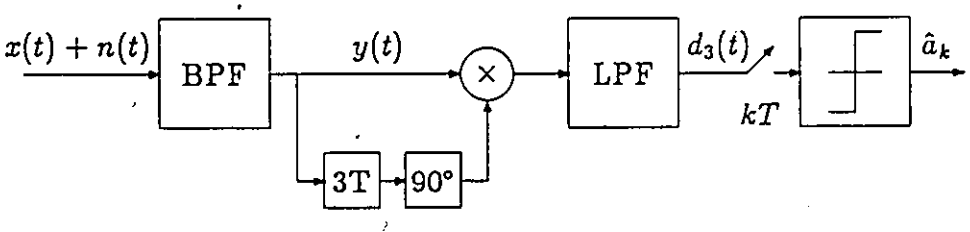

Figure 4.9: Block diagram of a three-bit differential detector.

The values of U_i for different B_tT have been tabulated in Table 4.5. The

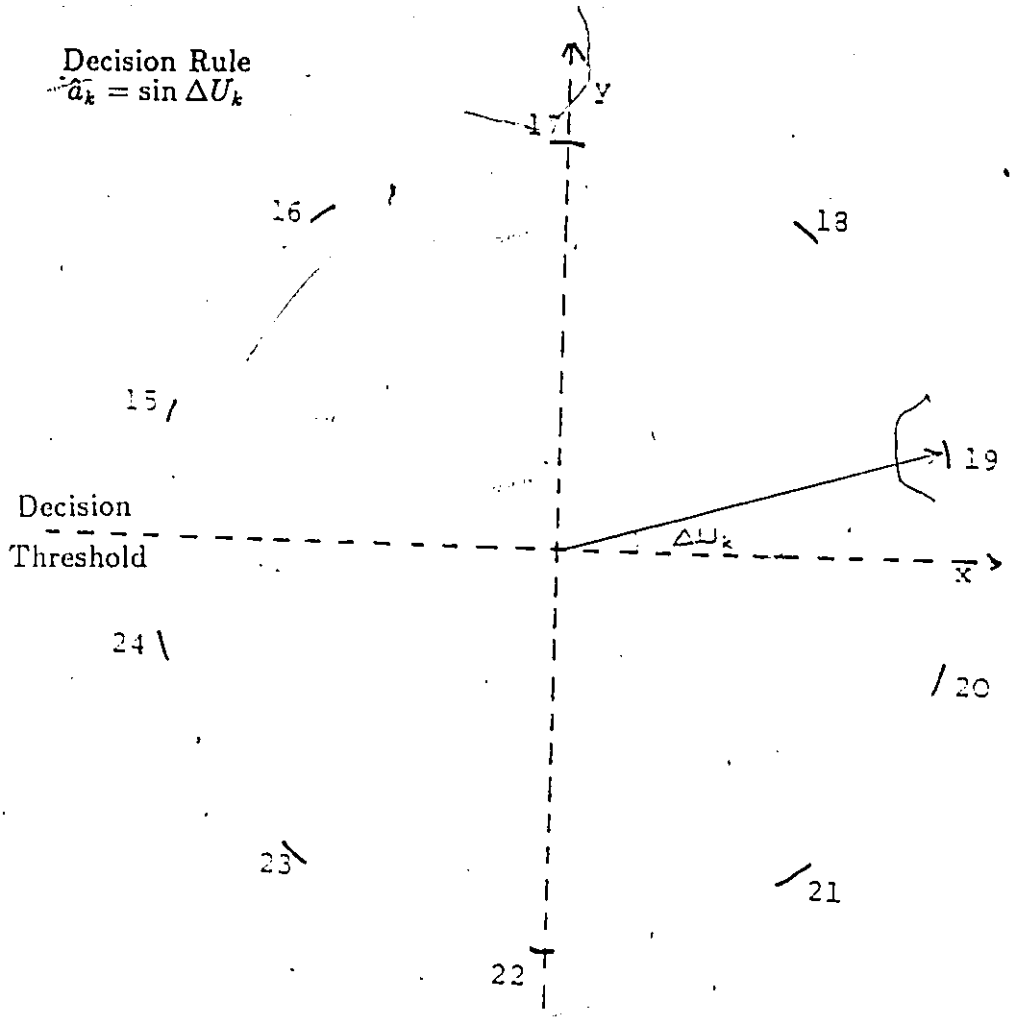

Figure 4.10: Phase-state diagram of three-bit differential detector.

B_tT	U_{-2}	U_{-1}	U_0	U_1	U_2	U_3	U_4	ΔU_{min}	ΔU_{min}^{DF}
0.15	4.85	26.7	63.0	80.3	63.0	26.7	4.85	—	52.4
0.2	1.7	22.3	67.7	86.6	67.7	22.3	1.7	—	84.0
0.25	0.6	18.8	71.2	88.8	71.2	18.8	0.6	24.8	102.4
0.3	0.2	16.2	73.9	89.6	73.9	16.2	0.2	48.8	113.8
0.4	—	12.5	77.5	90.0	77.5	12.5	—	80.0	130.0
0.5	—	10.3	79.7	90.0	79.7	10.3	—	97.6	138.8
1.0	—	5.9	84.1	90.0	84.1	5.9	—	132.8	156.4
∞	—	—	90.0	90.0	90.0	—	—	180.0	180.0

Table 4.5: Phase-shifts (in degrees) corresponding to signal terms (U_o, U_1 and U_2) and ISI terms as a function of transmit Gaussian filter B_tT for the three-bit differential detector. ΔU_{min} and ΔU_{min}^{DF} are the minimum differential phase angles before and after applying decision feedback.

differential phase angles corresponding to all combinations of b_{k-3},b_{k-2},b_{k-1}, b_k, b_{k+1} are given in Table 4.6 for $B_tT = 0.25$ and plotted in Figure 4.10. We see that the signal has 10 distinct states (counting the states which are only a few degrees apart as one). Taking into account all the ISI terms, ΔU_{min} is calculated as 24.8°. In Figure 4.10, the decision threshold is the x-axis. When ΔU_k is positive, $(b_{k-2}b_{k-1}b_k)$ is "−1"; and when ΔU_k is negative, $(b_{k-2}b_{k-1}b_k)$ is "+1". Recall from (4.2) that when a three-bit differential encoder is used,

$$a_k = -b_k b_{k-1} b_{k-2}. \tag{4.27}$$

Hence,

$$\hat{a}_k = \text{sgn}[d_3(kT)]. \tag{4.28}$$

Although the conventional 3-bit differential detector has a slightly smaller minimum differential phase angle than the one-bit differential detector, as we shall see in Section 4.4, it is more suitable to decision feedback than the 1-bit differential detector.

By examining the differential phase angles for n=4,5,...; the trend we

Bit Combinations					State (in degrees)	ΔV_k
b_{k-3}	b_{k-2}	b_{k-1}	b_k	b_{k+1}		
1	-1	-1	-1	1	15	166.4
1	1	1	-1	1	16	126.4
1	-1	1	1	1	16	126.4
1	-1	-1	-1	-1	16	126.4
-1	-1	-1	-1	1	16	126.4
1	1	-1	1	1	17	91.2
-1	-1	-1	-1	-1	17	91.2
1	1	1	-1	-1	17	88.8
1	-1	1	1	-1	17	88.8
-1	1	1	-1	1	17	88.8
-1	-1	1	1	1	17	88.8
1	1	-1	1	-1	18	52.4
-1	1	-1	1	1	18	52.4
-1	1	1	-1	-1	18	51.2
-1	-1	1	1	-1	18	51.2
-1	1	-1	1	-1	19	16.0
1	-1	1	-1	1	20	-16.0
1	1	-1	-1	1	21	-51.2
1	-1	-1	1	1	21	-51.2
1	-1	1	-1	-1	21	-52.4
-1	-1	1	-1	1	21	-52.4
1	1	-1	-1	-1	22	-88.8
1	-1	-1	1	-1	22	-88.8
-1	1	-1	-1	1	22	-88.8
-1	-1	-1	1	1	22	-88.8
1	1	1	1	1	22	-91.2
-1	-1	1	-1	-1	22	-91.2
1	1	1	1	-1	23	-126.4
-1	-1	-1	1	-1	23	-126.4
-1	1	1	1	1	23	-126.4
-1	1	-1	-1	-1	23	-126.4
-1	1	1	1	-1	24	-166.4

Table 4.6: Differential phase angles ΔU_k of a three-bit detector.

have found leads to the conclusion that the 2-bit differential detector provides the largest minimum differential phase angle. It should also be noted that in mobile communications, as the delay duration increases, having a stable carrier phase over "n" bit duration may no longer be applicable.

4.4 APPLYING DECISION FEEDBACK TO DIFFERENTIAL DETECTORS

The previous section examined the operation of the conventional differential detectors. The phase-state diagrams of Figure 4.4, Figure 4.7 and Figure 4.10 indicate that a large amount of intersymbol interference is inherent in the received signal. In this section we demonstrate how the destructive effect of ISI can be reduced.

4.4.1 Decision Feedback in a One-Bit Differential Detector

For the one-bit differential detector, at the instant $t = kT$, $\Delta\theta_k$ depends not only on b_k but also on b_{k-1} and b_{k+1} (see (4.12) and (4.13)). When b_k is to be decided, the estimate of b_{k-1} (i.e., $\hat{b}_{k-1}$) is already available. Hence, introducing a phase shift equal to $(\hat{b}_{k-1}\theta_1)$ in the T second delay arm will cancel the effect of b_{k-1} on the signal phase.

Referring to Figure 4.4, we observe that in states 3 and 4, the effect of ISI is always destructive because $b_k \neq b_{k-1}$. Thus a phase shift equal to $(\hat{b}_{k-1}\theta_1)$ will increase the distance from the decision threshold by an angle θ_1. The corresponding new phases are:

$$\Delta\theta'_{k3} = \Delta\theta_{k3} + \theta_1 \tag{4.29}$$

and

$$\Delta\theta'_{k4} = \Delta\theta_{k4} - \theta_1. \tag{4.30}$$

Thus, for states 3 and 4, the destructive ISI effect of the previous pulse is removed and a larger value at the sampling instant is achieved.

For states 2 and 5, the effect of b_{k-1} can be constructive or destructive. By applying decision feedback, the effect of b_{k-1} is removed. Thus we obtain:

$$\Delta\theta'_{k2} = \Delta\theta_{k2} \pm \theta_1 \tag{4.31}$$

and

$$\Delta\theta'_{k5} = \Delta\theta_{k5} \pm \theta_1. \tag{4.32}$$

The states 1 and 6 always have the widest separation and a phase shift of $(\hat{b}_{k-1}\theta_1)$ reduces the phase angle $\Delta\theta_{k1}$ and $\Delta\theta_{k6}$ by θ_1. Thus we obtain:

$$\Delta\theta'_{k1} = \Delta\theta_{k1} - \theta_1 \tag{4.33}$$

and

$$\Delta\theta'_{k6} = \Delta\theta_{k6} + \theta_1. \tag{4.34}$$

Note that in determining the system performance, the critical states are 3 and 4. Hence the reduction in $\Delta\theta_k$ for states 1,2,5 and 6 is several times compensated by the increase in $\Delta\theta_{k3}$ and $\Delta\theta_{k4}$.

The phase-state diagram (for $B_tT = 0.25$) after applying decision feedback is shown in Figure 4.11. The eye-diagram obtained by using decision feedback is shown in Figure 4.12. A comparison of Figure 4.5 and Figure 4.12 reveals that the eye-opening is significantly increased.

The above analysis considered only the effect of b_{k-1} at the k^{th} decision instant. For systems with a $B_tT < 0.25$, the effect of b_{k-2} is not negligible. Then, the required phase shift in the T delay arm is $(\hat{b}_{k-1}\theta_1 + \hat{b}_{k-2}\theta_2)$.

The minimum differential phase angle after applying decision feedback can be defined as

$$\Delta\theta^{DF}_{min} = 2(\theta_0 - \sum_{i<1}\theta_i). \tag{4.35}$$

The values of $\Delta\theta^{DF}_{min}$ for different B_tT are shown in the last column of Table 4.1. From Table 4.1, we can conclude that by using decision feedback, a one-bit differential detection of GMSK is possible for B_tT values as low as 0.15[3].

[3]Recall that for the conventional one-bit differential detector the minimum permissible $B_tT = 0.22$.

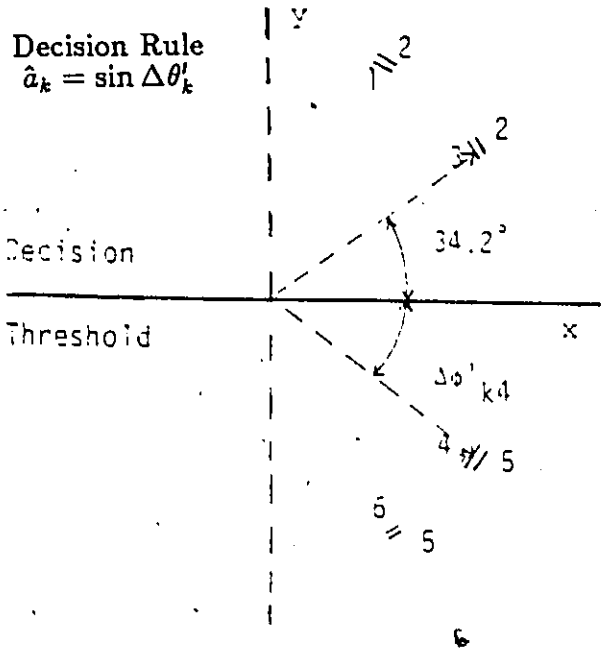

Figure 4.11: Phase-state diagram of one-bit differential detector after applying decision feedback.

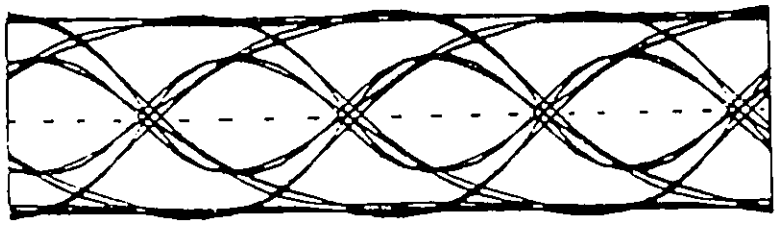

Figure 4.12: Eye-diagram of one-bit differential detector after applying decision feedback.

4.4.2 Decision Feedback in a Two-Bit Differential Detector

Having demonstrated that decision feedback increases the eye opening of the one-bit detector, we shall now apply the same concept to the two-bit detector.

Let us first assume that the effect of b_{k-3} and b_{k+2} is negligible. Observe from Figure 4.7 that the phase-states 10 and 14 are subject to the maximum amount of ISI. If the states 10 and 14 are ignored, then the y-axis represents the optimal decision threshold. Hence our objective is to move the state 10 clockwise and the state 14 counter-clockwise. While doing this, we also want to keep the other states as far away from the decision threshold (i.e. y-axis) as possible.

To meet these objectives, the phase of the $2T$ delayed signal is shifted by λ degrees. The phase shifting rule can be formulated as follows:

$$\lambda = \begin{cases} 2\hat{b}_{k-2}V_2 & \text{if} \quad \hat{b}_{k-1} \neq \hat{b}_{k-2} \\ 0 & \text{if} \quad \hat{b}_{k-1} = \hat{b}_{k-2}. \end{cases} \tag{4.36}$$

When the effect of b_{k-3} is not negligible, the required phase shifts are slightly different. Then, we have:

$$\lambda = \begin{cases} 2\hat{b}_{k-2}V_2 + 2\hat{b}_{k-3}V_3 & \text{if} \quad \hat{b}_{k-1} \neq \hat{b}_{k-3} \quad \text{and} \quad \hat{b}_{k-1} \neq \hat{b}_{k-2} \\ 2\hat{b}_{k-2}V_2 & \text{if} \quad \hat{b}_{k-1} = \hat{b}_{k-3} \quad \text{and} \quad \hat{b}_{k-1} \neq \hat{b}_{k-2} \\ 2\hat{b}_{k-3}V_3 & \text{if} \quad \hat{b}_{k-1} \neq \hat{b}_{k-3} \quad \text{and} \quad \hat{b}_{k-1} = \hat{b}_{k-2} \\ 0 & \text{if} \quad \hat{b}_{k-1} = \hat{b}_{k-3} \quad \text{and} \quad \hat{b}_{k-1} = \hat{b}_{k-2}. \end{cases} \tag{4.37}$$

The phase states (for $B_bT = 0.25$) after applying these phase shifts are shown in Figure 4.13. Note that the resulting phase states and the corresponding eye-diagram shown in Figure 4.14 are symmetric. Comparing the eye-diagram of the conventional two-bit differential detector, we observe that after applying decision feedback the eye-opening is significantly increased.

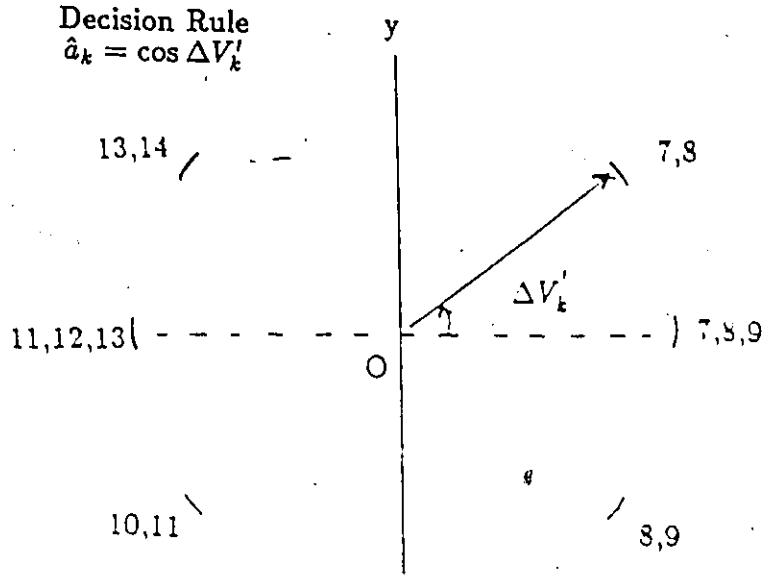

Figure 4.13: Phase state diagram of two-bit differential detector after applying decision feedback.

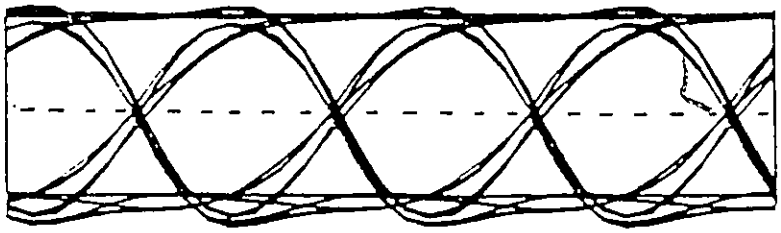

Figure 4.14: Eye-diagram of two-bit differential detector after applying decision feedback.

4.4.3 Decision Feedback in a Three-Bit Differential Detector

To determine how to apply the decision feedback to the 3-bit differential detector, let us compare Table 4.3 and Table 4.5. We see that $U_0 \simeq V_0$, $U_{-1} \simeq V_{-1}$, $U_2 \simeq V_1$ and $U_3 \simeq V_2$. Table 4.5 has a column for U_1 values which has no counterpart in Table 4.3. Noting these properties, we can transform the phase states of the conventional 3-bit differential detector to that of the 2-bit detector with decision feedback (see Figure 4.13). In order to do this, we first introduce a phase shift in the $3T$ delay arm which is equivalent to $(\hat{b}_{k-1}U_1)$. Then, we apply the phase shift rules which were used for the 2-bit detector (i.e., (4.36) or (4.37)). The only difference is that the bit corresponding to U_2 and U_3 are b_{k-2} and b_{k-3} respectively. Hence the amount of phase shift (χ) required in the 3-bit delay arm can be formulated as follows.

$$\chi = \begin{cases} \hat{b}_{k-1}U_1 + 2\hat{b}_{k-3}U_3 + 2\hat{b}_{k-4}U_4 & \text{if } \hat{b}_{k-2} \neq \hat{b}_{k-3} \text{ and } \hat{b}_{k-2} \neq \hat{b}_{k-4} \\ \hat{b}_{k-1}U_1 + 2\hat{b}_{k-3}U_3 & \text{if } \hat{b}_{k-2} \neq \hat{b}_{k-3} \text{ and } \hat{b}_{k-2} = \hat{b}_{k-4} \\ \hat{b}_{k-1}U_1 + 2\hat{b}_{k-4}U_4 & \text{if } \hat{b}_{k-2} = \hat{b}_{k-3} \text{ and } \hat{b}_{k-2} \neq \hat{b}_{k-4} \\ \hat{b}_{k-1}U_1 & \text{if } \hat{b}_{k-2} = \hat{b}_{k-3} \text{ and } \hat{b}_{k-2} = \hat{b}_{k-4}. \end{cases} \tag{4.38}$$

The eye-diagrams of the 3-bit detector before and after applying decision feedback are shown in Figure 4.15 and Figure 4.16 respectively (for $B_tT = 0.25$).

4.5 SIGNAL COMBINING AND PROPOSED RECEIVERS

The last section demonstrated that applying decision feedback to differential detectors significantly increases the corresponding eye-openings. The next step is to use the outputs of two detectors jointly.

The structure of the envisioned receiver can be established by using the maximum likelihood ratio test (MLRT) (see Section 3.6). The MLRT indicates that the optimal utilization of more than one detector requires a nonlinear receiver. In order to reduce the complexity of such an optimal

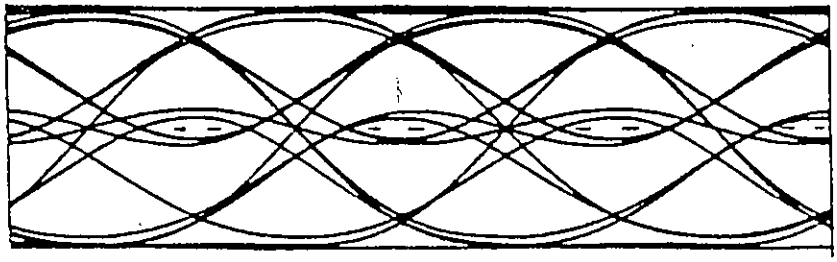

Figure 4.15: Eye-diagram of a three-bit differential detector before applying decision feedback.

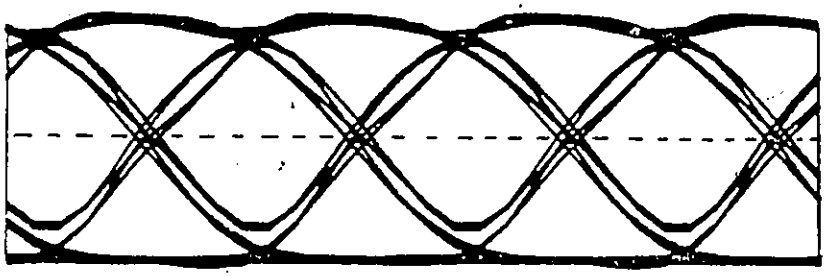

Figure 4.16: Eye-diagram of a three-bit differential detector after applying decision feedback.

receiver, we propose two suboptimal linear receivers.

In the first receiver, the decision feedback is applied to the one-bit and two-bit detectors. Then the outputs of these detectors are combined. This receiver is denoted by 1+2DF. The decision law for the 1+2DF receiver is given by

$$\hat{a}_k = \text{sgn}[d_1'(kT) - c_1 \hat{a}_{k-1} d_2'(kT)] \tag{4.39}$$

where $d_1'(kT)$, $d_2'(kT)$ are respectively the sampled outputs of the one and two-bit detectors after decision feedback, and c_1 is the combining coefficient ($c_1 > 1$). The structure of the proposed receiver is that of the combining with feedback (CWF) detector and its block diagram is shown in Figure 4.17. Note that the transmitter corresponding to the 1+2DF receiver does not employ a differential encoder.

In the second proposed receiver, the decision feedback is applied to the two-bit and the three-bit detectors, and then the outputs are combined. This receiver is denoted as 2+3DF. The decision law of the 2+3DF receiver is given by

$$\hat{a}_k = \text{sgn}[d_2'(kT) - c_2 \hat{a}_{k-1} d_3'(kT)] \tag{4.40}$$

where $d_2'(kT)$, $d_3'(kT)$ are respectively the sampled outputs of the two and three-bit detectors after decision feedback, and c_2 is the combining coefficient ($c_2 < 1$). The block diagram of the 2+3DF receiver is shown in Figure 4.18. Note that the transmitter corresponding to the 2+3DF receiver requires a differential encoder (see Section 4.2 and equation (4.1)).

4.6 RESULTS

We used a computer simulation approach to evaluate the BER performances of various DGMSK configurations. The simulation was based on the Monte Carlo error counting technique[4].

The configurations we evaluated were:

- one-bit differential detection with decision feedback (1DF);

[4]Program listings are given in Appendix B.

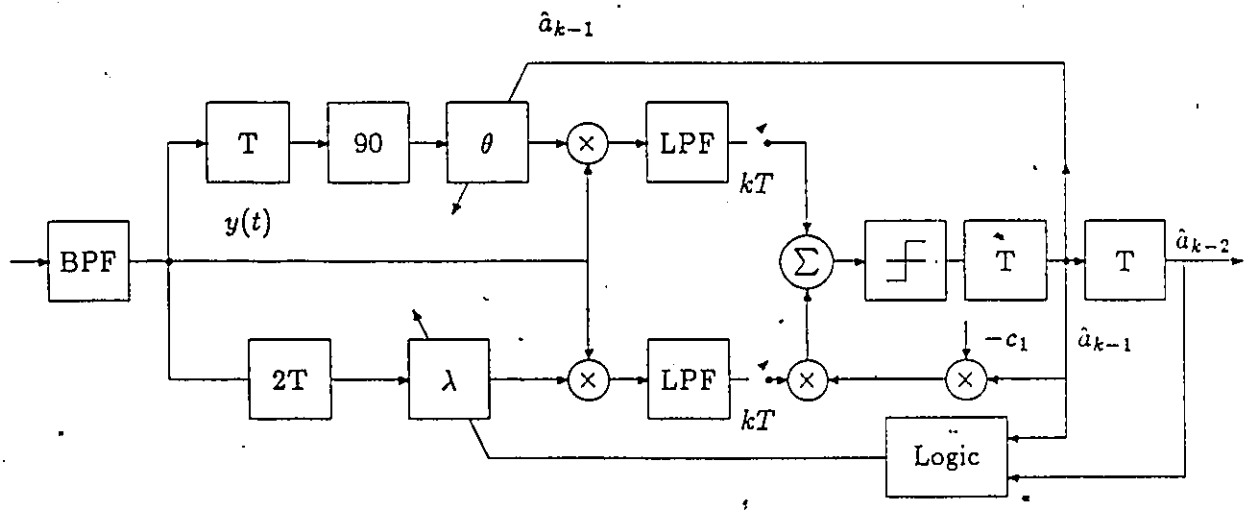

Figure 4.17: Block diagram of 1+2DF receiver.

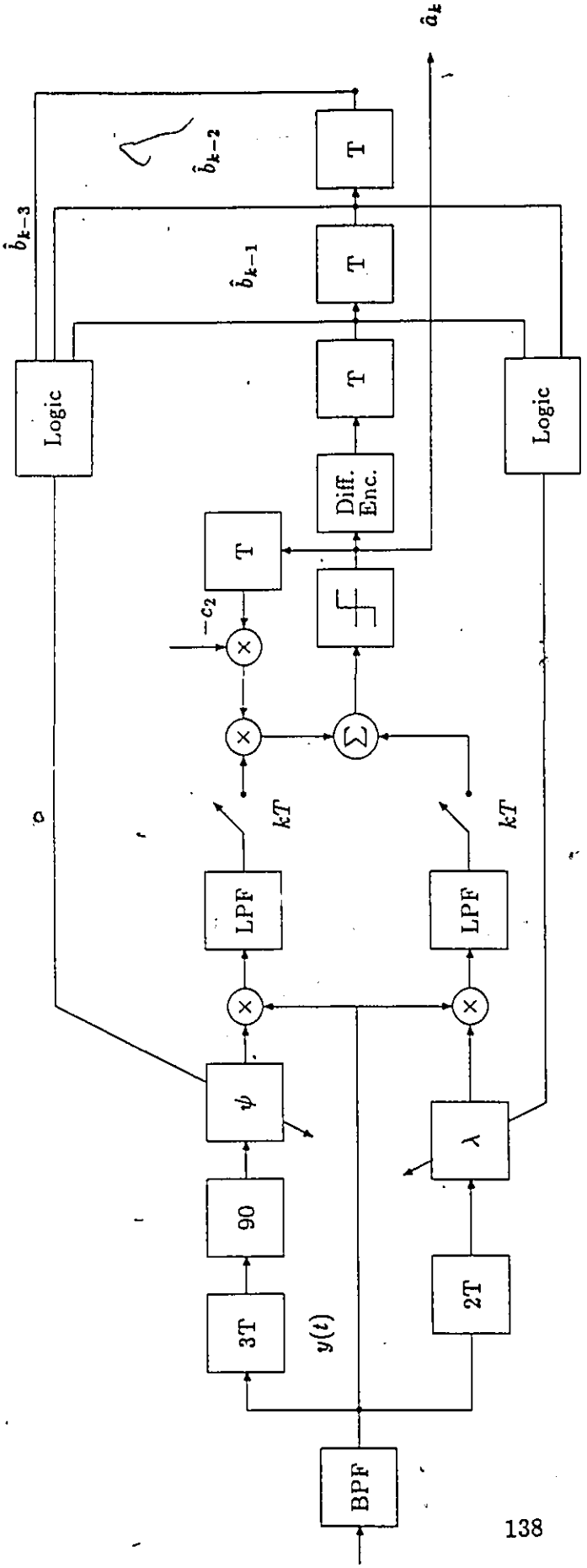

Figure 4.18: Block diagram of 2+3DF receiver.

- combined one and two-bit detection with decision feedback (1+2DF);
- combined two and three-bit detection with decision feedback (2+3DF).

For comparison purposes, we also evaluated

- conventional one-bit differential detection (1C);
- conventional two-bit differential detection using a Gaussian predetection filter(2CG) [110];
- conventional two-bit differential detection using a Butterworth predetection filter(2CBW).

The individual performances of the receivers which use decision feedback are as follows.

1DF

The BER performance of the 1DF receiver for various B_tT values is plotted in Figure 4.19. In the same figure, we also show the performance of the conventional one-bit detector (1C). The predetection BPF used for both configurations is a fourth-order Butterworth with a $BT = 1.0$ (which yields a better performance than a Gaussian filter). Observe that for the B_tT value of 0.3, at a BER of 10^{-3}, the decision feedback configuration requires about 4.5 dB less E_b/N_0 than the conventional detector. For smaller values of B_tT the advantage of the 1DF increases. Furthermore, the 1DF configuration can operate at B_tT values which are prohibitive for the conventional system (e.g., $B_tT = 0.2$).

1+2DF

Although the decision feedback drastically improves the performance of one-bit differential detection, a comparison of 1DF and 2CG [110] indicates that 1DF does not provide any advantages by itself. However, the improved one-bit differential detector permits the utilization of one and two bit detectors jointly, i.e., the 1+2DF configuration.

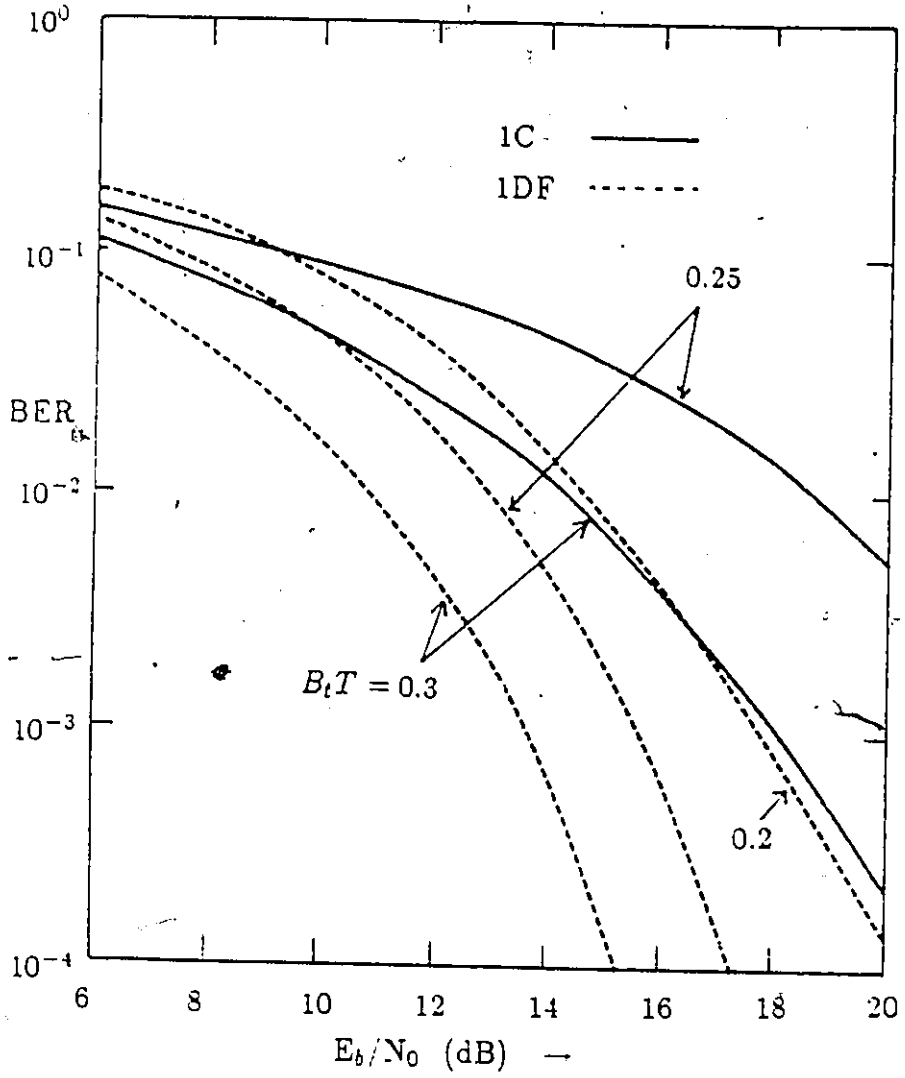

Figure 4.19: BER performances of one-bit differential detectors (1C: conventional, 1DF: using decision feedback).

The BER performance of the 1+2DF receiver for various B_tT values is plotted in Figure 4.20. The predetection BPF used is a fourth-order Butterworth with a BT=1.0, and we have optimized the combining coefficient c_1 for different values of E_b/N_o. For GMSK, the best differential detector reported in the literature is the conventional two-bit detector which uses a Gaussian predetection BPF [110,105]. We have found that using a fourth-order Butterworth filter provides about 0.5 dB improvement in the performance of the conventional two-bit differential detector. This can be observed by comparing the curves for 2CG and 2CBW in Figure 4.20.

When the performances of 1+2DF and 2CBW detectors are compared, we see from Figure 4.20 that for B_tT =0.2 the improvement of decision feedback is about 4 dB (at BER=10^{-3}). Note that the improvement is a function of the B_tT value, and as B_tT is reduced, the improvement becomes greater.

2+3DF

In Section 4.4 we have shown that the three-bit differential detector using decision feedback provides a larger eye opening than a one-bit differential detector with decision feedback. Consequently, the performance of the 2+3DF structure is expected to be better than that of the 1+2DF receiver.

The BER performance of the 2+3DF receiver for various B_tT values is plotted in Figure 4.21. The predetection BPF is a fourth-order Butterworth with a BT=1.0, and the combining coefficient c_2 is optimized. By comparing the performances of 2+3DF and 2CBW detectors, we see that at a BER of 10^{-3} and for a B_tT value of 0.2, the 2+3DF configuration provides about 5 dB E_b/N_o advantage. Again, the improvement varies as a function of the B_tT value.

Overall Comparison

Having evaluated the new receivers individually, let us compare the performances of different receivers for a given B_tT. For this purpose we chose the GMSK system with a B_tT=0.25. This value of B_tT maximizes the spectrum efficiency of digital land mobile radio [113]. The BER curves obtained are shown in Figure 4.22. We can observe that 2+3DF has the best performance among the differential detectors. For example, at BER of

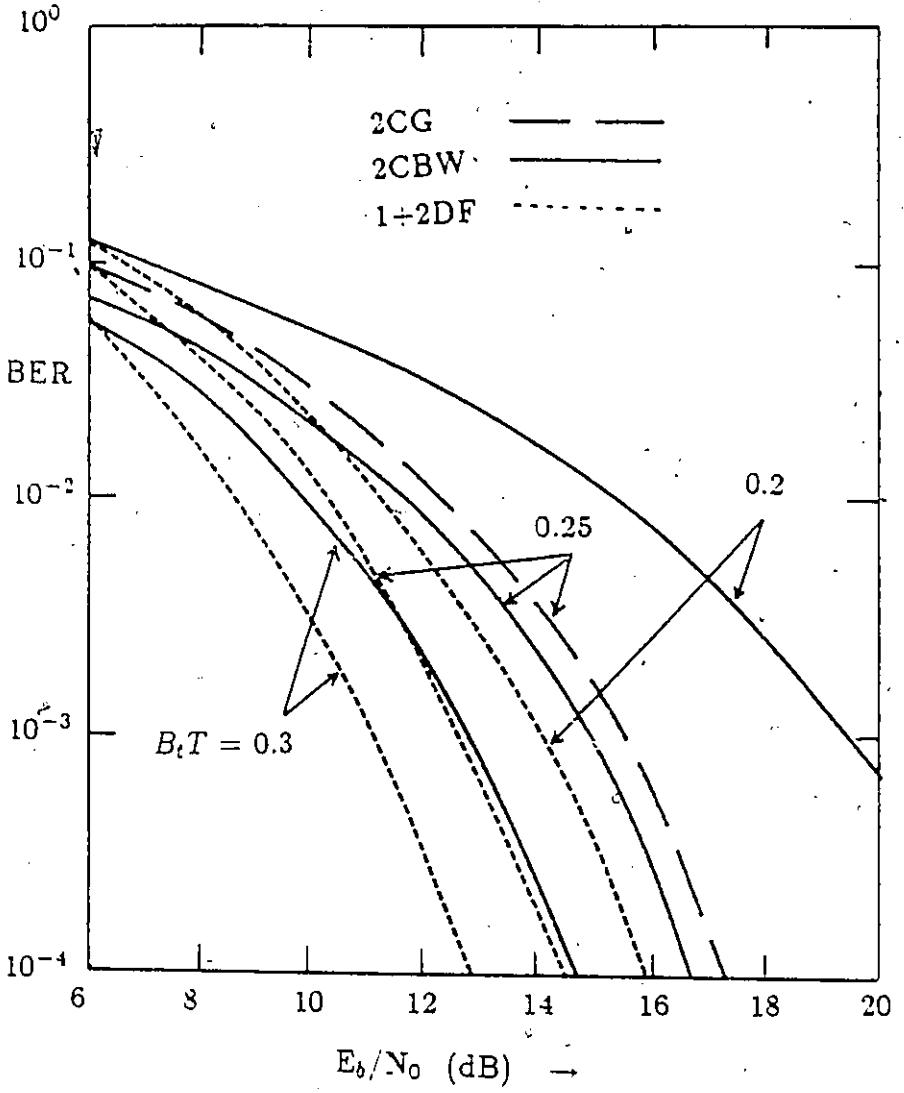

Figure 4.20: BER performances of conventional two-bit differential detector (2C), and combined one and two-bit differential detectors with decision feedback (1−2DF).

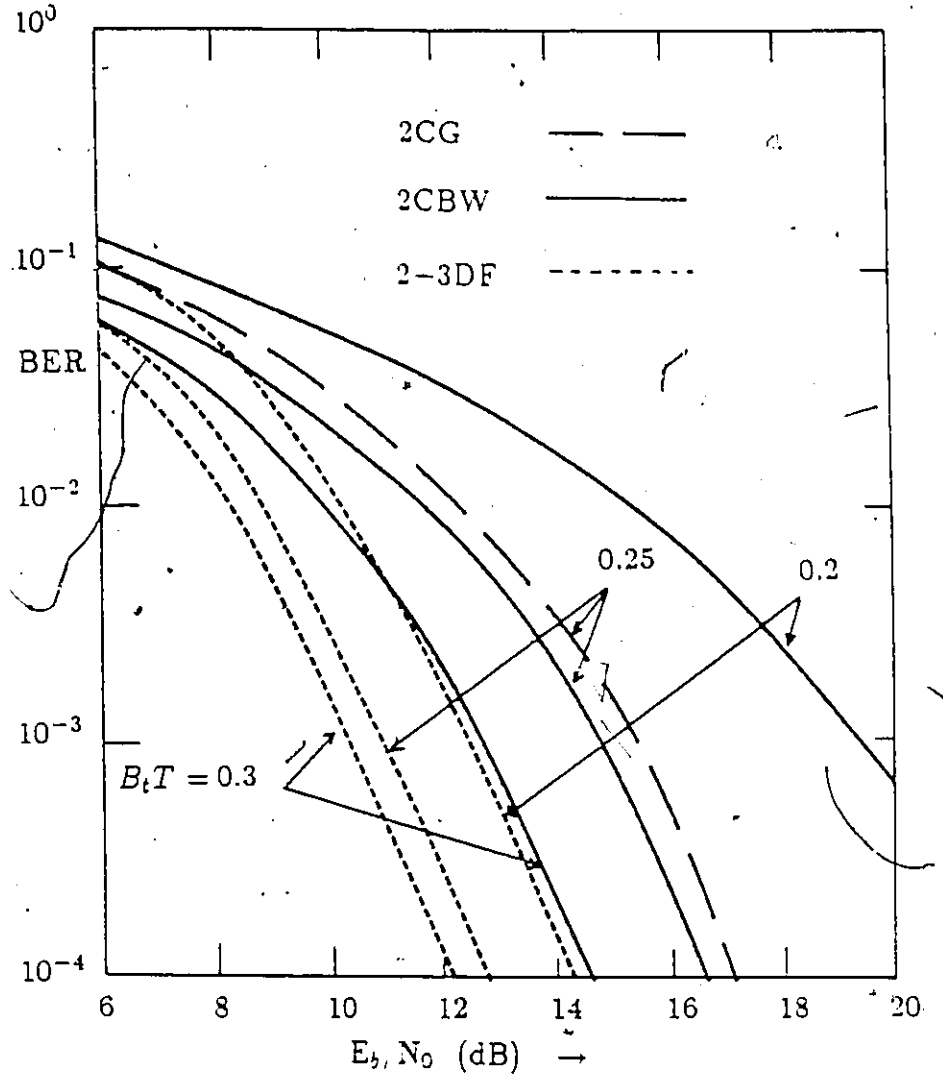

Figure 4.21: BER performances of conventional two-bit differential detector (2C), and combined two and three-bit differential detectors with decision feedback (2−3DF).

10^{-4} it offers a 1 dB and a 4.0 dB E_b/N_0 advantage over 1+2DF and 2CBW receivers respectively. In Figure 4.22 we have also plotted the performance of coherent GMSK in a AWGN channel [94]. It can be observed that the 2+3DF receiver is only 3 dB away from the coherent receiver, while the problems associated with carrier recovery are avoided.

4.7 CONCLUSIONS

The principle of the differential detection of GMSK has been examined for one-bit, two-bit and three-bit differential detectors. The phase-state diagrams introduced here provide an insight into the intersymbol interference mechanisms of these differential detectors. By applying decision feedback to these differential detectors, the effect of destructive ISI has been partially removed. The improved differential detectors may be utilized in configurations where the outputs of two detectors are combined. The best BER performance is obtained when the outputs of the modified two-bit and three-bit differential detectors are jointly utilized. For a system with a $B_tT = 0.25$, this new receiver provides about a 4 dB E_b/N_o advantage over currently known DGMSK receivers. Furthermore, the improvement is greater for systems with B_tT values smaller than 0.25.

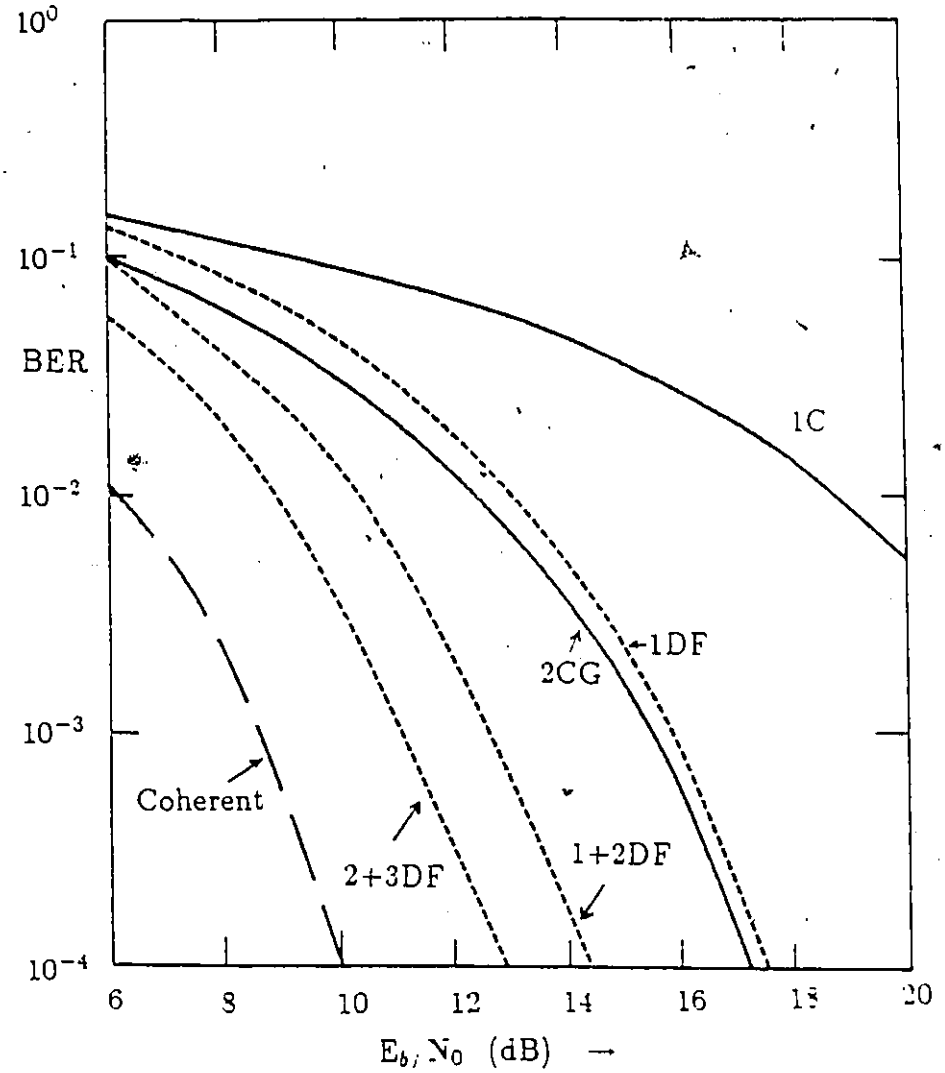

Figure 4.22: BER performance of various DGMSK receivers ($B_tT = 0.25$).

Chapter 5

SUMMARY AND SUGGESTIONS FOR FURTHER RESEARCH

5.1 SUMMARY

This thesis has presented new transmit/receive processing techniques to improve the bandwidth efficiency and/or detection efficiency of systems using differential detection. The contributions of the thesis can be summarized as follows:

1) *The DCTPSK modem has been introduced.*
This modem employs a new signal format which can be demodulated using a conventional differential detector. The DCTPSK modem is suitable to frequency division multiple access operations when the channel includes nonlinearities.

The bit error rate performance of the DCTPSK modem in a hardlimited channel has been evaluated. It has been shown that in an adjacent channel interference environment, more carriers can share the same channel using DCTPSK modems compared to using DQPSK or DMSK modems. Similarly, for certain bandwidth efficiencies, a DCTPSK modem requires less transmit power than a DQPSK or a DMSK modem.

As a proof of concept, we implemented a DCTPSK modem. The design principle of the modem has been discussed and the circuit diagrams have been given. The performance of the modem has been evaluated using a back-to-back configuration, and also via a satellite link. The experimental results indicate that the modem suffers about a 2 dB E_b/N_0 degradation due to various hardware imperfections. We also identified various sources of impairments when the modem was evaluated over a satellite link.

2) *Two new receiver processing techniques have been introduced.* The new receivers use twice the number of differential detectors and additional baseband processing to improve the BER performance of the DCTPSK modem.

The first new technique uses a symbol-by-symbol detector which combines the outputs of one-bit and two-bit differential detectors. Thus, an E_b/N_0 improvement of 1.2 dB is achieved (at BER=10^{-4}).

The second receiver processing technique is based on using a four-state sequential decoder. The E_b/N_0 improvement achieved with this technique is about 1.7 dB.

The new receiver processing techniques are also applicable to DQPSK systems, and the same concepts can be utilized for other modulation techniques as well.

3) *New receiver structures have been introduced to improve the BER performance of differentially detected Gaussian Minimum Shift Keying.* DGMSK systems can provide much higher bandwidth efficiencies than DQPSK, DMSK or DCTPSK systems. But the price paid for the increased bandwidth efficiency is a loss in detection efficiency due to a significant amount of ISI. Hence, to improve the performance of the DGMSK sytems, the effect of ISI had to be reduced as a first step. For this purpose, the principle of the differential detection of GMSK has been examined for one-bit, two-bit and three-bit differential detectors. The phase-state diagrams introduced here provide insight to the intersymbol interference mechanisms of the differential detectors. By applying decision feedback to the differential detectors, the effect of destructive ISI has been partially removed. The modified differential detectors may be utilized in configurations where the outputs of two detectors are combined. The best BER performance found here is obtained when the outputs of the modified two-bit and three-bit dif-

ferential detectors are jointly utilized. For a system with a $B_tT = 0.25$, this new receiver provides about a 4 dB E_b/N_o advantage over currently known DGMSK receivers. Furthermore, the improvement is greater for systems with B_tT values smaller than 0.25.

5.2 SUGGESTIONS FOR FURTHER RESEARCH

5.2.1 Using Decision Feedback in Differential Detection of CPM Signals

The compact main lobe and low sidelobes of the GMSK spectrum is achieved by using pulse shapes which extend over several symbol intervals. There are several CPM signals offering similar advantages such as TFM and Duobinary MSK. In all these CPM signals, ISI is inherent in the transmitted signal, and employing conventional differential detectors results in rather poor BER performances.

The decision feedback structure which we introduced for GMSK can in principle be applied to other CPM signals. Therefore, for the CPM signals of interest, the exact structure of the receiver might be determined and the performance of the system might be evaluated.

5.2.2 Sequential Decoder for CPM Signals

The sequential decoder presented in Section 3.6 provided about a 1.7 dB improvement over a conventional differential detector. Following a similar approach, sequential decoders for GMSK and other CPM signals can be developed. Since the CPM pulses extend over several symbol intervals, the sequential decoders required here will be rather complex. But in return, the BER improvements obtained by using such a sequential detector are expected to be higher than the decision feedback structure presented in this thesis.

5.2.3 Designing CPM Signals With Asymmetric Pulse Shapes

In Chapter 4, we have seen that by using decision feedback, the ISI due to past symbols can be removed. When the pulse shapes utilized are symmetric (e.g., GMSK or TFM), the ISI due to future symbols is still significant. By using asymmetric pulse shapes, the ISI due to future symbols can be kept at a low level. Thus the BER performance will improve. For this purpose, the bandwidth efficiency versus detection efficiency of various asymmetric pulse shapes need to be investigated.

5.2.4 Performance of Differential Detection in Fading Channels

In this thesis the impairments considered were the additive white Gaussian noise, ISI and ACI. In mobile radio and satellite communications, the other major sources of impairments are fading and shadowing. The performance degradations caused by fading and shadowing on systems using differential detection, particularly the new systems presented here, are worth studying.

5.2.5 Applying Differential Detection to Coded Modulations

In recent years, powerful coded modulation techniques have been introduced [126]. Coded modulations offer the attractive possibility of achieving performance improvements without any bandwidth expansion when compared to uncoded modulations. Coded modulations are currently being applied to voice-band data transmission [127], and future satellite communication systems are expected to utilize them as well [128,129].

The existing coded modulation techniques are designed for coherent detection. Designing coded modulation constellations suitable to differential detection is a challenging and potentially fruitful area.

Appendix A

DCTPSK MODEM DETAILS

This appendix consists of two parts. Section A.1 serves as a user's manual for the proof-of-concept DCTPSK modem, while in Section A.2 the circuit diagrams of the modem are documented.

A.1 DCTPSK Modem User Manual

This section intends to serve as a user's manual for anyone interested in using the DCTPSK modem. All the equipment needed is currently available in the Digital Communication Group laboratory. Following the steps described below, the user can reproduce the results presented in this thesis.

A.1.1 Equipment Needed

- Data Error Analyzer (e.g. HP 1645)
- Oscilloscope (bw $<$ 70 MHz, with a x-y display option)
- Spectrum Analyzer (e.g. Anritsu MS62D)
- RMS Powermeter (e.g. HP 435B)

- Power Supply (+15 V, +5 V, -12 V)
- Signal Generator (4.096 MHz, e.g. HP 606A)
- Signal Generator (70.256 MHz, 10dBm; e.g. Marconi 2019)
- IF filter @ 70 MHz (noise bw known, e.g. K&L 3C20-70/1-B/B)
- IF Noise Source (e.g. DCD 3002)
- Combiner (e.g. MCL ZFSC2-1)
- Variable Attenuators, Cables, T connectors, 50 Ω termination.

A.1.2 Setting Up The Modem

The DCTPSK modem consists of 5 cards (Vector plugboard 4610 construction) plugged into a module cage (Vector-Pak) which can accommodate up to 8 cards. Power supply connections are on the right side of the box. All other external connections are made from the front panel using BNC connectors. In Figure A.1 the front panel of the modem is shown and the external connections are indicated. Note that the recommended power levels for the external connections are underlined.

The modem is set-up as follows.

1) Supply the following dc power levels:

- green: +15 V,
- red: +5 V,
- yellow: -12 V,
- black: ground

2) Observe that the internally generated 64 kHz data clock is available at port **2**. This clock is fed to a PRBS generator (e.g. HP 1645).

3) Connect the output of the PRBS generator (Data Out) to the modem "Data In" port (i.e. **1**).

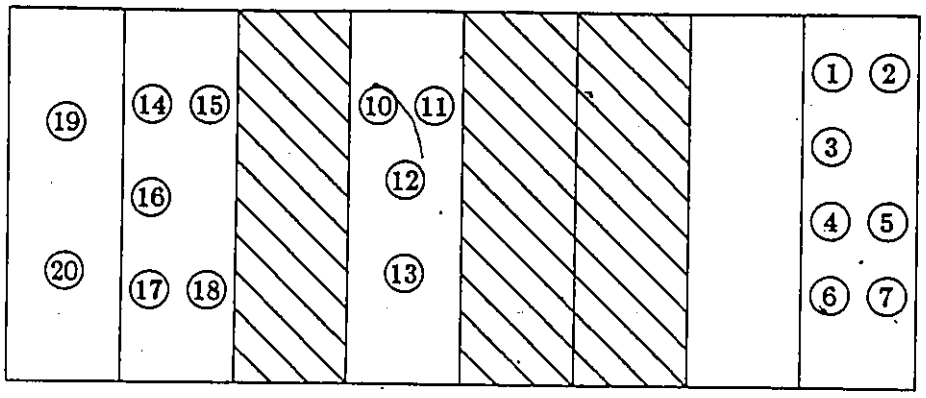

Figure A.1: Front panel of the modem. Hatched sections not used.

1. Data In (from HP 1645) (TTL)
2. 64 kHz Clock Out (to HP 1645)
3. 256 Clock Out (UNUSED)
4. Differentially Encoded I-Channel (test point)
5. Differentially Encoded Q-Channel (test point)
6. I-Channel after S/P
7. Q-Channel after S/P
8. Baseband DCTPSK I-Channel (to **11**)
9. Baseband DCTPSK Q-Channel (to **10**)
10. Input to 70 MHz Mixer (from **9**)
11. Input to 70 MHz Mixer (from **8**)
12. UNUSED
13. Transmitted Data Out (IF: 70 MHz) (to combiner or Test Loop Translator)
14. Received IF Signal In (70 MHz) (from BPF or D/C) (-30 dBm)
15. IF Local Oscillator In (70.256 MHz) (from Marconi 2019) (10 dBm)
16. Down Converted IF Signal Out (@ 256 kHz) (to **19**)
17. Decoded Data Out (to Error Analyzer Data In)
18. Integrated Q-Channel Eye-Diagram (for fine adjustment)
19. Received Signal @ 256 kHz (from **16**)

20 Clock In for the Differential Detector (4096 kHz from HP 606A) (10 dBm)

A.1.3 Baseband Signals

4) At this point the following waveforms can be observed on the scope.

- Serial to parallel converted data is available at ports **6, 7**;
- The differentially encoded I and Q channel signals are available at ports **4, 5** respectively. Note that ports **4–7** are test points; the signals observed at these points are connected to the other stages of the modem internally.

5) The baseband I and Q channel DCTPSK signals are available at ports **8, 9** respectively. By connecting these ports to a scope and using the 64 kHz clock for external triggering, the eye-diagrams of the I and Q-channel signals can be viewed (see Chapter 3, Figure 3.20). With the same connections, if the scope is switched to x-y mode, the signal space diagram (SSD) of the DCTPSK modem can be observed (see Chapter 3, Figure 3.21).

A.1.4 Modulated Signal

6) The baseband DCTPSK signals are fed into a quadrature modulator. The center frequency of the modulator is 70 MHz and this is provided by an internal crystal oscillator. To obtain the modulated signal, port **8** is connected to port **11** and port **9** is connected to port **10**. The transmitted IF signal can be observed at port **13**. The spectrum of the signal can be observed on a spectrum analyzer (see Chapter 3, Figure 3.6).

A.1.5 BER Measurements Using a Noise Generator

7) The transmitted 70 MHz signal (from port **13**) and the noise from the IF noise generator are externally combined. Signal plus noise are passed through a BPF of a known bandwidth. The output of the BPF is connected to port **14**. The output of the 70 MHz BPF is also connected to the power meter for carrier and noise power measurements.

The decoded data out (port **17**) is connected to the "data in" port of the Data Error Analyzer (e.g. HP 1645). The data Error Analyzer also requires a receive clock. For this purpose the received clock is the same as the transmit clock (i.e., hardwired).

A.2 Circuit Diagrams

A block diagram showing the operations performed on each card is given in Figure A.2. The associated circuit diagrams are given in Figures A.3 to A.7. The correspondence between the cards, operations performed, and the circuit diagrams are tabulated in Table A.1.

Card No.	Functions Performed	Corresponding Figure(s)
1	Serial to Parallel Conversion	Figure A.3
1	Differential Encoding	Figure A.3
1	Selecting Transitions	Figure A.4
2	DCTPSK Processors	Figure A.5
3	Quadrature Modulator	Figure A.6
4	70 MHz to 256 kHz D/C	Figure A.7
4	Phase Comparator	Figure A.8
4	PWM Decoder	Figure A.8
5	Digital Delay & Phase shifting	Figure A.9

Table A.1: Functions performed on each card and corresponding circuit diagrams.

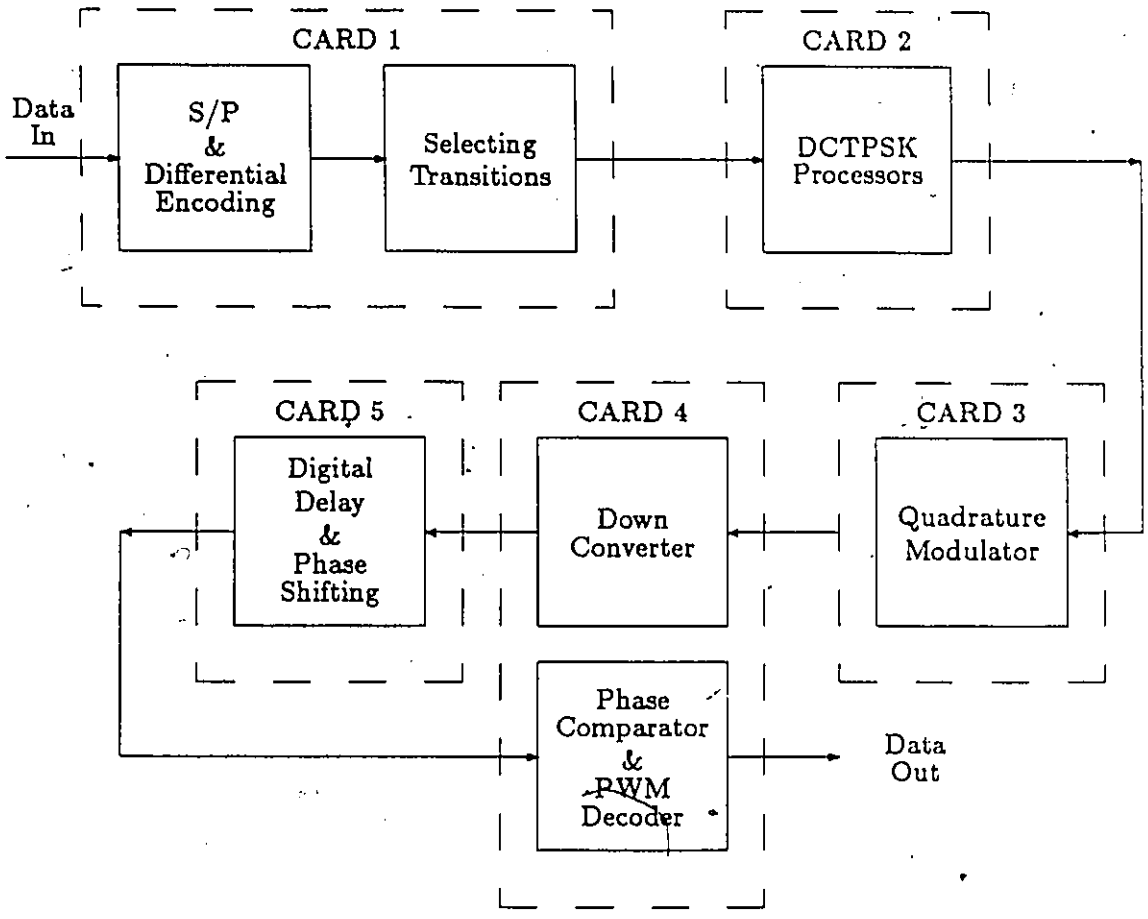

Figure A.2: Block diagram of operations performed on each card of the modem.

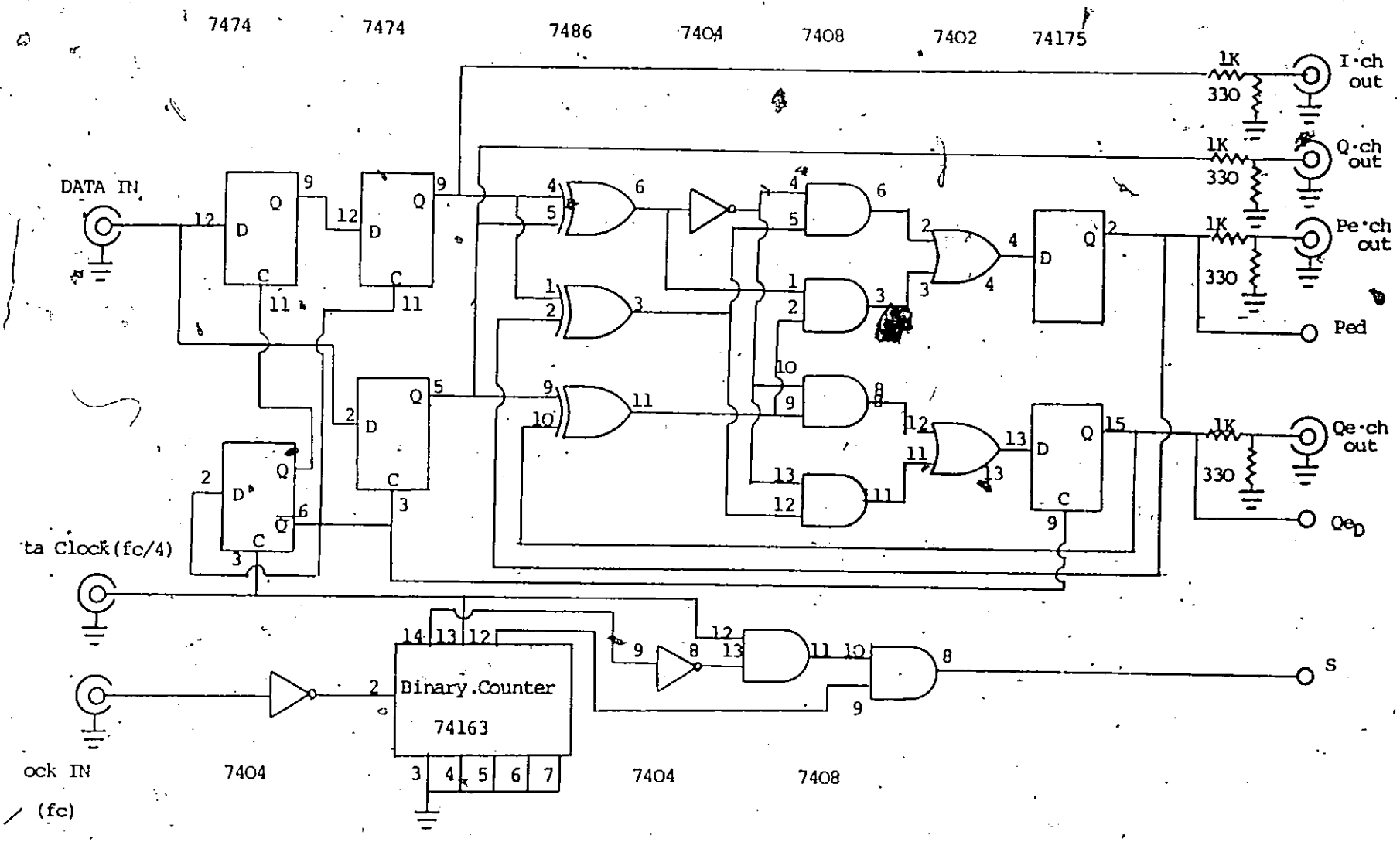

Figure A.3: Circuit diagram of serial-to-parallel converter and differential encoder.

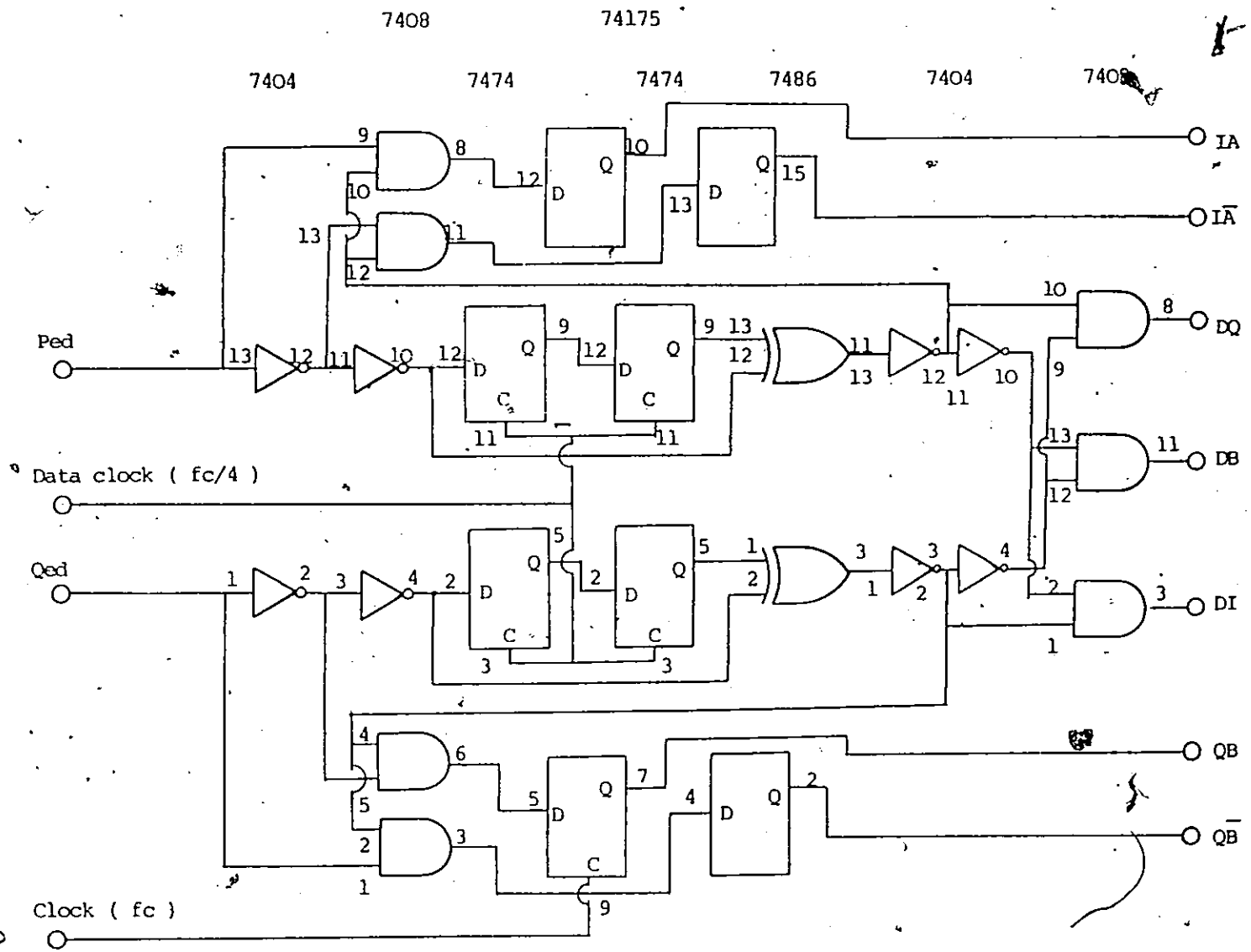

Figure A.4: Circuit diagram of selecting the transitions.

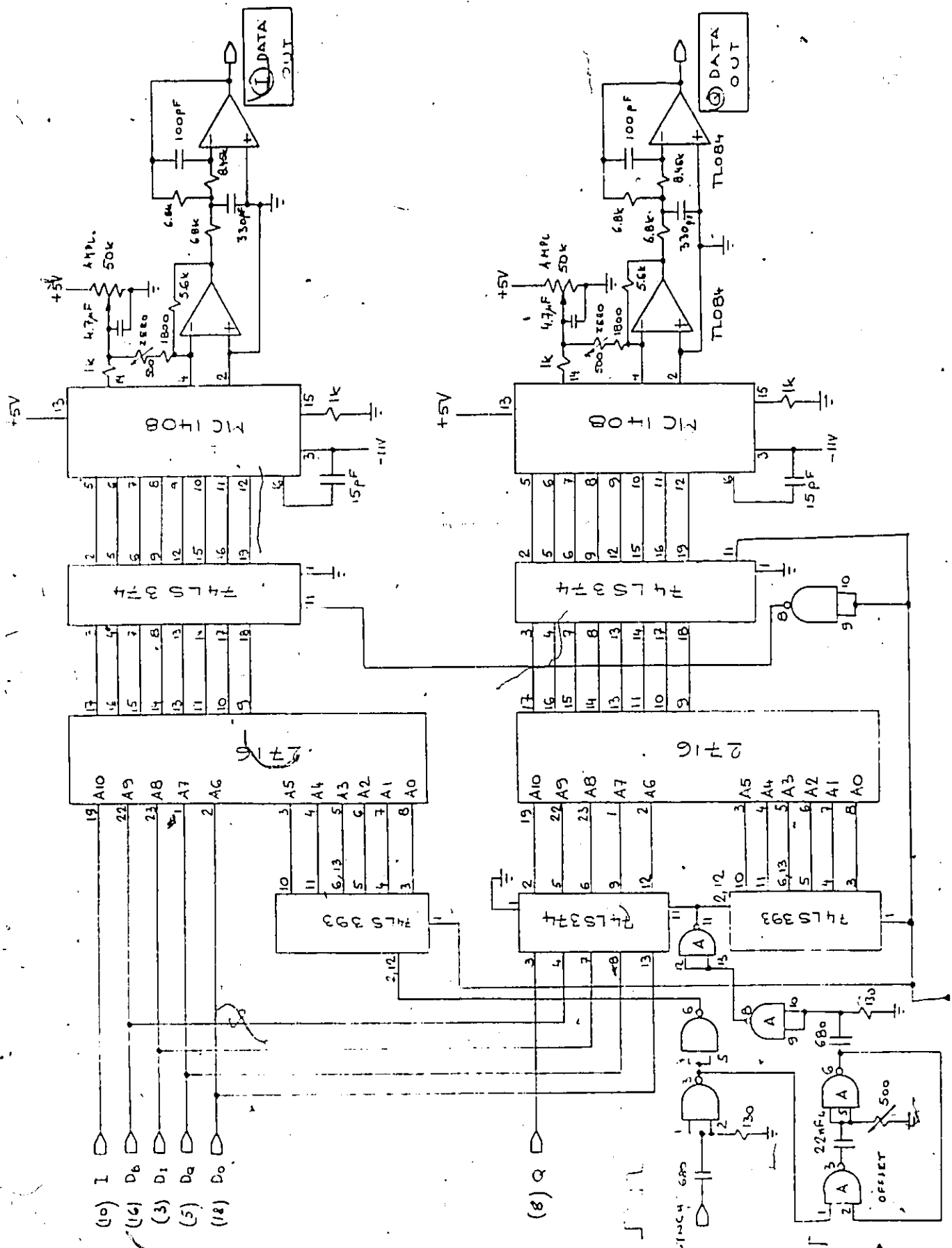

Figure A.5: Circuit diagram of DCTPSK processors.

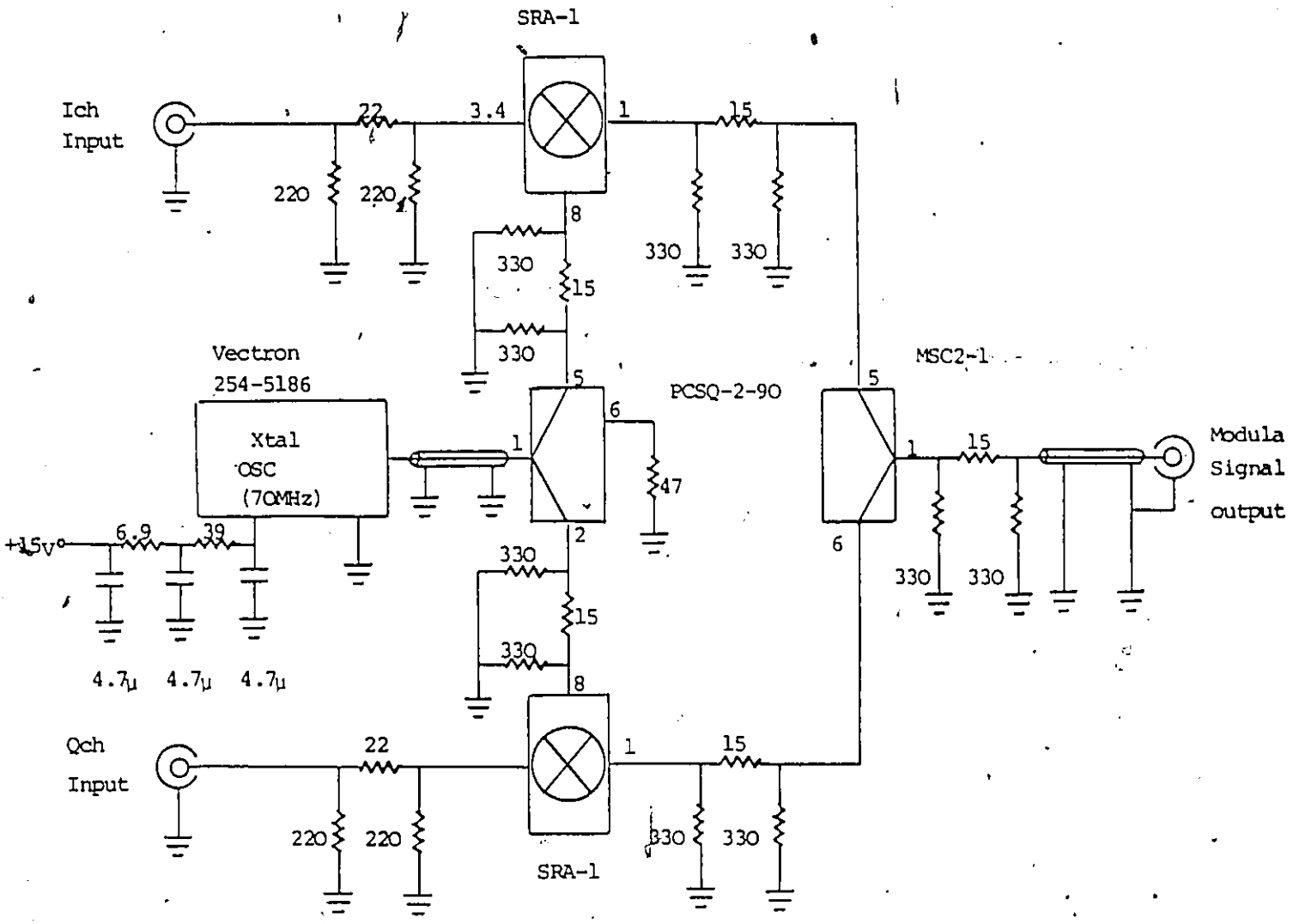

Figure A.6: Circuit diagram of quadrature modulators.

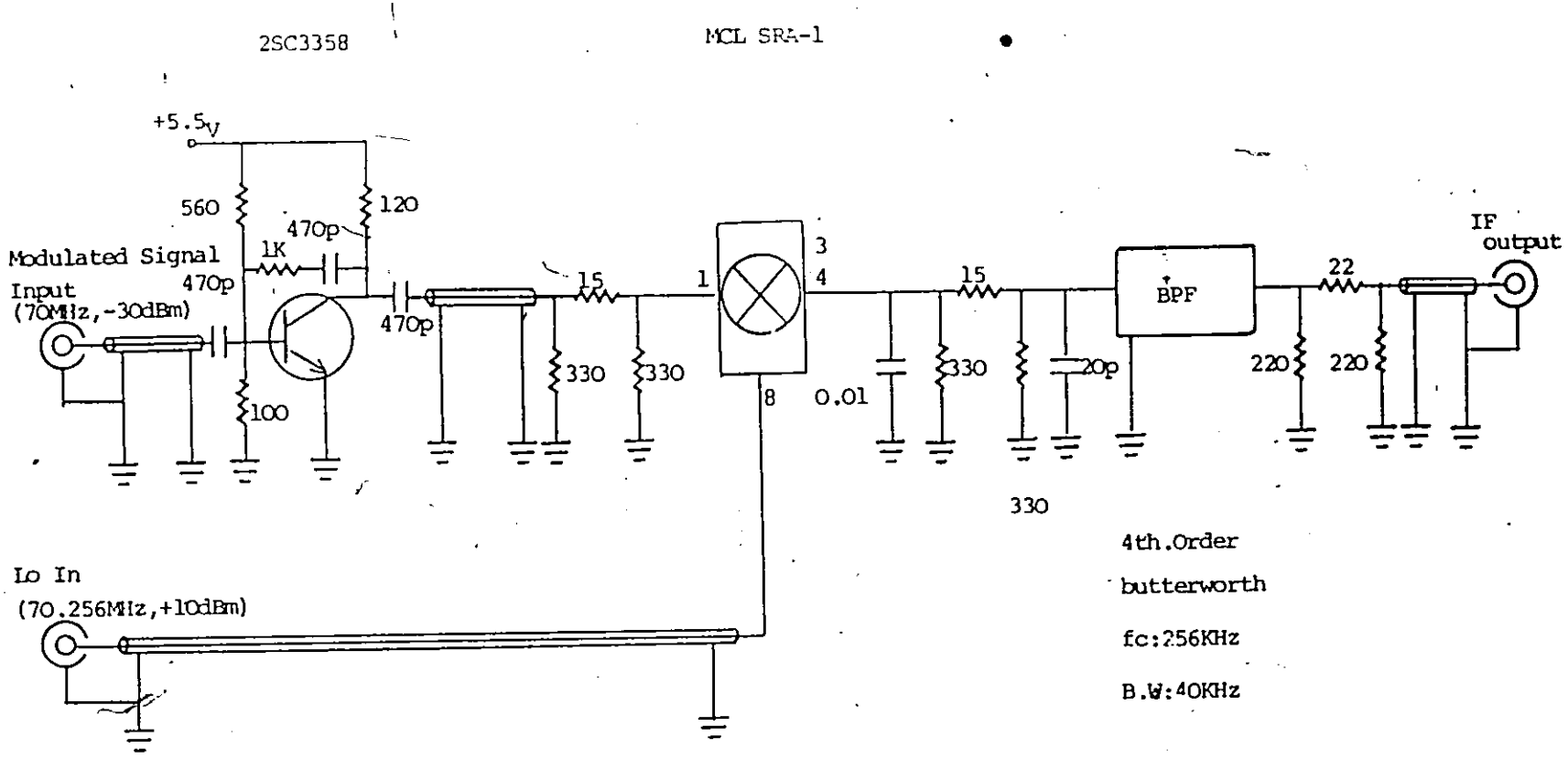

Figure A.7: Circuit diagram of 70 MHz to 256 kHz down converter.

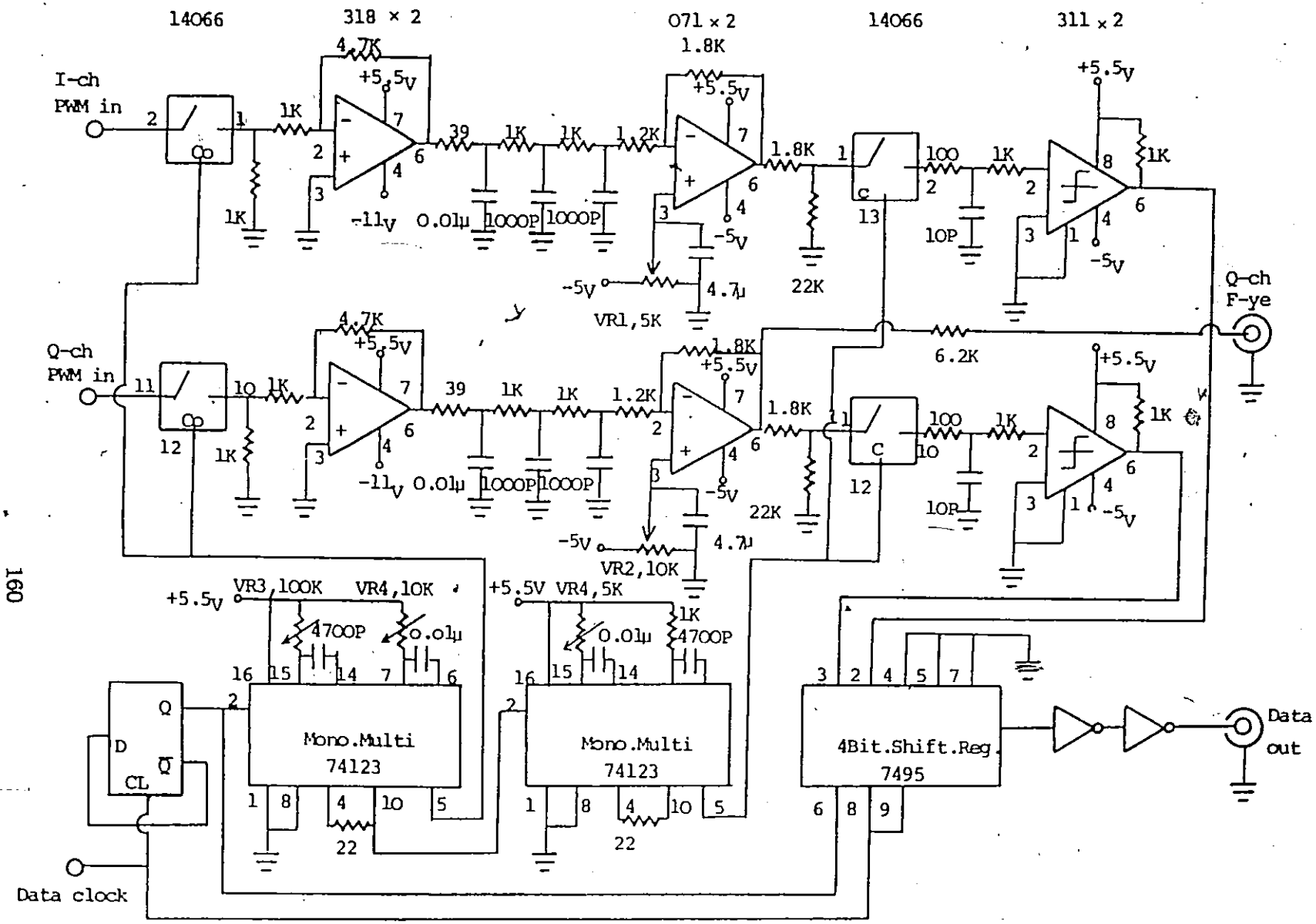

Figure A.8: Circuit diagram of phase comparator and PWM decoder.

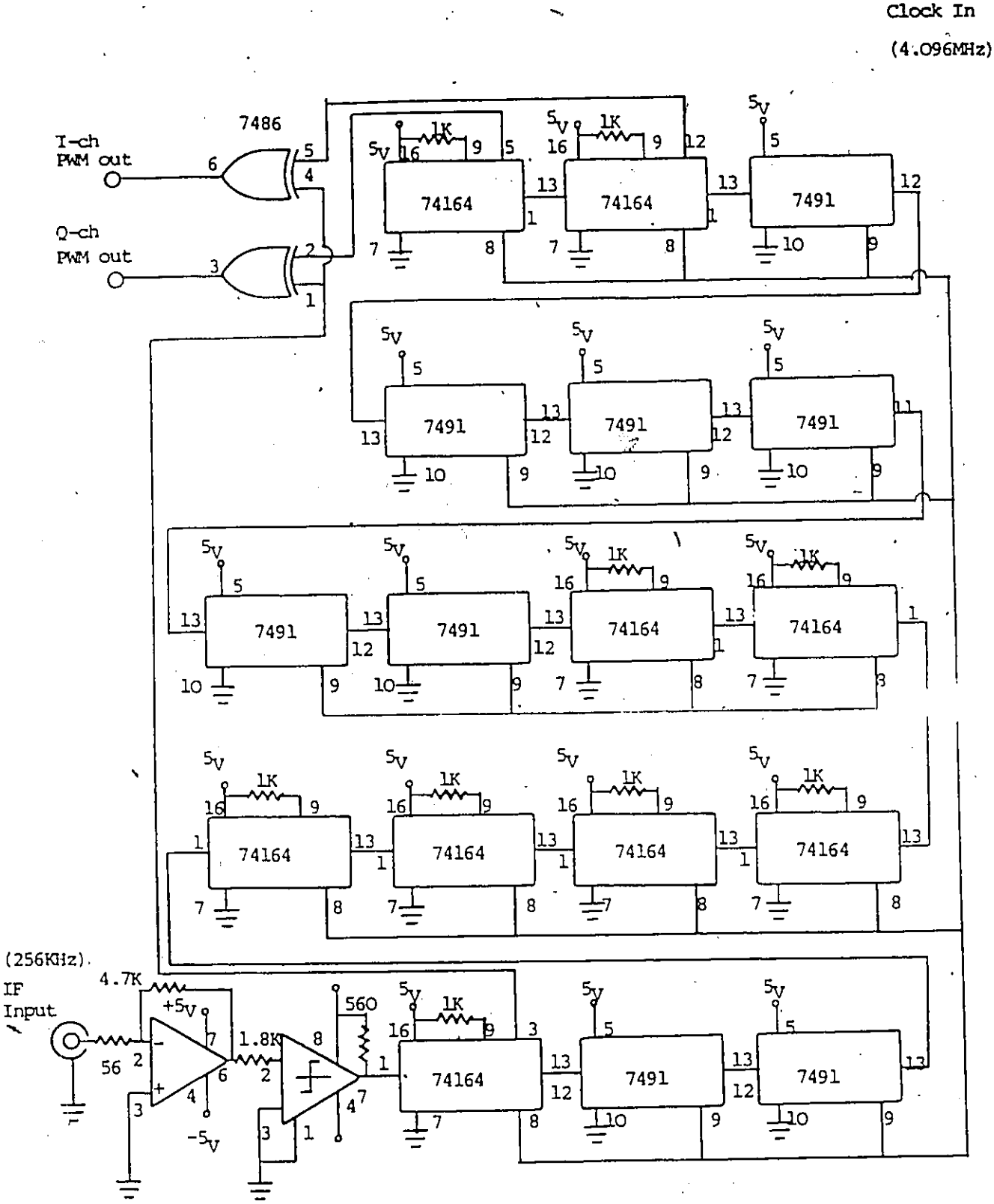

Figure A.9: Circuit diagram of digital delay and phase shifter.

Appendix B

COMPUTER SIMULATIONS AND PROGRAM LISTINGS

B.1 Simulation Considerations

There are many situations where explicit performance evaluation of a communication system defies analytical methods and meaningful results can best be obtained through computer simulations. This is particularly true when the channel includes composite sources of impairments or the detection process is nonlinear. For the systems considered in this thesis, both conditions exist.

To simulate the communication system, we have considered two simulation approaches. These are

1. Quasi analytical approach,
2. Direct Monte Carlo method.

Let us briefly discuss the capabilities and the features of the two approaches.

Quasi Analytical Approach

The complex samples of the signal (without noise) are processed through all the simulation modules of the system. The interfering signals are also processed in a similar fashion, and then added to the desired signal at an

appropriate stage. In the absence of timing offset or jitter, the detected signal value is taken as the one corresponding to the widest vertical eye-opening. Additive Gaussisian noise is not simulated but the effective noise power is calculated using the filter transfer functions and input noise spectral density. The probability of error is calculated for each symbol using an analytical expression. The average probability of error is calculated by directly averaging over several symbol durations. This technique is applicable to the class of receivers for which demodulation can be modelled as a linear process. This technique results in a considerable saving in computer run-time by avoiding direct noise simulation and error counting.

Direct Monte Carlo Method

The signal representation and generation techniques for the direct Monte Carlo method are similar to the quasi analytical approach. However the random noise samples and interference samples are now both generated and added to the signal samples at the appropriate places. The signal is demodulated and the bit errors are then counted directly. A major disadvantage of this approach is that the run-time required to estimate the average bit error probability, P_b, is inversely proportional to the P_b. To obtain reasonable accuracy in P_b, about 100 errors should be observed, which requires a run length of $100/P_b$ bits. For example at $P_b=10^{-6}$, a run length of 10^8 bits is required, which results in long CPU time on most computers.

The quasi analytical approach is not suited to the systems investigated in this thesis, because the proposed receivers are not linear. Therefore the direct Monte Carlo method has been used.

Accuracy Considerations

The usefulness of a simulation package depends strongly on the reliability and accuracy of the results it produces. For this reason, considerable attention has been paid to modelling and validation.

In order to obtain accurate results, the sample sizes used in the programs were sufficiently large. This is particularly important because we used the Monte Carlo method, where the evaluation of the BER performance was performed by simply counting the error occurences.

If the error events have a binomial distribution, which would be the

case for coherent detection with no ISI, the accuracy of the Monte Carlo method is measured by the variance

$$\sigma_p^2 = \frac{P_b(1-P_b)}{N}$$

where P_b is the probability of bit error and N is the sample size.

When the signal is differentially detected, the distribution of error events depends on the joint probability density of both the noise and the signal. In other words, the noise is signal dependent. We observed that for differential detection the variance of the simulation results tends to be larger than the binomial case. Therefore, in all BER estimations, we counted at least 200 errors. This limited us to estimating bit error rates greater than 10^{-5}.

For the validation of our simulation programs, whenever it was possible, the simulations results were compared with the analytical results (e.g., see Figure 2.23).

B.2 Program Listings

The listing of the computer programs which were used to evaluate the bit error rate performances of systems employing differential detection are given below. The programs are written in FORTRAN and ran on the Amdahl 470/V8 computer.The listings are given for running in an interactive mode. However, when user becomes familiar with the program parameters, it is recommended to make the few necessary changes and run the programs in the batch mode.

The listings consist of 4 main programs which simulate the following systems:

1. The program DDPSK: calculates the BER performances of
   - DBPSK,
   - DQPSK,
   - DOQPSK,
   - DCTPSK.

The receivers considered in this program are conventional.

2. The program IMPDCT: calculates the BER performance of the DCTPSK system with the improved receivers (see Section 3.6).
3. The program DGMSK calculates the BER performances of
   - One-bit conventional differential detection of MSK or GMSK,
   - One-bit differential detection of GMSK using decision feedback,
   - Two-bit conventional differential detection of MSK or GMSK.
4. The program IMPDGM: calculates the BER performances of differentially detected GMSK when decision feedback is used and
   - outputs of one-bit and two-bit differential detectors are combined,
   - outputs of two-bit and three-bit differential detectors are combined.

Each main program calls up a series of subroutines, each routine simulates one subsystem of the communication link. Dividing the program into small subroutines simplifies the debugging process. Furthermore, adding a subsytem to the communication link (or deleting one) is done with less effort.

The subroutines are divided into three categories:

- specific subroutines (used by only one main program),
- shared subroutines, and
- IMSL library subroutines [130].

```
C PROGRAM NAME: DDPSK
C
C  WRITTEN ON APR.17 1984 BY ABBAS YONGACOGLU
C
C    THIS PROGRAM SIMULATES  CONVENTIONAL DIFFERENTIAL DETECTION
C       OF THE FOLLOWING PSK TYPE SIGNALS
C
C               1) BINARY PSK (DBPSK)
C               2) QUATERNARY PSK (DQPSK)
C               3) OFFSET QPSK (DOQPSK)
C               4) DCTPSK
C
C
C  THE SIMULATION IS IN BASEBAND.
C
C
C   THE SUBROUTINES USED IN THIS PROGRAM ARE :
C
C  *** 1) IMSL ***
C
C   FFT2C     GGNML
C
C  *** 2) SHARED WITH OTHER PROGRAMS
C
C   ENERGY  FILT    FILTER   HLIM    PRBS    RCOSFA    REIM
C
C   COMP   CHOFIL  DATA   REIM   RDRCOS   RDBWG
C
C
C  *** 3) SPECIFIC TO THIS PROGRAM ***
C
C   DBPSK   TXQPSK  TXOQP    RDNONL
C
C   RXDBPS  RXDQPS  RXOQPS    SAMTIM   SETFI
C
C
C   NOTE: IPF= NUMBER OF SAMPLES PER BIT
C
C
C    SIGNAL    — TX AND RX SIGNAL (LDIM)
C    TXF,PREFI— CONTAIN FILTER COEFF.
C    AR,AI     — REAL AND IMAGINARY PARTS OF SIGNAL (LDIM)
C
C
C
      DOUBLE PRECISION DSEED
      COMMON LDIM,PI,IPF,NSYM
      COMMON/PARA/NO1,NO2,SYMRAT,SBANDW
      COMMON/IOPUT/ITTI,ITTO,LPT
      COMPLEX SIGNAL(2048),SIG1(2048),SIG2(2048),TXF(2048),PREFI(2048)
      COMPLEX SAMSIG(256),B2(2048)
      DIMENSION THETA(2048)
```

```
      DIMENSION THETA2(2048)
      INTEGER IE(36)
      COMPLEX SIG1I(2044),SIG1Q(2048),B1I(2048),B1Q(2048)
      DIMENSION AR(2200),AI(2200),DUM(2200)
      INTEGER II(256),IQ(256),IID(256),IQD(256),IORI(258)
      INTEGER JAI(29000)
      INTEGER II1(256),IQ1(256)
      DIMENSION D1I(2048),D1Q(2048)
C
C   INITIALIZE
C
C******************
      IPF=8
      NSYM=256
      L=11
C******************
      NP=2**L
      LDIM=NSYM*IPF
      IF(LDIM.NE.NP)WRITE(6,654)
654   FORMAT(5X,'DIMENSIONS DO NOT MATCH')
      IPFT2=IPF*2
      NSYMM1=NSYM-1
      NSYMO2=NSYM/2
      WRITE(6,100)IPF
      INC=6
      PI=3.141592653589793
      SYMRAT=1.0
      BITRAT=1.0
      EBIN=1.0
      SBANDW=IPF*SYMRAT
      NO=LDIM/2
      NO1=NO+1
      NO2=NO1+1
      ITER=0
C-----------------------------------------
C
C   START FOR EACH NEW RUN
C
1111  ITER=ITER+1
      DO 362 I=1,36
362   IE(I)=0
      IDUM=13
      DSEED=268943D0
      ITTI=7
      ITTO=7
      LPT=6
C*********************************************************
C   CHOOSING THE MODULATION TYPE
C*********************************************************
      WRITE(7,2803)
2803  FORMAT('BPSK=1, OQPSK=2  QPSK=3  DCTPSK=4 ')
      READ(7,6001)ICOD
```

```
C
      IF(ICOD.EQ.2)WRITE(7,831)
 831  FORMAT('THRESHOLD IN DEGREES ?')
      IF(ICOD.EQ.2)READ(7,3001)TH
3001  FORMAT(F5.2)
      WRITE(7,6010)
        READ(7,6004)JRUN
      IF(JRUN.LE.50)GOTO 210
      WRITE(7,7001)
        READ(7,6004)JRUN
210   CONTINUE
C
      INOBIT=28000
      ISYBEF=0
C
      WRITE(7,6003)
        READ(7,8004)DB
      DBR=DB/10.0
      PN0IN=1.0/(BITRAT*(10.0**DBR))*IPF
C
C     GENERATE A LONG PRBS OF LENGTH INOBIT
C
      CALL PRBS(JAI,15,1,15,INOBIT)
C
C————————CHOOSING THE FILTERS————————
C
      WRITE(7,7006)
7006  FORMAT('VARIABLE FILTER PARAMETERS PRESS 1')
      READ(7,6001)IVARFI
      IF(IVARFI.EQ.1)GOTO 360
      ITXFI=1
      IPREFI=1
      CALL SETFI(TXF,PREFI)
      GOTO 950
C
C  TX FILTER
C
360   WRITE(7,8100)
      READ(7,6001)ITXFI
      IF(ITXFI.NE.1)WRITE(6,8109)
      IF(ITXFI.EQ.1)CALL CHOFIL(TXF,1)
C
C  PREMOD FILTER
C
550   WRITE(7,9100)
      READ(7,6001)IPREFI
      IF(IPREFI.NE.1)WRITE(6,9109)
      IF(IPREFI.EQ.1)CALL CHOFIL(PREFI,2)
C
C————————————————————————————
950   WRITE(7,8201)
8201  FORMAT('DO YOU WANT A HARDLIMITER ? YES=1')
```

```
      READ(7,6001)IHLIM
      WRITE(7,2045)
C*****************************************************************
C     ADJACENT CHANNEL INTERFERENCE PARAMETERS
C
2045  FORMAT('IF ACI  IS TO BE SIMULATED THEN PRESS 1')
      READ(7,6001)IACI
      IF(IACI.NE.1)GOTO 201
      WRITE(ITTO,897)
897   FORMAT('B/S/HZ ?')
      READ(ITTI,890)BPSPHZ
      CHASPA=1.0/BPSPHZ
      WRITE(ITTO,797)
797   FORMAT('REL. ATTENUATION')
      READ(ITTI,890)ATT
890   FORMAT(F8.3)
C*****************************************
            IFCN1=NSYM*CHASPA
            IFCN2=LDIM-IFCN1
      WRITE(7,178)IFCN1,IFCN2
178   FORMAT('IFCN1=',I4,6X,'IFCN2=',I4)
      CALL ACGEN(SIG1,SIG2,TXF,ICOD,ITXFI,IHLIM
     ?,L,IFCN1,IFCN2,ATT)
C*****************************************
201   CONTINUE
C-------------------------------
      ISTART=1
C
1900  ICHE=JRUN*INC+NSYM+IDUM
      IF(INOBIT.LE.ICHE)WRITE(6,689)
      IF(INOBIT.LE.ICHE)STOP
C
C
C   START OF EACH ITERATION
C
C
      NSYMP2=NSYM+2
      DO 888 KRUN=ISTART,JRUN
      WRITE(7,3300)KRUN
      CALL DATA(JAI,IORI,NSYMP2,IDUM)
C
      IF(ICOD.EQ.1) CALL DBPSK(IORI,SIGNAL,AR,AI,IID)
C
      IF(ICOD.EQ.2)CALL TXOQP(SIGNAL,AR,AI,IORI,II,IQ,IID,IQD)
C
      IF(ICOD.EQ.3.OR.ICOD.EQ.4)CALL TXQPSK(IORI,II,IQ,SIGNAL,AR,AI,IID
     ?,IQD,ICOD)
C
C PASS THE SIGNAL THROUGH THE TRANSMIT FILTER
C
      IF(ITXFI.EQ.1)CALL FILTER(SIGNAL,TXF,LDIM,L)
C
```

```
C      **********************
C          HARDLIMITER
C      **********************
      IF(IHLIM.EQ.1)CALL HLIM(SIGNAL,LDIM)
C
C         CALCULATE THE ENERGY PER BIT
C
      CALL ENERGY(SIGNAL,EB)
      IF(IACI.EQ.1)CALL ACI(SIGNAL,SIG1,SIG2)
C
C     GENERATE AND SCALE THE NOISE
C
C
      CALL GGNML(DSEED,LDIM,DUM)
      PN0=PN0IN*EB
C
      DO 53 I=1,LDIM
53    DUM(I)=DUM(I)*SQRT(PN0)
C  **************
C     ADD NOISE
C  **************
      DO 63 I=1,LDIM
63    SIGNAL(I)=SIGNAL(I)+CMPLX(DUM(I),DUM(LDIM+1-I))
C
C
C   PREMOD FILTERING
C
      IF(IPREFI.EQ.1)CALL FILTER(SIGNAL,PREFI,LDIM,L)
C
C ***********************************************
C                 DECODING
C*************************************************************
C
      IF(ICOD.EQ.1)CALL RXDBPS(SIGNAL,SIG1I,IORI,IE,D1I,ISAMPO)
C
      IF(ICOD.EQ.2)CALL RXOQPS(SIGNAL,B2,AR,AI,THETA,THETA2,IE,TH,IORI
     ?,ISAMPO)
C
      IF(ICOD.EQ.3.OR.ICOD.EQ.4)CALL RXDQPS(SIGNAL,SAMSIG,II,IQ,IE,
     ?B1I,B1Q,D1I,D1Q,SIG1I,SIG1Q,ISAMPO)
C ***********************************************
C
      IDUM=IDUM+INC
888   CONTINUE
      WRITE(7,9701)(I,IE(I),I=1,ISAMPO)
9701  FORMAT(I2,6X,I6)
      CALL SAMTIM(IE,ISAMPO,ISYBEF)
C*************************************************
C
C
196   WRITE(7,3613)ISYBEF
3613  FORMAT('ISYBEF =',I4)
```

```
      BERBEF=FLOAT(ISYBEF)/FLOAT((NSYM-4)*JRUN)
      WRITE(6,929)BERBEF
      WRITE(7,929)BERBEF
  929 FORMAT('BER = ',F10.6)
C
C
C
      WRITE(7,712)DB
  296  WRITE(7,5005)
         READ(7,6001)ICONT
       IF(ICONT.NE.1)GO TO 369
       WRITE(7,8202)
         READ(7,6004)IINC
      IF(IINC.LE.50)GOTO 211
      WRITE(7,7001)
        READ(7,6004)IINC
  211  ISTART=1+JRUN
       JRUN=JRUN+IINC
       GO TO 1900
  369 WRITE(7,7005)
 7005 FORMAT('FOR A NEW RUN PRESS 1')
      READ(7,6001)NEWRUN
      IF(NEWRUN.EQ.1)GOTO 1111
C
C  READ FORMATS
C
 6004 FORMAT(I3)
 8004 FORMAT(F10.4)
 6001 FORMAT(I1)
C
C
 7001 FORMAT('IS IT A MISTAKE? TRY AGAIN')
 6010 FORMAT('NO OF RUNS=? (I3)')
  100 FORMAT(5X,'IPF=',I4)
 6003 FORMAT(' DB= ? (F10.4)')
 8100 FORMAT('DO YOU WANT A TX FILTER ? (YES=1)')
 8109 FORMAT('NO TRANSMIT FILTERING')
 9100 FORMAT('DO YOU WANT A PRE-MOD FILTER ? (YES=1)')
 9109 FORMAT('NO PREMOD   FILTERING')
  689 FORMAT(2X,'INCREASE INOBIT')
 3300 FORMAT(5X,'KRUN=',I4)
  258 FORMAT(10X,'ENERGY BEF MOD',F10.6)
  712 FORMAT(10X,'DB=',F10.4)
 5005  FORMAT('DO YOU WANT TO CONTINUE ?',/,'IF YES PRESS 1')
 8202  FORMAT('NO OF RUNS')
      STOP
      END
C
C
C   TRANSMITTER SUBROUTINES
C
C
```

```
C*****************************************************************
C THIS SUBR. FIRST DIFFERENTIALLY ENCODES THE INPUT DATA
C THEN GENERATES THE BASEBAND BPSK SIGNAL.
C SUBROUTINES USED:  STAYB, REVB, BPSK
C*****************************************************************
      SUBROUTINE DBPSK(II,SIGNAL,AR,AI,IID)
C*****************************************************************
      COMMON LDIM,PI,IPF,NSYM
      COMPLEX SIGNAL(1)
      DIMENSION AR(1),AI(1)
      INTEGER II(1),IID(1)
C
C     DIFFERENTIALLY ENCODE
C
      II(1)=1
      IID(1)=II(1)
      DO 3000 I=2,NSYM
      IF(II(I).EQ.1)CALL STAYB(IID,I)
      IF(II(I).EQ.-1)CALL REVB(IID,I)
3000  CONTINUE
C
C       ****************************************
C             GENERATE THE BASEBAND SIGNALS
C       ****************************************
C
      CALL BPSK(AR,AI,IID)
C
      CALL COMP(SIGNAL,AR,AI,LDIM)
      RETURN
      END
C*****************************************************************
      SUBROUTINE STAYB(II,I)
      INTEGER II(1)
      II(I)=II(I-1)
      RETURN
      END
C*****************************************************************
      SUBROUTINE REVB(II,I)
      INTEGER II(1)
      II(I)=-II(I-1)
      RETURN
      END
C*****************************************************************
C THIS SUBROUTINE GENERATES THE BPSK SIGNAL
C*****************************************************************
      SUBROUTINE BPSK(AR,AI,IID)
      COMMON LDIM,PI,IPF,NSYM
      DIMENSION AR(1),AI(1)
      INTEGER IID(1)
      DO 12 I=1,NSYM
      DO 12 J=1,IPF
      AR((I-1)*IPF+J)=IID(I)
```

```
      AI((I-1)*IPF+J)=0.0
12    CONTINUE
      RETURN
      END
C*****************************************************************
C GENERATES THE TRANSMITTED DQPSK OR DCTPSK SIGNAL
C
C THE SUBROUTINES CALLED ARE:
C 1) SEPA, 2) QPSKDE,   3) QPSK,  4) DCTPSK
C*****************************************************************
      SUBROUTINE TXQPSK(IORI,II,IQ,SIGNAL,AR,AI,IID,IQD,ICOD)
C*****************************************************************
      COMMON LDIM,PI,IPF,NSYM
      COMPLEX SIGNAL(1)
      DIMENSION AR(1),AI(1)
      INTEGER IORI(1),II(1),IQ(1),IID(1),IQD(1)
C
C     SERIAL TO PARALEL CONVERSION
C
      CALL SEPA(IORI,II,IQ,NSYM)
C
C        DIFFERENTIALLY ENCODE THE I AND Q CHANNEL DATA
C
      CALL QPSKDE(II,IQ,IID,IQD,NSYM)
C
C        GENERATE THE BASEBAND SIGNALS
C
      IF(ICOD.EQ.3)CALL QPSK(AR,AI,IID,IQD)
      IF(ICOD.EQ.4)CALL DCTPSK(AR,AI,IID,IQD)
      CALL COMP(SIGNAL,AR,AI,LDIM)
      RETURN
      END
C*****************************************************************
C THIS SUBROUTINE DIFFERENTIALLY ENCODES THE QPSK (OR DCTPSK) DATA
C
C THE SUBROUTINES CALLED ARE:  1) STAY, 2) PO90, 3) NE90, 4)REV
C
C*****************************************************************
      SUBROUTINE QPSKDE(II,IQ,IID,IQD,NSYM)
C*****************************************************************
      INTEGER II(1),IQ(1),IID(1),IQD(1)
      NSYMO2=NSYM/2
C
      II(1)=1
      IQ(1)=1
      IID(1)=II(1)
      IQD(1)=IQ(1)
C
      DO 2000 I=2,NSYMO2
      IF(II(I).EQ.1.AND.IQ(I).EQ.1)CALL STAY(IID,IQD,I)
      IF(II(I).EQ.1.AND.IQ(I).EQ.-1)CALL PO90(IID,IQD,I)
      IF(II(I).EQ.-1.AND.IQ(I).EQ.1)CALL NE90(IID,IQD,I)
```

```
      IF(II(I).EQ.-1.AND.IQ(I).EQ.-1)CALL REV(IID,IQD,I)
2000  CONTINUE
      RETURN
      END
C*****************************************************************
      SUBROUTINE STAY(II,IQ,I)
      INTEGER II(1),IQ(1)
      II(I)=II(I-1)
      IQ(I)=IQ(I-1)
      RETURN
      END
C*****************************************************************
      SUBROUTINE REV(II,IQ,I)
      INTEGER II(1),IQ(1)
      II(I)=-II(I-1)
      IQ(I)=-IQ(I-1)
      RETURN
      END
C*****************************************************************
      SUBROUTINE PO90(II,IQ,I)
      INTEGER II(1),IQ(1)
      COMPLEX X,Y
      A=II(I-1)
      B=IQ(I-1)
      X=CMPLX(A,B)
      Y=X*CMPLX(0.0,1.0)
      C=REAL(Y)
      D=AIMAG(Y)
      II(I)=C
      IQ(I)=D
      RETURN
      END
C*****************************************************************
      SUBROUTINE NE90(II,IQ,I)
      INTEGER II(1),IQ(1)
      COMPLEX X,Y
      A=II(I-1)
      B=IQ(I-1)
      X=CMPLX(A,B)
      Y=X*CMPLX(0.0,-1.0)
      C=REAL(Y)
      D=AIMAG(Y)
      II(I)=C
      IQ(I)=D
      RETURN
      END
C*****************************************************************
C THIS SUBROUTINE ENCODES THE QPSK SIGNAL
C*****************************************************************
      SUBROUTINE QPSK(AR,AI,IID,IQD)
      COMMON LDIM,PI,IPF,NSYM
      DIMENSION AR(1),AI(1)
```

```
      INTEGER IID(1),IQD(1)
      NSYMO2=NSYM/2
      IPFT2=IPF*2
      DO 12 I=1,NSYMO2
      DO 12 J=1,IPFT2
      AR((I-1)*IPFT2+J)=IID(I)
      AI((I-1)*IPFT2+J)=IQD(I)
12    CONTINUE
      RETURN
      END
C*************************************************************
C  THIS SUBR. GENERATES THE BASEBAND DCTPSK SIGNALS
C
C  SUBROUTINES USED: CO34, SHAPE1, DUZ
C*************************************************************
      SUBROUTINE DCTPSK(AR,AI,II,IQ)
C*************************************************************
      COMMON LDIM,PI,IPF,NSYM
      DIMENSION AR(1),AI(1)
      INTEGER II(1),IQ(1)
      IPFT2=IPF*2
      NSYMO2=NSYM/2
      DO 3 I=1,IPFT2
      AR(I)=II(1)
3     AI(I)=IQ(1)
C
      DO 4 K=2,NSYMO2
      ISTI=0
      ISTQ=0
      IBOTH=0
      IF(II(K).NE.II(K-1))ISTI=1
      IF(IQ(K).NE.IQ(K-1))ISTQ=1
      IF(ISTI.EQ.1.AND.ISTQ.EQ.1)IBOTH=1
      IF(IBOTH.EQ.1)CALL CO34(AR,AI,II,IQ,K)
      IF(ISTI.EQ.1.AND.ISTQ.EQ.0)CALL SHAPE1(AR,AI,II,IQ,K)
      IF(ISTI.EQ.0.AND.ISTQ.EQ.1)CALL SHAPE1(AI,AR,IQ,II,K)
      IF(ISTI.EQ.0.AND.ISTQ.EQ.0)CALL DUZ(AR,AI,II,IQ,K)
4     CONTINUE
      RETURN
      END
C*************************************************************
      SUBROUTINE CO34(AR,AI,II,IQ,K)
C*************************************************************
      COMMON LDIM,PI,IPF,NSYM
      DIMENSION AR(1),AI(1)
      INTEGER II(1),IQ(1)
      IPFT2=IPF*2
      NSYMO2=NSYM/2
      IPO4=IPFT2/4
      IPO4P1=IPO4+1
      IPO4T3=IPO4*3
      IP43P1=IPO4T3+1
```

```
      FIPT2=IPFT2
      DO 1 I=1,IPO4
      AR((K-1)*IPFT2+I)=II(K-1)
1     CONTINUE
      DO 2 I=IPO4P1,IPFT2
      TI=I-IPO4P1
      X1=COS(PI*TI/FLOAT(IPO4T3))
      AR((K-1)*IPFT2+I)=II(K-1)*X1
2     CONTINUE
      DO 3 I=IP43P1,IPFT2
      AI((K-1)*IPFT2+I)=IQ(K)
3     CONTINUE
      DO 4 I=1,IPO4T3
      TI=I-1
      X1=COS(PI*TI/FLOAT(IPO4T3))
      AI((K-1)*IPFT2+I)=IQ(K-1)*X1
4     CONTINUE
      RETURN
      END
C*************************************************************
      SUBROUTINE SHAPE1(X,Y,MV,MC,K)
C*************************************************************
      COMMON LDIM,PI,IPF,NSYM
      DIMENSION X(1),Y(1)
      INTEGER MV(1),MC(1)
      IPFT2=IPF*2
      FIPT2=IPFT2
      DO 1 I=1,IPFT2
      FI=I-1
      X((K-1)*IPFT2+I)=MV(K-1)*COS(PI*FI/FIPT2)
      Y((K-1)*IPFT2+I)=MC(K)
1     CONTINUE
      RETURN
      END
C*************************************************************
      SUBROUTINE DUZ(AR,AI,II,IQ,K)
C*************************************************************
      COMMON LDIM,PI,IPF,NSYM
      DIMENSION AR(1),AI(1)
      INTEGER II(1),IQ(1)
      IPFT2=IPF*2
      DO 1 I=1,IPFT2
      AR((K-1)*IPFT2+I)=II(K)
1     AI((K-1)*IPFT2+I)=IQ(K)
      RETURN
      END
C*********************************
      SUBROUTINE TXOQP(SIGNAL,AR,AI,IORI,II,IQ,IID,IQD)
      COMMON LDIM,PI,IPF,NSYM
      COMPLEX SIGNAL(1)
      DIMENSION AR(1),AI(1)
      INTEGER IORI(1),II(1),IQ(1),IID(1),IQD(1)
```

```
      NSO2P1=NSYM/2+1
      NSYMP2=NSYM+2
C
C     SERIAL TO PARALLEL CONVERSION
C
      CALL SEPA(IORI,II,IQ,NSYMP2)
C
C     DIFFERENTIALLY ENCODE EACH QUADRATURE CHANNEL
C
      CALL DENCOD(II,IID,NSO2P1)
      CALL DENCOD(IQ,IQD,NSO2P1)
C       ****************************************
C             GENERATE THE BASEBAND SIGNALS
C       ****************************************
      CALL OQPS(AR,AI,IID,IQD)
      CALL COMP(SIGNAL,AR,AI,LDIM)
      RETURN
      END
C*************************************************************
      SUBROUTINE OQPS(AR,AI,IID,IQD)
C*************************************************************
      COMMON LDIM,PI,IPF,NSYM
      DIMENSION AR(1),AI(1)
      INTEGER IID(1),IQD(1)
      NSO2P1=NSYM/2+1
      IPFT2=IPF*2
      DO 22 J=1,NSO2P1
      DO 22 I=1,IPFT2
      J1=(J-1)*IPFT2+I
      FI1=J1-1
      AR(J1)=IID(J)
22    AI(J1)=IQD(J)
      DO 23 I=1,LDIM
23    AR(I)=AR(IPF+I)
      RETURN
      END.
C
C
C     RECEIVER SUBROUTINES
C
C
C ***********************************************************
C  THIS SUBR. DIFFERENTIALLY DECODES THE RECEIVED BPSK SIGNAL
C***********************************************************
      SUBROUTINE  RXDBPS(SIGNAL,SIG1I,II,IE,D1I,ISAMPO)
C***********************************************************
      COMMON LDIM,PI,IPF,NSYM
      COMPLEX SIGNAL(1),SIG1I(1)
      DIMENSION D1I(1)
      INTEGER II(1),IE(1)
      NSYMM1=NSYM-1
      IPFP1=IPF+1
```

```
      ISAMPO=IPF+2
      DO 112 I=IPFP1,LDIM
112   SIG1I(I)=SIGNAL(I)*CONJG(SIGNAL(I-IPF))
662   CALL REIMN(SIG1I,D1I,LDIM)
C
      DO 160 J=2,NSYMM1
      DO 160 I=1,ISAMPO
      J1=(J-1)*IPF+I
      IX=-1
      IF(D1I(J1).GT.0.0)IX=1
160   IF(IX.NE.II(J))IE(I)=IE(I)+1
      RETURN
      END
C*************************************************************
C THIS SUBR. PERFORMS THE DIFFERENTIAL DECODING OF QPSK
C OR DCTPSK SIGNALS.
C SUBR. USED: YARQPS, SH45, SHM45, DELMUL, REIMN
C*************************************************************
      SUBROUTINE  RXDQPS(SIGNAL,SAMSIG,II,IQ,IE,B1I,B1Q,D1I,D1Q,
     ?SIG1I,SIG1Q,ISAMPO)
C*************************************************************
      COMMON LDIM,PI,IPF,NSYM
      COMPLEX SIGNAL(1),SAMSIG(1),B1I(1),B1Q(1)
      COMPLEX SIG1I(1),SIG1Q(1)
      DIMENSION D1I(1),D1Q(1)
      INTEGER II(1),IQ(1),IE(1)
      NSYMO2=NSYM/2
      IPFT2=IPF*2
      ISAMPO=IPFT2+2
      CALL SH45(SIGNAL,B1I,LDIM)
      CALL DELMUL(SIG1I,SIGNAL,B1I,IPFT2,LDIM)
      CALL REIMN(SIG1I,D1I,LDIM)
C
      CALL SHM45(SIGNAL,B1Q,LDIM)
      CALL DELMUL(SIG1Q,SIGNAL,B1Q,IPFT2,LDIM)
      CALL REIMN(SIG1Q,D1Q,LDIM)
C
      CALL YARQPS(D1I,D1Q,IE,II,IQ)
C
      RETURN
      END
C*************************************************************
      SUBROUTINE  YARQPS(D1I,D1Q,IE,II,IQ)
C*************************************************************
      COMMON LDIM,PI,IPF,NSYM
      DIMENSION D1I(1),D1Q(1)
      INTEGER II(1),IQ(1),IE(1)
C
C
      IPFT2=IPF*2
      NSO2=NSYM/2
      NSO2M1=NSO2-1
```

```
C
      ISAMPO=IPFT2+2
C
      DO 180 J=2,NSO2M1
      DO 180 I=1,ISAMPO
      J1=(J-1)*IPFT2+I
      IX=-1
      IY=-1
      IF(D1I(J1).GT.0.0)IX=1
      IF(D1Q(J1).GT.0.0)IY=1
      IF(IX.NE.II(J))IE(I)=IE(I)+1
180   IF(IY.NE.IQ(J))IE(I)=IE(I)+1
      RETURN
      END
C*************************************************************
      SUBROUTINE SH45(SIGNAL,B,LDIM)
C*************************************************************
C SHIFT + 45 DEGREES
      COMPLEX SIGNAL(1),B(1)
      SQ2=1.0/SQRT(2.0)
      DO 1 I=1,LDIM
1     B(I)=SIGNAL(I)*CMPLX(SQ2,SQ2)
      RETURN
      END
C*************************************************************
      SUBROUTINE SHM45(SIGNAL,B,LDIM)
C*************************************************************
C     SHIFT -45 DEGREES
      COMPLEX SIGNAL(1),B(1)
      SQ2=1.0/SQRT(2.0)
      DO 1 I=1,LDIM
1     B(I)=SIGNAL(I)*CMPLX(SQ2,-SQ2)
      RETURN
      END
C*************************************************************
      SUBROUTINE REIMN(SIGNAL,AR,LDIM)
      COMPLEX SIGNAL(1)
      DIMENSION AR(1)
      DO 1 I=1,LDIM
1     AR(I)=REAL(SIGNAL(I))
      RETURN
      END
C*************************************************************
C  MULTIPLIES THE SIGNAL WITH A DELAYED VERSION OF ITSELF
C*************************************************************
      SUBROUTINE DELMUL(A,B,C,IDEL,LDIM)
      COMPLEX  A(1),B(1),C(1)
      ID1=IDEL+1
      DO 1 I=ID1,LDIM
1     A(I)=B(I)*CONJG(C(I-IDEL))
      RETURN
      END
```

```
C*************************************************************
C   THIS SUBR. SETS THE TRANSMIT AND RECEIVE FILTERS TO RAISED COSINE
C   WITH ALPHA=1 (WITH EQUAL SPLITTING PLUS AMPLITUDE EQUALIZER).
C
C   CALLS SUBROUTINE RCOSFA
      SUBROUTINE SETFI(F1,F2)
      COMPLEX F1(1),F2(1),F3(1)
      CALL RCOSFA(0.5,F1,1.0,1,1)
      CALL RCOSFA(0.5,F2,1.0,1,0)
      RETURN
      END
C*************************************************************
      SUBROUTINE SH90(SIGNAL,B,LDIM)
C*************************************************************
      COMPLEX SIGNAL(1),B(1)
      DO 1 I=1,LDIM
1     B(I)=SIGNAL(I)*CMPLX(0.0,1.0)
      RETURN
      END
C*************************************************************
      SUBROUTINE SEPA(IORI,II,IQ,NSYM)
C*************************************************************
      INTEGER IORI(1),II(1),IQ(1)
      NSYMO2=NSYM/2
      DO 2 I=1,NSYMO2
      II(I)=IORI(2*I-1)
2     IQ(I)=IORI(2*I)
      RETURN
      END
C*************************************************************
      SUBROUTINE  RXOQPS(SIGNAL,B2,AR,AI,THETA,THETA2,IE,TH,IORI,ISAMPO
C  RECEIVER FOR OQPSK
      COMMON LDIM,PI,IPF,NSYM
      COMPLEX SIGNAL(1),B2(1)
      INTEGER IORI(1)
      DIMENSION AR(1),AI(1),THETA(1),THETA2(1)
      NSYMO2=NSYM/2
      IPFT2=IPF*2
      IPFP1=IPF+1
      ISAMPO=IPF+2
      DO 647 I=IPFP1,LDIM
647   B2(I)=SIGNAL(I)*CONJG(SIGNAL(I-IPF))
      CALL REIM(B2,AR,AI,LDIM)
      CALL TANABS(AR,AI,THETA,LDIM,PI)
      DO 142 I=1,LDIM
142   THETA2(I)=THETA(I)*180.0/PI
      CALL YAROQP(THETA2,IORI,IE,TH)
      RETURN
      END
C*************************************************************
C THIS SUBROUTINE DECODES DIFFERENTIAL OQPSK
C*************************************************************
```

```
      SUBROUTINE YAROQP(THETA2,IPNI,IE,TH)
      COMMON LDIM,PI,IPF,NSYM
      INTEGER IPNI(1),IPNQ(1),IE(1)
      DIMENSION THETA2(1)
      NSYMM1=NSYM-3
      ISAMPO=IPF+2
      DO 110 J=2,NSYMM1
      DO 100 K=1,ISAMPO
      J1=(J-1)*IPF+K
      IX=1
      IF(THETA2(J1).GT.TH)IX=-1
      IF(IX.NE.IPNI(J+1)) IE(K)=IE(K)+1
  100 CONTINUE
  110 CONTINUE
      RETURN
      END
C*************************************************************
C     FIND THE BEST SAMPLING INSTANT
C*************************************************************
      SUBROUTINE SAMTIM(IE,ISAMPO,NERROR)
      INTEGER IE(1)
      NERROR=10000
      DO 823 I=1,ISAMPO
      IF(IE(I).LE.NERROR)NERROR=IE(I)
  823 CONTINUE
      RETURN
      END
C*************************************************************
      SUBROUTINE DENCOD(II,IID,NSYM)
C*************************************************************
      DIMENSION II(1),IID(1)
      IID(1)=II(1)
      DO 3 I=2,NSYM
    3 IID(I)=IID(I-1)*II(I)
      RETURN
      END
C*************************************************************
      SUBROUTINE TANABS(AR,AI,THETA,LDIM,PI)
C*************************************************************
      DIMENSION AR(1),AI(1),THETA(1)
      DO 1 I=1,LDIM
      IF(AR(I).EQ.0.0)AR(I)=0.00001
      YY=ABS(AI(I)/AR(I))
      THETA(I)=ATAN(YY)
    1 CONTINUE
      RETURN
      END
C*************************************************************
      SUBROUTINE ACGEN(SIG1,SIG2,TXF,ICOD,ITXFI,IHLIM,L,IFCN1,IFCN2,ATT
C*************************************************************
      COMMON LDIM,PI,IPF,NSYM
      DIMENSION AR1(2048),AR2(2048),AI1(2048),AI2(2048)
```

```
      INTEGER JI1(514),JQ2(514)
      COMPLEX SIG1(1),SIG2(1),TXF(1)
      INTEGER IQ1(514),II2(514),IQ2(514),II1(514),LWK(15)
      INTEGER IID1(514),IQD1(514),IORI1(514)
      INTEGER IID2(514),IQD2(514),IORI2(514)
      NSY2=NSYM*2
      NSY2P2=NSY2+2
      IDUM1=4
      IDUM2=17
      INOBIT=514
      NSYMP2=NSYM+2
C
      CALL PRBS(JI1,15,1,15,INOBIT)
      CALL DATA(JI1,IORI1,NSYMP2,IDUM1)
C
      IF(ICOD.EQ.1) CALL DBPSK(IORI1,SIG1,AR1,AI1,IID1)
C
      IF(ICOD.EQ.2)CALL TXOQP(SIG1,AR1,AI1,IORI1,II1,IQ1,IID1,IQD1)
C
      IF(ICOD.EQ.3.OR.ICOD.EQ.4)CALL TXQPSK(IORI1,II1,IQ1,SIG1,AR1,AI1,
     ?IID1,IQD1,ICOD)
C
      CALL PRBS(JQ2,15,1,15,INOBIT)
      CALL DATA(JQ2,IORI2,NSYMP2,IDUM2)
C
      IF(ICOD.EQ.1) CALL DBPSK(IORI2,SIG2,AR2,AI2,IID2)
C
      IF(ICOD.EQ.2)CALL TXOQP(SIG2,AR2,AI2,IORI2,II2,IQ2,IID2,IQD2)
C
      IF(ICOD.EQ.3.OR.ICOD.EQ.4)CALL TXQPSK(IORI2,II2,IQ2,SIG2,AR2,AI2,
     ?IID2,IQD2,ICOD)
C PASS THE SIGNAL THROUGH THE TRANSMIT FILTER
C
C
      IF(ITXFI.EQ.1)CALL FILTER(SIG1,TXF,LDIM,L)
      IF(ITXFI.EQ.1)CALL FILTER(SIG2,TXF,LDIM,L)
C
      IF(IHLIM.EQ.1)CALL HLIM(SIG1,LDIM)
      IF(IHLIM.EQ.1)CALL HLIM(SIG2,LDIM)
      CALL FFT2C(SIG1,L,LWK)
      CALL FFT2C(SIG2,L,LWK)
C  ROTATE
      CALL ROTATE(SIG1,LDIM,IFCN1)
      CALL ROTATE(SIG2,LDIM,IFCN2)
C
      CALL INVERS(SIG1,LDIM,L)
      CALL INVERS(SIG2,LDIM,L)
      DO 172 I=1,LDIM
      SIG2(I)=ATT*SIG2(I)
172   SIG1(I)=ATT*SIG1(I)
      RETURN
      END
```

```
C     ********************************************************
      SUBROUTINE ROTATE(SIG,LDIM,IRO)
      COMPLEX SIG(1),XX,YY
      DO 1 K=1,IRO
      XX=SIG(1)
      SIG(1)=SIG(LDIM)
      DO 2 I=2,LDIM
      YY=SIG(I)
      SIG(I)=XX
    2 XX=YY
    1 CONTINUE
      RETURN
      END
C*************************************************************
C     THE FOLLOWING SUBROUTINE PERFORMS THE INVERSE FFT
C     PROCESS ON THE DATA SEQUENCE.
C*************************************************************
      SUBROUTINE INVERS(SIGNAL,LDIM,L)
      COMPLEX SIGNAL(1)
      DIMENSION IWK(15)
      DO 1 I=1,LDIM
    1 SIGNAL(I)=CONJG(SIGNAL(I))
      CALL FFT2C(SIGNAL,L,IWK)
      DO 2 I=1,LDIM
    2 SIGNAL(I)=CONJG(SIGNAL(I))/FLOAT(LDIM)
      RETURN
      END
C************************************
      SUBROUTINE ACI(SIGNAL,SIG1,SIG2)
      COMMON LDIM,PI,IPF,NSYM
      COMPLEX SIG1(1),SIG2(1),SIGNAL(1) ,XX
      DO 529 I=1,LDIM
      XX=SIGNAL(I)
  529 SIGNAL(I)=SIGNAL(I)+SIG1(I)+SIG2(I)
      RETURN
      END
```

```
C PROGRAM NAME: IMPDCT
C
C  WRITTEN ON FEBRUARY 9 1986 BY ABBAS YONGACOGLU
C
C    THIS PROGRAM IS USED FOR EVALUATING THE BER PERFORMANCE OF
C    DQPSK AND DCTPSK WITH VARIOUS RECEIVERS.
C    THESE RECEIVERS USE:
C            1) CONVENTIONAL DECODERS
C            2) NONREDUNDANT ERROR CORRECTION DECODER
C            3) COMBINING WITH FEEDBACK DECODER
C            4) A 4-STATE SEQUENTIAL DECODER.
C
C
C  THE SIMULATION IS IN BASEBAND.
C
C
C   THE SUBROUTINES USED IN THIS PROGRAM ARE :
C
C  *** 1) IMSL ***
C
C   FFT2C     GGNML
C
C  *** 2) SHARED WITH OTHER PROGRAMS
C
C   ENERGY  FILT    FILTER     PRBS    RCOSFA    REIM
C
C   COMP  CHOFIL  DATA   REIMN  RDRCOS   RDBWG   SETFI
C
C   SH45  SHM45  DCTPSK  STAY  REV  PO90  NE90  CONJUG
C
C  *** 3) SPECIFIC TO THIS PROGRAM ***
C
C   SEC    CWF    SEQUEN   MAP
C
C
C
C    TO SPEED UP THE COMPUTATIONS, ONLY EVERY IPF/2 SAMPLE IS USED.
C
C    ICODE= 0   QPSK
C         = 1   CTPSK
C
C    IPF = NUMBER OF SAMPLES PER SYMBOL
C
C
C    SIGNAL— (LDIM) TX AND RX SIGNAL
C    TXF,PREFI— CONTAIN FILTER COEFF.
C    AR,AI—     REAL AND IMAGINARY PARTS OF SIGNAL
C    SAMSIM — (NSYM) CONTAINS THE SAMPLED VALUES OF RX'D SIGNAL
C
      DOUBLE PRECISION DSEED
      COMMON LDIM,PI,IPF,NSYM
      COMMON/PARA/NO1,NO2,SYMRAT,SBANDW
```

```
      COMMON/IOPUT/ITTI,ITTO,LPT
      COMPLEX SIGNAL(2048),TXF(2048),PREFI(2048)
      COMPLEX SAMSIG(256)
      COMPLEX SIG1I(256),SIG1Q(256),B1I(256),B1Q(256)
      DIMENSION AR(2200),AI(2200),DUM(2200)
      COMPLEX SIG2I(256),SIG2Q(256)
      DIMENSION P1(256),PM1(256),QM1(256),X1(256),XM1(256)
      INTEGER IX1(512),IXM1(512),IV1(256)
      INTEGER II(256),IQ(256),IID(256),IQD(256)
      INTEGER JAI(29000),JAQ(29000),IB(256),IB2(256),ICO(256)
      INTEGER ISEC(256),II1(256),IQ1(256),IPR(256),ICOPR(256)
      INTEGER II2(256),IQ2(256),IED(256),IS(256),IT(256),IIND(256)
      DIMENSION D1I(256),D1Q(256)
      DIMENSION D2I(256),D2Q(256)
      INTEGER KDEC(256),MD(256)
C
C   INITIALIZE
      ITTI=7
      ITTO=7
      LPT=6
C     DSEED=748943D0
      DSEED=467238D0
      PI=3.141592653589793
C******************
      IPF=8
      NSYM=256
      L=11
C******************
      NP=2**L
      IPFT2=IPF*2
      NSYMP1=NSYM+1
      NSYMM1=NSYM-1
      NSYMM2=NSYM-2
      NSY2=NSYM*2
      WRITE(6,100)IPF
      INC=6
      IPF1=IPF+1
      LDIM=NSYM*IPF
      IF(LDIM.NE.NP)WRITE(6,654)
      SYMRAT=1.0
      SBANDW=IPF*SYMRAT
      NO=LDIM/2
      NO1=NO+1
      NO2=NO1+1
      ITER=0
C-------------------------------
C
C   START FOR EACH NEW RUN
C
1111  ITER=ITER+1
      IDUM=148
C
```

```
C
      WRITE(7,800)
800   FORMAT('DQPSK =0, DCTPSK =1')
        READ(7,6001)ICODE
      WRITE(7,6010)
        READ(7,6004)JRUN
      IF(JRUN.LE.50)GOTO 210
      WRITE(7,7001)
        READ(7,6004)JRUN
210   CONTINUE
C
      INOBIT=28000
      IERCOM=0
      ISYBEF=0
      ISYSEC=0
      IESEQ1=0
      IESEQ2=0
C
      WRITE(7,6003)
        READ(7,8004)DB
      DBR=DB/10.0
      EBIN=1.0
      PN0IN=1.0/((2.0)*(10.0**DBR))*IPF
C
C     GENERATE  PRBS FOR I AND Q SEPARATELY
C
C
      CALL PRBS(JAI,15,1,15,INOBIT)
      CALL PRBS(JAQ,22,1,22,INOBIT)
C
C
C----------CHOOSING THE FILTERS----------
C
      WRITE(ITTO,7006)
7006  FORMAT('VARIABLE FILTER PARAMETERS PRESS 1')
      READ(ITTI,6001)IVARFI
      IF(IVARFI.EQ.1)GOTO 360
      ITXFI=1
      CALL SETFI(TXF,PREFI)
      GOTO 950
C
C  TX FILTER
C
360   WRITE(ITTO,8100)
      READ(ITTI,6001)ITXFI
      IF(ITXFI.NE.1)WRITE(LPT,8109)
      IF(ITXFI.EQ.1)CALL CHOFIL(TXF,1)
C
C  PREMOD FILTER
C
550   WRITE(ITTO,9100)
      READ(ITTI,6001)IPREFI
```

```
      IF(IPREFI.NE.1)WRITE(LPT,9109)
      IF(IPREFI.EQ.1)CALL CHOFIL(PREFI,2)
C
C-------------------------------------
950   WRITE(ITTO,8201)
8201  FORMAT('DO YOU WANT A HARDLIMITER ?-YES=1')
      READ(ITTI,6001)IHLIM
C-------------------------------------
      ISTART=1
C
1900  ICHE=JRUN*INC+NSYM+IDUM
      IF(INOBIT.LE.ICHE)WRITE(6,689)
      IF(INOBIT.LE.ICHE)STOP
      ISYMT=(NSYM-2)*2*JRUN
C
C
C   START OF EACH ITERATION
C
C
      DO 888 KRUN=ISTART,JRUN
      WRITE(7,3300)KRUN
C
C GENERATE THE DATA
      CALL DATA(JAI,II,NSYM,IDUM)
      CALL DATA(JAQ,IQ,NSYM,IDUM)
C
C   EXPRESS INPUT DATA AS 4 DISTINCT PHASES
C
      CALL MAP(II,IQ,IT)
C
C
C    DIFFERENTIALLY ENCODE THE DATA
C
      II(1)=1
      IQ(1)=1
      IID(1)=II(1)
      IQD(1)=IQ(1)
      DO 2000 I=2,NSYM
      IF(II(I).EQ.1.AND.IQ(I).EQ.1)CALL STAY(IID,IQD,I)
      IF(II(I).EQ.1.AND.IQ(I).EQ.-1)CALL PO90(IID,IQD,I)
      IF(II(I).EQ.-1.AND.IQ(I).EQ.1)CALL NE90(IID,IQD,I)
      IF(II(I).EQ.-1.AND.IQ(I).EQ.-1)CALL REV(IID,IQD,I)
2000  CONTINUE
C
C     DETERMINE INITIAL PHASE CHANGE (FOR PRED AND COMBINING)
C
      IF(II(2).EQ.1.AND.IQ(2).EQ.1)MINI=0
      IF(II(2).EQ.-1.AND.IQ(2).EQ.-1)MINI=2
      IF(II(2).EQ.1.AND.IQ(2).EQ.-1)MINI=1
      IF(II(2).EQ.-1.AND.IQ(2).EQ.1)MINI=3
C       ****************************************
C             GENERATE THE BASEBAND SIGNALS
```

```
C      ******************************************
C
      IF(ICODE.EQ.1)CALL DCTPSK(AR,AI,IID,IQD)
      IF(ICODE.EQ.0)CALL QPSK(AR,AI,IID,IQD)
C
      CALL COMP(SIGNAL,AR,AI,LDIM)
C
C TX FILTER
C
      IF(ITXFI.EQ.1)CALL FILTER(SIGNAL,TXF,LDIM,L)
C
C            HARDLIMITER
C
      IF(IHLIM.EQ.1)CALL HLIM(SIGNAL,LDIM)
C
C
      CALL ENERGY(SIGNAL,EB)
      IF(KRUN.EQ.1)WRITE(6;258)EB
C
C
C     GENERATE AND SCALE THE NOISE
C
C
      CALL GGNML(DSEED,LDIM,DUM)
      PN0=PN0IN*EB
C
      DO 53 I=1,LDIM
53    DUM(I)=DUM(I)*SQRT(PN0)
C  ***************
C     ADD NOISE
C  ***************
      DO 63 I=1,LDIM
63    SIGNAL(I)=SIGNAL(I)+CMPLX(DUM(I),DUM(LDIM+1-I))
C
C   PREMOD FILTERING
C
C
      IF(IPREFI.EQ.1)CALL FILTER(SIGNAL,PREFI,LDIM,L)
C
C ******************************************
C                DECODING
C ******************************************
      MK=IPF/2
      IF(ICODE.EQ.1)MK=MK+IPF/2+1
C
C    SAMPLE THE RECEIVED SIGNAL
C
      DO 4555 I=1,NSYMM1
      M=(I-1)*IPF+MK
      SAMSIG(I)=SIGNAL(M)
4555  CONTINUE
C
```

```
C    1-SYMBOL DELAYED PATH
C
     CALL SH45(SAMSIG,B1I,NSYM)
     CALL CONJUG(SIG1I,SAMSIG,B1I,1,NSYM)
     CALL REIMN(SIG1I,D1I,NSYM)
C
     CALL SHM45(SAMSIG,B1Q,NSYM)
     CALL CONJUG(SIG1Q,SAMSIG,B1Q,1,NSYM)
     CALL REIMN(SIG1Q,D1Q,NSYM)
C
C
C
C  ************** 2 SYMBOL DELAYED ****************
C
     CALL CONJUG(SIG2I,SAMSIG,B1I,2,NSYM)
     CALL REIMN(SIG2I,D2I,NSYM)
C
     CALL CONJUG(SIG2Q,SAMSIG,B1Q,2,NSYM)
     CALL REIMN(SIG2Q,D2Q,NSYM)
C
C  DETERMINE THE POLARITY OF THE
C  I AND Q CHANNEL RECEIVED SIGNALS
C
C  1-BIT OUTPUTS ARE USED IN CONVENTIONAL DETECTOR
C
C  1 AND 2-BIT OUTPUTS ARE USED IN SEC
C
C
C
     DO 180 I=3,NSYMM1
     II1(I)=-1
     IQ1(I)=-1
     II2(I)=-1
     IQ2(I)=-1
     IF(D2I(I).GT.0.0)II2(I)=1
     IF(D2Q(I).GT.0.0)IQ2(I)=1
     IF(D1I(I).GT.0.0)II1(I)=1
180  IF(D1Q(I).GT.0.0)IQ1(I)=1
C
C    MAP I AND Q CHANNEL BITS TO 4 DISTINCT PHASES
C
     CALL MAP(II1,IQ1,IB)
C
C
C   APPLY SINGLE ERROR CORRECTION   (I.E., NONREDUNDANT
C   ERROR CORRECTION)
C
     CALL SEC(II2,IQ2,IB,IB2,IS,IED,ISEC)
C
C
C    APPLY COMBINING  WITH FEEDBACK
C
```

```
C
      CALL CWF(D1I,D1Q,D2I,D2Q,MINI,ICO,0)
C
C
C*****************************************
C
C   4 STATE SEQUENTIAL DECODER
C*****************************************
C
      CALL SEQUEN(D1I,D1Q,D2I,D2Q,KDEC,MD)
C77    FORMAT(9I7)
C
C
C     COUNT THE ERRORS
C
C
      NSH=NSYMM2-3
      DO 542 I=5,NSH
      IF(KDEC(I).NE.IT(I))IESEQ2=IESEQ2+1
      IF(MD(I+1).NE.IT(I))IESEQ1=IESEQ1+1
      IF(IT(I).NE.IB(I))ISYBEF=ISYBEF+1
      IF(IT(I).NE.ISEC(I))ISYSEC=ISYSEC+1
      IF(IT(I).NE.ICO(I))IERCOM=IERCOM+1
542   CONTINUE
      WRITE(7,3613)ISYBEF,ISYSEC,IERCOM
3613  FORMAT('ISYBEF =',I4,3X,'ISYSEC =',I4,3X,'IERCOM =',I4)
      WRITE(7,623)IESEQ1,IESEQ2
623   FORMAT('IESEQ1= ',I4,10X,'IESEQ2 = ',I4)
      IDUM=IDUM+INC
888   CONTINUE
C
C
C
C
      FNSYM=FLOAT(NSH-4)*2.0*JRUN
      BERBEF=FLOAT(ISYBEF)/FNSYM
      BERCOM=FLOAT(IERCOM)/FNSYM
      BERSEC=FLOAT(ISYSEC)/FNSYM
      BERSQ1=FLOAT(IESEQ1)/FNSYM
      BERSQ2=FLOAT(IESEQ2)/FNSYM
      WRITE(7,1400)BERBEF,BERCOM,BERSEC,BERSQ1,BERSQ2
      WRITE(6,1400)BERBEF,BERCOM,BERSEC,BERSQ1,BERSQ2
1400  FORMAT('BERBEF =',F10.6,/,'BERCOM =',F10.6,/,'BERSEC =',F10.6,/,
     ?'BERSQ1 =',F10.6,/,'BERSQ2 =',F10.6)
C
      WRITE(7,712)DB
       WRITE(7,5005)
          READ(7,6001)ICONT
       IF(ICONT.NE.1)GO TO 369
       WRITE(7,8202)
          READ(7,6004)IINC
      IF(IINC.LE.50)GOTO 211
```

```
      WRITE(7,7001)
        READ(7,6004)IINC
211    ISTART=1+JRUN
       JRUN=JRUN+IINC
       GO TO 1900
369    WRITE(ITTO,7005)
7005   FORMAT('FOR A NEW RUN PRESS 1')
       READ(ITTI,6001)NEWRUN
       IF(NEWRUN.EQ.1)GOTO 1111
C
C  READ FORMATS
C
6004   FORMAT(I3)
8004   FORMAT(F10.4)
6021   FORMAT(I1,/,I1)
6001   FORMAT(I1)
C
C    WRITE ON ITTI
C
C
C    WRITE ON LPT/ITTO
C
7001   FORMAT('IS IT A MISTAKE? TRY AGAIN')
6010   FORMAT('NO OF RUNS=? (I3)')
100    FORMAT(5X,'IPF=',I4)
654    FORMAT(5X,'BOYUTLAR UYUMSUZ')
6003   FORMAT(' DB= ? (F10.4)')
8100   FORMAT('DO YOU WANT A TX FILTER ? (YES=1)')
8109   FORMAT('NO TRANSMIT FILTERING')
9100   FORMAT('DO YOU WANT A PRE-MOD FILTER ? (YES=1)')
9109   FORMAT('NO PREMOD   FILTERING')
9200   FORMAT('DO YOU WANT A POSTMOD FILTER ? (YES=1)')
4109   FORMAT('NO POSMOD   FILTERING')
6200   FORMAT(5X,'TX FILTER BANDWIDTH= ',F10.2)
6201   FORMAT(5X,'PRE-DET FILTER BANDWIDTH= ',F10.2)
5001   FORMAT('DO YOU WANT VARIABLE NO OF RUNS',/,'IF YES PRESS 1')
689    FORMAT(2X,'INCREASE INOBIT')
3300   FORMAT(5X,'KRUN=',I4)
258    FORMAT(10X,'ENERGY BEF MOD',F10.6)
 366    FORMAT(2X,'I=',I5,5X,F10.4,5X,F10.4)
266    FORMAT(2X,'I=',I5,5X,F10.4,5X,F10.4)
712    FORMAT(10X,'DB=',F10.4)
5005    FORMAT('DO YOU WANT TO CONTINUE ?',/,'IF YES PRESS 1')
8202    FORMAT('NO OF RUNS')
       STOP
       END
C*************************************************************
       SUBROUTINE MAP(II,IQ,IB)
       INTEGER II(1),IQ(1),IB(1)
       COMMON LDIM,PI,IPF,NSYM
       DO 1 K=3,NSYM
       IF(II(K).EQ.1.AND.IQ(K).EQ.1)IB(K)=0
```

```
      IF(II(K).EQ.1.AND.IQ(K).EQ.-1)IB(K)=1
      IF(II(K).EQ.-1.AND.IQ(K).EQ.1)IB(K)=3
      IF(II(K).EQ.-1.AND.IQ(K).EQ.-1)IB(K)=2
1     CONTINUE
      RETURN
      END
C*************************************************
      SUBROUTINE ISDET(IS,IB,IB2,K)
      INTEGER IS(1),IB(1),IB2(1)
      IS(K)=IB(K)+IB(K-1)-IB2(K)
      CALL MOD4(IS,K)
      RETURN
      END
C*************************************************************
      SUBROUTINE MOD4(IS,K)
      INTEGER IS(1)
      IF(IS(K).GE.4)IS(K)=IS(K)-4
      IF(IS(K).LT.0)IS(K)=IS(K)+4
      RETURN
      END
C*************************************************
C
      SUBROUTINE CWF(D1I,D1Q,D2I,D2Q,MINIT,IRI,KSE)
C
C*************T*************************************
      COMMON LDIM,PI,IPF,NSYM
      DIMENSION D1I(1),D1Q(1),D2I(1),D2Q(1)
      INTEGER IRI(1)
      MINI=MINIT
      NSYMM1=NSYM-1
      PI2=PI/2.0
      PI4=PI/4.0
      DO 344 K=3,NSYMM1
      NPHA=3
C
      DO 244 I=1,3
      N1=NPHA
      N2=I-1
      ARG1=N1*PI2-PI4
      ARG2=N2*PI2-PI4
      ARG7=PI2*(N1+MINI)
      ARG8=PI2*(N2+MINI)
      ARG3=(N1+MINI)*PI2-PI4
      ARG4=(N2+MINI)*PI2-PI4
      T1=D1I(K)*(COS(ARG1)-COS(ARG2))
      T2=D1Q(K)*(SIN(ARG2)-SIN(ARG1))
      T3=D2I(K)*(COS(ARG3)-COS(ARG4))
      T4=D2Q(K)*(SIN(ARG4)-SIN(ARG3))
C
      T5=2.0*D1I(K)*(COS(ARG1)-COS(ARG2))
      T6=2.0*D1Q(K)*(SIN(ARG1)-SIN(ARG2))
      T7=(D1Q(K)*D1Q(K-1)-D1I(K)*D1I(K-1))*(SIN(ARG8)-SIN(ARG7))
```

```
      T8=(D1Q(K)*D1I(K-1)+D1I(K)*D1Q(K-1))*(COS(ARG7)-COS(ARG8))
      NPHA=N1
      QU0=T1+T2+T3+T4
C     QU0=T3+T4
      QU1=T5-T6+T7+T8
      QU2=QU0+QU1
      QUAN=QU0
      IF(KSE.EQ.1)QUAN=QU1
      IF(KSE.EQ.2)QUAN=QU2
      IF(QUAN.LT.0.0)NPHA=N2
C     WRITE(7,392)NPHA,QUAN
392   FORMAT('NPHA=',I3,5X,'QUAN',F10.4)
244   CONTINUE
      IRI(K)=NPHA
344   MINI=NPHA
C
C
4520  FORMAT(I4,4X,4F10.3)
      RETURN
      END
C*****************************************************************
      SUBROUTINE SEC(II2,IQ2,IB,IB2,IS,IED,IRI)
C*****************************************************************
      COMMON LDIM,PI,IPF,NSYM
      INTEGER II2(1),IQ2(1),IB(1),IB2(1),IS(256),IED(256),IRI(1)
      NSYMM1=NSYM-1
      CALL MAP(II2,IQ2,IB2)
C
      IS(2)=0
      IED(2)=0
      DO 135 K=3,NSYMM1
      KM1=K-1
      CALL ISDET(IS,IB,IB2,K)
C
      IED(K-1)=0
      IF(IS(K).NE.0.AND.IS(K).EQ.IS(KM1))IED(KM1)=IS(K)
      IRI(KM1)=IB(KM1)-IED(KM1)
      CALL MOD4(IRI,KM1)
135   CONTINUE
      RETURN
      END
C*****************************************************************
C   SEQUENTIAL DECODING
C*****************************************************************
      SUBROUTINE SEQUEN(D1I,D1Q,D2I,D2Q,KDEC,MD)
      COMMON LDIM,PI,IPF,NSYM
C     DIMENSION P1(256),PM1(256),QM1(256),X1(256),XM1(256)
C     INTEGER IX1(512),IXM1(512),IV1(256)
      DIMENSION D1I(1),D1Q(1)
      DIMENSION D2I(1),D2Q(1)
      DIMENSION S0(256),S1(256),S2(256),S3(256),Q0(4),Q1(4),Q2(4),Q3(4)
      INTEGER MG0(256),MG1(256),MG2(256),MG3(256),MD(1)
```

```
      INTEGER KDEC(1),MP(256)
      NSYMM2=NSYM-2
C
C
      S0(4)=0.0
      S1(4)=0.0
      S2(4)=0.0
      S3(4)=0.0
C
C
C
      DO 236 I=5,NSYMM2
      QY1=-D2I(I)-D2Q(I)
      QY2=-D2I(I)+D2Q(I)
      QY3=-QY1
      QY4=-QY2
C
C
C
      CT1=D1I(I)+D1Q(I)
      AM0M0=-(CT1-QY1)
      AM1M0=-(CT1-QY2)
      AM2M0=-(CT1-QY3)
      AM3M0=-(CT1-QY4)
C
      CT2=D1I(I)-D1Q(I)
      AM0M1=-(CT2-QY2)
      AM1M1=-(CT2-QY3)
      AM2M1=-(CT2-QY4)
      AM3M1=-(CT2-QY1)
C
      CT3=-D1I(I)-D1Q(I)
      AM0M2=-(CT3-QY3)
      AM1M2=-(CT3-QY4)
      AM2M2=-(CT3-QY1)
      AM3M2=-(CT3-QY2)
C
      CT4=-D1I(I)+D1Q(I)
      AM0M3=-(CT4-QY4)
      AM1M3=-(CT4-QY1)
      AM2M3=-(CT4-QY2)
      AM3M3=-(CT4-QY3)
C
C
C   DETERMINE AND CHOOSE S0(I)
      Q0(1)=S0(I-1)+AM0M0
      Q0(2)=S1(I-1)+AM1M0
      Q0(3)=S2(I-1)+AM2M0
      Q0(4)=S3(I-1)+AM3M0
C
      CALL SES(Q0,S0,I,MG0)
C
```

```
C   DETERMINE AND CHOOSE S1(I)
C
      Q1(1)=S0(I-1)+AM0M1
      Q1(2)=S1(I-1)+AM1M1
      Q1(3)=S2(I-1)+AM2M1
      Q1(4)=S3(I-1)+AM3M1
C
C
      CALL SES(Q1,S1,I,MG1)
C
C   DETERMINE AND CHOOSE S2(I)
C
      Q2(1)=S0(I-1)+AM0M2
      Q2(2)=S1(I-1)+AM1M2
      Q2(3)=S2(I-1)+AM2M2
      Q2(4)=S3(I-1)+AM3M2
C
C
      CALL SES(Q2,S2,I,MG2)
C
C   DETERMINE AND CHOOSE S3(I)
C
      Q3(1)=S0(I-1)+AM0M3
      Q3(2)=S1(I-1)+AM1M3
      Q3(3)=S2(I-1)+AM2M3
      Q3(4)=S3(I-1)+AM3M3
C
      CALL SES(Q3,S3,I,MG3)
C
      CALL SELTRA(S0,S1,S2,S3,MD,I,MG0,MG1,MG2,MG3,MP)
      CALL SQU3(MD,MP,MG0,MG1,MG2,MG3,NSYM,KDEC)
  236 CONTINUE
   77 FORMAT(9I7)
      RETURN
      END
C*****************************************
      SUBROUTINE SES(Q,S,K,MG)
      DIMENSION Q(1),S(1)
      INTEGER MG(1)
      NPHA=1
      DO 1 I=2,4
      N1=NPHA
      N2=I
    1 IF(Q(N1).GT.Q(N2))NPHA=N2
      S(K)=Q(NPHA)
      MG(K)=NPHA-1
      RETURN
      END
C*********************************
      SUBROUTINE SELTRA(S0,S1,S2,S3,MD,I,MG0,MG1,MG2,MG3,MP)
      DIMENSION S0(1),S1(1),S2(1),S3(1)
      INTEGER MD(1),MG0(1),MG1(1),MG2(1),MG3(1),MP(1)
```

```
      SMIN=S0(I)
      NMIN=MG0(I)
      MMIN=0
C
      IF(S1(I).LT.SMIN)NMIN=MG1(I)
      IF(S1(I).LT.SMIN)MMIN=1
      IF(S1(I).LT.SMIN)SMIN=S1(I)
C
      IF(S2(I).LT.SMIN)NMIN=MG2(I)
      IF(S2(I).LT.SMIN)MMIN=2
      IF(S2(I).LT.SMIN)SMIN=S2(I)
C
      IF(S3(I).LT.SMIN)NMIN=MG3(I)
      IF(S3(I).LT.SMIN)MMIN=3
      IF(S3(I).LT.SMIN)SMIN=S3(I)
      MD(I)=NMIN
      MP(I)=MMIN
      RETURN
      END
C**********************************
      SUBROUTINE SQU3(MD,MP,MG0,MG1,MG2,MG3,NSYM,KDEC)
      INTEGER MD(1),MG0(1),MG1(1),MG2(1),MG3(1),KDEC(1)
      INTEGER MP(1)
      NSYMM2=NSYM-2
      NSYMM4=NSYM-4
C
      DO 1 I=7,NSYMM2
      M=I-2
      IF(MP(I).NE.0)GOTO 11
      IF(MG0(I).EQ.0)KDEC(I-2)=MG0(I-1)
      IF(MG0(I).EQ.1)KDEC(I-2)=MG1(I-1)
      IF(MG0(I).EQ.2)KDEC(I-2)=MG2(I-1)
      IF(MG0(I).EQ.3)KDEC(I-2)=MG3(I-1)
      GOTO 1
C
11    IF(MP(I).NE.1)GOTO 22
      IF(MG1(I).EQ.0)KDEC(M)=MG0(I-1)
      IF(MG1(I).EQ.1)KDEC(M)=MG1(I-1)
      IF(MG1(I).EQ.2)KDEC(M)=MG2(I-1)
      IF(MG1(I).EQ.3)KDEC(M)=MG3(I-1)
      GOTO 1
C
22    IF(MP(I).NE.2)GOTO 33
      IF(MG2(I).EQ.0)KDEC(M)=MG0(I-1)
      IF(MG2(I).EQ.1)KDEC(M)=MG1(I-1)
      IF(MG2(I).EQ.2)KDEC(M)=MG2(I-1)
      IF(MG2(I).EQ.3)KDEC(M)=MG3(I-1)
      GOTO 1
C
33    IF(MG3(I).EQ.0)KDEC(M)=MG0(I-1)
      IF(MG3(I).EQ.1)KDEC(M)=MG1(I-1)
      IF(MG3(I).EQ.2)KDEC(M)=MG2(I-1)
```

```
      IF(MG3(I).EQ.3)KDEC(M)=MG3(I-1)
   1  CONTINUE
C
      RETURN
      END
```

```
C PROGRAM NAME: DGMSK
C* WRITTEN BY A. YONGACOGLU,  SEPT. 9 1985
C
C*** THIS PROGRAM SIMULATES DIFFERENTIAL DETECTION OF MSK OR GMSK
C
C     THE BER PERFORMANCE OF THE FOLLOWING RECEIVERS CAN BE EVALUATED:
C
C     1) CONVENTIONAL ONE-BIT DIFFERENTIAL DETECTION
C     2) ONE-BIT DIFFERENTIAL DETECTION USING DECISION FEEDBACK
C     3) CONVENTIONAL TWO-BIT DIFFERENTIAL DETECTION
C
C     FOR THE ONE-BIT DIFFERENTIAL DETECTION
C     THERE IS NO DIFFERENTIAL ENCODING AT TRANSMITTER.
C
C    AT THE RECEIVER, THE CORRECT SAMPLING TIME IS KNOWN,
C    THEREFORE ONLY ONE SAMPLE PER BIT IS PROCESSED.
C
C    THE SIMULATION IS IN BASEBAND.
C
C    THE SUBROUTINES CALLED:
C
C    1) SPECIFIC TO THIS PROGRAM
C
C    NRZ   FMMOD   RX1BIT   RX2BIT
C
C    2)  SHARED WITH OTHER PROGRAMS
C
C     PRBS     DATA    DENCOD  ENERGY
C     SETFI   CHOFI    COMP    REIM
C
C    ALSO THE FOLLOWING IMSL ROUTINES ARE NEEDED
C    1) GGNML   2) FFT2C
C
      DOUBLE PRECISION DSEED
      COMMON LDIM,PI,IPF,NSYM
      COMMON/IORUT/ITTI,ITTO,LPT
      COMMON/PARA/NO1,NO2,SYMRAT,SBANDW
      COMPLEX SIGNAL(2048),TXF(2048),PREFI(2048)
      COMPLEX SIG(256),YG(256)
      DIMENSION AR(2048),AI(2048),DUM(2200)
      INTEGER JAI(29000),IN1(256),IN1DF(256)
      INTEGER IORI(256),IN2(256),IDE(256)
C
C   INITIALIZE THE FIXED PARAMETERS
C
      PI=3.141592653589793
C*********************************
      L=11
      NP=2**L
      IPF=16
      NSYM=128
C*********************************
```

```
      FIPF=IPF*2.0
      INC=6
      LDIM=NSYM*IPF
      IF(LDIM.NE.NP)WRITE(7,654)
654   FORMAT(5X,'DIMENSIONS DO NOT MATCH')
      SYMRAT=1.0
      SBANDW=IPF*SYMRAT
      EBIN=1.0
      NO=LDIM/2
      NO1=NO+1
      NO2=NO1+1
      ITTI=7
      ITTO=7
      LPT=6
      ITER=0
C-----------------------------------------
C   INITIALIZE THE PARAMETERS FOR EACH ADDITIONAL RUN
C
C
1111  ITER=ITER+1
      DSEED=268943D0
      IDUM=24
         WRITE(7,6010)
         READ(7,6004)JRUN
      IF(JRUN.LE.50)GOTO 210
         WRITE(7,7001)
         READ(7,6004)JRUN
210   CONTINUE
C
      INOBIT=28000
      IER1=0
      IER1DF=0
      IER2=0
C
      SHIFT1=0.0
         WRITE(7,108)
108   FORMAT('FOR ONE-BIT PRESS 1, FOR TWO-BIT PRESS 2')
         READ(7,6001)I1OR2
      IF(I1OR2.EQ.1)GOTO 112
         WRITE(7,4027)
4027  FORMAT('THRESHOLD = ?')
         READ(7,8004)TH
      GOTO 15
C
C DECISION FEEDBACK OR NOT
C
112      WRITE(7,816)
816   FORMAT('IF YOU WANT DECISION FEEDBACK PRESS 1')
         READ(7,6001)ISHI
      IF(ISHI.NE.1)GOTO 15
         WRITE(7,5285)
5285  FORMAT('SHIFT VALUE IN DEGREES  ? (FOR BT=0.25 ENTER 18.2)')
```

```
        READ(7,8014)SHIFT1
8014  FORMAT(F8.4)
      SHIFT1=SHIFT1*PI/180.0
15      WRITE(7,6003)
        READ(7,8004)DB
      DBR=DB/10.0
C*****************************************
      PN0IN=1.0/((10.0**DBR))*IPF
C*****************************************
        WRITE(7,8254)
8254  FORMAT('ENTER THE SAMPLING TIME, NOMINAL VALUE: 00  (I2)')
        READ(7,9367)MOFF
9367  FORMAT(I2)
C
      CALL PRBS(JAI,15,1,15,INOBIT)
C
C----------CHOOSING THE FILTERS----------
C
        WRITE(7,591)
591   FORMAT('FILTER PARAM. USER DEFINED=1, SET=0, SAME AS LAST RUN=2')
        READ(7,6001)IVARFI
      IF(IVARFI.EQ.1)GOTO 360
      IF(IVARFI.EQ.2)GOTO 950
      ITXFI=1
      IPREFI=1
      CALL SETFI(TXF,PREFI)
      GOTO 950
C  TX FILTER
C
360     WRITE(7,8100)
        READ(7,6001)ITXFI
      IF(ITXFI.NE.1)GOTO 450
      CALL CHOFIL(TXF,1)
      GOTO 550
450     WRITE(6,8109)
C
C  PREMOD FILTER
C
550     WRITE(7,9100)
        READ(7,6001)IPREFI
      IF(IPREFI.NE.1)GOTO 650
      CALL CHOFIL(PREFI,2)
      GOTO 950
650     WRITE(6,9109)
C
950   CONTINUE
C-----------------------------------
      ISTART=1
C
1900  ICHE=JRUN*INC+NSYM+IDUM
      IF(INOBIT.LE.ICHE)WRITE(6,689)
      IF(INOBIT.LE.ICHE)STOP
```

```
C
C
C   START OF EACH ITERATION
C
C
      DO 888 KRUN=ISTART,JRUN
         WRITE(7,3300)KRUN
C
C LOAD NSYM FROM THE GENERATED PRBS
C
      CALL DATA(JAI,IORI,NSYM,IDUM)
C
C   IF 2-BIT DIF. DETECTION, DIFFERENTIALLY ENCODE THE DATA
C
      IF(I1OR2.EQ.2)CALL DENCOD(IORI,IDE,NSYM)
C
C    GENERATE NRZ SIGNALS, IPF SAMPLES PER BIT
C
      IF(I1OR2.EQ.1)CALL NRZ(AR,AI,IORI,NSYM,IPF)
      IF(I1OR2.EQ.2)CALL NRZ(AR,AI,IDE,NSYM,IPF)
      CALL COMP(SIGNAL,AI,AR,LDIM)
C
C PASS THE SIGNAL THROUGH TRANSMIT FILTER
C
      IF(ITXFI.EQ.1)CALL FILTER(SIGNAL,TXF,LDIM,L)
C
C       FILTERED NRZ SIGNAL IS FED TO THE FM MODULATOR
C
      CALL FMMOD(SIGNAL,AR,AI)
C
C    CALCULATE ENERGY PER BIT
C
      CALL ENERGY(SIGNAL,EB)
C
C    GENERATE WHITE GAUSSIAN NOISE AND SCALE IT
C
C
      CALL GGNML(DSEED,LDIM,DUM)
      PN0=PN0IN*EB
C
      DO 53 I=1,LDIM
53    DUM(I)=DUM(I)*SQRT(PN0)
C  ***************
C     ADD NOISE
C  ***************
      DO 63 I=1,LDIM
63    SIGNAL(I)=SIGNAL(I)+CMPLX(DUM(I),DUM(LDIM+1-I))
C
C    PASS THE SIGNAL THROUGH PREDETECTION FILTER
C
      IF(IPREFI.EQ.1)CALL FILTER(SIGNAL,PREFI,LDIM,L)
C
```

```
C ***************************
C    DIFFERENTIAL DECODING
C ***************************
C
C  SAMPLE THE SIGNAL
C
      DO 2444 I=1,NSYM
      YG(I)=CMPLX(0.0,0.0)
2444  SIG(I)=SIGNAL(I*IPF-MOFF)
C
C     CONVENTIONAL 2-BIT DIFFERENTIAL DETECTION
C
      IF(I1OR2.NE.2)GOTO 28
      CALL RX2BIT(SIG,IORI,IN2,TH,IER2)
      GOTO 422
C
C     CONVENTIONAL 1-BIT DIFFERENTIAL DETECTION
C
28    CALL RX1BIT(SIG,YG,IORI,IN1,0.0,IER1,NSYM)
C
C     2-BIT DIFFERENTIAL DETECTION USING DECISION FEEDBACK
C
      IF(ISHI.EQ.1)CALL RX1BIT(SIG,YG,IORI,IN1DF,SHIFT1,IER1DF,NSYM)
422   IDUM=IDUM+INC
888   CONTINUE
C
C
C
      PRE1=FLOAT(IER1)/FLOAT((NSYM-3)*JRUN)
      IF(I1OR2.EQ.1)WRITE(7,562)IER1,PRE1
562   FORMAT('NO. OF ERRORS',I4,6X,'PROB. ERROR 1-BIT CONV. =',F12.6)
C
      PRE1DF=FLOAT(IER1DF)/FLOAT((NSYM-3)*JRUN)
      IF(I1OR2.EQ.1.AND.ISHI.EQ.1)WRITE(7,562)IER1DF,PRE1DF
762   FORMAT('NO.OF ERRORS',I4,6X,'PROB. ERROR 1-BIT DF. =',F12.6)
C
      PRE2=FLOAT(IER2)/FLOAT((NSYM-3)*JRUN)
      IF(I1OR2.EQ.2)WRITE(7,262)IER2,PRE2
262   FORMAT('NO OF ERRORS',I4,6X,'PROB. ERROR 2-BIT CONV. =',F12.6)
      WRITE(6,712)DB
      WRITE(7,712)DB
       WRITE(7,5005)
          READ(7,6001)ICONT
       IF(ICONT.NE.1)GO TO 369
       WRITE(7,8202)
          READ(7,6004)IINC
      IF(IINC.LE.50)GOTO 211
      WRITE(7,7001)
        READ(7,6004)IINC
211    ISTART=1+JRUN
       JRUN=JRUN+IINC
       GO TO 1900
```

```
369   WRITE(7,7005)
7005  FORMAT('FOR A NEW RUN PRESS 1')
      READ(7,6001)NEWRUN
      IF(NEWRUN.EQ.1)GOTO 1111
C
C  READ FORMATS
C
6004  FORMAT(I3)
8004  FORMAT(F10.4)
6001  FORMAT(I1)
C
7001  FORMAT('IS IT A MISTAKE? TRY AGAIN')
6010  FORMAT('NO OF RUNS=? (I3)')
100   FORMAT(5X,'IPF=',I4)
6003  FORMAT(' ENTER EB/NO IN DB= ? (F10.4)')
8100  FORMAT('DO YOU WANT A TX FILTER ? (YES=1)')
8109  FORMAT('NO TRANSMIT FILTERING')
9100  FORMAT('DO YOU WANT A PRE-MOD FILTER ? (YES=1)')
9109  FORMAT('NO PREMOD   FILTERING')
689   FORMAT(2X,'INCREASE INOBIT')
3300  FORMAT(5X,'KRUN=',I4)
258   FORMAT(10X,'ENERGY BEF MOD',F10.6)
266   FORMAT(2X,'I=',I5,5X,F10.4,5X,F10.4)
712   FORMAT(10X,'DB=',F10.4)
5005   FORMAT('DO YOU WANT TO CONTINUE ?',/,'IF YES PRESS 1')
8202   FORMAT('NO OF RUNS')
      STOP
      END
C*****************************************************
C  SET THE TRANSMIT AND PREDETECTION FILTER PARAMETERS
      SUBROUTINE SETFI(F1,F2)
      COMPLEX F1(1),F2(1)
      CALL FILT(0.25,0.0,F1,9)
      CALL FILT(0.5,0.0,F2,9)
      RETURN
      END
C*********************************************
C   PERFORMING THE FM MODULATION
      SUBROUTINE FMMOD(SIGNAL,AR,AI)
      COMMON LDIM,PI,IPF,NSYM
      COMPLEX SIGNAL(1)
      DIMENSION AR(1),AI(1)
C
      CALL REIM(SIGNAL,AI,AR,LDIM)
C
      FIPF=IPF*2
      SUMI=0.0
      DO 36 I=1,NSYM
      DO 36 J=1,IPF
      M=((I-1)*IPF+J)
      SUMI=SUMI+AI(M)
      AR(M)=COS(PI/FIPF*SUMI)
```

```
36    AI(M)=SIN(PI/FIPF*SUMI)
C
      CALL COMP(SIGNAL,AR,AI,LDIM)
      RETURN
      END
C ***************************************************************
C     2-BIT DIFFERENTIAL DECODING SUBROUTINE
C ***************************************************************
      SUBROUTINE RX2BIT(SIG,IORI,IN2,TH,IER2)
      COMMON LDIM,PI,IPF,NSYM
      COMPLEX SIG(1)
      INTEGER IORI(1),IN2(1)
      NSYMM2=NSYM-2
C
      DO 547 I=3,NSYMM2
      C2=REAL(SIG(I)*CONJG(SIG(I-2)))-TH
      IN2(I)=-1
      IF(C2.LT.0.0)IN2(I)=1
      IF(IN2(I).NE.IORI(I))IER2=IER2+1
547   CONTINUE
      RETURN
      END
C***************************************************************
C       DIFFERNTIALLY ENCODING THE DATA
      SUBROUTINE DENCOD(II,IID,NSYM)
C***************************************************************
      DIMENSION II(1),IID(1)
      IID(1)=II(1)
      DO 3 I=2,NSYM
3     IID(I)=IID(I-1)*II(I)
      RETURN
      END
C***************************************************************
C       REPRESENTING THE SIGNAL WITH IPF SAMPLES
      SUBROUTINE NRZ(AR,AI,II,NSYM,IPF)
C***************************************************************
      DIMENSION AR(1),AI(1)
      INTEGER II(1)
      DO 35 I=1,NSYM
      DO 35 J=1,IPF
      M=((I-1)*IPF+J)
      AR(M)=0.0
35    AI(M)=II(I)
      RETURN
      END
C***************************************************************
C  THIS SUBROUTINE PERMITS INTERACTIVE ENTRY OF FILTER PARAMETERS
C  SUBROUTINES CALLED: 1) RDRCOS, 2) RCOSFA, 3) RDBWG, 4) FILT
C***************************************************************
      SUBROUTINE CHOFIL(FI,MFIL)
      COMPLEX FI(1)
      COMMON/IOPUT/ITTI,ITTO,LPT
```

```
      WRITE(ITTO,8101)
     ,READ(ITTI,6001)IKIN
      IF(IKIN.NE.1)GOTO 451
      CALL RDRCOS(ALPHA,FN,ISQRT,IAMP,MFIL)
C
      CALL RCOSFA(FN,FI,ALPHA,ISQRT,IAMP)
C
      RETURN
451   IF(IKIN.NE.2)GOTO 352
      CALL RDBWG(BT,IBWG,MFIL)
C
      CALL FILT(BT,0.0,FI,IBWG)
      RETURN
352   WRITE(ITTO,8108)
6001  FORMAT(I1)
8101  FORMAT('RCOS=1,  BUTW/GAUSS=2')
8108  FORMAT('INCORRECT FILTER TYPE SPEC')
      RETURN
      END
C*****************************************************************
C THIS SUBROUTINE PERFORMS THE ONE-BIT DIFFERENTIAL DETECTION
C (CONVENTIONAL OR USING DECISION FEEDBACK)
C
C SUBROUTINE CALLED: 1) PS1
C*****************************************************************
      SUBROUTINE RX1BIT(SIG,YG,II,IN,SHIFT,IER,NSYM)
      COMPLEX SIG(1),YG(1)
      INTEGER II(1),IN(1)
C
      NSK=NSYM-2
      IG=2
      IN(IG)=II(IG)
C
      DO 547 I=3,NSK
      XX=IN(I-1)*SHIFT
      CALL PS1(SIG,YG,I,XX)
      A1C=REAL(SIG(I)*CONJG(YG(I)))
      IN(I)=-1
      IF(A1C.GT.0.0)IN(I)=1
      IF(IN(I).NE.II(I))IER=IER+1
547   CONTINUE
      RETURN
      END
C*****************************************************************
C   THIS SUBR. SHIFTS THE PHASE OF THE 1-BIT DELAYED SIGNAL
C   FOR CONVENTIONAL 90 DEGREES
C   FOR DECISION FEEDBACK ADDITIONAL (X=IN(I-1)*SHIFT) DEGREES
      SUBROUTINE PS1(SIGNAL,B,I,X)
C*****************************************************************
      COMPLEX SIGNAL(1),B(1)
      PIO2=3.14159/2.0
      AA=COS(X+PIO2)
      BB=SIN(X+PIO2)
      B(I)=SIGNAL(I-1)*CMPLX(AA,BB)
      RETURN
      END
```

```
C PROGRAM NAME: IMPDGM
C
C  WRITTEN ON JULY 12 1986 BY ABBAS YONGACOGLU
C
C    THIS PROGRAM IS USED FOR EVALUATING THE BER PERFORMANCE OF
C    DGMSK RECEIVERS WHICH USE DECISION FEEDBACK. MORE SPECIFICALLY
C    THAT OF:
C            1) 1+2DF RECEIVER
C            2) 2+3DF
C            3) OFFSET QPSK (DOQPSK)
C            4) DCTPSK
C
C
C  THE SIMULATION IS IN BASEBAND.
C
C
C    THE SUBROUTINES USED IN THIS PROGRAM ARE :
C
C  *** 1) IMSL ***
C
C    FFT2C     GGNML
C
C  *** 2) SHARED WITH OTHER PROGRAMS
C
C    ENERGY  FILT    FILTER     PRBS    RCOSFA    REIM
C
C    COMP  CHOFIL  DATA   REIM   RDRCOS   RDBWG
C
C
C  *** 3) SPECIFIC TO THIS PROGRAM ***
C
C    DF12      DF23
C
C    TO SPEED UP THE COMPUTATIONS, ONLY EVERY IPF/2 SAMPLE IS USED.
C
      DOUBLE PRECISION PID,DSEED
      COMMON LDIM,PI,IPF,NSYM
      COMMON/PARA/NO1,NO2,SYMRAT,SBANDW
      COMMON/IOPUT/ITTI,ITTO,LPT
      COMPLEX SIGNAL(2048),TXF(2048),PREFI(2048)
      COMPLEX SIG(256)
      DIMENSION AR(2200),AI(2200),DUM(2200)
      INTEGER JAI(59000)
      INTEGER IORI(1024),IDE(1024),IOUT(300),IOUT3(300)
C
C
C    INITIALIZE
      ITTI=7
      ITTO=7
      LPT=6
      PI=3.141592653589793
      L=11
```

```
      NP=2**L
      IPF=16
      FIPF=IPF*2
      IPFP1=IPF+1
      IPFO2=IPF/2
      IPO2P1=IPFO2+1
      SQ2=SQRT(2.0)
      NSYM=128
      NSYMP1=NSYM+1
      NSYMM1=NSYM-1
      WRITE(6,100)IPF
      INC=6
      LDIM=NSYM*IPF
      IF(LDIM.NE.NP)WRITE(6,654)
      SYMRAT=1.0
      SBANDW=IPF*SYMRAT
      NO=LDIM/2
      NO1=NO+1
      NO2=NO1+1
      ITER=0
C-----------------------------------
C
C   START FOR EACH ADDITIONAL RUN
C
1111  ITER=ITER+1
      DSEED=268943D0
      IDUM=24
      WRITE(7,6010)
         READ(7,6004)JRUN
      IF(JRUN.LE.50)GOTO 210
      WRITE(7,7001)
         READ(7,6004)JRUN
210   CONTINUE
C
      INOBIT=58000
      IERROR=0
      WRITE(7,120)
120   FORMAT('FOR 1+2DF RECEIVER ENTER 1, FOR 2+3DF ENTER 2')
      READ(7,6001)IRX
C
      WRITE(7,1572)
1572  FORMAT('COMBINING COEFFICIENT ?')
      READ(7,8014)COMCOF
C
      WRITE(7,5285)
5285  FORMAT('ENTER THE SHIFT VALUES IN DEGREES ?')
      READ(7,8019)SHIFT1,SHIFT2
8019  FORMAT(F8.4,/,F8.4)
8014  FORMAT(F8.4)
      SHIFT1=SHIFT1*PI/180.0
      SHIFT2=SHIFT2*PI/180.0
      WRITE(7,6003)
```

```
      READ(7,8004)DB
      DBR=DB/10.0
      EBIN=1.0
C*****************************************
      PN0IN=1.0/((10.0**DBR))*IPF
C*****************************************
C
      CALL PRBS(JAI,15,1,15,INOBIT)
C
C---------CHOOSING THE FILTERS----------
C
      WRITE(ITTO,591)
591   FORMAT('FILTER PARAM.  VAR=1, SET=0, SAME=2')
      READ(ITTI,6001)IVARFI
      IF(IVARFI.EQ.1)GOTO 360
      IF(IVARFI.EQ.2)GOTO 950
      ITXFI=1
      IPREFI=1
      CALL SETFI(TXF,PREFI)
      GOTO 950
C  TX FILTER
C
360   WRITE(ITTO,8100)
      READ(ITTI,6001)ITXFI
      IF(ITXFI.NE.1)GOTO 450
      CALL CHOFIL(TXF,1)
      GOTO 550
450   WRITE(LPT,8109)
C
C  PREMOD FILTER
C
550   WRITE(ITTO,9100)
      READ(ITTI,6001)IPREFI
      IF(IPREFI.NE.1)GOTO 650
      CALL CHOFIL(PREFI,2)
      GOTO 950
650   WRITE(LPT,9109)
C
950   CONTINUE
C-------------------------------------
8602  ISTART=1
C
1900  ICHE=JRUN*INC+NSYM+IDUM
      IF(INOBIT.LE.ICHE)WRITE(6,689)
      IF(INOBIT.LE.ICHE)STOP
C
C
C   START OF EACH ITERATION
C
C
      DO 888 KRUN=ISTART,JRUN
      WRITE(7,3300)KRUN
```

```
C
C GENERATE THE DATA
      CALL DATA(JAI,IORI,NSYM,IDUM)
      IF(IRX.EQ.2)CALL DENCOD(IORI,IDE,NSYM)
      IF(IRX.EQ.1)CALL FILLIN(IORI,IDE,NSYM)
      DO 35 I=1,NSYM
      DO 35 J=1,IPF
      M=((I-1)*IPF+J)
      AR(M)=0.0
35    AI(M)=IDE(I)
C
      CALL COMP(SIGNAL,AI,AR,LDIM)
C
C TX FILTER
C
      IF(ITXFI.EQ.1)CALL FILTER(SIGNAL,TXF,LDIM,L)
      CALL REIM(SIGNAL,AI,AR,LDIM)
C
C     WRITE(7,3273)(I,AI(I),AR(I),I=1,32)
3273  FORMAT(I4,3X,2F12.5)
C
      SUMI=0.0
      DO 36 I=1,NSYM
      DO 36 J=1,IPF
      M=((I-1)*IPF+J)
      SUMI=SUMI+AI(M)
      AR(M)=COS(PI/FIPF*SUMI)
36    AI(M)=SIN(PI/FIPF*SUMI)
C
      CALL COMP(SIGNAL,AR,AI,LDIM)
C
C
      CALL ENERGY(SIGNAL,EB)
      IF(KRUN.EQ.1)WRITE(6,258)EB
C
C
C
C
      CALL GGNML(DSEED,LDIM,DUM)
      PN0=PN0IN*EB
C
      DO 53 I=1,LDIM
53    DUM(I)=DUM(I)*SQRT(PN0)
C  ***************
C     ADD NOISE
C  ***************
      DO 63 I=1,LDIM
63    SIGNAL(I)=SIGNAL(I)+CMPLX(DUM(I),DUM(LDIM+1-I))
C
      IF(IPREFI.EQ.1)CALL FILTER(SIGNAL,PREFI,LDIM,L)
C
C
```

```
C
C ***************************
C    DIFFERENTIAL DECODING
C ***************************
C     SAMPLE THE RECEIVED SIGNAL
C
      DO 2444 I=1,NSYM
2444  SIG(I)=SIGNAL(I*IPF-2)
C
C   1+2DF RECEIVER
C
      IF(IRX.EQ.1)CALL DF12(IORI,IOUT,SIG,SHIFT1,SHIFT2,COMCOF)
C
C   2+3DF RECEIVER
C
      IF(IRX.EQ.2)CALL DF23(IDE,IORI,IOUT,SIG,SHIFT1,SHIFT2,COMCOF)
C
C     COUNTING THE ERRORS
C-------------------------------------
      NSK=NSYM-4
      DO 3666 I=6,NSK
      IF(IOUT(I).NE.IORI(I))IERROR=IERROR+1
3666  CONTINUE
      WRITE(ITTO,620)IERROR
620   FORMAT('IERROR =',I4)
      IDUM=IDUM+INC
888   CONTINUE
      PRE=FLOAT(IERROR)/FLOAT((NSK-4)*JRUN)
      WRITE(7,562)PRE
562   FORMAT('PROB. OF ERROR =',F12.6)
      WRITE(7,712)DB
       WRITE(7,5005)
          READ(7,6001)ICONT
       IF(ICONT.NE.1)GO TO 369
       WRITE(7,8202)
          READ(7,6004)IINC
      IF(IINC.LE.50)GOTO 211
      WRITE(7,7001)
         READ(7,6004)IINC
211   ISTART=1+JRUN
       JRUN=JRUN+IINC
       GO TO 1900
369   WRITE(ITTO,7005)
7005  FORMAT('FOR A NEW RUN PRESS 1')
      READ(ITTI,6001)NEWRUN
      IF(NEWRUN.EQ.1)GOTO 1111
C
C  READ FORMATS
C
6004  FORMAT(I3)
8004  FORMAT(F10.4)
6021  FORMAT(I1,/,I1)
```

```
6001  FORMAT(I1)
C
C   WRITE ON ITTI
C
C
C   WRITE ON LPT/ITTO
C
7001  FORMAT('IS IT A MISTAKE? TRY AGAIN')
6010  FORMAT('NO OF RUNS=? (I3)')
100   FORMAT(5X,'IPF=',I4)
654   FORMAT(5X,'BOYUTLAR UYUMSUZ')
6003  FORMAT(' DB= ? (F10.4)')
8100  FORMAT('DO YOU WANT A TX FILTER ? (YES=1)')
8109  FORMAT('NO TRANSMIT FILTERING')
9100  FORMAT('DO YOU WANT A PRE-MOD- FILTER ? (YES=1)')
9109  FORMAT('NO PREMOD   FILTERING')
5001  FORMAT('DO YOU WANT VARIABLE NO OF RUNS',/,'IF YES PRESS 1')
689   FORMAT(2X,'INCREASE INOBIT')
3300  FORMAT(5X,'KRUN=',I4)
258   FORMAT(10X,'ENERGY BEF MOD',F10.6)
266   FORMAT(2X,'I=',I5,5X,F10.4,5X,F10.4)
712   FORMAT(10X,'DB=',F10.4)
5005   FORMAT('DO YOU WANT TO CONTINUE ?',/,'IF YES PRESS-1')
8202   FORMAT('NO OF RUNS')
      STOP
      END
C*************************************************************
      SUBROUTINE DENCOD(II,IID,NSYM)
C*************************************************************
      DIMENSION II(1),IID(1)
      IID(1)=II(1)
      DO 3 I=2,NSYM
3     IID(I)=-IID(I-1)*II(I)
      RETURN
      END
C*************************************************************
      SUBROUTINE SETFI(F1,F2)
      COMPLEX F1(1),F2(1)
      CALL FILT(0.25,0.0,F1,9)
      CALL FILT(0.5,0.0,F2,9)
      RETURN
      END
C ***************************
C    DIFFERENTIAL DECODING
C ***************************
      SUBROUTINE DF23(IDE,IORI,IOUT,SIG,SHIFT1,SHIFT2,COMCOF)
      COMMON LDIM,PI,IPF,NSYM
      COMPLEX SIG(1),XG(256),WG(256)
      INTEGER IN(256),IDE(1),IORI(1),IOUT(1)
C
      DO 2444 I=1,NSYM
      XG(I)=CMPLX(0.0,0.0)
```

```
2444  WG(I)=CMPLX(0.0,0.0)
C
      J1=1
      J2=2
      J3=3
      J4=4
      IN(1)=IDE(J1)
      IN(2)=IDE(J2)
      IN(3)=IDE(J3)
      IN(4)=IDE(J4)
      IOUT(J3)=IORI(J3)
      IOUT(J4)=IORI(J4)
C*************************
      DO 547 I=5,NSYM
C
C   2-BIT
C
      WW=0.0
      IF(IN(I-1).NE.IN(I-2))WW=IN(I-2)*SHIFT1*2.0
      IF(IN(I-1).NE.IN(I-3))WW=IN(I-3)*SHIFT2+WW
      CALL PS2(SIG,XG,I,WW)
      FR=REAL(SIG(I)*CONJG(XG(I-2)))
C
C
C   3-BIT
C
      SS=PI/2.0*IN(I-1)
      SHI2=SHIFT1*2
      IF(IN(I-2).NE.IN(I-3))SS=IN(I-3)*SHI2+SS
      IF(IN(I-2).NE.IN(I-4))SS=IN(I-4)*SHIFT2+SS
      CALL PS3(SIG,WG,I,SS)
      SR=REAL(SIG(I)*CONJG(WG(I-3)))
C
      SG=-SR*IOUT(I-1)+FR*COMCOF
      IOUT(I)=-1
      IF(SG.GT.0.0)IOUT(I)=1
      IN(I)=-IN(I-1)*IOUT(I)
547   CONTINUE
      RETURN
      END
C *************************
C   DIFFERENTIAL DECODING
C *************************
      SUBROUTINE DF12(IORI,IN1,SIG,SHIFT1,SHIFT2,COMCOF)
      COMMON LDEM,PI,IPF,NSYM
      COMPLEX SIG(1),XG(256),WG(256)
      INTEGER IN1(256),IORI(1)
C
      DO 2444 I=1,NSYM
      XG(I)=CMPLX(0.0,0.0)
2444  WG(I)=CMPLX(0.0,0.0)
C
```

```
      J1=1
      J2=2
      J3=3
      IN1(J1)=IORI(J1)
      IN1(J2)=IORI(J2)
      IN1(J3)=IORI(J3)
C*****************************
      DO 547 I=4,NSYM
C
C   1-BIT
C
      XX=IN1(I-1)*SHIFT1+IN1(I-2)*SHIFT2
      CALL PS1(SIG,XG,I,XX)
      CR=REAL(SIG(I)*CONJG(XG(I)))
C
C   2-BIT
C
      WW=0.0
      IF(IN1(I-1).NE.IN1(I-2))WW=IN1(I-2)*(SHIFT1+SHIFT2)*2.0
      IF(IN1(I-1).NE.IN1(I-3))WW=IN1(I-1)*(SHIFT2)*2.0+WW
      CALL PS2(SIG,WG,I,WW)
      FR=REAL(SIG(I)*CONJG(WG(I-2)))
      FG=-IN1(I-1)*FR*COMCOF
      TOT=CR+FG
      IN1(I)=-1
      IF(TOT.GT.0.0)IN1(I)=1
547   CONTINUE
      RETURN
      END
C*********************************************************************
      SUBROUTINE FILLIN(IORI,IDE,NSYM)
      INTEGER IORI(1),IDE(1)
      DO 1 I=1,NSYM
1     IDE(I)=IORI(I)
      RETURN
      END
C*************************************************************
      SUBROUTINE PS1(SIGNAL,B,I,X)
C*************************************************************
      COMPLEX SIGNAL(1),B(1)
      PIO2=3.14159/2.0
      AA=COS(X+PIO2)
      BB=SIN(X+PIO2)
C     B(I-1)=SIGNAL(I-1)*CMPLX(AA,BB)
      B(I)=SIGNAL(I-1)*CMPLX(AA,BB)
      RETURN
      END
C*************************************************
      SUBROUTINE PS2(SIGNAL,B,I,X)
C*************************************************************
      COMPLEX SIGNAL(1),B(1)
      AA=COS(X)
```

```
      BB=SIN(X)
      B(I-2)=SIGNAL(I-2)*CMPLX(AA,BB)
      RETURN
      END
C*****************************************************
      SUBROUTINE PS3(SIGNAL,B,I,X)
C*****************************************************
      COMPLEX SIGNAL(1),B(1)
      AA=COS(X)
      BB=SIN(X)
      B(I-3)=SIGNAL(I-3)*CMPLX(AA,BB)
      RETURN
      END
```

```
C*************************************************
      SUBROUTINE SEPA(IORI,II,IQ,NSYM)
C  SERIAL TO PARALLEL CONVERSION
C*************************************************
      INTEGER IORI(1),II(1),IQ(1)
      NSYMO2=NSYM/2
      DO 2 I=1,NSYMO2
      II(I)=IORI(2*I-1)
2     IQ(I)=IORI(2*I)
      RETURN
      END
C*************************************************************
      SUBROUTINE DENCOD(II,IID,NSYM)
C  DIFFERENTIAL ENCODING (FOR DBPSK OR DOQPSK)
C*************************************************************
      DIMENSION II(1),IID(1)
      IID(1)=II(1)
      DO 3 I=2,NSYM
3     IID(I)=IID(I-1)*II(I)
      RETURN
      END
C*************************************************************
      SUBROUTINE RCOSFA(FBANDW,TF,ALPHA,ISQ,IAMP)
C  GENERATING RAISED COSINE FILTER CHARACTERISTICS
C*************************************************************
      COMMON LDIM,PI,IPF,NSYM
      COMMON/PARA/NO1,NO2,SYMRAT,SBANDW
      COMPLEX TF(1)
      IF (ALPHA.EQ.0) ALPHA=0.0001
      FN=LDIM*(FBANDW/SBANDW)
      F1=(1.-ALPHA)*FN
      F2=(1.+ALPHA)*FN
      IFN=IFIX(FN)
      IF1=IFIX(F1)+1
      IF2=IFIX(F2)+1
      B1=2.0*FN
      A1=PI/B1
      TF(1)=CMPLX(1.,0.0)
      DO 8 I=2,IF1
      FJ=I-1
      A2=1.0
      B2=FJ*A1
      SB2=SIN(B2)
      IF(SB2.LT.1.0E-10)SB2=1.0E-10
      B3=1.0-4.0*FJ*FJ/B1/B1
      IF(IAMP.EQ.1)A2=B2/SB2
      IF(IAMP.EQ.2)A2=2.0*B2*B3/SIN(2.0*B2)
      IF(IAMP.EQ.3)A2=B2*B2/SB2/SB2
      TF(I)=CMPLX(A2,0.0)
    8 CONTINUE
      JK=IF1+1
      DO 9 J=JK,IF2
```

```
      FJ=J-1
      A3=1.0
      B2=FJ*A1
      SB2=SIN(B2)
      IF(SB2.LT.1.0E-10)SB2=1.0E-10
      B3=1.0-4.0*FJ*FJ/B1/B1
      IF(IAMP.EQ.1)A3=B2/SB2
      IF(IAMP.EQ.2)A3=2.0*B2*B3/SIN(2.0*B2)
      IF(IAMP.EQ.3)A3=B2*B2/SB2/SB2
      A=(PI/(2.0*ALPHA))*(FJ/FLOAT(IFN)-1.)
      TF(J)=CMPLX(SQRT(0.5*(1.0-SIN(A))),0.0)
      IF(ISQ.EQ.0)TF(J)=CMPLX((0.5*(1.0-SIN(A))),0.0)
      IF(ISQ.EQ.2)TF(J)=CMPLX(SQRT(SQRT(0.5*(1.0-SIN(A)))),0.0)
      TF(J)=TF(J)*CMPLX(A3,0.0)
    9 CONTINUE
      JH=IF2+1
      DO 10 I=JH,NO1
      TF(I)=CMPLX(0.0,0.0)
   10 CONTINUE
      DO 5 I=NO2,LDIM
      TF(I)=CONJG(TF(LDIM+2-I))
    5 CONTINUE
      RETURN
      END
C*************************************************************
      SUBROUTINE FILT(F3DB,FCN,TF,IFIL)
C  GENERATING BUTTERWORTH OR GAUSSIAN FILTER CHARACTERISTICS
C*************************************************************
      COMMON LDIM,PI,IPF,NSYM
      COMMON /PARA/NO1,NO2,SYMRAT,SBANDW
      COMPLEX TF(1),S,T
C
      LL=LDIM/2
      LLP1=LL+1
      OMEGAC=F3DB*LDIM/SBANDW
C
      DO 21 I=1,LLP1
      FI=I
      S=CMPLX(0.0,FI/OMEGAC)
      IF(IFIL.EQ.4)T=1./((S**2+0.765*S+1)*(S**2+1.848*S+1))
      IF(IFIL.EQ.2)T=1./(S**2+1.414*S+1)
      OMEGA=CABS(S)
      IF(OMEGA.GT.22.0)TT=0.00001
      IF(OMEGA.GT.22.0)GOTO 93
      IF(IFIL.EQ.9)XT=EXP(0.34657*(OMEGA)**2)
      IF(IFIL.EQ.9)TT=1.0/XT
93    IF(IFIL.EQ.2.OR.IFIL.EQ.4)TT=CABS(T)
      TF(I)=CMPLX(TT,0.0)
21    CONTINUE
C
      DO 22 I=2,LL
      TF(LDIM+2-I)=TF(I)
```

```
22      CONTINUE
C
        ICENTR=LDIM*FCN/IPF
       IF(ICENTR.EQ.0)GOTO 60
        DO 24 II=1,ICENTR
        L=LDIM-1
        TEMP=TF(LDIM)
        DO 25 I=1,L
        TF(LDIM+1-I)=TF(LDIM-I)
25      CONTINUE
        TF(1)=TEMP
24      CONTINUE
C
        DO 26 I=2,LL
        TF(LDIM+2-I)=TF(I)
26      CONTINUE
C
60     CONTINUE
        RETURN
       END.
C*************************************************************
C      THE FOLLOWING SUBROUTINE PERFORMS THE FILTERING
C      PROCESS ON THE DATA SEQUENCE.
C*************************************************************
       SUBROUTINE FILTER(SIGNAL,TF,LDIM,L)
       COMPLEX SIGNAL(1),TF(1)
       DIMENSION IWK(15)
       CALL FFT2C(SIGNAL,L,IWK)
       DO 1 I=1,LDIM
     1 SIGNAL(I)=CONJG(SIGNAL(I)*TF(I))
       CALL FFT2C(SIGNAL,L,IWK)
       DO 2 I=1,LDIM
   2   SIGNAL(I)=CONJG(SIGNAL(I))/FLOAT(LDIM)
       RETURN
       END
C*************************************************************
C BIT ENERGY COMPUTATION
C *************************************************************
       SUBROUTINE ENERGY(DATA,EB)
       COMMON LDIM,PI,IPF,NSYM
       COMMON/PARA/NO1,NO2,SYMRAT,SBANDW
       COMPLEX DATA(1)
       WATTS=0.
       DO 1 I=1,LDIM
       WATTS=WATTS+((CABS(DATA(I)))**2.)
1      CONTINUE
       WATTS=WATTS/FLOAT(LDIM)
        EB=WATTS/(2.0*SYMRAT)
       RETURN
       END
C*************************************************************
       SUBROUTINE PRBS(JA,N,KTAP1,KTAP2,INOBIT)
```

```
C GENERATING A PSEUDO RANDOM BINARY SEQUENCE
C*************************************************************
      INTEGER KR(30),JA(1)
      J=0
      K1=N+1
      K2=N+2
      DO 5 I=1,N
5     KR(I)=1
      N1=N-1
      DO 25 K=1,INOBIT
      KR(K1)=KR(KTAP1)
      KR(K2)=KR(KTAP2)
      DO 10 I=1,N1
10    KR(N+1-I)=KR(N-I)
      KR(1)=-KR(K1)*KR(K2)
      J=J+1
25    JA(J)=KR(1)
      RETURN
      END
C*************************************************************
      SUBROUTINE HLIM(DATA,LDIM)
C*************************************************************
      COMPLEX DATA(1),X
      X=CABS(CMPLX(1.0,1.0))
      DO 10 I=1,LDIM
10    DATA(I)=DATA(I)/CABS(DATA(I))*X
      RETURN
      END
C*************************************************************
C*************************************************************
C  THIS SUBROUTINE PERMITS INTERACTIVE ENTRY OF FILTER PARAMETERS
C  SUBROUTINES CALLED: 1) RDRCOS, 2) RCOSFA, 3) RDBWG, 4) FILT
C*************************************************************
      SUBROUTINE CHOFIL(FI,MFIL)
      COMPLEX FI(1)
      COMMON/IOPUT/ITTI,ITTO,LPT
      WRITE(7,8101)
      READ(7,6001)IKIN
      IF(IKIN.NE.1)GOTO 451
      CALL RDRCOS(ALPHA,FN,ISQRT,IAMP,MFIL)
C
      CALL RCOSFA(FN,FI,ALPHA,ISQRT,IAMP)
C
      RETURN
451   IF(IKIN.NE.2)GOTO 352
      CALL RDBWG(BT,IBWG,MFIL)
C
      CALL FILT(BT,0.0,FI,IBWG)
      RETURN
352   WRITE(7,8108)
6001  FORMAT(I1)
8101  FORMAT('RCOS=1,  BUTW/GAUSS=2')
```

```
8108  FORMAT('INCORRECT FILTER TYPE SPEC')
      RETURN
      END
C*************************************************************
C     READ RAISED-COS FILTER PARAMETERS
C*************************************************************
      SUBROUTINE RDRCOS(ALPHA,FN,ISQRT,IAMP,MFIL)
      COMMON/IOPUT/ITTI,ITTO,LPT
      WRITE(ITTO,8102)
8102  FORMAT('ALPHA=?')
      READ(ITTI,8004)ALPHA
      WRITE(ITTO,8103)
8103  FORMAT('F NYQUIST/F SYMRATE =?')
      READ(ITTI,8004)FN
      WRITE(ITTO,8104)
8104  FORMAT('SQUARE ROOT=1')
      READ(ITTI,6001)ISQRT
      WRITE(ITTO,8105)
8105  FORMAT('AMP EQUALIZER=1, OTHERWISE=0')
      READ(ITTI,6001)IAMP
8004  FORMAT(F10.4)
6001  FORMAT(I1)
      IF(MFIL.EQ.1)WRITE(LPT,8007)
      IF(MFIL.EQ.2)WRITE(LPT,8008)
      IF(MFIL.EQ.3)WRITE(LPT,8009)
8007  FORMAT('TRANSMIT FILTER PARAMETERS',/)
8008  FORMAT('PRE-MODULATION FILTER PARAMETERS',/)
8009  FORMAT('POST-MODULATION FILTER PARAMETERS',/)
      WRITE(LPT,8010)ALPHA
8010  FORMAT('ALPHA=',F10.4)
      WRITE(LPT,8011)FN
8011  FORMAT('F NYQUIST/ F SYMBOL RATE =',F10.4)
      IF(ISQRT.EQ.1)WRITE(LPT,8012)
8012  FORMAT('FILTER IS SQUARE ROOT RAISED COSINE')
      IF(IAMP.EQ.1)WRITE(LPT,8013)
8013  FORMAT('FILTER INCLUDES AN AMPLITUDE EQUALIZER')
      RETURN
      END
C*************************************************************
C     READ BUTTERWORTH OR GAUSSIAN FILTER PARAMETERS
C*************************************************************
      SUBROUTINE RDBWG(BT,IBWG,MFIL)
      COMMON/IOPUT/ITTI,ITTO,LPT
      WRITE(ITTO,8106)
8106  FORMAT('BW2=2, BW4=4, GAUSS=9')
      READ(ITTI,6001)IBWG
      WRITE(ITTO,8107)
8107  FORMAT('BT PRODUCT= ?')
      READ(ITTI,8004)BT
6001  FORMAT(I1)
8004  FORMAT(F10.4)
      IF(MFIL.EQ.1)WRITE(LPT,8007)
```

```
      IF(MFIL.EQ.2)WRITE(LPT,8008)
      IF(MFIL.EQ.3)WRITE(LPT,8009)
 8007 FORMAT('TRANSMIT FILTER PARAMETERS',/)
 8008 FORMAT('PRE-MODULATION FILTER PARAMETERS',/)
 8009 FORMAT('POST-MODULATION FILTER PARAMETERS',/)
      IF(IBWG.EQ.2)WRITE(LPT,8016)
 8016 FORMAT('FILTER IS A SECOND ORDER BUTTERWORTH',/)
      IF(IBWG.EQ.4)WRITE(LPT,8017)
 8017 FORMAT('FILTER IS A FOURTH ORDER BUTTERWORTH',/)
      IF(IBWG.EQ.9)WRITE(LPT,8018)
 8018 FORMAT('FILTER IS GAUSSIAN',/)
      WRITE(LPT,8019)BT
 8019 FORMAT('3 DB BANDWIDTH * SYMBOL DURATION (I.E. BT) =',F10.4,/)
      RETURN
      END
```

Bibliography

[1] K. Hirade et al., "Error-Rate Performance of Digital FM with Differential Detection in Land Mobile Radio Channels", IEEE Trans. on Vehicular Tech., Vol. VT-28, pp. 204-212, Aug. 1979.

[2] S. Goode, "A Comparison of Gaussian Minimum Shift Keying to Frequency Shift Keying for Land Mobile Radio", Proc. of IEEE Veh. Tech. Conf., pp. 136-141, May 1984.

[3] F. Adachi, "Postdetection Selection Diversity Effects on Digital Land Mobile Radio", IEEE Trans. on Vehicular Tech., Vol. VT-31, pp. 166–172, Nov. 1982.

[4] J.E. Stjernvall and J. Uddenfeldt, "Gaussian MSK with Different Demodulators and Channel Coding for Mobile Telephony", ICC–84, pp. 219–222, May 1984.

[5] T. Aulin and C.W. Sundberg, "Partially Coherent Detection of Digital Full Response Continuous Phase Modulated Signals", IEEE Trans. on Comm., Vol. COM-30, pp. 1096-1116, May 1982.

[6] T. Aulin and C.W. Sundberg, "Synchronization Properties of Continuous Phase Modulation", GLOBECOM-82, pp. 877–883, Dec. 1982.

[7] T.A. Fitch, "The Effects of Rayleigh Distributed Multipath Fading on Carrier Recovery Performance", Proc. of IEEE Veh. Tech. Conf., pp. 252-255, May 1986.

[8] W.C. Hagmann, "Carrier Synchronizer for Overlapped Raised Cosine Pulse Amplitude Modulation", COMSAT Tech. Rev., Vol. 14, No. 1, pp. 25–52, Spring 1984.

[9] F.M. Gardner, *Phaselock Techniques*, John Wiley & Sons, Inc., New York, 1979.

[10] G.J. Saulnier and W. Rafferty, "DSP-Based Noncoherent Dual Detector Demodulator for Land Mobile Radio Channels", ICC-86, pp. 32.2.1 – 32.2.5, June 1986.

[11] H.P. Kuchenbecker and M. Aldinger, "Digital Speech Transmission on Mobile Radio Channels", *Signal Processing II: Theories and Applications*, Elsevier Science Publishers B.V.(North-Holland), pp. 535-538, EURASIP, 1983.

[12] J.P. McGeehan and A.J. Bateman,"Phaselocked Transparent Tone in Band (TTIB): A New Spectrum Configuration Particularly Suited to the Transmission of Data Over SSB Mobile Radio Networks", IEEE Trans. on Comm., Vol. COM-30, pp. 81-87, Jan. 1984.

[13] R. Wells, "SSB for VHF Mobile Radio at 5 kHz Channel, Spacing", IERE Conf. Proc. Radio Receivers and Associated Systems, Southhampton, pp. 29-36, July 1978.

[14] M. Yokoyama, " BPSK System with Sounder to Combat Rayleigh Fading in Mobile Radio Communication", IEEE Trans. on Vehicular Tech., Vol. VT-34, pp. 35-40, Feb.1985.

[15] B.B. Lusignan, "Single-Sideband Transmissions for Land Mobile Radio", IEEE Spectrum, pp. 33-37, July 1978.

[16] F. Davarian, " Comments on " BPSK System with Sounder to Combat Rayleigh Fading in Mobile Radio Communication"", IEEE Trans. on Vehicular Tech., Vol. VT-34, pp. 154-156 Nov.1985.

[17] A.J. Bateman et al., "Speech and Data Communications Over 942 MHz TAB and TTIB Single Sideband Mobile Radio Systems Incorporating Feed-Forward Signal Regeneration", IEEE Trans. on Vehicular Tech., Vol. VT-34, pp. 13-21, Feb.1985.

[18] Y. Daido et al., "256 QAM Modem for High Capacity Digital Radio Systems", GLOBECOM-84, pp. 16.8.1–16.8.5, Dec. 1984.

[19] M.K. Simon, "Dual-Pilot Tone Calibration Technique", IEEE Trans. on Vehicular Tech., Vol. VT-35, pp. 63–70, May 1986.

[20] M.S. Roden, *Digital and Data Communication Systems*, Prentice-Hall, Inc., Englewood Cliffs, N.J., 1982.

[21] M.K. Simon and C.C. Wang, "Differential Versus Limiter-Discriminator Detection of Narrow-Band FM" IEEE Trans. on Comm., Vol. COM-31, pp. 1227–1234, Nov. 1983.

[22] S.N. Carney, "Co-Channel Interference Comparison for Conventional Land Mobile Frequency Modulation and 2400 bps LPC/FSK Systems", Proc. of IEEE Vehicular Tech. Conf., pp. 131 – 135, May 1984.

[23] W.R. Bennett and J. Salz, "Binary Data Transmission by FM over a Real Channel", Bell System Technical Journal, pp. 2387 – 2426, Sept. 1963.

[24] S.A. Rhodes et al., "Signal Design for Inmarsat Standard C Ship Earth Station", GLOBECOM-82, pp. E5.5.1–E5.5.10, 1982.

[25] K.J.P. Fonseka and N. Ekanayake, "Differential Detection of Narrow-Band FM", IEEE Trans. on Comm., Vol. COM-33, pp. 725–729, July 1985.

[26] P.E.K. Chow and D.H.S. Ko, "Improving DCPSK Transmission by Means of Error Control", IEEE Trans. on Comm. Tech., pp. 715-719, Oct. 1971.

[27] M. Kato and H. Inose, "Majority Logic Detection Scheme of Differentially Phase Modulated Waves", Electronics and Communications in Japan, Vol. 55-A, No.1, 1972.

[28] T. Masamura et al., "Differential Detection of MSK with Nonredundant Error Correction", IEEE Trans. on Comm., Vol. COM-27, pp. 912–918, June 1979.

[29] K. S. Chung, "A Noncoherent Receiver for GTFM Signals", GLOBECOM-82, pp. B3.5.1-B3.5.5, Dec. 1982.

[30] S. Samejima et al., "Differential PSK Systems with Nonredundant Error Correction", IEEE Jour. on Selected Areas in Comm., Vol. SAC-1, pp. 74–81, Jan. 1983.

[31] S. Bellini, M. Sonzogni and G. Tartara, "Noncoherent Detection of Tamed Frequency Modulation", IEEE Trans. on Comm., Vol. COM-32, pp. 218 – 224, March 1984.

[32] M. Hirono, T. Miki and K. Murota, "Multilevel Decision Method for Band-limited Digital FM with Limiter Discriminator Detection", IEEE Trans. on Veh. Tech. Vol. VT-33, pp. 114-122, Aug. 1984.

[33] A. Svensson, "On an Improved Differential Detector for Continuous Phase Modulation", ICC-86, pp. 31.3.1–31.3.7, June 1986.

[34] T.T. Tjhung, K.K. Yeo and P.H. Wittke, "Effects of Pulse Shaping and Soft Decisions on the Performance of Digital FM with Discriminator Detection", IEEE Trans. on Comm., Vol. COM-34, pp. 1116 – 1122, Nov. 1986.

[35] I. Kalet et al., "Examples of Continuous Phase Modulation Using Discriminator Detection", IEEE Trans. on Comm., Vol. COM-34, pp. 1148 - 1150, Nov. 1986.

[36] N.A.B. Svensson and C.E.W. Sundberg, "Performance Evaluation of Differential and Discriminator Detection of Continuous Phase Modulation", IEEE Trans. on Vehicular Tech., Vol. VT-35, pp. 106–117, Aug. 1986.

[37] G, Boudreau and P.J. McLane, "Differential Detection of Duobinary CPFSK", IEEE Trahs. on Comm., Vol. COM-35, pp. 181–184, Feb. 1987.

[38] D. Makrakis, A. Yongaçoğlu and K. Feher, "Discriminator Detection Using Noise Prediction–Cancellation Techniques For Mobile Communications", to appear in Proceedings of ICC–87, June 1987.

[39] M. Lopriore, "The Design of a 30/20 GHz Regenerative Payload for Satellite Applications", 5th International Conference on Digital Satellite Communications, Genoa, Italy, March 1981.

[40] G. Ohm, "Experimental 14/11 GHz Regenerative Repeater for Communication Satellites", 5th International Conference on Digital Satellite Communications, pp. 445–451, Genoa, Italy, March 1981.

[41] Y.S. Lee, "Simulation Analysis for Differentially Coherent Quaternary PSK Regenerative Repeater", COMSAT Tech. Rev., pp. 447–474, Fall 1977.

[42] H.J. Apple, "An Onboard Baseband Switched Matrix for SS-TDMA", 5th International Conference on Digital Satellite Communications, Genoa, Italy, March 1981.

[43] S.J. Campanella, F. Assal and A. Berman, "On Board Regenerative Repeater", ICC-77, pp. 6.2.121–125, June 1977.

[44] W.H. Childs et al., "A 120-Mbit/s 14-GHz Regenerative Receiver for Spacecraft Applications", COMSAT Tech. Rev., Vol. 11 No. 1, Spring 1981.

[45] L. Moreno, F. Pattini and P.P. Giusto, "Implementation Imperfections of a 4ϕ-DCPSK On-Board Demodulator: Performance Degradations and Measurement Results", 5th International Conference on Digital Satellite Communications, pp. 469–476, Genoa, Italy, March 1981.

[46] W. Sandrin et al., "Aeronautical Satellite Data Link Study", COMSAT Tech. Rev., pp. 1-36, Spring-85.

[47] Y:Miyakagi, N.Morinaga and T.Namekawa, "Error Rate Performance of M-ary DPSK in Satellite/Aircraft Communications", ICC-79, pp. 34.6.1– 34.6.5, June 1979.

[48] F. Davarian, "Channel Simulation to Facilitate Mobile-Satellite Communications Research", IEEE Trans. on Comm., Vol. COM-35, pp. 47–56, Jan. 1987.

[49] J. E. Nicholson, J.D.B. Kent and J.T. Sydor, "MSAT Mobile Terminal Design Considerations", Proc. of IEEE Veh. Tech. Conf., pp. 347 - 351, May 1983.

[50] "MSAT System Concept Document", Communications Research Center, Canada, March 22, 1983.

[51] CCIR Report 599-1, "Aeronautical Satellite Tests in Band 9 (UHF)", Vol. VIII, Mobile Services, Geneva, 1982.

[52] Y. Miyakagi et al., "Double Symbol Error Rates for m-ary DPSK Systems in Satellite-Aircraft Multipath Channel", IEEE Trans. on Comm., Vol. COM-31, pp. 1285–1289, Dec. 1983.

[53] S.G. Wilson, R.W. Sutton and E.H. Schroeder, "Differential-Phase Shift Keying Performance on L-band Aeronautical Satellite Channels: Test Results and a Coding Evaluation", IEEE Trans. on Comm., Vol. COM-24, pp. 374–380, March 1976.

[54] H. Salwen, "Differential Phase-Shift Keying Performance under Time Varying Multipath Fading", IEEE Trans. on Comm., Vol. COM-23, pp. 383–385, March 1975.

[55] L.J. Mason " Error Probability Evaluation For Systems Employing Differential Detection in a Rician Fast Fading Environment and Gaussian Noise", IEEE Trans. on Comm., Vol. COM-35, pp. 39 – 46, Jan. 1987.

[56] W.C.Y. Lee, *Mobile Communications Engineering*, McGraw-Hill, New York, 1982.

[57] W.R. Bennett and J.R. Davey, *Data Transmission*, McGraw-Hill, New York, 1965.

[58] M.F. Choquet and H.J. Nussbaumer, "Microcoded Modem Transmitters", IBM J. Res. Dev., pp. 338-351, July 1974.

[59] J.J. Bussgang and M. Leiter, "Error Performance of Differential Phase-Shift Transmission Over a Telephone Line", IEEE Trans. on Comm., Vol. COM-16, pp. 411–418, June 1968.

[60] J. Salz, "Modulation and Detection for Coherent Lightwave Communications", IEEE Communications Magazine, pp. 38-49, June 1986.

[61] T. E. Bell, "Technology '87: Communications", IEEE Spectrum, pp. 42-44, Jan. 1987.

[62] J.K. Holmes, *Coherent Spread Spectrum Systems*, John Wiley & Sons, Inc., New York, 1982.

[63] M.K. Simon, "The Performance of M-ary FH-DPSK in the Presence of Partial-Band Multitone Jamming", IEEE Trans. on Comm., Vol. COM-30, pp. 953-958, May 1982.

[64] P.S. Henry, "Spectrum Efficiency of a Frequency Hopped DPSK Mobile Radio System", Proc. of IEEE Vehicular Tech. Conf., pp. 7-12, 1979.

[65] M.K. Simon and C.C. Wang, "Two-Bit Differential Detection of MSK", GLOBECOM-84, pp. 22.3.1–22.3.6, Dec. 1984.

[66] M.L. Doelz, E.T. Heald and D.L. Martin, "Binary Data Transmission Techniques for Linear Systems", Proc. of IRE, pp. 656–661, May 1957.

[67] C.R. Cahn, "Performance of Digital Phase-Modulation Communication Systems", IRE Trans. Commun. Syst., Vol.CS-7, pp. 3-6, May 1959.

[68] J.G. Lawton, "Comparison of Binary Data Transmission", Proc. 1958 Conf. on Military Electronics.

[69] S. Stein, "Unified Analysis of Certain Coherent and Noncoherent Binary Communication Systems", IEEE Trans. on Information Theory, Vol. IT-10, pp. 43-51, Jan. 1964.

[70] J.T. Fleck, "Alternate Derivation of the Error Rate of Differentially Coherent PSK System", Cornell Aero. Lab. Memo, June 1958.

[71] J.C. Henry, "DPSK versus FSK with Frequency Uncertainty", IEEE Trans. on Comm., Vol. COM-18, pp. 814–817.

[72] P.A. Kullstam, "DC Demodulation of BPSK and QPSK Signals in the Presence of Doppler and Phase Noise", NTC–74, pp.221–227, 1974.

[73] J.J. Spilker, *Digital Communications by Satellite*, Prentice-Hall, Inc., Englewood Cliffs, N.J., 1977.

[74] J.G. Proakis, *Digital Communications*, McGraw-Hill, New York, 1983.

[75] W.C. Lindsey and M.K. Simon, *Telecommunication System Engineering*, Prentice-Hall, Inc., Englewood Cliffs, N.J., 1973.

[76] S. Stein and J.J. Jones, *Modern Communications Principles*, McGraw-Hill, New York, 1967, Ch.12.

[77] A.J. Viterbi, *Principles of Coherent Communications*, McGraw-Hill, New York, 1966.

[78] J.H. Park, "On Binary DPSK Detection", IEEE Trans. on Comm., Vol. COM-26, pp.484-486, April 1978.

[79] R.W. Lucky, J. Saltz and J. Weldon, *Principles of Data Communications*, McGraw-Hill, New York, 1968.

[80] O. Shimbo, M.I. Celebiler and R.J. Fang, "Performance Analysis of DPSK Systems in Both Thermal Noise and Intersymbol Interference", IEEE Trans. on Comm., Vol. COM-19, pp. 1179-1188, Dec.1971.

[81] L.E. Miller and J.S. Lee, "The Probability Density Function for the Output of an Analog Cross-Correlator with Correlated Bandpass Inputs", IEEE Trans. on Information Theory, Vol. IT-20, pp. 433-440, July 1974.

[82] K. Feher, *Digital Communications Satellite-Earth Station Engineering*, Prentice-Hall, Inc., Englewood Cliffs, N.J., Jan. 1983.

[83] R.L. Horlacher and H.C. Schroeder, "Voiceband Four-Phase Data Set for Global Communication", IEEE Trans. on Comm., Vol. COM-17, pp. 390-394, June 1969.

[84] P. Monsen, "Modern HF Communications, Modulation and Coding", AGARD Lecture Series No. 127, June 1983.

[85] R.F. Pawula, S.O. Rice and J.H. Roberts, "Distribution of the Phase Angle Between Two Vectors Perturbed by Gaussian Noise", IEEE Trans. on Comm., Vol. COM-30, pp. 1228-1241, Aug. 1982.

[86] V.K. Prabhu and J. Salz, "On the Performance of Phase-Shift Keying Systems", Bell System Technical Journal, pp. 2307–2343, Dec. 1981.

[87] H. Okinaka, "Performance Characteristics of QPSK Signal Passing Nonlinear Channel in Digital Ship Earth Station System", Trans. of IECE of Japan, pp. 864-871, Aug. 1985.

[88] M.C. Austin and M.U. Chang, "Quadrature Overlapped Raised-Cosine Modulation", IEEE Trans. on Comm., Vol. COM-29, pp.237-249, March 1981.

[89] T. Le-Ngoc and K. Feher, "Power and Bandwidth Efficient ISI and Jitter Free (IJF) Transmission Techniques", ICC-81, June 1981.

[90] S. Kato and K. Feher, "XPSK: A New Cross-Correlated Phase Shift Keying Modulation TJchnique", IEEE Trans. on Comm., Vol. COM-31, pp.701–706, May 1983.

[91] J.S. Seo and K. Feher, "SQAM – A New Superposed QAM Modem Technique", IEEE Trans. on Comm., Vol. COM-33, pp. 296 - 300, March 1985.

[92] D. Muilwijk, "Correlative Phase Shift Keying: Bandwidth and Power Efficient Constant Envelope Modulation", ICC'80, pp. 26.6.1-26.6.8. June 1980.

[93] C.E. Sundberg, "Continuous Phase Modulation", IEEE Communications Magazine, Vol.24, pp. 25–38, April 1986.

[94] K. Murota and K.Hirade, "GMSK Modulation for Digital Mobile Radio Telephony", IEEE Trans. on Comm., Vol. COM-29, pp.1044–1050, July 1981.

[95] M. El-Tanany, J.S. Wight and H.M. Hafez, "The Optimization of a Quadrature Coherent Detector for Partial Response Continuous Phase Modulation with Modulation Index 1/2", GLOBECOM-82, pp. 884-889, Dec. 1982.

[96] M.L. Doelz and E.T. Heald, "Minimum-Shift Data Communication System", Collins Radio Co., U.S. Patent 2 977 417, March 28, 1961.

[97] W.M. Hubbard, "The Effect of Intersymbol Interference on Error Rtae in Binary Differentially-Coherent Phase Shift Keyed Systems", Bell System Technical Journal, Vol. 46, pp. 1149-1172, Aug. 1967.

[98] S. Crozier B. Mazur and R. Matyas, "Performance Evaluation of Differential Detection of MSK", GLOBECOM-82, pp. A5.1.1–A5.1.5, Dec. 1982.

[99] I. Tezcan and K. Feher, "Performance Evaluation of Differential MSK (DMSK) Systems in an ACI and AWGN Environment", IEEE Trans. on Comm., Vol. COM-34, pp. 727–733, July 1986.

[100] M.K. Simon, "Double Symbol Error Rates for Differential Detection of Narrow-Band FM", IEEE Trans. on Comm., Vol. COM-33, pp. 394–398, May 1985.

[101] L.J. Mason, "Analysis and Simulation of a DMSK Receiver", Satellite Communications Conference, pp. 5.7.1–5.7.5, Ottawa, June 1983.

[102] H. Suzuki, "Optimum Gaussian Filter for Differential Detection of MSK", IEEE Trans. on Comm., Vol. COM-29, pp. 916–918, June 1981.

[103] V.K. Bhargava, D. Haccoun, R. Matyas and P.P. Nuspl, *Digital Communications by Satellite : Modulation, Multiple Access and Coding*, John Wiley & Sons, Inc., New York, 1981.

[104] S. Pasupathy, "Minimum Shift Keying: A Spectrally Efficient Modulation", IEEE Communications Magazine, Vol.17, pp. 14–22, July 1979.

[105] S. Ogose and K. Murota, "Differentially Encoded GMSK with 2-Bit Differential Detection", Trans. IECE Japan, vol. J64-B, no. 4, pp. 248-254, April 1981.

[106] A. Yongaçoğlu and K. Feher, "DCTPSK: An Efficient Modulation Technique for Differential Detection", ICC'85, Chicago, June 23-26, 1985.

[107] K. Kinoshita et al., "Evaluation of 16 kbit/s Digital Voice Transmission for Mobile Radio", IEEE Trans. on Vehicular Tech., Vol. VT-3 , pp. 321-327, Nov.1984.

[108] F. de Jager and C.B. Dekker, "Tamed Frequency Modulation: A Novel Method to Achieve Spectrum Economy in Digital Transmission", IEEE Trans. on Comm., Vol. COM-26, pp. 534–542, May 1978.

[109] S. Asakawa and F. Sugiyama, "A Compact Spectrum Constant Envelope Digital Phase Modulation", IEEE Trans. on Vehicular Tech., Vol. VT-29, pp. 102-111, Aug. 1981.

[110] M.K. Simon and C.C. Wang, "Differential Detection of Gaussian MSK in a Mobile Radio Environment", IEEE Trans. on Vehicular Tech., Vol. VT-32, pp. 307-320, Nov. 1984.

[111] A. Yongaçoğlu, D. Makrakis and K. Feher, "One-bit Differential Detection of GMSK with Data-Aided Phase Control", ICC–86, pp. 57.8.1-57.8.5, June 1986.

[112] K. Murota, " Spectrum Efficiency of GMSK Land Mobile Radio", IEEE Trans. on Vehicular Tech., Vol. VT-34, pp. 69–75, May 1985.

[113] CCIR Report 903, "Digital Transmission in the Land Mobile Service", Vol. VIII, p. 100, 1983.

[114] G.D. Boudreau and P.J. McLane, "Differential Detection of Duobinary MSK", GLOBECOM'85, pp. 21.4.1-21.4.7, Dec. 1985.

[115] F. Amoroso, "The Bandwidth of Digital Data Signals", IEEE Commun. Mag., Vol. 18, pp. 13 - 24, Nov. 1980.

[116] T. Aulin and C.E. Sundberg, "CPM–The Effect of Filtering and Hardlimiting", International Journal of Satellite Communications, Vol. 2, No.4, pp. 219–240, Oct.-Dec. 1984.

[117] R. Bainbridge, A.G. Wacker and D.E. Dodds, "Effects of Hardlimiting in Differential MSK Demodulation", Electronicom'85, Toronto, pp. 562–565, Oct. 1985.

[118] D. Chakraborty and C.J. Wolejsza, "A Survey of Modem Design and Performance in Digital Satellite Communications", IEEE Jour. on Selected Areas in Comm., Vol. SAC-1, pp. 5-20, Jan. 1983.

[119] G.D. Forney, "The Viterbi Algorithm", Proc. IEEE, Vol. 61, pp. 268–278, March 1973.

[120] A. Papoulis, *Probability, Random Variables and Stochastic Processes*, Mc-Graw-Hill, New York, 1965.

[121] "University of Ottawa 12/14 GHz Anik B Earth Terminal" SED Systems Inc., Saskatoon, Nov. 1981.

[122] A. Yongaçoğlu, D. Makrakis, H.Ohnishi and K. Feher, "A New Receiver For Differential Detection of GMSK", GLOBECOM-86, pp. 29.5.1–29.5.6, Dec. 1986.

[123] H.L. Van Trees, *Detection, Estimation, and Modulation Theory*, John Wiley and Sons, Inc., Ch.2, 1968.

[124] K. Hirade, M. Ishizuka and F. Adachi, "Error-Rate Performance of Digital FM with Discriminator-Detection in the Presence of Co-channel Interference under Fast Rayleigh Fading Environment", Trans. of IECE of Japan, Vol. E 61, pp. 704-709, Sept. 1978.

[125] H. Suzuki et al., "Digital Portable Transceiver Using GMSK Modem and ADM Codec", IEEE Jour. on Selected Areas in Comm., Vol. SAC-2, pp. 604–610, July 1984.

[126] G. Ungerboeck, "Channel Coding with Multilevel/Phase Signals", IEEE Trans. on Inform. Theory, Vol. IT-28, pp. 55-67, Jan. 1982.

[127] H.K. Thapar, "Real-Time Application of Trellis Coding to High-Speed Voiceband Data Transmission", IEEE Jour. on Selected Areas in Comm., Vol. SAC-2, pp. 648–658, Sept. 1984.

[128] Statement of Work on Advanced Digital Modulation, INTELSAT, RFP INTEL–547, 16 Sept. 1985.

[129] D. Divsalar and M.K. Simon, "Trellis Coded Modulation for 4800–9600 bits/s Transmission Over a Fading Mobile Satellite Channel", IEEE Jour. on Selected Areas in Comm., Vol. SAC-5, pp. 162-175, Feb. 1987.

[130] IMSL Library Reference Manual, June 1982, Texas.